

VENT SIZING OF OIL FIELD CHEMICALS

SANJALA RIZVAN NASHIN



VENT SIZING OF OIL FIELD CHEMICALS

by

© SANJALA RIZVAN NASHIN

A thesis presented to the School of Graduate Studies of Memorial University of Newfoundland
in partial fulfillment of the requirements leading to the award of Master of Engineering

Department of Mechanical Engineering
Faculty of Engineering & Applied Science
Memorial University of Newfoundland

August, 2010

St. John's

Newfoundland

DEDICATION

I would like to dedicate my thesis to my beloved parents

(T. I. M. Abu Masud and Tahera Banu)

and sister (Zakia Iffat)

ABSTRACT

High temperature and pressure conditions occur very frequently in the oil and gas operation. A variety of oil field chemicals, such as corrosion inhibitors and hydrogen sulfide scavengers, are commonly used. These two chemicals are generally hydrocarbons, volatile and vulnerable in heating conditions. The objective of this work is to evaluate the hazard associated with three liquid (Nox Rust 1100, Nox Rust 9800, and Brenntag) and one solid (VCI 1 powder) corrosion inhibitors, and one hydrogen sulfide scavenger formulated with Formaldehyde and Monoethanolamine.

The Vent Sizing Package (VSP2) and the Advanced Reactive System Screening Tool (ARSST) are used to evaluate the thermal properties for hazard assessment and vent sizing. ARSST is used for rapidly screening and characterizing the system, and it provides directly scalable relief-system design data for reactive systems. Whereas, VSP2 continuously tracks pressure and adiabatic temperature which makes it a useful tool for measuring temperature and pressure rise rates. Vent sizing methods such as Leung's, Fauske's standard, and Fauske's short form equation are applied to the studied systems. The derived vent sizing areas are compared to determine the most appropriate one.

The studied corrosion inhibitors and the hydrogen sulfide scavenger show three kinds of system behaviors: non-reactive vapor, reactive vapor and gassy. The hydrogen sulfide scavenger sample is found to be the most reactive sample with two exotherms. Among the corrosion inhibitors, Nox Rust 9800 requires the largest area to volume ratio ($2.15 \times 10^{-4} \text{ m}^{-1}$) and VCI 1 powder require the lowest ($7.26 \times 10^{-6} \text{ m}^{-1}$).

ACKNOWLEDGEMENT

I would like to acknowledge Dr. Silvia Vargas in the first place, post doctorate fellow working with Dr. Khan and Dr. Kelly Hawboldt, for her remarkable guidance and supervision throughout the entirety of this project. Without her amazing ideas, unwavering support, and words of encouragement, this work would have been impossible.

I owe my deepest gratitude to Dr. Faisal Khan and Dr. Kelly Hawboldt for providing the opportunity to work in the field of adiabatic calorimetry with these very expensive and infrequent instruments (VSP2 and ARSST). Their guidance and supervision has enriched the work. I would like to thank NSERC, INCO Innovation Center, and Dr. Shafiq Alam for providing financial assistance.

It is a pleasure to thank Corrine Smith for providing assistance during the experimental work. I am indebted to the members of Fauske and Associates (J. P. Burelbach, Amy E. Theis, Charles F. Askonas, and R. Gabe Wood) for their continuous helps and suggestions throughout the work.

I would also like to pay my gratitude to Moya Crocker, as she was always there to solve any official problems or provide any possible help. It is a pleasure to pay tribute also to all of the faculty members, official and technical staff who helped me at any context.

It would have been next to impossible for me to come to the end of this long and tough journey without the moral support and affection from Sanjida Moury, who was my family in St. John's, thousands of miles away from my home.

I would like to pay my gratitude to Aminul Islam and Suvra Saha for being by the side of me in this journey. Thanks to my friends, Tahmina Akter, Mohidur Rahman, Tanjila Haque, Omit Mehruz, Punyama Jayasinghe, Rachel Moore, and Clemente Miranda, for their encouragement and support in different context.

I am nowhere without my family. I am grateful to them as they are always by the side of me in any circumstances. It is their continuous encouragement and good wishes, which led me to achieve my goal.

Finally, I offer my regards and blessing to all of those who were important to the successful realization of thesis, as well as expressing my apology that I could not mention personally one by one.

Table of Contents

| | |
|--|-----|
| ABSTRACT | iii |
| ACKNOWLEDGEMENT | iv |
| List of Tables | x |
| List of Figures | xi |
| List of Abbreviations | xv |
| List of Appendices | xvi |
| 1 INTRODUCTION | 1 |
| 1.1 Background | 1 |
| 1.1.1 Process Safety and Emergency Relief System Design | 1 |
| 1.1.2 Assessing the Importance of ERS Design for Certain Oil Field Chemicals | 3 |
| 1.2 Objectives | 4 |
| 1.3 Justification | 5 |
| 1.4 Problem Formulation | 5 |
| 1.5 Assumption | 6 |
| 1.6 Hypotheses | 6 |
| 1.7 Variables | 7 |
| 1.7.1 Independent variables | 7 |
| 1.7.2 Dependent variables | 7 |
| 1.8 Novel Contribution | 8 |
| 2 LITERATURE REVIEW | 9 |
| 2.1 Different Vent Sizing Methodologies | 9 |
| 2.1.1 Factory Insurance Association (FIA) Method | 11 |
| 2.1.2 American Petroleum Institute (API) Method | 13 |

| | | |
|-------|---|----|
| 2.1.3 | Boyle's Method | 19 |
| 2.1.4 | DIERS Method | 23 |
| 2.1.5 | Leung's Method | 25 |
| 2.1.6 | Fauske's Method | 30 |
| 2.1.7 | Fauske's Short Form Equation | 35 |
| 2.1.8 | Monogram Method | 36 |
| 2.1.9 | Fauske's Screening Equation for Reactive System | 37 |
| 2.2 | Evaluation of Different Methodologies | 38 |
| 2.3 | Oil Field Chemicals | 39 |
| 2.3.1 | Corrosion Inhibitors | 39 |
| 2.3.2 | Hydrogen Sulfide Scavenger | 40 |
| 3 | EXPERIMENTAL METHODOLOGY | 42 |
| 3.1 | Equipment | 42 |
| 3.1.1 | Advanced Reactive System Screening Tool (ARSST) | 42 |
| 3.1.2 | Vent Sizing Package 2 (VSP2) | 44 |
| 3.1.3 | DSC | 47 |
| 3.2 | Materials | 49 |
| 3.2.1 | 25% DTBP (Di-tert-butylperoxide) in Toluene | 49 |
| 3.2.2 | Corrosion inhibitors | 50 |
| 3.2.3 | H ₂ S Scavenger Components | 52 |
| 3.2.4 | Acetone | 53 |
| 3.3 | Procedure | 53 |
| 3.3.1 | Advanced Reactive System Calorimeter (ARSST) | 53 |
| 3.3.2 | Vent Sizing Package 2 (VSP 2) | 55 |
| 3.3.3 | Differential Scanning Calorimeter (DSC) | 55 |

| | | |
|-------|---|-----|
| 3.4 | Software for Data Processing | 59 |
| 3.4.1 | Reduce | 59 |
| 4 | HEAT CAPACITY CALCULATION | 61 |
| 4.1 | Corrosion Inhibitors | 64 |
| 4.1.1 | Nox Rust 1100 | 64 |
| 4.1.2 | Nox Rust 9800 | 65 |
| 4.1.3 | Brenntag Corrosion Inhibitor | 67 |
| 4.1.4 | VCI 1 Powder | 68 |
| 4.2 | H ₂ S Scavenger Components | 70 |
| 4.2.1 | Formaldehyde | 70 |
| 4.2.2 | Monoethanolamine | 71 |
| 5 | VENT SIZING: OIL FIELD CORROSION INHIBITORS | 73 |
| 5.1 | Brenntag Corrosion Inhibitor | 73 |
| 5.1.1 | ARSST Data | 73 |
| 5.1.2 | VSP2 Data | 76 |
| 5.1.3 | Vent Sizing Calculation | 82 |
| 5.2 | Nox Rust 9800 | 85 |
| 5.2.1 | ARSST Data | 85 |
| 5.2.2 | VSP2 Data | 87 |
| 5.2.3 | Vent Sizing | 91 |
| 5.3 | Nox Rust 1100 | 92 |
| 5.3.1 | ARSST Data | 92 |
| 5.3.2 | VSP2 Data | 94 |
| 5.3.3 | Vent Sizing | 97 |
| 5.4 | VCI 1 Powder | 102 |

| | | |
|-------|---|-----|
| 5.4.1 | ARSST Data | 102 |
| 5.4.2 | VSP2 Data | 105 |
| 5.4.3 | Vent Sizing | 110 |
| 5.5 | Discussion | 115 |
| 6 | VENT SIZING: HYDROGEN SULFIDE SCAVENGER | 118 |
| 6.1 | Formaldehyde | 118 |
| 6.1.1 | VSP2 Data | 118 |
| 6.1.2 | Vent Sizing | 123 |
| 6.2 | Monoethanolamine | 125 |
| 6.2.1 | VSP2 Data | 125 |
| 6.2.2 | 6.2.2 Vent Sizing | 129 |
| 6.3 | Hydrogen Sulphide Scavenger | 132 |
| 6.3.1 | Heat of Mixing Calculation | 133 |
| 6.3.2 | VSP-2 Data for Second Step | 135 |
| 6.3.3 | Vent Sizing Calculation | 147 |
| 6.4 | Discussion | 149 |
| 7 | CONCLUSION AND RECOMMENDATION | 152 |
| 7.1 | Conclusion | 152 |
| 7.1.1 | Specific Heat Capacity | 152 |
| 7.1.2 | Oil Field Corrosion Inhibitor | 152 |
| 7.1.3 | Hydrogen Sulphide Scavenger | 153 |
| 7.2 | Recommendation | 154 |
| 8 | Bibliography | 158 |

List of Tables

| | |
|--|-----|
| Table 4-1: Weight Loss of the Samples during Test | 63 |
| Table 5-1: Mass Loss of Brenntag Corrosion Inhibitor for ARSST Tests | 75 |
| Table 5-2: Mass Loss of Nox Rust 9800 for ARSST Tests | 86 |
| Table 5-3: Independent and Dependent Variables for Vent Sizing for Nox Rust 9800 | 90 |
| Table 5-4: Mass Loss of Nox Rust 1100 for ARSST Tests | 93 |
| Table 5-5: Area to Volume Ratio for Nox Rust 1100 | 102 |
| Table 5-6: Mass Loss of VCI 1 Powder for ARSST Tests | 105 |
| Table 6-1: Area to Volume Ratio for Monoethanolamine | 130 |
| Table 6-2: Weight, Mass Fraction and Molar Quantity of the H ₂ S Scavenger Components | 133 |

List of Figures

| | |
|---|----|
| Figure 2.1 : Mechanism of Corrosion Inhibitor Protection [Source: (Kelland, 2009)] | 40 |
| Figure 2.2 : Reaction of Formaldehyde with H ₂ S [Source: (Kelland, 2009)] | 41 |
| Figure 3.1 : Key features of ARSST [Source: (Burelbach & Theis, 2005)] | 43 |
| Figure 3.2: Advanced Reactive System Screening Tool (ARSST) | 44 |
| Figure 3.3 : Key Features of VSP2 Calorimeter [Source: (Askonas, Burelbach, & Leung, 2000)] | 46 |
| Figure 3.4: Vent Sizing Package 2 (VSP 2) | 46 |
| Figure 3.5 : Schematic Diagram of DSC [Source: (Vargas, 2009 a)] | 47 |
| Figure 3.6: METTLER TOLEDO DSC 1 | 48 |
| Figure 3.7: Aluminium Hermetic Pan. | 56 |
| Figure 4.1: Specific heat capacity thermal curves [Source: (ASTM, 2005)] | 61 |
| Figure 4.2: Specific Heat Capacity Vs Temperature for Nox Rust 1100 | 65 |
| Figure 4.3: Specific Heat Capacity Vs Temperature for Nox Rust 9800 | 66 |
| Figure 4.4: Specific Heat Capacity Vs Temperature for Brenntag Corrosion Inhibitor | 67 |
| Figure 4.5: Specific Heat Capacity Vs Temperature for VCI 1 Powder | 68 |
| Figure 4.6: Heat Flow Vs Temperature Plot for VCI 1 Powder (Fauske's Laboratory) | 69 |
| Figure 4.7: Specific Heat Capacity Vs Temperature for Formaldehyde | 70 |
| Figure 4.8: Specific Heat Capacity Vs Temperature for Monoethanolamine | 71 |
| Figure 4.9: Specific Heat Capacity Values as a Function of Temperature for Literature and Experimental Value | 72 |
| Figure 5.1: Temperature History for Brenntag Corrosion Inhibitor (ARSST Tests) | 74 |
| Figure 5.2: Pressure History for Brenntag Corrosion Inhibitor (ARSST Tests) | 74 |

| | |
|--|-----|
| Figure 5.3: Mass Loss as a Function of Time for Brenntag Corrosion Inhibitor (ARSST Tests) | 75 |
| Figure 5.4: Self Heat Rate as a Function of Temperature for Brenntag Corrosion Inhibitor (VSP2 Test) | 76 |
| Figure 5.5: Temperature History for Brenntag Corrosion Inhibitor (VSP2 Test) | 78 |
| Figure 5.6: Pressure History for Brenntag Corrosion Inhibitor (VSP2 Test) | 79 |
| Figure 5.7: Pressure as a Function of Temperature for Brenntag Corrosion Inhibitor (VSP2 Test) | 80 |
| Figure 5.8: Temperature History for Nox Rust 9800 (ARSST Tests) | 85 |
| Figure 5.9: Pressure History for Nox Rust 9800 (ARSST Tests) | 86 |
| Figure 5.10: Mass Loss as a Function of Time for Nox Rust 9800 (ARSST Tests) | 87 |
| Figure 5.11: Self Heat Rate as a Function of Temperature for Nox Rust 9800 (VSP2 Test) | 88 |
| Figure 5.12: Temperature History for Nox Rust 9800 (VSP2 Test) | 88 |
| Figure 5.13: Pressure History for Nox Rust 9800 (VSP2 Test) | 89 |
| Figure 5.14: Pressure as a Function of Temperature for Nox Rust 9800 (VSP2 Test) | 89 |
| Figure 5.15: Temperature History for Nox Rust 1100 (ARSST Tests) | 92 |
| Figure 5.16: Pressure History for Nox Rust 1100 (ARSST Tests) | 93 |
| Figure 5.17: Mass Loss as a Function of Time for Nox Rust 1100 (ARSST Tests) | 94 |
| Figure 5.18: Self Heat Rate as a Function of Temperature for Nox Rust 1100 (VSP2 Test 1) | 95 |
| Figure 5.19: Temperature History for Nox Rust 1100 (VSP2 Test 1) | 95 |
| Figure 5.20: Pressure History for Nox Rust 1100 (VSP2 Test 1) | 96 |
| Figure 5.21: Pressure as a Function of Temperature for Nox Rust 1100 (VSP2 Test 1) | 96 |
| Figure 5.22: Pressure Rate as a Function of Temperature for Nox Rust 1100 (VSP2 Tests) | 98 |
| Figure 5.23: Temperature History for VCI 1 Powder (ARSST Tests) | 103 |

| | |
|--|-----|
| Figure 5.24: Pressure History for VCI 1 Powder (ARSST Tests) | 104 |
| Figure 5.25: VCI 1 Powder before Test (Left) and ARSST Test Cell Containing VCI 1 Powder after Test (Right) | 104 |
| Figure 5.26: Temperature History for VCI 1 Powder (VSP2 Test) | 106 |
| Figure 5.27: Pressure History for VCI 1 Powder (VSP2 Test) | 106 |
| Figure 5.28: Self Heat Rate as a Function of Temperature for VCI 1 Powder (VSP2 Test) | 107 |
| Figure 5.29: Pressure as a Function of Temperature for VCI 1 Powder (VSP2 Test) | 108 |
| Figure 5.30: Deformed Closed Test Cell for VSP2 after Test with VCI 1 Powder | 109 |
| Figure 5.31: Pressure Rate as a Function of Temperature for VCI 1 Powder (VSP2 Test) | 110 |
| Figure 5.32: Inside View of Containment Vessel after Performing Open Cell Test in VSP2 | 114 |
| Figure 5.33: Deposited Product on the Defector Plot after Open Cell Test in VSP2 | 114 |
| Figure 5.34: Comparison of A/V Ratio Calculated by Leung's Method and Fauske's method for External Heating | 115 |
| Figure 5.35: Comparison of A/V Ratio for Nox Rust 1100 | 116 |
| Figure 5.36: Comparison of A/V Ratio for VCI 1 Powder | 116 |
| Figure 6.1: Temperature History for Formaldehyde (VSP2 Test) | 119 |
| Figure 6.2: Pressure History for Formaldehyde (VSP2 Test) | 120 |
| Figure 6.3: Self Heat Rate as a Function of Temperature for Formaldehyde (VSP2 Test) | 120 |
| Figure 6.4: Pressure as a Function of Temperature for Formaldehyde (VSP2 Test) | 121 |
| Figure 6.5: Pressure Rate as a Function of Temperature for Formaldehyde (VSP2 Test) | 122 |
| Figure 6.6: Temperature History for Monoethanolamine (VSP2 Test) | 125 |
| Figure 6.7: Pressure History for Monoethanolamine (VSP2 Test) | 126 |
| Figure 6.8: Self Heat Rate as a Function of Temperature for Monoethanolamine (VSP2 Test) | 126 |

| | |
|---|-----|
| Figure 6.9: Pressure as a Function of Temperature for Monoethanolamine (VSP2 Test) | 127 |
| Figure 6.10: Pressure Rate as a Function of Temperature for Monoethanolamine (VSP2 Test) | 128 |
| Figure 6.11: Area to Volume Ratio as a Function of gas Molecular Weight | 131 |
| Figure 6.12: Temperature History due to the Heat of Mixing (VSP 2 Test) | 134 |
| Figure 6.13: Temperature History for H ₂ S Scavenger (VSP2 Tests) | 136 |
| Figure 6.14: Pressure History for H ₂ S Scavenger (VSP2 Tests) | 136 |
| Figure 6.15: Pressure Rate as a Function of Temperature for H ₂ S Scavenger (VSP2 Tests) | 137 |
| Figure 6.16: Pressure as a Function of Temperature for H ₂ S Scavenger (VSP 2 Tests) | 140 |
| Figure 6.17: Self Heat Rate as a Function of Temperature for H ₂ S Scavenger (VSP 2 Tests) | 142 |
| Figure 6.18: Comparison of A/V Ratio for 37% Formaldehyde | 149 |
| Figure 6.19: Comparison of A/V Ratio for Monoethanolamine | 149 |
| Figure 6.20: Comparison of A/V Ratio for H ₂ S Scavenger Sample | 150 |

List of Abbreviations

| | |
|-------|---|
| API | American Petroleum Institute |
| ARC | Accelerating Rate Calorimetry |
| ARSST | Advanced Reactive System Screening Tool |
| BLEVE | Boiling Liquid Expanding Vapor Explosion |
| CCPS | Centre for Chemical Process Safety |
| DIERS | Design Institute of Emergency Relief System |
| DSC | Differential Scanning Calorimetry |
| ERS | Emergency Relief System |
| FIA | Factory Insurance Association |
| VSP2 | Vent Sizing Package 2 |

List of Appendices

| | |
|---|-----|
| APPENDIX 1 | 164 |
| A1.1 EXPERIMENTAL SETUP | 164 |
| A1.1.1 Pre Test Steps | 164 |
| A1.1.2 Making Test Cell Assembly | 166 |
| A1.1.3 Making Final Vessel Assembly | 178 |
| A1.1.4 Pressure Calibration | 184 |
| A1.1.5 Experimental Run | 186 |
| A1.2 TROUBLESHOOTING | 188 |
| A1.2.1 Changing Heater Gland | 188 |
| A1.2.2 Checking Pressure leak | 190 |
| A1.2.3 Fixing Nonzero Gauge Pressure Reading in Atmospheric Condition | 191 |
| APPENDIX 2 | 192 |
| A2.1 EXPERIMENTAL SETUP | 192 |
| A2.1.1 Test Cell Setup | 192 |
| <i>A2.1.1.1 Choice of test cell and the primary information</i> | 192 |
| <i>A2.1.1.2 Checking continuity and resistance of different parts</i> | 193 |
| <i>A2.1.1.3 Insulating and installing test cell into heaters</i> | 196 |
| <i>A2.1.1.4 Double checking continuity of heaters</i> | 200 |
| A2.1.2 Containment Vessel Setup | 202 |
| <i>A2.1.2.1 Test cell and vessel connectoins</i> | 202 |
| <i>A2.1.2.2 Thermocouple connections inside the vessel</i> | 205 |
| <i>A2.1.2.3 Insulation</i> | 209 |

| | |
|--|-----|
| A2.1.3 Vessel Assembly | 209 |
| A2.1.4 Checking Resistance of Thermocouples and Heater Glands | 214 |
| A2.1.5 Thermocouple Connections outside the Vessel | 217 |
| A2.1.6 Calibration of Thermocouples | 222 |
| A2.1.7 Calibration of Pressure Transducers | 224 |
| A2.1.8 Checking Leak in the Test Cell | 228 |
| A2.1.9 Applying Vacuum in the Test Cell and Containment Vessel | 231 |
| A2.1.10 Loading Sample in the Test Cell | 232 |
| <i>A2.1.10.1 Liquid sample</i> | 232 |
| <i>A2.1.10.2 Solid sample</i> | 232 |
| A2.1.11 Running Test | 233 |
| A2.2 BASIC CONCERNS | 235 |
| A2.3 TROUBLESHOOTING | 237 |
| APPENDIX 3 | 239 |
| APPENDIX 4 | 246 |
| A4.1 Brenntag Corrosion Inhibitor | 246 |
| A4.2 Nox Rust 9800 | 247 |
| A4.2.1 Different Parameters to design Vent size | 247 |
| A4.2.2 Vent Sizing Calculation | 250 |
| A4.3 Nox Rust 1100 | 251 |
| A4.4 VCI 1 Powder | 253 |
| APPENDIX 5 | 256 |
| A5.1 Heat of Mixing Calculation for Test 2 | 256 |
| A5.2 Different Parameters | 257 |
| A5.3 Vent Sizing Calculation | 261 |

1 INTRODUCTION

1.1 Background

1.1.1 Process Safety and Emergency Relief System Design

In any process that deals with hazardous chemicals, unexpected events such as fires, explosions and accidental releases are not uncommon. Process safety deals with the prevention of unintentional releases of chemicals, energy or other potentially harmful materials that can affect the plant or environment detrimentally (Marshall & Ruhemann, 2001). An emergency Relief System (ERS) is one of the line defenses to achieve process safety (ioMosaic Corporation, 2006). Due to the increasing public concern of environmental issues, on average 25-30% of the total process cost was invested in 1996 by the industries to ensure safe release of the chemicals. (Duffield, Nijsing, & Brinkhof, 1996).

The reason behind sudden excessive pressure rise is either unexpected heating of the vessel due to external causes such as external fire or uncontrolled reactions within the vessel (CCPS, 1993). An analysis of 190 accident case histories indicated that accidents happened more frequently in batch reactors (57%) than continuous process plants (10%) (Rasmussen, 1988). Surprisingly, a large percentage of accidents (24%) happened during holding or storage operation (Rasmussen, 1988). In a batch reactor containing a multi component liquid mixture, a chemical reaction (usually exothermic) may initiate a thermal runaway process. It becomes dangerous if the generation of the reaction heat due to malfunctioning exceeds the heat removal capacity of the equipment (Duffield et al., 1996). If this situation cannot be controlled by operational measures, the temperature will rise to the level where the volatile components of the liquid start to

evaporate or even gas might be produced due to undesired secondary decomposition reactions (CCPS, 1993; Duffield et al., 1996). Even endothermic reactions can cause a pressure increase if the reaction products are gases or liquids which are more volatile than the reactants (CCPS, 1993). However, exothermic reactions are potentially more dangerous because of the increase in temperature, which leads to accelerated chemical reaction rates. As the system pressure increases, it is necessary to discharge the fluid mixture from the vessel at an adequate rate to prevent the over pressurization (CCPS, 1993; Duffield et al., 1996). If the ERS is not correctly sized, vessel failure may occur, which leads to uncontrolled release to the environment. One of the main challenges for designing an ERS is to determine whether it should be designed for a single or two phase vapor-liquid flow (Fisher et al., 1992). Two phase flow requires vent sizes 2 to 10 times larger than for single phase vapors (Duffield et al., 1996). The designed vent size should be large enough to ensure that the over pressure stays within safe limits during relief.

The basic data needed to design an emergency relief system requires a careful experimental program which uses representative samples, such as Accelerating Rate Calorimeter (ARC), Vent Sizing Package 2 (VSP 2) and Advanced Reactive System Screening Tool (ARSST). VSP2 and ARSST are the two bench scale apparatus developed for DIERS (Design Institute for Emergency Relief System) testing for acquiring vent sizing data. The key feature for both of the instruments is the use of a unique low thermal mass test cell to reduce the thermal inertia (Fauske, 2000).

1.1.2 Assessing the Importance of ERS Design for Certain Oil Field Chemicals

Though vent sizing techniques are studied for different process field chemicals, no studies of vent sizing for oil field chemicals (such as corrosion inhibitors, H₂S scavenger) are available in literature (Vargas, 2009 b). In oil and gas production industry, internal corrosion which is enhanced by the presence of carbon dioxide and hydrogen sulphide continues to be a challenge (Palmer, Hedges, & Dawson, 2004). Yearly, approximately 1.34 billion US dollars are invested to mitigate corrosion problems in U.S. oil and gas production industry (Ruschau & Al-Anezi, 2006).

Corrosion inhibitors are widely used in the oil and gas industries to combat corrosion during production, transportation and refining. North America is the leading consumer of oil field chemicals and corrosion inhibitors in the world, and the consumption of these chemicals is increasing daily (Muller, Rizvi, Yokose, & Jackel, 2009). For example, total consumption of corrosion inhibitors in the United States has doubled (from roughly \$ 600 million to \$ 1.1 billion) in 16 years (from 1982 to 1998) (Ruschau & Al-Anezi, 2006). Corrosion inhibitors are toxic and volatile in nature and are available in liquid, solid and gas phases (Andreev & Kuznetsov, 1998; Palmer et al., 2004). However, the exact chemical nature and composition of the corrosion inhibitors are not revealed due to proprietary protection (Fink, 2003; Vargas, 2009 b).

Hydrogen sulphide is a naturally occurring gas that introduces various problems in the oil and gas industry such as toxicity, corrosion, emulsion, surface equipment problems, etc. (Tung, Hung, Tien, & Loi, 2001). The amount of hydrogen sulphide in the oil products needs to be below 4 ppm to meet the sales specification (Kelland, 2009). This is why the use of hydrogen

sulphide scavengers has seen significant growth. In fact, \$172 million was invested in the North American region in 1995 and \$220 million was invested only in USA in 2004 for scavenging operations in oil and gas industries (Houston, 1996). However, the chemical composition and physical and thermal properties of H₂S scavengers are entirely unknown (Kelland, 2009).

The momentous importance of corrosion inhibitors and hydrogen sulphide scavengers in the oil and gas fields, and the cost involved in applying these chemicals have ascertained the importance of accessing vent sizing application for their safe storage and process conditions.

1.2 Objectives

1. The purpose of this work is to apply the DIERS based calorimetry to oil field chemicals (three liquid corrosion inhibitors, one solid corrosion inhibitor and one hydrogen sulphide scavenger) to perform thermal analysis which will help to understand their behaviour at high temperature and pressure.
2. To apply vent sizing methods that do not require detailed physical and chemical properties to ERS design for particular chemicals.
3. To determine the safe storage and process conditions for corrosion inhibitors and scavengers.

1.3 Justification

The liquid corrosion inhibitors used in the oil and gas industries are mainly oil based (Fink, 2003). Being hydrocarbon, the liquid corrosion inhibitor is highly susceptible to fire exposure. When introduced to fire, they may produce various hazardous decomposition products such as carbon monoxide, carbon dioxide, oxides of sulfur and miscellaneous hydrocarbons (Kelland, 2009; Fink, 2003). The fine solid corrosion inhibitors are also generally hydrocarbon based, which may be explosive (dust or mist explosion) in the presence of an ignition source in case of mixing with air in critical proportion. It may produce different hazardous hydrocarbons due to decomposition (Kelland, 2009).

In addition, the corrosion inhibitors may be susceptible to runaway reaction when heated as they are a blend of different components. Runaway reactions result in a sudden raise of temperature and pressure, which can trigger a process accident.

Thermal analysis of the corrosion inhibitors will help to understand their thermal and pressure characterization, and their behavior in case of extreme operating conditions. This analysis will lead to enhanced process safety, one of the noteworthy goals in oil and gas production facility.

1.4 Problem Formulation

The queries that are the driving force behind conducting this research are as follows:

1. What is the thermal and pressure behaviour of the oil field chemicals?
2. Will there be occurrence of runaway reactions for the chemicals?
3. How can the hazard be characterized due to external fire conditions?
4. Will there be any chemical loss due to high temperature introduction?

1.5 Assumption

- i. Both of the calorimeters (VSP2 and ARSST) are capable of providing adiabatic conditions, as the phi factors for a standard ARSST test cell and a standard VSP2 test cell are close to unity (Fauske, 2000).
- ii. The ARSST heater components and test cells are capable of producing repeatability in case of reuse when the cells are not burned after use. This assumption was made on the basis of the results for 25% DTBP in toluene. However, VSP2 cells are not re-usable.
- iii. The existing polynomials (heater calibrations) for running tests in ARSST in single ramp polynomial control mode are adequate as the properties of the corrosion inhibitors are unknown.

1.6 Hypotheses

The corresponding hypotheses are listed as follows:

1. As the oil field chemicals are mainly hydrocarbon based, they will be vulnerable to external fire conditions.
2. The oil field chemicals that are a blend of different proprietary protected components may cause runaway reactions.

1.7 Variables

1.7.1 Independent variables

- Temperature (The experiments are carried out from a temperature range of 20 °C- 300 °C).
- Time.
- Molecular weight.
- Density of the liquid.
- Density of the solid.

1.7.2 Dependent variables

- Pressure (The pressure range for the experiments is -14.7 Psig to 700 Psig).
- Temperature increase rate.
- Self heat rate.
- Pressure increase rate.
- Energy release rate/ Heat generation rate.
- Specific heat capacity.
- Vapour density.
- Latent heat of vaporization.
- Area to volume ratio (A/V ratio) for vent.

1.8 Novel Contribution

1. The thermal and pressure behaviour of the premeditated corrosion inhibitors (Nox Rust 1100, Nox Rust 9800, Brenntag, and VCI 1 Powder) and scavenger (mixture of Formaldehyde and Monoethanolamine) are studied for the first time. This study has a significant importance to the oil field research, as their chemical properties and chemistry are proprietary protected.
2. Specific heat capacity values of these six chemicals from 30 °C prior to their boiling point are determined in order to perform vent sizing calculations. The specific heat capacity values are imperative to know, as there are no published values for these compositions. It is a novel addition to the published literature.
3. The calculated vent area will help to assess the safe storage and process conditions for the studied oil field chemicals.
4. As more complex blends of different chemicals are used in oil and gas fields, the calculated vent areas for the studied chemicals in isolation will help to predict the actual scenario.

2 LITERATURE REVIEW

2.1 Different Vent Sizing Methodologies

There is no unified approach that can be used to design an emergency relief system (ERS) because of the diversity of the systems and materials involved in process industries. Chemical systems can be broadly classified into non-reactive systems and reactive systems, and a reactive system can be subsequently classified as vapor, gassy or hybrid. If a reactive system contains components whose vapor- liquid equilibrium controls the system temperature and reaction rate, it is considered as a vapor reactive system. A gassy system has non condensable reactions or decomposition products and a hybrid system exhibits both vapor and gassy characteristics. Each system has a unique set of emergency conditions depending on the specific risk and hazard analysis for the system. According to Fauske (1985), the steps that must be considered in any ERS design are:

1. Defining upset conditions for that particular system.
2. Designing basis envelope including the worst case scenario for that system.
3. Determining vent size and flow rate considering the design basis envelope.
4. During designing, investigating type of vented material.

Steps 2 and 3 are achieved by applying a combined experimental and analytical approach for possible upset conditions. To analyze the upset conditions, experimental simulation with bench scale equipment is required in addition to conducting a detailed risk analysis.

There are numerous vent sizing methods available. The most commonly applied and documented methods are American Petroleum Institute (API) (American Petroleum Institute, 2008; American

Petroleum Institute, 2003; American Petroleum Institute, 2007), Factory Insurance Association (FIA) (Duxbury, 1980; Mannan & Frank, 2005; Sestak, 1965), Boyle, Design Institute for Emergency Relief Systems (DIERS) (Fauske, 2000; Fisher, 1985; Fisher, et al., 1992; Kemp, 1983; Swift, 1984), Leung (Leung, 1986), Fauske's standard (Fauske, 2000), Fauske's short form (Fauske, 1984 a) and Monogram (Fauske, 1984 b). Each method has different nomenclature and parameters. In subsequent sections, a brief description of these methods is presented. To avoid complexity, each method is printed using their original nomenclature.

The basic data needed to design an ERS requires careful experimental programs that use representative samples such as Vent Sizing Package 2 (VSP 2) and Advanced Reactive System Screening Tool (ARSST). VSP2 and ARSST are the two bench scale apparatus developed by DIERS for acquiring vent sizing data. The key feature for both of the instruments is the use of a unique low thermal mass test cell to reduce the thermal inertia. According to Townsend and Tou (1980), the phi (ϕ) factor (also known as thermal inertia) is simply the ratio of the combined thermal capacity of the reacting sample and the sample container to that of the sample alone. It can be defined mathematically as follows:

$$\phi = 1 + \frac{m_b C_{pb}}{m_s C_{ps}}$$

Equation 2.1

Where, m_s = mass of the sample.

m_b = mass of the test cell.

C_{ps} = specific heat of the sample.

C_{pb} = specific heat of the test cell.

A ϕ factor of unity means that the reacting sample is truly adiabatic. Factors greater than 1 indicate that the temperature rise of the sample by reaction heat will be lower than in perfect adiabatic condition. For instance, a ϕ factor of 2 means that half of the reaction heat will be used to heat the sample container, and the temperature rise due to sample reaction is only half of that in a truly adiabatic case. VSP2 and ARSST are benefited with test cells having a phi factor close to unity and therefore provide a nearly true adiabatic environment. The low thermal inertia of the VSP2 and ARSST help to understand the magnitude of self heat rate and the adiabatic temperature rise. These equipments also have mechanism for automatic pressure tracking continuously.

2.1.1 Factory Insurance Association (FIA) Method

FIA method (Sestak, 1965) is a well known empirical approach proposed by Factory Insurance Association. FIA method is a quick and easy method and can serve as a preliminary assessment tool. This method is no longer recommended because it is based in “exothermicity” (Sestak, 1965), which is defined as the heat release per unit volume. The degree of exothermicity can be determined from the examples presented in the work of Sestak (1965). The required vent area (A) is considered (approximately) proportional to the reactor capacity (V) to the power 0.92. The graphical relationship is represented by Equation 2.2 where K is a constant.

$$A = KV^{0.92}$$

Equation 2.2

The value of K is dependent on the degree of exothermicity and the capacity of the reactor. For exothermic reactions categorized as A (very low), B (low), and C (moderately high), the (approximate) values of K are 0.0056, 0.021, and 0.095, respectively (for $V \leq 10,000$). For exothermic reactions with extraordinarily high heat releases, categorized as D, the approximate value of K is 0.48 (for $V \leq 4,000$). The value of K is considered as 0.0056 for endothermic reactions. The vent areas can be calculated as bands of approximately $\pm 50\%$ of the values derived from Equation 2.2 (Mannan & Frank, 2005).

The limitations of FIA method are summarized by Duxbury (1980) as follows:

- FIA's guidelines are not always sufficient to determine the degree of exothermicity.

The severity of exothermic reaction is considered as highest and may lead to over sizing.

- There is no reference in the guidelines for gas phase reactions. Thus, it might not be appropriate to categorize the reactions on the basis of "exothermicity".

- The physical properties of the reactor content (e.g. viscosity) are not considered.

- The method is based on only 100 to 125 psig vessels. Pressure higher than 125 psig may lead to marked over sizing of the vent area. FIA method fails to consider the effect of allowable reactor pressure on the vent size.

- It does not take into account the length of the vent line; no. of bends, etc.

- FIA chart does not consider the effect of the vessel capacity less than 10US gallons.

- FIA method ignores the effect of fill ratio and is only based on reactor capacity.

2.1.2 American Petroleum Institute (API) Method

API recommended practices provide guidelines for heat input. Guidelines are provided for examining principal causes of overpressure; determining individual relieving rates; and selecting and designing disposal systems. It considers components such as vessels, flares, and vent stacks. Solutions are suggested considering design, economic, and safety issues related to pressure-relieving. It also includes a new section on flare gas recovery.

The latest upgrade on API RP 521 was in 2008 and was addressed as “Pressure-Relieving and Depressurizing Systems” (American Petroleum Institute, 2007). It is a guide for plant engineers in the design, installation, and operation of pressure-relieving and depressurizing systems, and supplements API Recommended Practice 520, Part I. A detailed discussion of potential causes of over pressure is also given in API 521.

API RP 520 gives the guidelines to determine the effective area in generating or heating vapour and the relieve valve rate of discharge (American Petroleum Institute, 2008). API RP 520 also provides the guidelines for equipment failure (tube rupture or air cooler failures of heat exchangers), and the sizing equation for gas or vapour relief, steam relief, and liquid relief. Though API RP 520 recommends methods for sizing pressure relief devices in two phase flow services, there are currently no pressure relief devices with certified capacities for two phase flow as testing methods for certification are not available (American Petroleum Institute, 2008). The necessary equations for gas or vapour, steam and liquid relief systems for calculation in SI units are described below. The methods for calculation in USC units are not listed here and it is important to note that the formulae for these two units are different. The equations are developed

analytically on the basis of the assumption of isentropic nozzle flow for homogeneous fluid. The API RP 520 provides the details.

2.1.2.1 Vent Sizing for Gas or Vapor Relief

Critical flow in pipe for gas or vapour occurs when the downstream pressure is less than or equal to the critical flow pressure, whereas subcritical flow occurs when the downstream pressure exceeds the critical flow pressure. Depending on whether the flow is critical or subcritical, the sizing equation for pressure relief devices can be divided into two different categories. Upstream pressure refers to the pressure in a pipe or duct on the inlet side and downstream pressure refers to the pressure in the outlet of the pipe or duct.

For critical flow, effective discharge area (A in mm^2) can be calculated using any of the equations (American Petroleum Institute, 2008) from Equation 2.3 to Equation 2.5.

$$A = \frac{W}{CK_d P_1 K_b K_c} \sqrt{\frac{TZ}{M}}$$

Equation 2.3

$$A = \frac{2.676 \times V \sqrt{TZM}}{CK_d P_1 K_b K_c}$$

Equation 2.4

$$A = \frac{14.41 \times V \sqrt{TZG_v}}{CK_d P_1 K_b K_c}$$

Equation 2.5

Where,

$$C = 0.03948 \sqrt{k \left(\frac{2}{k+1} \right)^{\frac{(k+1)}{(k-1)}} \frac{\sqrt{kg \times kg - mole \times K}}{mm^2 \times hr \times kPa}}$$

Equation 2.6

For subcritical flow, the effective discharge area (A) can be calculated by using any of the equations (American Petroleum Institute, 2008) from Equation 2.7 to Equation 2.9.

$$A = \frac{17.9 \times W}{F_2 K_d K_c} \sqrt{\frac{ZT}{M \times P_1 (P_1 - P_2)}}$$

Equation 2.7

$$A = \frac{47.95 \times V}{F_2 K_d K_c} \sqrt{\frac{ZTM}{P_1 (P_1 - P_2)}}$$

Equation 2.8

$$A = \frac{258 \times V}{F_2 K_d K_c} \sqrt{\frac{ZT G_v}{P_1 (P_1 - P_2)}}$$

Equation 2.9

Here,

W = Required flow through the device (Kg/h).

C = A function of the ratio of the ideal gas specific heats ($k = C_p/C_v$) of the gas or vapour at inlet relieving temperature.

K = Ratio of specific heats (C_p/C_v) for an ideal gas at relieving temperature. The ideal gas specific heat ratio is independent of pressure.

K_d = Effective coefficient of discharge. For preliminary sizing the following values are used:
0.975, when a PRV is installed with or without a rupture disk in combination for gas/vapour/ steam relief sizing
0.65, when a PRV is installed with or without a rupture disk in combination for liquid relief sizing
0.62, when a PRV is not installed and sizing is for a rupture disk

P_1 = Upstream relieving pressure, which is the summation of set pressure, the allowable overpressure and atmospheric pressure (kPa).

P_2 = Backpressure (kPa).

K_b = Capacity correction factor due to backpressure.

K_c = Combination correction factor for installations with a rupture disk upstream of the pressure relief valve (PRV) (1.0, when a rupture disk is not installed; 0.9 when a rupture disk is installed in combination with a PRV and the combination does not have a certified value).

T = Relieving temperature of the inlet gas or vapour (K)

Z = Compressibility factor for the deviation of the actual gas from a perfect gas, a ratio evaluated at inlet relieving conditions.

M = Molecular weight of the gas or vapour at inlet relieving conditions (kg/kg-mole). This value should be obtained from the process data.

V = Required flow through the device (Nm^3/min at 0°C and 101.325 kPa).

F_2 = Co-efficient of subcritical flow.

G_v = Specific gravity of gas at standard conditions referred to air at standard conditions.

2.1.2.2 Sizing for Steam Relief

Pressure relief devices in steam service operated at critical flow conditions may be sized using Equation 2.10 (American Petroleum Institute, 2008).

$$A = \frac{190.5 \times W}{P_1 K_d K_b K_c K_N K_{SH}}$$

Equation 2.10

The correction factor for the Napier Equation, K_N , is equal to 1 if P_1 is lower than 1500 psia (10,339 kPa) (American Petroleum Institute, 2008). When P_1 ranges from 1500 psia (10,339 kPa) to 3200 psia (22,057 kPa), the value of K_N can be calculated using Equation 2.11 (American Petroleum Institute, 2008).

$$K_N = \frac{0.02764 \times P_1 - 1000}{0.03324 \times P_1 - 1061}$$

Equation 2.11

The superheat correction factor (K_{SH}) is listed in Table 9 of API 520 (American Petroleum Institute, 2008). For saturated steam at any pressure, $K_{SH} = 1.0$.

2.1.2.3 Sizing for Liquid Relief

API 520 recommends relief valves in liquid service that are designed in accordance with the ASME Code, which requires capacity certification and can be initially sized using Equation 2.12. The ASME Code requires that the capacity certification includes testing to determine the rated coefficient of discharge for the liquid pressure relief valves (PRV) at 10% overpressure (American Petroleum Institute, 2008).

$$A = \frac{11.78 \times Q}{K_d K_w K_c K_v} \sqrt{\frac{G_l}{P_1 - P_2}}$$

Equation 2.12

Here,

P_2 = Backpressure (KPa).

Q = Flow rate for liquid sizing relief (L/min).

K_w = Correction factor due to backpressure. If the backpressure is atmospheric, value for K_w is used as 1.0.

G_l = The specific gravity of the liquid at the flowing temperature referred to water at standard conditions.

K_v = Viscosity correction factor. K_v is estimated and used in Equation 2.12.

When a PRV is sized for viscous liquid service, firstly it is to be sized as if it were for a non-viscous type application (i.e. $K_v = 1.0$) so that a preliminary required discharge area can be obtained from Equation 2.11 (American Petroleum Institute, 2008).

API method is only applicable to single phase flow. API RP 520 and 521 do not address emergency relief for runaway reaction in batch reactors. API 520 uses the equation of ideal gases for sizing. Thus, the discharge area calculated for high pressures is oversized. This results, for example, in high implementation and operation costs, as well as potential vibration and pulsation problems.

API method is capable of providing a vent area estimation having good agreement with a real situation when the following conditions are fulfilled: (i) maximum allowable working pressure is lower than 15psig, (ii) the vessel is not subjected to external fire consideration and (iii) thermo physical properties are known (American Petroleum Institute, 2008; American Petroleum Institute, 2003; American Petroleum Institute, 2007).

2.1.3 Boyle's Method

Before Boyle's method, a typical approach to calculate relief area for a reactor was based on the assumption that vapor is to be vented. An adequate relief area is defined as one being large enough to have a vapor venting rate such that the internal pressure in the reactor does not continue to rise after the rupture disk bursts. This assumption is observed being violated for some cases where the required vapor venting area is as high as three to four times the designed vapor

venting area. As a result, this encourages the idea to consider 100% liquid venting. However, this idea cannot be completely true as vapor does get generated in the kettle to maintain the vapor pressure. It is observed that if the percentage of the vented liquid is greater (such as 90%) than the percentage of vented vapor, assumption of venting 100% liquid will provide a good assumption of the required venting area.

Boyle (1967) proposed an iterative method for the sizing of relief area for polymer reactors. At first, a vent Diameter (D in feet), reasonable for that particular reactor, is assumed. A venting velocity (V) is also assumed, and the Reynolds number (Re) for that velocity is calculated. The value of contraction co-efficient (K_c) is taken on the basis of the derived Reynolds number and ranges from 0.40 to 1.10 (Boyle, 1967). Then the value of friction factor (f) is determined from the plot of the Reynolds number versus friction factor. The value of f and K_c are substituted in the Equation 2.13, which is solved for the venting velocity (V).

$$\frac{\Delta P}{\rho} + (Z_2 - Z_1) = \left(\frac{4fL}{D} + K_c + 1.0 \right) \frac{V^2}{2g}$$

Equation 2.13

Here,

$\Delta P = P_2$ (Upstream Pressure, lb./sq. ft.) – P_1 (Downstream Pressure, lb./sq. ft.), which is the rating of the relief device.

$Z_1 =$ Upstream elevation above datum plane, ft.

$Z_2 =$ Downstream elevation above datum plane, ft.

$\rho =$ Density, lb./cu. ft.

L = Equivalent length of vent piping.

g = Acceleration of gravity (32.2 ft./sec²).

If the value of the venting velocity (V) from Equation 2.13 matches with the assumed venting velocity, then the assumption is proved to be valid. This initial velocity is then converted to flow rate (Q in gallon/ minute) according to Equation 2.14 (Boyle, 1967) as follows:

$$Q = \left(V \frac{\text{ft.}}{\text{sec.}} \right) \left(\frac{\pi}{4} D^2 \text{ sq. ft.} \right) \times \left(7.48 \frac{\text{gal.}}{\text{cu. ft.}} \right) \left(60 \frac{\text{sec.}}{\text{min.}} \right)$$

Equation 2.14

The flow rate is divided by the total volume of the batch in the reactor (M in gallons) to calculate the venting time.

The next step is to determine the rate of temperature rise. The system is assumed adiabatic, which means all the exothermic heat of polymerization is involved to raise the batch temperature. The rate of temperature rise is given by Equation 2.15 (Boyle, 1967).

$$\frac{dT}{dt} = \frac{W_m \times \Delta H \times R}{W_b \times C_p}$$

Equation 2.15

Here,

W_m = Total amount of monomers in batch, lb.

ΔH = Heat of polymerization for monomers, Btu/lb.

W_b = Total weight of batch, lb.

C_p = Average heat capacity of batch over temperature range involved, Btu/lb-°F.

$R =$ Conversion rate, %conversion/hr.

The log rate of conversion is expressed as Equation 2.16 (Boyle, 1967), where a and b are constants and T is temperature in °F.

$$\log_e R = aT - b$$

Equation 2.16

Substituting R from Equation 2.16 into Equation 2.15 results in Equation 2.17 (Boyle, 1967), where c is a constant.

$$\frac{dT}{dt} = \frac{W_m \times \Delta H \times ce^{aT}}{W_b \times C_p}$$

Equation 2.17

By combining all the constants in a single constant (K_1), Equation 2.17 can be expressed as Equation 2.18 (Boyle, 1967), as shown below.

$$\frac{dT}{dt} = K_1 e^{aT}$$

Equation 2.18

Integrating Equation 2.18 in the range of T_1 to T_2 gives the time (in minutes) required to raise the temperature from T_1 to T_2 , as given by Equation 2.19 (Boyle, 1967).

$$\Delta t = -K_2 [e^{-aT_2} - e^{-aT_1}]$$

Equation 2.19

If $T_2 = \infty$, the reaction is considered to be explosive. By substituting this value of T_2 , the time to raise the temperature from T_1 to the explosive condition can be derived as follows (Boyle, 1967):

$$\Delta t = K e^{-aT_1}$$

Equation 2.20

A plot of venting time versus temperature can be achieved by using Equation 2.20.

The pressure as function of temperature for the particular system is also plotted. In case of multi phase system, the total reactor pressure may be calculated by adding the vapor pressures of the main components.

The calculated vent area is multiplied by a safety factor of 2 or 3 while designing the reactor for providing a conservative specified relief area for safety purposes.

Hand calculations are practicable in Boyle's method, which is comparatively quicker to apply as it considers the calculation of reactor conditions and the calculation of fluid flow separately. Boyle's method usually leads to a larger vent area than the steady state vapor venting approach. Hence, it provides safer approximation in some cases.

2.1.4 DIERS Method

Under the patronage of AIChE, a syndicate of 29 companies was formed in 1976 named The Design Institute of Emergency Relief Systems (DIERS) (Fisher, 1985; Kemp, 1983; Swift, 1984). As the name indicates, the role of this consortium is to develop methods for the design of emergency relief systems. Pressure relief requirements for chemical reactive systems can be obtained by two approaches (Fauske, 2000):

1. Using Computer simulation methods (e.g. DIERS-developed SAFIRE code and Super Chems for DIERS) requires all basic physical, thermodynamic, and kinetic properties of the system.
2. Calculating the vent area by directly using data of runaway calorimetry tests used in special-case venting models.

The first approach is not preferable in many cases as the required physical and kinetic data are rarely available in the range of emergency relief conditions and they are also time consuming and costly to generate. Hence, the second approach has become the most-frequently-used as it is a more user-friendly technique.

The DIERS methodology for vent sizing includes the following basic steps:

- 1.** Definition of the worst credible deviation of the process, to provide the design case for vent sizing.
- 2.** Characterization of the reacting system behaviour, using pseudo adiabatic experimental techniques. The reacting systems are divided in three classes: high vapour systems, gassy reactions, and hybrid systems.
- 3.** Acquisition of the experimental data necessary for vent sizing. The nature of the data required depends on the nature of the reacting system. The data must be obtained under conditions close to adiabatic for a correct simulation of the runaway behaviour.
- 4.** Choice of the vent sizing method and of the two phase flow calculation method, according to the system behaviour.

Generally the limit of venting pressure is about 1.1 times the Maximum Allowable Working Pressure (MAWP) of the vessels for the reactive cases and about 1.2 times this factor for the non-reactive volatile fire exposure cases (Fauske, 2000). Fisher (1992) provides more details.

The original 1985 DIERS Methods and even the Simplified Methods are complex and time consuming because of the complicated equations for each of the reaction systems (Noronha, 1999). Further, no generally accepted procedures were available to estimate venting pressures prior to the DIERS Technology Methods. Most companies had to base their decisions primarily on prevention. The DIERS method is applicable for two phase flow. DIERS Risk Guidelines recommend appropriate additional preventive and protective measures when the venting pressures are high.

2.1.5 Leung's Method

Leung classified venting modes as homogeneous vessel venting, all vapor venting and all liquid venting which are considered under two different energy sources: run away chemical reactions and external heating (Leung, 1986).

2.1.5.1 Homogeneous Vessel Venting with Runaway Reaction

This method (Leung, 1986) is based on the following assumptions: (i) During the over pressure transient, mass flux (G) is almost invariant; (ii) An appropriate average value for the reaction energy per unit mass (q) is considered as constant; (iii) Other properties such as liquid specific heat at constant volume (C_v), latent heat of vaporization (h_{fg}), specific volume (ϑ) are also

considered constant. The relief mass flow rate or vent rate (W) can be calculated from Equation 2.21 in this case.

$$W = GA = \frac{m_o q}{\left[\left(\frac{V}{m_o} \frac{h_{fg}}{\vartheta_{fg}} \right)^{1/2} + (C_v \Delta T)^{1/2} \right]^2}$$

Equation 2.21

Where,

A = Ideal vent area (m^2).

G = Critical mass flux (Kg/m^2 -s).

m_o = Initial instantaneous mass in the vessel (Kg).

q = Energy flow rate (J/ Kg-s).

V = Volume of vessel (m^3).

ϑ_{fg} = Specific volume difference between gas (vapor) phase and liquid phase (m^3/ Kg).

h_{fg} = Latent heat of vaporization (J/ Kg).

C_v = Specific heat at constant volume (J/ cm^3 - K) (Specific heat capacity at constant pressure, C_p (J/Kg- K) can be used instead of C_v as $C_p = C_v$ for incompressible fluid (Leung, 1986)

ΔT = Over temperature (Peak temperature, T_m – Set temperature, T_s) (K).

For no over pressure (that is for $\Delta P = 0$, $\Delta T = 0$), Equation 2.21 turns into a simple equation and is used to calculate for zero over pressure vent area (A_0) (Leung, 1986):

$$A_0 = \frac{m_0 q_s \vartheta_{fg}}{G \vartheta h_{fg}}$$

Equation 2.22

The reaction heat release rate per unit mass (q) can be calculated in a number of ways, some of which are:

- i. $q = q_m$ (at turn around)
- ii. $q = \frac{1}{2} (q_s + q_m)$ (arithmetic average)
- iii. $q = (q_s q_m)^{1/2}$
- iv. $q = (q_m - q_s) / \ln (q_m / q_s)$ (log mean)

Where, q_s is the energy release rate at the set temperature, q_m is the energy release rate at the turnaround temperature, and q is related to the temperature rise rate in a non-vented system according to the following equation (Leung, 1986; Fauske, 1985):

$$q = \frac{1}{2} C_p \left[\left(\frac{dT}{dt} \right)_s + \left(\frac{dT}{dt} \right)_m \right]$$

Equation 2.23

Where, $\left(\frac{dT}{dt} \right)_s$ is the temperature rate at set temperature (K/s) and $\left(\frac{dT}{dt} \right)_m$ is the temperature rate at turnaround temperature (K/s).

2.1.5.2 All Vapor and All Liquid Venting with Runaway Reaction

Both of the venting modes (all vapor venting and all liquid venting) for vessels exhibit complete vapor-liquid phase separation or disengagement, which leads to the similar final equation. Thus, they are discussed together, and the relief vent rate can be implicitly calculated from the following equation (Leung, 1986):

$$T_m - T_s = \frac{m_0 q}{G A C_v} \left(1 - \frac{A}{A_0}\right) + \frac{\vartheta_i h_{fg}}{\vartheta_{fg} C_\vartheta} \ln\left(\frac{A}{A_0}\right)$$

Equation 2.24

Where, ϑ_i (initial specific volume) = ϑ_g (specific volume at gas phase) for all vapour venting, and ϑ_i (initial specific volume) = ϑ_f (specific volume at liquid phase) for all liquid venting.

For no over pressure, Equation 2.24 turns to the following correct limiting form (Leung, 1986):

$$A_0 = \frac{m_0 q_s \vartheta_{fg}}{G \vartheta_f h_{fg}}$$

Equation 2.25

2.1.5.3 Homogeneous Vessel Venting with External Heating

Equation 2.26 is implicit in relief vent area where GA is calculated either by iteration or graphical method (Leung, 1986):

$$T_m - T_s = \frac{Q_T}{G A C_\vartheta} \left[\ln\left(\frac{m_0}{V} \frac{Q_T}{G A} \frac{\vartheta_{fg}}{h_{fg}}\right) - 1 \right] + \frac{V h_{fg}}{m_0 C_0 \vartheta_{fg}}$$

Equation 2.26

Here, Q_T is the total heat input or release rate. For the special case of no over pressure, Equation 2.25 turns to the following limiting form (Leung, 1986):

$$A_0 = \frac{Q_T m_0 \vartheta_{fg}}{G V h_{fg}}$$

Equation 2.27

Equation 2.27 is similar to Equation 2.22 with $Q_T = m_o q$ and $\vartheta = V/m_o$. It is applicable in the case of fire exposure of storage vessels.

2.1.5.4 All Vapor and All Liquid Venting with External Heating

For the all vapor venting case, no overpressure is considered, which will result in the following expression for vent area estimation (Leung, 1986):

$$A_o = \frac{Q_T v_{fg}}{G v_g h_{fg}}$$

Equation 2.28

For all liquid venting, the vent rate is given by the following equation (Leung, 1986):

$$W = GA = \frac{Q_T}{\left[\vartheta_f \frac{h_{fg}}{\vartheta_{fg}} + \frac{C_p \Delta T}{2.303} \right]}$$

Equation 2.29

For no over pressure, Equation 2.29 turns to the following form (Leung, 1986):

$$A_o = \frac{Q_T \vartheta_{fg}}{G \vartheta_f h_{fg}}$$

Equation 2.30

The simplified equation for homogeneous discharge flow (Q) (Leung, 1986) for Leung's method is:

$$G \approx 0.9 \frac{h_{fg}}{v_{fg}} \left(\frac{1}{C_p T} \right)^{0.5} = 0.9 G_L$$

Equation 2.31

Where, G_L = Limiting flow corresponding to ERM model (Kg/m²-s).

Leung's simplified vent sizing equations are preferred over other methods because they are simple, require only relevant physical property and thermal data, and lead to quick but precise vent size predictions. These vent sizing equations are applicable over a wide range of overpressure situation, which can be reduced to the correct limit at no over pressure. Leung's method demonstrates relative merit as it allows for over pressure in various venting modes. Therefore, Leung's method results in smaller vent area (due to mass depletion in the reactor by venting) with realistic approximation.

Leung's methods are only limited to liquid phase systems, not extended to pure gaseous phase and solid phase systems. The two phase quality entering the relief vent can be substantially higher than the expected amount based on homogeneous assumption. This leads to higher volumetric flow and smaller required vent area than that of homogeneous vessel treatment.

2.1.6 Fauske's Method

DIERS low-phi-factor calorimetry methodology provides relevant data to develop equations for relief area calculations. For a realistic and safe design, knowledge of the prevailing flow regime is necessary. DIERS practice is mainly based on "foamy" conditions (i.e., homogeneous vessel situations); thus, overestimating in the safe side. However, Fauske (2000) developed a set of equations for different flow conditions, which are discussed in the subsequent sections.

2.1.6.1 Non Foamy Behavior- Non Reactive System

These equations are developed assuming that all vapors vent, which is consistent with traditional approach. The required vent area (A) is given by the following expressions (Fauske, 2000):

$$\text{For critical flow, } A = \frac{\dot{Q}}{C_D 0.61 (P/\rho_v)^{1/2}}$$

Equation 2.32

$$\text{For highly sub critical flow, } A = \frac{\dot{Q}}{C_D (2\Delta P/\rho_v)^{1/2}}$$

Equation 2.33

Where,

\dot{Q} = Vapor release rate (m^3s^{-1}).

P = Venting pressure (Pa).

ρ_v = Vapor density (Kg m^{-3}).

ΔP = Overpressure relative to the ambient pressure (Pa).

C_D = Appropriate discharge co-efficient (based on the length to diameter ratio of the nozzle).

Experiments were conducted to assess the accuracy of the prediction by Equation 2.32 and Equation 2.33 (Fauske, 2000). The estimated vent area for atmospheric water is in good agreement with real data and the estimated relief area for propane is a bit bigger than the actual one (Fauske, 2000).

2.1.6.2 Foamy behavior - non reactive system

A very high void fraction regime ($\alpha > 0.99$) enters the vent line that leads to a larger vent area and reduces the potentiality of BLEVE (boiling liquid expanding vapor explosion). Replacing ρ_v in Equation 2.32 with $\rho_l (1-\alpha) + \rho_g \alpha$ gives a higher value of vent area for critical flow conditions of foamy behavior of non-reactive system. For the highly sub critical flow condition, ρ_v in Equation 2.33 is replaced with $\rho_l (1-\alpha) + \rho_g \alpha$ to get the relief vent area for foamy condition of non-reactive system (Fauske, 2000).

2.1.6.3 Reactive system-Hybrid

A hybrid system is a reactive system where both gas production and vapor production occur simultaneously. Here, the total pressure is equal to the sum of the gas partial pressure and the vapor pressure. The rate of temperature rise and the rate of pressure rise are needed to determine the proper vent size for a specified venting pressure.

Considering gas-vapor venting, the vent area to volume ratio is calculated from the following equations (Fauske, 2000):

$$\text{For critical flow, } \frac{A}{V} = \frac{1}{0.61 C_D} \left[\frac{\rho c \dot{T}}{\lambda P} \left(\frac{R \dot{T}}{M_{\omega, g}} \right)^{1/2} + \frac{\rho \vartheta \dot{P}}{m_t P} \left(\frac{M_{\omega, g}}{RT} \right)^{1/2} \right]$$

Equation 2.34

$$\text{For highly sub critical flow, } \frac{A}{V} = \frac{1}{C_D} \left[\frac{\rho c \dot{T}}{\lambda P} \left(\frac{R \dot{T}}{M_{\omega, g}} \right)^{1/2} + \frac{\rho \vartheta \dot{P}}{m_t P} \left(\frac{M_{\omega, g}}{RT} \right)^{1/2} \right] \left[\frac{1}{2 \left(1 - \frac{P_b}{P} \right)} \right]^{1/2}$$

Equation 2.35

Where,

$A/V =$ Vent area to volume ratio (m^{-1}).

$\rho =$ Loading density (kg m^{-3}).

$c =$ Liquid specific heat ($\text{JKg}^{-1}\text{K}^{-1}$).

$T =$ Temperature (K).

$\lambda =$ Latent heat of vaporization (JKg^{-1}).

$R =$ Gas constant ($8314 \text{ Pa}\cdot\text{m}^3/\text{K}\cdot\text{Kg mole}$).

$\dot{T} =$ Self heat rate (Ks^{-1}).

$\dot{P} =$ Maximum rate of pressure rise (Pas^{-1}).

$M_{w,v} =$ Vapor molecular weight (Kg-Kmol).

$M_{w,g} =$ Gas molecular weight (Kg-Kmol).

$\vartheta =$ Test freeboard volume (m^3).

$m_t =$ Test sample mass (Kg).

$P_b =$ Back pressure (Pa).

2.1.6.4 Reactive System-Vapor

In a vapor system, the reaction is entirely tempered by the latent heat of vaporization. This results in lowest practical relief set pressure, which leads to smallest relief area requirement. The principal parameter determining the vent area is the rate of temperature rise at the relief set pressure. The necessary equations (Fauske, 2000) are:

$$\text{For critical flow, } \frac{A}{V} = \frac{1}{0.61 C_D} \frac{\rho c \dot{T}}{\lambda P} \left(\frac{RT}{M_{\omega, g}} \right)^{1/2}$$

Equation 2.36

$$\text{For highly sub critical flow, } \frac{A}{V} = \frac{1}{C_D} \frac{\rho c \dot{T}}{\lambda P} \left(\frac{RT}{2 \left(1 - \frac{P}{P^*} \right) M_{\omega, g}} \right)^{1/2}$$

Equation 2.37

2.1.6.5 Reactive System-Gassy

In gassy reactive system, the total pressure is equal to the non-condensable gas pressure. The principal parameter for determining the vent area is the maximum rate of pressure rise. Fauske (2000) provides more details on this topic. The vent area is estimated using Equation 2.38.

$$\frac{A}{V} = \frac{1}{0.61 C_D} \frac{\rho \vartheta \dot{P}}{m_t P} \left(\frac{M_{\omega, g}}{RT} \right)^{1/2}$$

Equation 2.38

DIERS calorimetry methodology data, which can be scaled directly to full size application, is the basis of this method. It is a simple and relatively economical approach to relief system sizing. Fauske (2000) showed that this method is capable of producing good agreement with a large number of large scale venting tests.

2.1.7 Fauske's Short Form Equation

The design of the venting area for a liquid-gas flow is more critical than that for gas flow. Understanding a flow regime, which can be categorized as bubbly and/or foamy, churn turbulent, or droplet flows helps to determine whether the venting flow will be gas or liquid-gas. It is not possible to generalize and differentiate between disengaged and homogenous behavior for even simple systems. The degree of bubbly and/or foamy behavior is highly dependent on the system properties. Assuming the two phase mixture entering the relief line as well mixed and homogeneous, Fauske's short form of equation is valid for most of the cases. This leads to a good approximation of the vent area. Based on these assumptions, the simple expression for the vent area (Fauske, 1984 a) is:

$$A = V\rho (TC)^{-1/2} \frac{q_s}{\Delta P}$$

Equation 2.39

Fauske's simple form of equation can also be expressed as follows (Leung, 1986):

$$A = \frac{m_o}{\Delta P} \left(\frac{C_p}{T_s} \right)^{1/2} \left(\frac{dT}{dt} \right)_s$$

Equation 2.40

Where,

V = Volume of the vessel (m^3).

q_s = Heat release rate J/ Kg-s.

m_o = Initial instantaneous mass in the vessel (Kg).

ΔP = Over pressure (Pa).

C_p = Specific heat at constant pressure (J/Kg- K).

T_s = Set temperature (K).

$\left(\frac{dT}{dt}\right)_s$ = The temperature rate at set temperature (K/s).

Fauske's design method is for overpressure in the range of 10 to 30% (Fauske, 1984 a). It predicts a vent size area up to 2 times larger than that predicted by a detailed integral analysis assuming homogeneous vessel behavior and homogeneous equilibrium flashing flow (Fauske, 1984 a). Thus, the short form equation is capable of estimating a safe but conservative vent area.

2.1.8 Monogram Method

The generalized vent sizing monogram (Fauske, 1984 b) is based on Fauske's guidelines (Fauske, 1984 b). For a given self heat rate and set pressure, the chart provides a vent sizing envelope for both runaway chemical reactions, including gassy reactions and for uncontrolled heating or without chemical reactions. The monogram is based on the Equation 2.39, which assumes that flow in the vent line is homogeneous and turbulent. This method is intended for use where there is a modest overpressure over 10-30% (e.g. 20%).

The main advantage of this method is that it only requires knowledge of the adiabatic self heat rate corresponding to tempered reactions (where the system pressure is equal to the component vapor pressure) at the specific set pressure of the relief device. No other thermo kinetic and physical property information is required.

This monogram is valid, as long as these are tempered at the specific relief set pressure and the turbulent flow regime prevails in the vent line (Fauske, 1984 b). For a frictionless vent line, Equation 2.39 predicts a vent area larger by a factor of less than 2 compared to integral model,

assuming homogeneous vessel behaviour and homogeneous liquid flow. Thus, it is also capable of estimating a safe but not a conservative vent area.

2.1.9 Fauske's Screening Equation for Reactive System

Fauske (2000) developed a screening equation to characterize a hybrid system by considering the thermal and physical properties of water from the detailed equation (Equation 2.34). This equation is further modified using data from an open test performed in ARSST, as shown in Equation 2.41 (Burelbach, 2001).

$$\frac{A}{V} = \frac{3.5 \times 10^{-3} (\dot{T} + \dot{P})}{C_D P \left[1 + \frac{1.98 \times 10^{-3}}{P^{1.75}} \right]^{0.286}}$$

Equation 2.41

Here,

P = Venting pressure (Psia)

\dot{P} = Maximum pressure rate (Psi/min)

\dot{T} = Temperature rate at set point (°C/min)

For characterizing a vapor system, the pressure rate term (\dot{P}) is omitted and for a gassy system, the temperature rate term (\dot{T}) is omitted in Equation 2.41 (Burelbach, 2001).

While characterizing for a vapor system for a closed test VSP 2 test, the same screening equation as for an open test ARSST test can be used. But for characterization of a gassy or hybrid system for a closed test VSP 2 test, the \dot{P} term in Equation 2.41 is multiplied by a factor of $\left(\frac{120-v}{350} \times \frac{10}{m} \right)$; where, v = volume of the sample in the closed test cell of VSP 2 (mL) and m = mass of sample (gm) (Burelbach, 2001).

2.2 Evaluation of Different Methodologies

The FIA method is the simplest, quickest method for calculating vent area, and it provides an initial idea about the required vent size. However, it is limited by numerous assumptions, and it does not consider the thermo physical properties of the element. These factors may lead to oversized vent size. Boyle's method is also quick and simple, yet it is prone to overestimation. And Boyle's method described here is only limited to the polymerization reactors. Thus, among the quick and easy methods, Fauske's short form equation and monograph method has a better applicability and ability to provide better vent size designs. API 520 methods are applicable in the places where the properties of the elements are well known and the conditions satisfy the initial assumption.

Leung's method has the advantage of being simple to calculate and it considers two phase flow. Recently developed Fauske's detailed method is capable of providing accurate results for different conditions. However, it requires exact properties of the elements and flow regime.

As the detailed physical and chemical properties of the chemicals are unknown, Leung's method (both for reactive and non-reactive system), Fauske's detailed method for non reactive system, Fauske's short form of equation and Fauske's screening equation based on Fauske's detailed method would be implemented in this present work to evaluate the vent sizing design consideration for the oil field chemicals.

2.3 Oil Field Chemicals

Oil stream fluids being a mixture of liquid hydrocarbon, gaseous hydrocarbon and associated water, are transported from the reservoir through the processing system (Kelland, 2009). Oil field chemicals are used to overcome or minimize the effects of the production chemistry problems. As the number of crude oil sources is decreasing day by day, more sophisticated methods for exploitation of oil sources is becoming significant, which leads to escalated oil field chemicals uses (Fink, 2003). It is predicted that the global demand of oilfield chemicals will grow 5.7% annually through 2012 (Freedonia Group, 2008). There are several types of oil field chemicals such as scale inhibitors, corrosion inhibitors, wax inhibitors, cement additives, antifreeze agents, surfactants, drilling fluids, hydrate inhibitors, enhanced oil recovery (EOR) fluids, etc. (Fink, 2003). Among these, corrosion inhibitors and hydrogen sulfide scavengers are some of the most widely used in oil field industries (Vargas, 2009 b). The current study will be limited to these two types of oil field chemicals.

2.3.1 Corrosion Inhibitors

Corrosion inhibitors are used to inhibit corrosion caused by CO₂, chlorides, and H₂S throughout production, transportation and refining (Kelland, 2009; Fink, 2003). Corrosion inhibitors can be broadly categorized as: passive (anodic), cathodic, vapor phase or volatile, and film forming (Palme et al., 2004; Sastri, 1998; Rosenfeld, 1977). Among these, film forming corrosion inhibitors are mainly used for production of oil, condensate and gas production lines (Kelland, 2009).

Most of the films forming corrosion inhibitors have a polar head group and hydrophobic tail, where the polar head group is attracted to the metal surface and the hydrophobic tail is attracted

to liquid hydrocarbons forming an oily film which prevents the metal surface from corrosion (Kelland, 2009) as shown in

Figure 2.1.

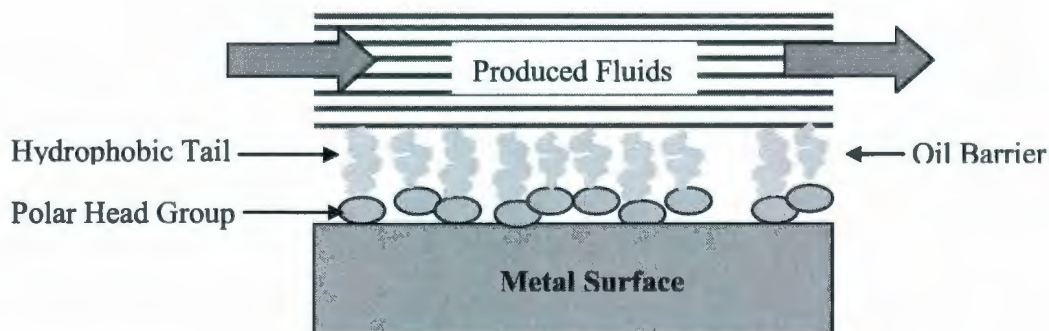


Figure 2.1 : Mechanism of Corrosion Inhibitor Protection [Source: (Kelland, 2009)]

Corrosion inhibitors can be amides & imidazolines, nitrogenous bases with carboxylic acids, nitrogen quaternaries, nitrogen heterocyclic, carbonyl compounds, phosphate esters, silicate based and polyxylated amines, amides & imidazolines, etc. or a blend of these compounds (Fink, 2003).

2.3.2 Hydrogen Sulfide Scavenger

A hydrogen sulfide scavenger can be broadly classified as regenerative (such as monoethanolamine, diethanolamine, N-methyldiethanolamine, diglycolamine etc.) and non-regenerative (such as aldehydes, amines, triazines, metal carboxylates and chelates etc.) (Kelland, 2009). For the present work a hydrogen sulfide scavenger sample, which is a mixture

of formaldehyde and monoethanolamine is used. While an amine based H₂S scavenger is applied, generally the nitrogen in the aromatic chain of the scavenger is replaced by the sulfur presented in the H₂S and the sulfur is removed from the process fluid (Vargas, 2010). Formaldehydes mainly forms 1, 2, 3 – trithane, a nonregenerative ring compound, with the presence of H₂S, as shown in Figure 2.2 (Kelland, 2009).

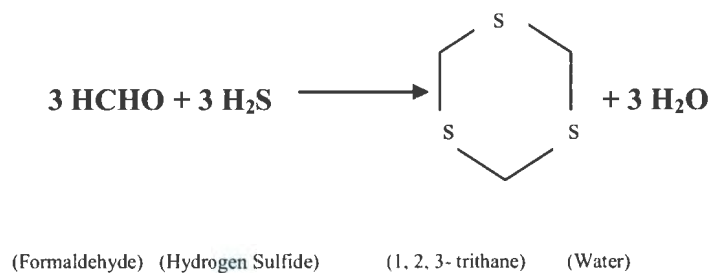


Figure 2.2 : Reaction of Formaldehyde with H₂S [Source: (Kelland, 2009)]

3 EXPERIMENTAL METHODOLOGY

3.1 Equipment

3.1.1 Advanced Reactive System Screening Tool (ARSST)

The Advanced Reactive System Screening Tool (ARSST) is a calorimeter to characterize chemical behaviour and acquire relief-system design data in a relatively fast and economic fashion (compared to other calorimeters such as ARC and VSP). The ARSST provides energy and gas release rates, which are directly applicable to full scale process conditions, and it yields temperature and pressure rise rates data, as well. The ARSST is said to be as user friendly as a DSC (Differential Scanning Calorimeter) with the benefit of having data accuracy similar to Vent Size Design Package (VSP) (Fisher et al., 1992). The ARSST has a broad range of scan rate (0-30 °C/min), an onset detection sensitivity as low as 0.1 °C/min in a heat-wait search mode, and capability to distinguish between foamy and non foamy behaviour with a flow regime detector (Burelbach & Theis, 2005).

The 10 ml open spherical glass test cell has a low phi factor or thermal inertia ranging from 1.03 to 1.06 (i.e. quite adiabatic considering that a perfectly adiabatic system has a phi factor of 1.00). The test cell is situated in a 350 cm³ stainless steel containment vessel for an experimental operation. The containment vessel holds 3000 psig pressure while the Hastelloy rupture disk can hold only 900 psig pressure. An external bottom heater is belted to the test cell directly, which provides effective heating. The sample in the test cell is heated for characterization in a pressurized vessel. Generally, open test cell tests are performed where the sample is charged in the test cell before installing it in the containment vessel. However, an external fill tube can also

be used to charge the sample, or to add reagents before or during a test. During the experiment, the pressure rise and pressure rate are measured by a 500 psig pressure transducer. A type K thermocouple is inserted in the test cell to continuously monitor the sample temperature. A type K thermocouple is chromel–alumel based general purpose thermocouple with a sensitivity of approximately $41 \mu\text{V}/^\circ\text{C}$. To provide a good mixing during the experiment, a magnetic stir bar, driven by an external magnetic stirrer, is placed in the test cell. A control box having heating power, a pressure amplifier, and temperature amplifier is used to continuously monitor and control pressure and temperature. The containment vessel and the magnetic stirrer along with the connection wires are kept in the fume hood for safety purposes. The detailed description of the basic experimental procedure for using ARSST is explained in Appendix 1. The key features of the instrument are illustrated in Figure 3.1 and Figure 3.2.

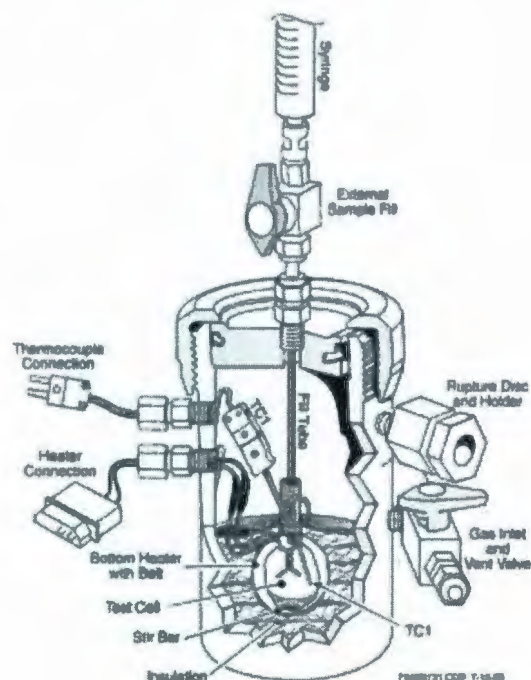


Figure 3.1 : Key features of ARSST [Source: (Burelbach & Theis, 2005)]

(©Fauske & Associates, Inc.)



Figure 3.2: Advanced Reactive System Screening Tool (ARSST)

3.1.2 Vent Sizing Package 2 (VSP2)

The VSP2 (Vent Sizing Package 2) calorimeter is an original DIERS Bench Scale Apparatus for characterizing runaway reactions and was introduced in 1985 (Askonas, Burelbach, & Leung, 2000). It has the benefit of having light test cell with a phi factor (ϕ) close to unity. Hence, it is capable of providing a nearly true adiabatic environment. The VSP2 allows continuous and automatic tracking of pressure and adiabatic temperature which makes it a useful tool for measuring temperature and pressure rise rates for thermal analysis and for vent sizing applications.

The basic principle behind VSP2 is well described by Askonas, Burelbach & Leung (2000). The test cell is situated in a 4 liter pressure vessel. The low ϕ factor test cell typically weights 35

grams and has a diameter of two inches with a capacity of 116 ml. It can be made of 304 or 316 stainless steel, Titanium, or Hastelloy C-276 (a Nickel-Molybdenum-Chromium alloy having the addition of Tungsten and has an excellent corrosion resistance). The test cell contains a magnetic stir bar, which is either Teflon™ coated or glass encapsulated. The apparatus measures four parameters: sample temperature (T1), sample pressure (P1), external temperature (T2), and containment vessel pressure (P2). To heat the sample to the temperature where runaway reaction occurs, the test cell is enclosed by test cell heater (also called main heater or auxiliary heater). The main heater assembly (surrounded by insulation) is enclosed by a guard heater. To provide an adiabatic condition at runaway temperature, the main heater is turned off and the guard heater is regulated to keep the temperature (T2) equal to the sample temperature (T1). For the closed test cell, the containment vessel pressure (P2) is also regulated to keep the pressure difference between test cell and containment vessel between 20-40 psig. This pressure balance allows having low mass test cells in the system. However, for open or vented test cells, it is not necessary to control the pressure as pressure equalization is done through the vent. The instrument has a rupture disk to combat with accidental situations. The detailed description of the basic experimental procedure of VSP2 use is explained and illustrated in Appendix 2. The key features of the instrument are illustrated in Figure 3.3 and Figure 3.4.

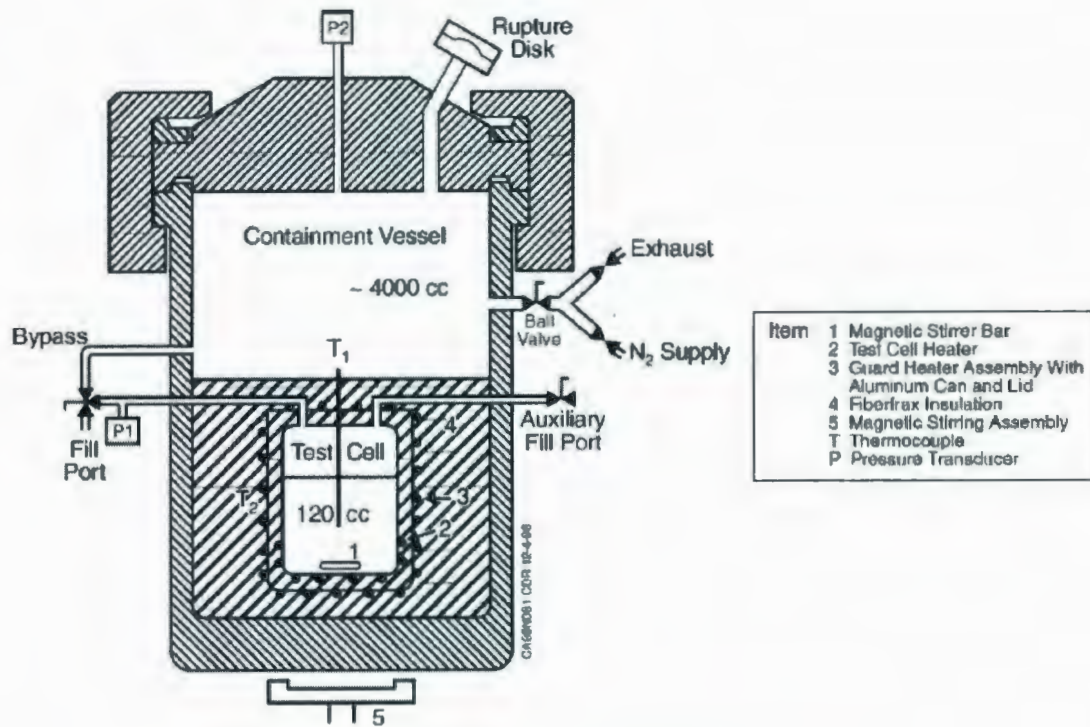


Figure 3.3 : Key Features of VSP2 Calorimeter
 [Source: (Askonas, Burelbach, & Leung, 2000)]

(©Fauske & Associates, Inc.)



Figure 3.4: Vent Sizing Package 2 (VSP 2)

3.1.3 DSC

The Differential Scanning Calorimeter (DSC) is a thermal analysis instrument that determines the temperature and heat flow associated with material transitions as a function of time and temperature. DSC is classified into two types based on the mechanism of operation: (i) Heat flux DSC (a single furnace is used to heat sample and the reference pan) and (ii) Power Compensated DSC (two separate furnaces are used to heat sample and reference pan) (Hohne, Heminger, & Flammersheim, 2003).

A DSC consists of 3 basic units: (i) Furnace, (ii) Cooling system, and (iii) Computer. During the test, the sample material enclosed in a pan and an empty reference pan are heated at a linear heating rate under controlled conditions.

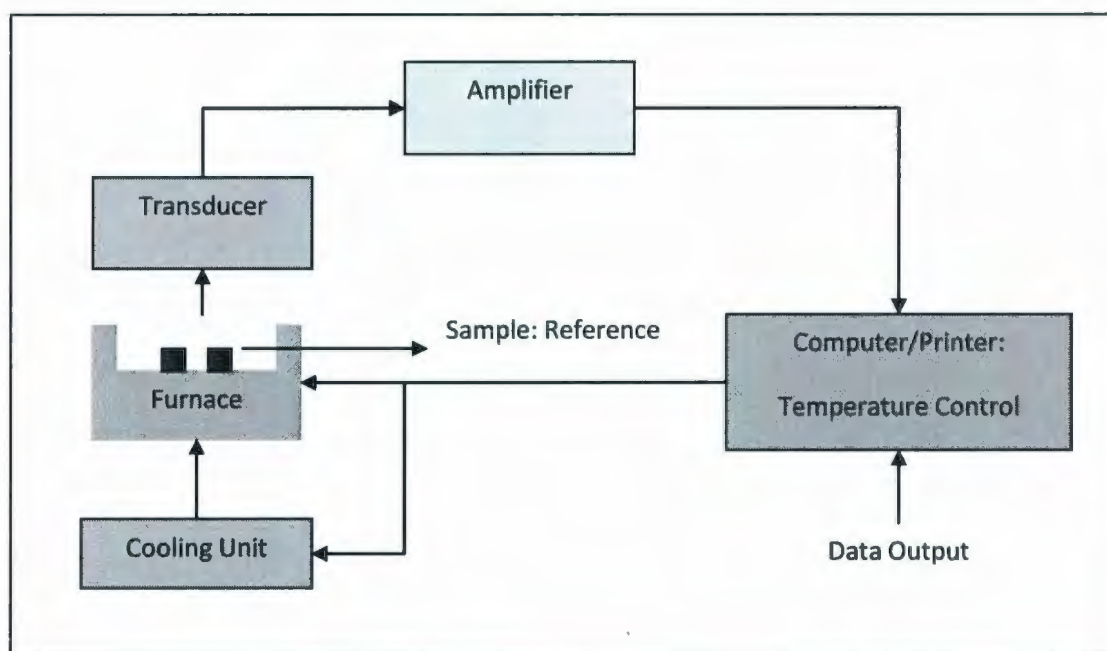


Figure 3.5 : Schematic Diagram of DSC [Source: (Vargas, 2009 a)]



Figure 3.6: METTLER TOLEDO DSC 1

When any material is heated or cooled, changes in the physical or chemical state generally result in a change of energy level (exothermic or endothermic). As a result, a heat flow occurs between the sample and the reference pan. The transducer (thermocouple) generates a voltage on the basis of this heat flow. This voltage is then amplified and stored in the computer for subsequent analysis.

Heat flux DSC is the most popular type and it has the advantages of improved baseline flatness due to the large mass furnace, higher sensitivity, and cell durability. For the experimental purpose, DSC 1 from METTLER TOLEDO having FRS5 sensor (made of ceramic) was used with 400 W power amplifier, GC200 gas controller, and Julabo FT100 intracooler (METTLER TOLEDO, 2007). The instrument can be operated from -80°C to 625°C . Industrial grade Nitrogen dried by Drierite (CaSO_4) was used as purge gas.

3.2 Materials

3.2.1 25% DTBP (Di-tert-butylperoxide) in Toluene

Thermal decomposition of di-tert-butyl peroxide (DTBP) in toluene is one of the most widely studied kinetic systems (Mannan, Aldeeb, & Rogers, 2002). It is used to calibrate the VSP2 and ARSST as the behaviour of this sample is already standardized by these two calorimeters. 25% DTBP is used for calibration mainly for three reasons: its first order kinetic behaviour, the importance of DTBP applications in process chemistry, and the number of fire and explosion incidents involving DTBP decomposition (Mannan et al., 2002).

Toluene is a colorless water insoluble liquid, which is widely used as an industrial solvent. It is an aromatic hydrocarbon and is considered hazardous by the OSHA Hazard Communication Standard. Toluene is a flammable liquid having a molecular weight of 92.15 g/mole, boiling point of 110.4 °C, and relative density of 0.867 (EMD Chemicals Inc, 2009 b).

Di-tert-butyl peroxide or DTBP is an organic compound consisting of a peroxide group flanked by two tert-butyl groups, it decomposes with or without the presence of air, and it generates a fuel source. DTBP is a clear liquid having a molecular weight of 146.23 g/mole, boiling point of 109-110 °C, and density of 0.794 g/cm³ (Sigma-Aldrich Canada, 2009).

3.2.2 Corrosion inhibitors

3.2.2.1 NOX RUST 1100

“Nox Rust 1100 VCI Liquid” is a petroleum oil based volatile corrosion inhibitor (VCI) produced by DAUBERT VCI, INC. It is used in ferrous and other metals in enclosed systems such as storage tanks, fuel tanks, hydraulic and coolant circulating systems, and transmissions. According to the manufacturer, Nox Rust 1100 inhibits corrosion and provides lubrication. When it is applied to any enclosed system, it is drained away from the metal surfaces in about six months. But the vapor evolving from the inhibitor will spread throughout the void of the system and inhibit the corrosion caused by moisture in the air and as well as protect the metal below the oil level (KPR ADCOR Inc, 2009).

Nox Rust 1100 is a light golden oil having a viscosity of 210 cps, specific gravity of 0.89, boiling point greater than 149°C, and flash point of 121°C (KPR ADCOR Inc, 2009). Being petroleum oil based, Nox Rust 1100 is highly susceptible to fire exposure and can produce different hazardous decomposition products such as carbon monoxide, carbon dioxide, oxides of sulfur and miscellaneous hydrocarbons.

3.2.2.2 NOX RUST 9800

“Nox Rust 9800 VCI Liquid” is a water soluble volatile corrosion inhibitor (VCI) produced by DAUBERT VCI, INC. This liquid corrosion inhibitor has a proprietary protected VCI formula. It is applied by fogging or spraying to inhibit corrosion and oxidation on ferrous and non-ferrous metals used in the enclosed spaces such as piping systems, tanks, turbines, and heating and cooling systems. When it comes in direct contact to metal surfaces, usually the volatile

component is attracted to the charged metal surfaces creating a molecular barrier against the oxidizing component. In this way, a complex shaped system or surface having hidden voids could be protected (KPR ADCOR Inc, 2003).

Nox Rust 9800 is a clear to hazy amber liquid having a density about 0.974 g/cm^3 , specific gravity of 0.97, and flash point of 80°C (KPR ADCOR Inc, 2003). Having 86% volatile components by volume, it is highly susceptible to fire exposure and can produce different hazardous decomposition products such as carbon monoxide, carbon dioxide, and miscellaneous hydrocarbons while introduced to fire.

3.2.2.3 VCI Powder

“VCI Powder-1” is a white crystalline powder that has a special water soluble proprietary formulation of volatile corrosion inhibitors (VCI) produced by KPR ADCOR INC. It can be applied either in a dry or a solution form. It can inhibit corrosion of ferrous and aluminium metals caused by adverse environmental condition such as high heat, humidity, seawater, or other oxidizing environments. It can be soluble up to 15% at room temperature (22°C) and the melting point is 198°C (KPR ADCOR Inc, 2007). It may be explosive in the presence of a source of ignition if mixed with air in critical proportion. It may produce carbon monoxide, carbon dioxide, and oxides of nitrogen while subjected to thermal decomposition or combustion.

3.2.2.4 *BRENNTAG Corrosion Inhibitor*

Brenntag Corrosion Inhibitor is a toxic mixture of aromatic hydrocarbons, oxygenated aliphatic hydrocarbons, and amine compounds. A major component (30-60%) of this corrosion inhibitor is Naphtha. The detailed composition and the inhibition mechanism of the product cannot be disclosed due to proprietary issues. The boiling point is greater than 82°C and the density is 0.90-0.92 g/cm³ (Brenntag Canada Inc, 2009).

3.2.3 *H₂S Scavenger Components*

3.2.3.1 *Formaldehyde Solution*

It is a proprietary product by Brenntag Canada Inc. It contains 37% formaldehyde and 12-15% methanol and the rest of the constituents are not disclosed. It has a boiling range of 90-100°C and density of 1.09 g/cm³ (Brenntag Canada Inc, 2007).

3.2.3.2 *Monoethanolamine Solution*

The exact composition of this product is property protected, yet the major component is monoethanolamine. The density of the solution is 1.01 g/cm³ at 25°C and the boiling range is 168-172°C (Brenntag Canada Inc, 2008).

3.2.4 Acetone

Acetone is a relatively low cost, volatile solvent that does not form any low boiling temperature azeotropic mixture with water. Hence, it is a common solvent for cleaning and rinsing laboratory glassware. For similar reasons, acetone is also used as a drying agent.

Acetone being an organic compound is a colorless, mobile, and flammable liquid. The molecular weight of acetone is 58.09 g/mol, relative density is 0.791, and the boiling point is 56.1°C (EMD Chemicals Inc, 2009 a). Acetone is believed to exhibit only slight toxicity in normal use, and there is no strong evidence of chronic health effects if basic precautions are followed.

3.3 Procedure

3.3.1 Advanced Reactive System Calorimeter (ARSST)

There are seven basic modes of operation in the ARSST software (Fauske and Associates Inc., 2007 a). The thermal scan method using a saved calibration that is the Single Ramp- Polynomial control mode is recommended while testing unknown samples, and it is the method used to conduct this work. The thermal scan method is also known as the Conventional RSST method, and it can be performed in two ways: calibrating in situ (directly on the sample) and by utilizing a saved calibration. While performing the test using saved polynomial, the heater power is supplied according to Equation 3.1 (Fauske and Associates Inc., 2007 a).

$$W = A + BT + CT^2$$

Equation 3.1

Where, W is the heater power (Watts), T is the temperature ($^{\circ}\text{C}$), and A, B, C are the polynomial coefficients obtained from a previous calibration test.

Thermal scan mode operation was used for all the samples as their properties are unknown due to the proprietary protection. Other modes of operation are not explained here as they are available in Fauske's user manual (Fauske and Associates Inc., 2007 a). The parameters used for the corrosion inhibitors (Nox Rust 1100, Nox Rust 9800, Brenntag and VCI 1 Powder) tests in the ARSST are listed below:

- Ramp Polynomial for initial gas pressure 300 Psig
A = 2.131E-01
B = 2.642E-02
C = 5.133E-05
- Ramp Polynomial for initial gas pressure of 15 Psig
A = 4.753E-01
B = 2.066E-02
C = 4.805E-05
- Auto Shutoff criteria
Temperature: 300 $^{\circ}\text{C}$
Pressure: 400 psig
Time: 500 minutes (8 hours 20 minutes)
- Data Logging Interval (min): 2
Data Logging Interval ($^{\circ}\text{C}$): 2
Data Logging Interval (psi): 2
- Magnetic Stirrer frequency: 400 rpm

Formaldehyde, monoethanolamine and H_2S scavenger mix were tested by Vargas (2010) using the same parameters listed above.

3.3.2 Vent Sizing Package 2 (VSP 2)

There are three modes of operation of VSP2 (based on operation of main heater): (i) Delta T mode, (ii) Constant Power mode, (iii) Constant Rate mode (Fauske and Associates Inc, 2002). VSP2 also has an Auto Heat Wait Search Function.

In constant power mode, heater power is maintained at a constant value. This mode was used for this work because it is the recommended mode for unknown sample behavior. Other modes of operation are explained in Fauske's user manual (Fauske and Associates Inc, 2002). The initial constant (low) power is 40% for all the corrosion inhibitors, as there is no sharp exotherm observed for the samples while tested in the ARSST. The H₂S scavenger test was carried out through two different sub tests: the first one is carried out during mixing monoethanolamine with formaldehyde without any application of external heat to determine the heat of mixing; the second one is carried out after the cooling down of the first sub test by a constant power mode with a 20% heating rate. The data logging interval is 3 (min, °C, psig) to avoid noisy data.

3.3.3 Differential Scanning Calorimeter (DSC)

Specific heat capacity measurements were conducted using the DSC by following the ASTM standard test method, E 1269-05 (ASTM, 2005). There are four basic steps for measuring heat capacity using DSC: (i) Sample preparation, (ii) Basic calibration, (iii) Heat capacity calibration and (iv) Experimental run.

3.3.3.1 Sample Preparation

Hermetic pans with sealed covers are capable for conducting studies of volatile liquids including specific heat, materials those sublime, aqueous solutions above 100°C, materials generating corrosive or condensable gases, and materials in self-generating atmospheres (TA Instruments, 2002). Aluminium hermetic pans by TA instruments with a temperature range of -180 °C to 600 °C are used for conducting this experimental work. These pans are unable to hold high pressure after a phase change and a significant mass loss is observed at a higher temperature. As opposed to the high pressure pan by TA, the hermetic pans match the pan requirements of METTLER TOLEDO. For this reason, the TA hermetic pans are used for the Cp tests as METTLER pans were not available at the time of the current test. The specific heat capacity measurement of the samples is conducted in a range from 25 °C to the boiling point of each sample. The mass of the sample is kept between 5mg to 8mg for better measurement and a sample encapsulation press is used to seal the pans.



Figure 3.7: Aluminium Hermetic Pan.

3.3.3.2 Basic Calibration

As recommended by the manufacturer, three major calibrations are performed for a METTLER TOLEDO DSC: (i) Temperature, (ii) Heat Flow, and (iii) Tau Lag. The Tau lag calibration is performed to achieve independency of temperature on the heating rate and was done by a fully automatic total calibration using Indium and Zinc. The calibrations for heat flow and temperature are done using Indium following the manufacturer recommended method (METTLER TOLEDO, 2007).

3.3.3.3 Specific Heat Calibration

The specific heat calibration consists of two steps: (i) Blank Run, and (ii) Sapphire Run.

(i) Blank Run:

The blank run procedure is described as follows:

- i. The DSC is purged with dried nitrogen gas at a flow rate of 50 mL/ min.
- ii. A clean empty aluminium hermetic pan (considered as reference pan) with lead is weighed and sealed.
- iii. Another clean empty aluminium hermetic pan (considered as sample pan) with lead is weighed and sealed.
- iv. The sample pan and the reference pan are properly placed on the sensor of the DSC.
- v. The DSC test chamber is heated or cooled to the initial temperature, 25°C.
- vi. The DSC chamber is held at the initial temperature for 4 min to establish equilibrium.

- vii. The furnace is heated from the initial temperature to the final temperature, 200°C, at a heating rate of 10°C/ min.
- viii. The DSC chamber is held at the final temperature for 4 min to establish equilibrium.
- ix. A steady state isothermal baseline at the upper temperature limit is recorded.
- x. After this period the thermal curve is terminated and the DSC test chamber is cooled to the ambient temperature.

(ii) Sapphire Run:

The procedure and parameters for the Sapphire run is the same as that for the blank run except a sample pan having a Sapphire disk is used instead of an empty sample pan. The weight of the Sapphire disk is 22.5 mg. It is necessary to check the weight of the Sapphire disk before and after the experiment to make sure that no weight loss has occurred.

3.3.3.4 Experimental Run

The same procedure as the blank run for the specific heat capacity calibration was used for experimental runs. Instead of having an empty sample pan, 5 to 8 mg of sample were used. The final temperature for heating up was chosen lower or equal to the boiling point (for liquid samples) or melting point (for solid sample). The sample weight prior and after the experiment has to be measured. If the sample mass loss is greater than or equal to 0.3%, the measurement is invalid (ASTM, 2005).

The specific heat capacity at different temperatures is calculated from the heat flow vs. temperature plots of blank, sapphire and experimental runs. The specific heat capacity calculation and results are described in Chapter 4.

3.4 Software for Data Processing

3.4.1 Reduce

Reduce software is developed by Fauske & Associates, LLC. This software package is used to process the raw data generated by the VSP2 and ARSST. It reduces raw data by calculating temperature and pressure rates (Fauske and Associates Inc, 2007 b). The features used to process the data from this work are as follows:

- (i) Smoothing the rate data by calculating the least square slope corresponding to an odd number of smooth over, and then assigning this slope to the central point of group of data points. 9 point smoothing is used for the data reduction for this work.
- (ii) Performing onset of time values in the case of starting a new test before an experiment of interest is conducted.
- (iii) Performing pad gas correction while the test is not started with a complete vacuum in the cell. Ideal gas law is used to estimate the pad pressure contribution at other temperatures.
- (iv) Reduction of temperature data and pressure data in case of tests performed in the VSP2.

Reduce software is capable of generating five output files: (i) <testname>.reduced (which has reduced data in tabular ASCII format), (ii) <testname>.xys (which is a XYPlot 2 script file that is used by XYPlot2 to automatically generate plots), (iii) <testname>.xls (which is reduced data in Microsoft Excel format), (iv) <raw ARSST data file>.d (which is only created when the raw data file contains non-US standard format numbers), and (v) <testname>.gcl (which is a MultiPlot script file that is used by MultiPlot to generate plots) (Fauske and Associates Inc, 2007 b).

The Excel output file is used for plotting and calculations. For more details, it is recommended to read the Reduce software user's manual (Fauske and Associates Inc, 2007 b).

4 HEAT CAPACITY CALCULATION

This chapter presents the result and analysis of the C_p measurements conducted on METTLER TOLEDO DSC 1 as per ASTM standard test method, E 1269-05 as presented in Section 3.3.3 of the experimental methodology chapter.

Figure 4.1 is a typical plot showing the heat flow as function of temperature for the blank run, sapphire run and sample run. From this plot, D_{st} which is the vertical distance between the blank run and sapphire run and D_s which is the vertical distance between the blank run and sample run are determined.

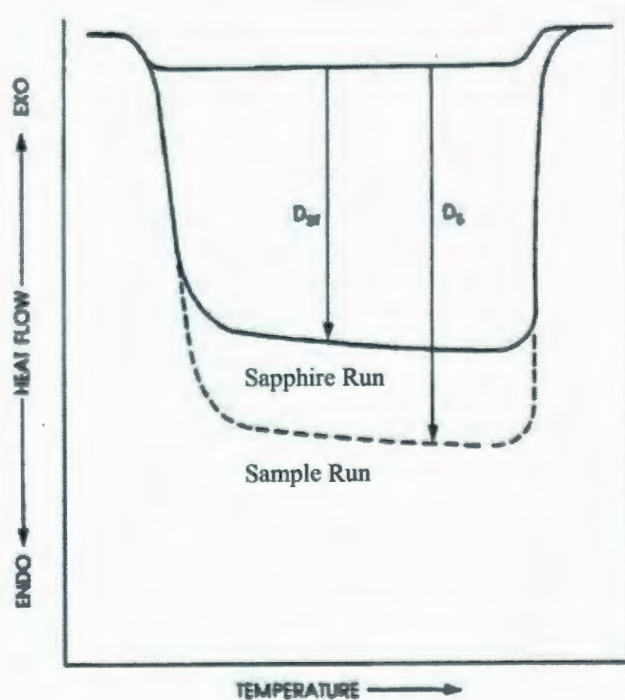


Figure 4.1: Specific heat capacity thermal curves [Source: (ASTM, 2005)]

The specific heat capacities of the samples at different temperatures are calculated according to Equation 4.1 and Equation 4.2 (ASTM, 2005):

$$E = \left[\frac{b}{(60 \times D_{st})} \right] [W_{st} \times C_p(st) + \Delta W \times C_p(c)]$$

Equation 4.1

Where,

b = Heating rate

D_{st} = Vertical distance between the thermal plots of blank run and sapphire run at a given temperature, mW

$C_p(st)$ = Specific heat capacity of Sapphire, J/ g- K

$C_p(c)$ = Specific heat capacity of specimen holder (which in this case is Aluminium), J/ g- K

W_{st} = Mass of Sapphire disk, mg

ΔW = Difference between the mass of the specimen holders used for blank run and Sapphire run, mg

Specific heat capacity of the sample (J/ kg- K):

$$C_p(s) = \left(\frac{60 \times E \times D_s}{W_s \times b} - \frac{\Delta W \times C_p(c)}{W_s} \right) \times 1000$$

Equation 4.2

Where,

D_s = Vertical distance between the thermal plots of blank run and experimental run at a given temperature, mW

W_s = Mass of sample, mg

ΔW = Difference between the mass of the specimen holders for blank run and experimental run, mg

The weight of the samples is ranged between 5 to 8 mg and the measurements were carried out from room temperature prior to the boiling point (for liquid) or melting point (for solid) of the samples. To validate the measurement, the weight loss of the samples after experimental run should be less than 0.3% (ASTM, 2005). The experimental runs for specific heat capacity measurements are valid as the results have good agreement and the weight loss of the samples after experiment are less than 0.3% as shown in Table 4-1. However, due to high amount of mass loss during the testing of VCI Powder, this sample was also tested at Fauske's Laboratory and the results are presented in the Section 4.1.4

Table 4-1: Weight Loss of the Samples during Test

| Name of Chemicals | Temperature Range (°C) | Weight of Sample (mg) | Mass Loss (%) |
|--------------------------|-------------------------------|------------------------------|----------------------|
| Nox Rust 1100 | 30 - 180 | 5.35±0.18 | 0.15±0.04 |
| Nox Rust 9800 | 30 - 90 | 6.22±0.02 | 0.25±0.04 |
| Brenntag | 30 - 80 | 5.72±0.31 | 0.03±0.01 |
| VCI 1 Powder | 30 - 180 | 5.36±0.33 | 0.36±0.05 |
| Formaldehyde | 30 - 90 | 7.35±0.16 | 0.23±0.06 |
| Monoethanolamine | 30 - 160 | 6.33±0.03 | 0.29±0.02 |

The specific heat capacity of the samples as a function of temperature plots is presented in Section 4.1 and Section 4.2. The tabulated values for the specific heat capacities and the heat flow vs. temperature plots are given in Appendix 3. The results of the studied samples indicate that the specific heat capacity of the samples increases with temperature. The database of "HSC Chemistry Chemical Reaction and Equilibrium Software – Version 5.1" was also utilized to find

out the specific heat capacity of the sample constituents in literature to compare with the experimentally determined values. The specific heat capacity values were not available for many of the constituents.

As some of the vents sizing methods require specific heat capacity values, the specific heat capacity measurements at higher temperature are very important. These values are utilized in Chapter 5 and Chapter 6 to characterize the emergency relief system for the studied chemicals.

4.1 Corrosion Inhibitors

4.1.1 Nox Rust 1100

The three main constituents of Nox Rust 1100 are petroleum oil, octanoic acid and morpholine (KPR ADCOR Inc, 2009). Among these, the specific heat capacity of morpholine is only found in the database of HSC Chemistry Software which is presented in Appendix 3. However, it is believed that the specific heat capacity of Nox Rust 1100 depends on the specific heat capacity of petroleum oil (KPR ADCOR Inc, 2009; Ergon Refining Inc, 2003) as it is the major component (more than 85%). The petroleum oil of Nox Rust 1100 is of severely hydro treated type which is obtained by treating a petroleum fraction with hydrogen in the presence of a catalyst (KPR ADCOR Inc, 2009; Ergon Refining Inc, 2003). Petroleum oil is a complex mixture of hydrocarbons in the range of C₁₅ through C₃₀ (Ergon Refining Inc, 2003; Environment Canada, 2008). Hence, the specific heat capacity of petroleum oil is not easy to obtain from literature (Ergon Refining Inc, 2003; Environment Canada, 2008).

The values from two experimental runs for Nox Rust 1100 have good agreement as shown in Figure 4.2. The specific heat capacity value increases from 2073.45J/ kg- K at 30 °C to 3086.16 J/ kg- K at 180 °C.

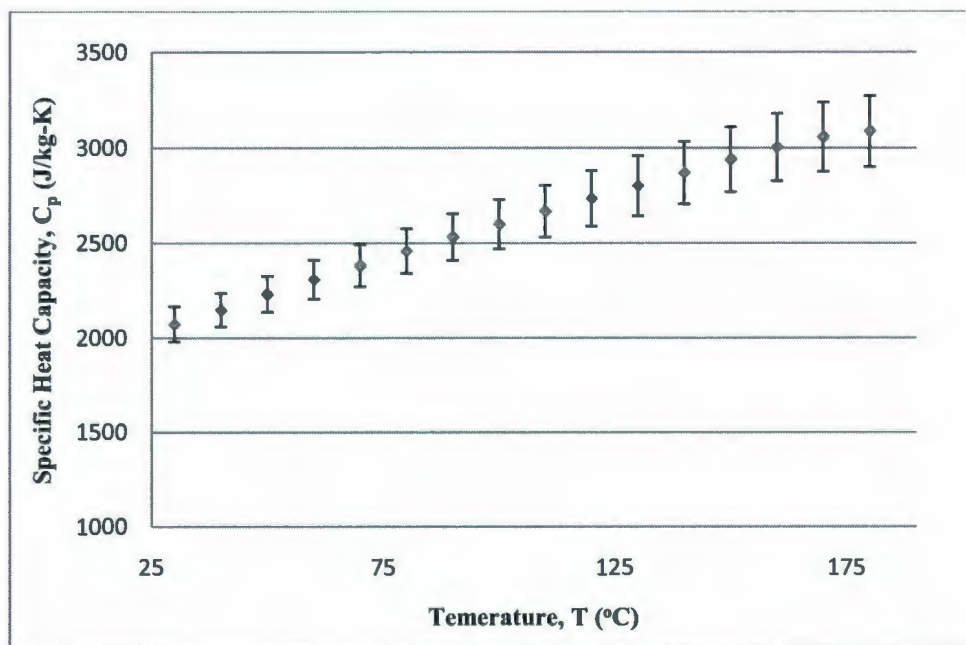


Figure 4.2: Specific Heat Capacity Vs Temperature for Nox Rust 1100

4.1.2 Nox Rust 9800

Nox Rust 9800 mainly consists of dipropylene glycol methyl ether (DPGME), dimethyl amino ethanol and phosphoric acid (KPR ADCOR Inc, 2003). Specific heat capacity values for dimethyl amino ethanol and phosphoric acid are well obtained from the database of HSC Chemistry and are illustrated in Appendix 3. But the specific heat capacity value of Nox Rust 9800 is expected to be governed by the specific heat capacity value of DPGME as it comprises more than 80% of the blend (KPR ADCOR Inc, 2003). DPGME is by itself a complex mixture of four isomers: methyldipropylene glycol; oxybispropanol, methyl ether; bis-(2-methoxypropyl)

ether (OECD/SIDS, 2001). Specific heat capacity value for DPGME is not observed in the database of HSC Chemistry Software. Though screening information data sets (SIDS) for DPGME were generated by Organisation for Economic Co-Operation (OECD), no specific heat capacity measurements were cited by them as well (OECD/SIDS, 2001).

From the Figure 4.3, it is seen that the values for two experimental runs have good agreement. With an increase in temperature from 30 °C to 90 °C, the specific heat capacity value increases from 2456.07 J/ kg- K to 2915.92 J/ kg- K.

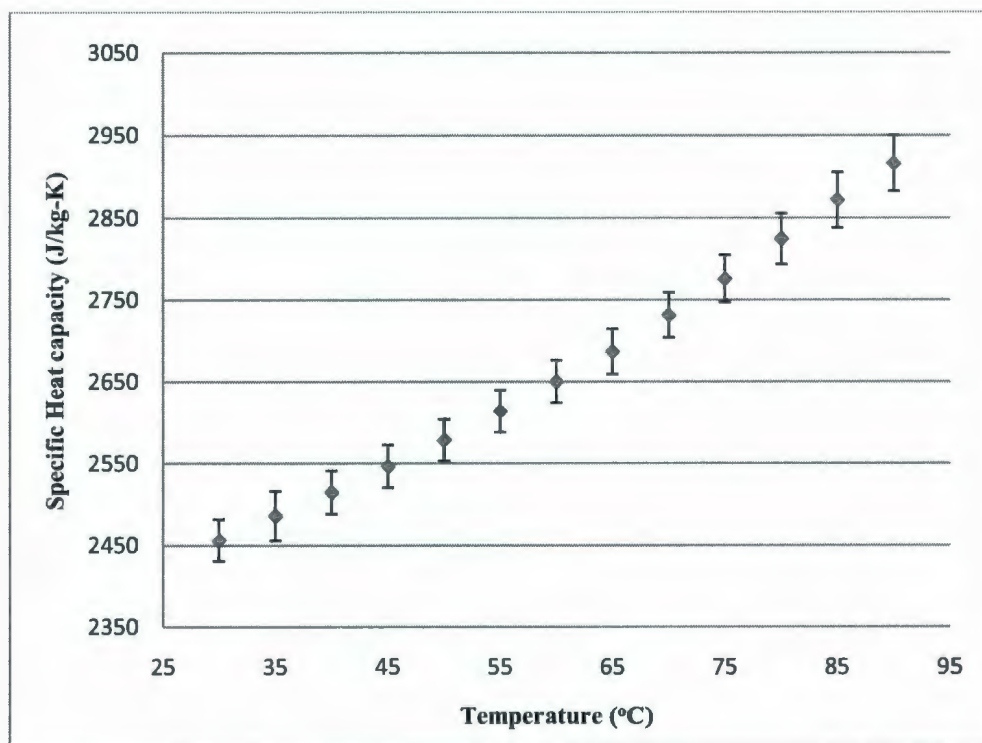


Figure 4.3: Specific Heat Capacity Vs Temperature for Nox Rust 9800

4.1.3 Brenntag Corrosion Inhibitor

Brenntag corrosion inhibitor is a proprietary protected complex mixture of different petroleum distilled components. One of the major components of this corrosion inhibitor is naphtha and other components are not disclosed due to proprietary protection (Brenntag Canada Inc, 2009). Naphtha is a highly volatile mixture of hydrocarbons and the proportion of the constituents can vary depending on source of Naphtha (Environment Canada, 2008). As a result, specific heat capacity of this particular naphtha mixture cannot be adopted from literature values.

The experimental runs are observed to have good repeatability as shown in Figure 4.4. The specific heat capacity value is observed to be increasing from 1998.69 J/ kg- K to 2296.71 J/ kg- K with the increase in temperature from 30 °C to 80 °C.

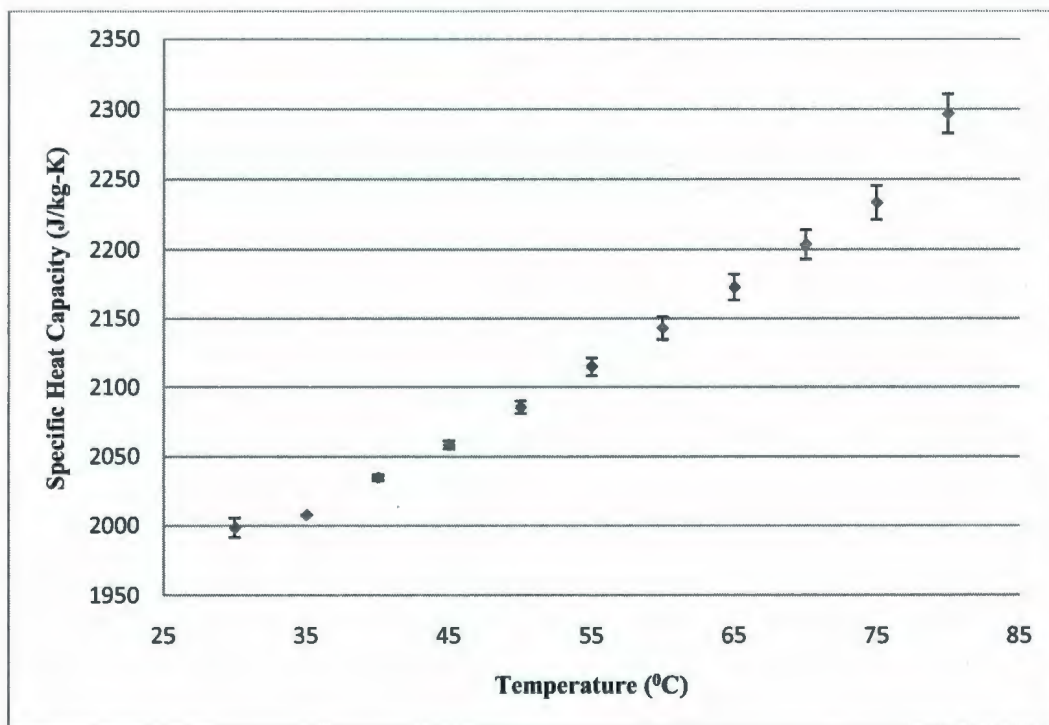


Figure 4.4: Specific Heat Capacity Vs Temperature for Brenntag Corrosion Inhibitor

4.1.4 VCI 1 Powder

VCI 1 powder is a completely proprietary protected formulation by KPR Adcor Inc (2007). Any indication about the chemical composition is not given in the MSDS of the product (KPR ADCOR Inc, 2007). The results from the two experimental runs are not in agreement with each other as shown in Figure 4.5. The mass losses for the experimental runs are also found to be higher, though the highest temperature is kept below the melting point. The specific heat capacity values for VCI 1 powder vary from 950.85 J/ kg- K (at 30 °C) to 1875.50 J/ kg- K (at 180 °C)..

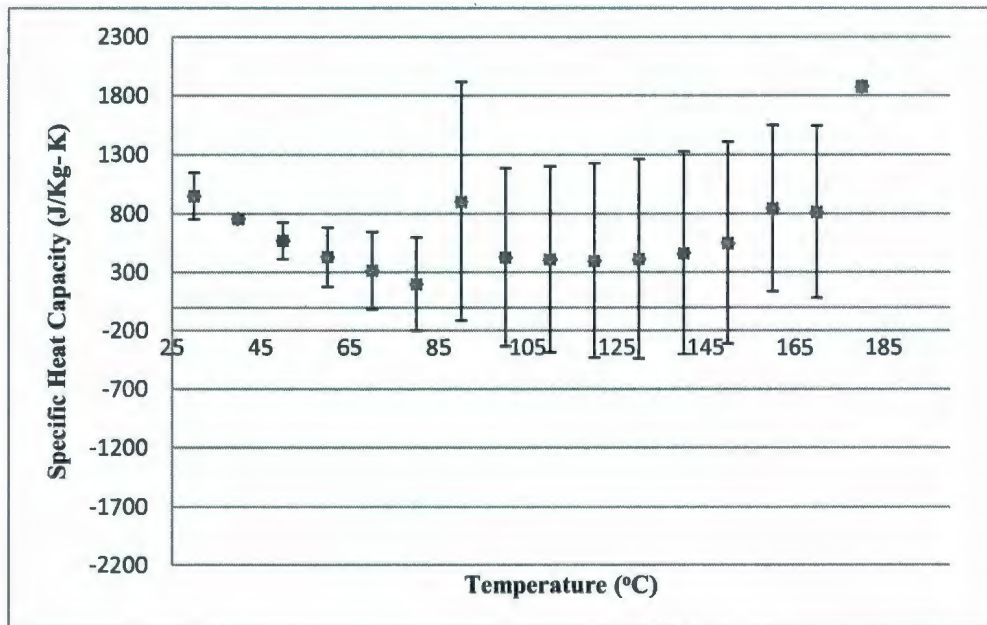


Figure 4.5: Specific Heat Capacity Vs Temperature for VCI 1 Powder

To obtain better Cp data, the VCI was later tested at Fauske Laboratory. The heat flow as a function of temperature is shown in Figure 4.6, and the calculated specific heat capacity value is 3489.96 J/ kg- K at 156 °C. The experimental run carried out in Fauske's Laboratory used 0.88 mg sample with 3 °C /min heating rate. This value is almost three times the value obtained using

the DSC at the C-Cart (Memorial University). The reason for this difference may be due to the uneven heat flow through the solid sample and as well as the high volatile nature of the sample. The aluminium hermetic pan that was used for experimental run (conducted at Memorial University) was not able to hold the high pressure evolved from the VCI decomposition, which leads to higher amount of mass loss. Higher than acceptable mass loss was also observed for the run conducted in Fauske's laboratory, though the test was carried out with high pressure pan. The specific heat capacity value determined by Fauske will be used for subsequent calculation. High pressure pans are recommended to be used in future experiments.

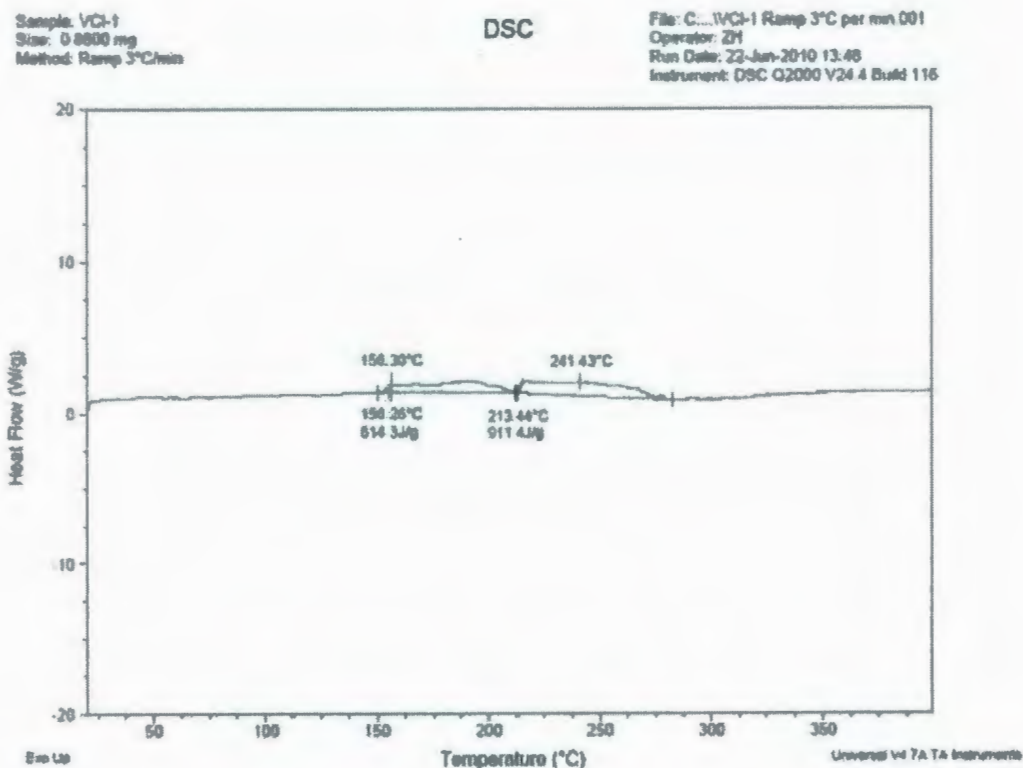


Figure 4.6: Heat Flow Vs Temperature Plot for VCI 1 Powder (Fauske's Laboratory)

4.2 H₂S Scavenger Components

4.2.1 Formaldehyde

The specific heat capacity value for this 37% Formaldehyde is observed to increase from 3105.80 J/ kg- K to 3645.73 J/ kg- K with the increase in temperature from 30 °C to 180 °C as shown in Figure 4.7. The manufacturer provided specific heat capacity value at room temperature is 3121 J/ kg- K (Brenntag Canada Inc, 2007; Vargas, 2010) which shows a good concurrence with experimentally determined value.

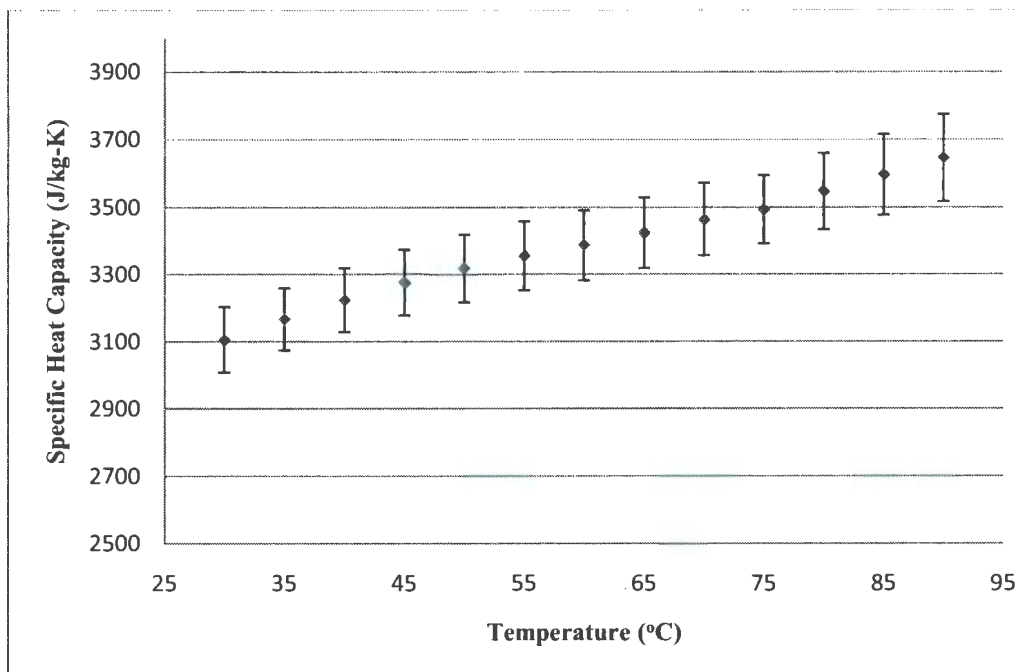


Figure 4.7: Specific Heat Capacity Vs Temperature for Formaldehyde

4.2.2 Monoethanolamine

The percentage of Monoethanolamine in the sample used may vary from 60 to 100% (Brenntag Canada Inc, 2008). The specific heat capacity changes significantly with the amount of Monoethanolamine present in the mixture (INEOS LLC, 2001). For 50% monoethanolamine, the specific heat capacity changes from 3480 J/ kg- K (at 20 °C) to 4130 J/ kg- K (at 120 °C) and for 100% monoethanolamine, the specific heat capacity changes from 2300 J/ kg- K (at 20 °C) to 2830 J/ kg- K (at 120 °C) (INEOS LLC, 2001). For the monoethanolamine used, the experimentally determined specific heat capacity values vary from 2867.70 J/ kg- K (at 30 °C) to 3281.47J/ kg- K (at 160 °C) as shown in Figure 4.8. Literature and experimental values of specific heat capacity of the Monoethanolamine are depicted in Figure 4.9 for the temperature range of 20 °C to 120 °C. From Figure 4.9, it can be inferred that the amount of Monoethanolamine in the sample studied in this work is within the range of 75% to 85%.

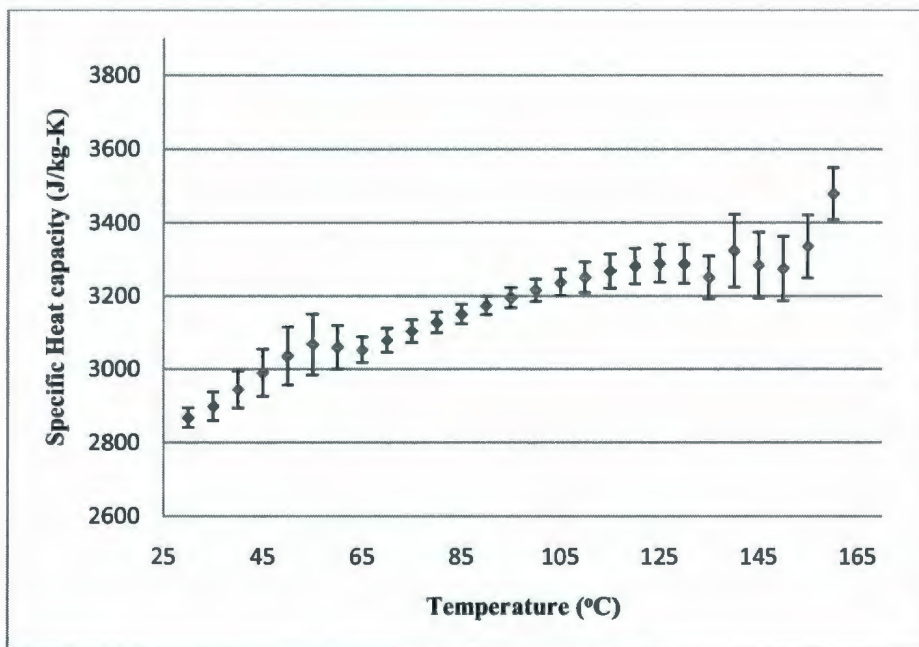


Figure 4.8: Specific Heat Capacity Vs Temperature for Monoethanolamine

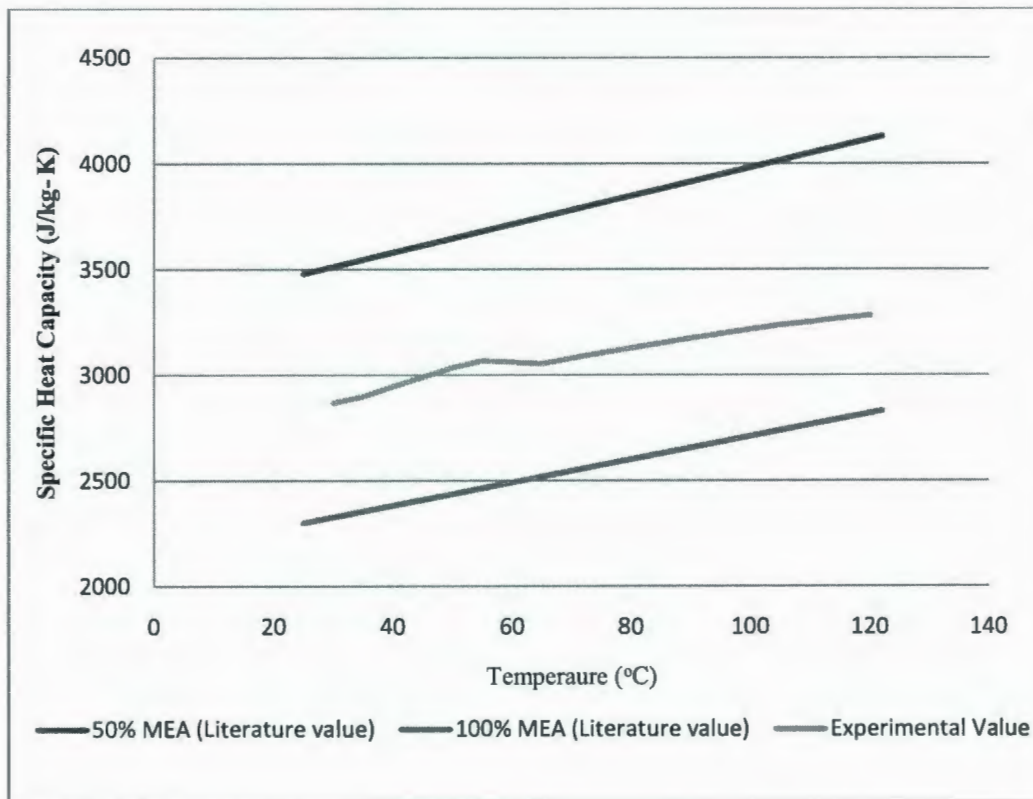


Figure 4.9: Specific Heat Capacity Values as a Function of Temperature for Literature and Experimental Value

5 VENT SIZING: OIL FIELD CORROSION INHIBITORS

This chapter represents the data analysis and vent sizing calculations for three liquid corrosion inhibitor samples (Brenntag, Nox Rust 1100, and Nox Rust 9800) and one solid corrosion inhibitor sample (VCI 1 powder) as described in Section 3.3.1 and Section 3.3.2. Experiments were conducted with the ARSST first, which helps to screen the reactivity of the system. Then the samples were tested with the VSP2 for having detailed thermal-pressure behavior of the systems. Mass loss of less than 5% was found when the corrosion inhibitor samples were tested in the VSP2 in closed test cells, but a higher amount of mass loss was observed while testing the samples in open test cells in the ARSST. The vent sizing calculations for the systems are done by using Leung's and Fauske's methods, which are earlier described in Sections 2.1.5, 2.1.6, and 2.1.9.

5.1 Brenntag Corrosion Inhibitor

5.1.1 ARSST Data

Two tests were carried out at 300 Psig pad gas pressure and two tests were carried out at 15 Psig pad gas pressure in the ARSST with 10 ml sample in open test cells. Figure 5.1 and Figure 5.2 depict the pressure and temperature history respectively for test 1. The pressure and temperature history for the second test are included in Appendix 4. The cut off temperature, pressure, and time are 300 °C, 400 Psig, and 500 minutes, respectively for Brenntag corrosion inhibitor, as described in Section 3.3.1. Though there is an increase in temperature due to the constant external heating, no sudden temperature rise (exotherm) or pressure rise is observed. From the

observation, it can be said that Brenntag corrosion inhibitor is a non-reactive chemical. ARSST is a screening tool for reactive systems (vapor, gassy, and hybrid) and is not an analytical tool. So, it is not unexpected to observe variations in the test data.

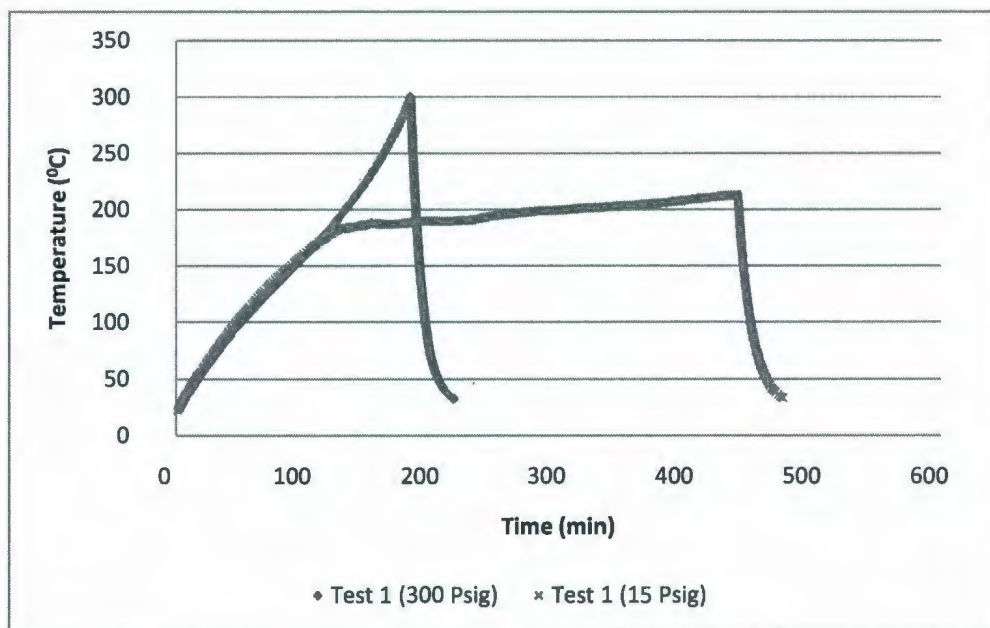


Figure 5.1: Temperature History for Brenntag Corrosion Inhibitor (ARSST Tests)

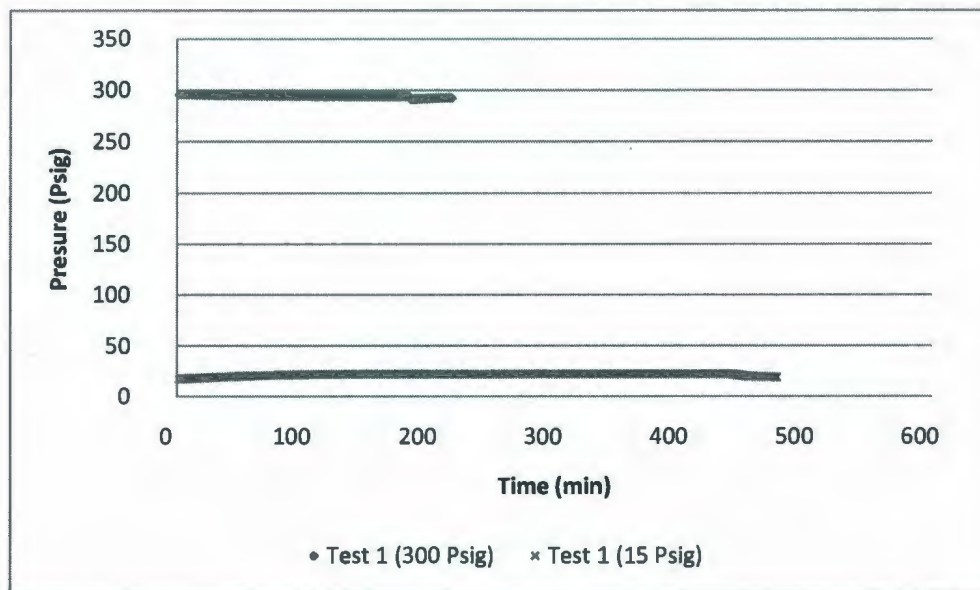


Figure 5.2: Pressure History for Brenntag Corrosion Inhibitor (ARSST Tests)

The mass loss during the open cell tests performed in the ARSST is found to be significant as shown in Table 5.1. Thus, in the event that a Brenntag storage container is exposed to external heating, a release system is required to discharge the mass loss. Vent sizing is necessary for the system in case of external heating, though it is non-reactive. Hence, a VSP test was conducted to design the vent size.

Table 5-1: Mass Loss of Brenntag Corrosion Inhibitor for ARSST Tests

| | Initial Mass (g) | Final Mass (g) | Average Mass Loss (%) |
|-----------------------------------|-------------------------|-----------------------|------------------------------|
| 300 Psig Pad Pressure Test | 8.97±0.10 | 6.81±0.10 | 24.06±1.95 |
| 15 Psig Pad Pressure Test | 8.71±0.11 | 5.53±0.18 | 37.25±1.24 |

Mass loss as a function of time is depicted in Figure 5.3. It is evident from the plot that mass loss does not vary with the time for the each set of tests carried out in 300 Psig and 15 Psig pad gas pressure. But, the mass loss for 15 Psig pad gas pressure test is higher than that for 300 Psig pad gas pressure tests. It is because higher pad gas pressure provides higher barrier to vaporize the sample.

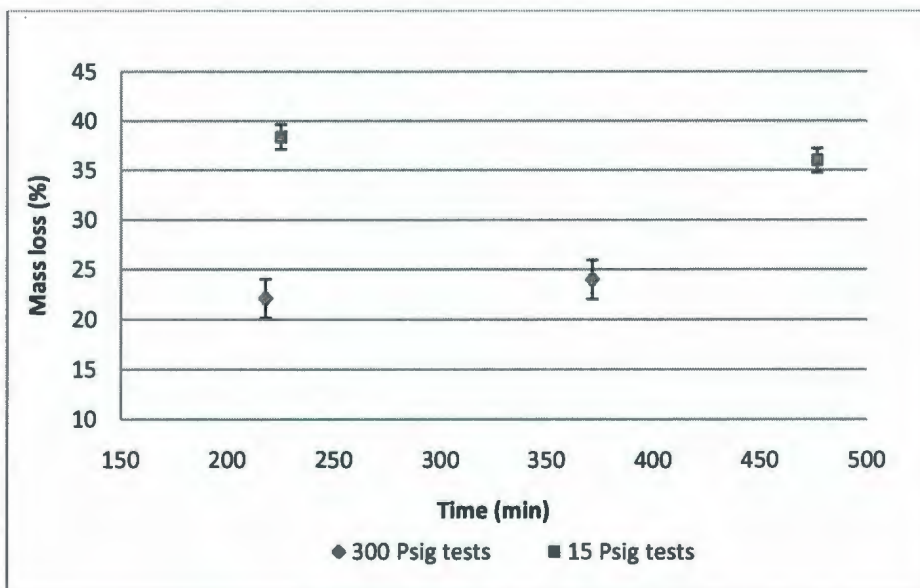


Figure 5.3: Mass Loss as a Function of Time for Brenntag Corrosion Inhibitor (ARSST Tests)

5.1.2 VSP2 Data

One closed cell VSP2 test was performed with 80 ml Brenntag corrosion inhibitor sample. As mentioned earlier, VSP2 tests are very expensive to conduct and, for this sample, the amount of sample provided by the manufacturer was also inadequate to perform multiple tests. The sample was heated up to 300 °C and then the test was turned off as the pressure rose as high as 500 Psig. The pressure and temperature profile of the test are depicted in Figure 5.5 and Figure 5.6.

From Figure 5.4, it is seen that there is no increase in self heat rate due to closed cell VSP2 testing. That means no exotherm occurred during the heating, which is in agreement with the ARSST behaviour. Figure 5.7 depicts the behaviour of pressure as function of temperature (1/T), which shows that the end initial pressure is equal to the initial pressure. No decomposition product or gas is observed to evolve during the testing. This is strengthening the conclusion from the ARSST tests that the system is non-reactive.

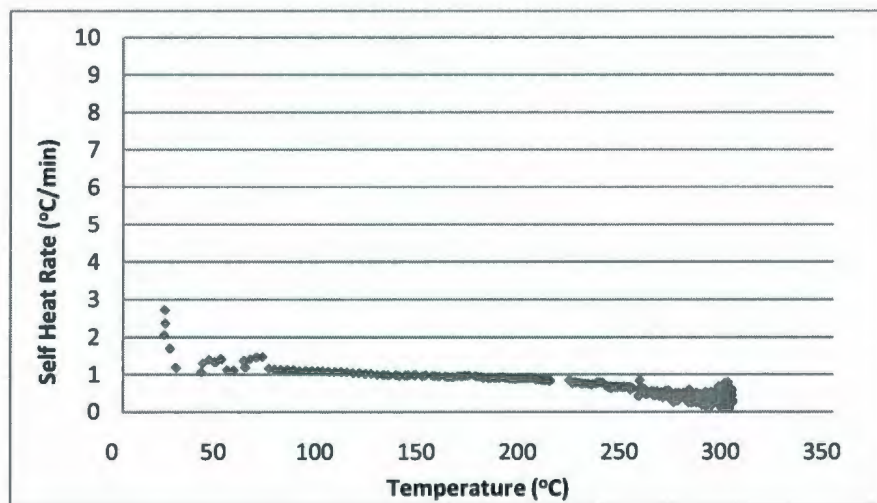


Figure 5.4: Self Heat Rate as a Function of Temperature for Brenntag Corrosion Inhibitor (VSP2 Test)

The parameters that are necessary for vent sizing calculation are described in the subsequent sections.

5.1.2.1 Phi factor (ϕ) calculation:

The phi factor of the test cell is calculated according to Equation 2.1 (Chapter 2). The vent sizing design is considered at a higher temperature than room temperature. Thus, specific heat capacity value of the sample determined at its boiling point, given in Chapter 0, is considered for calculation purposes.

Here,

Mass of the Brenntag sample, $m_s = 7.16 \times 10^{-2}$ kg

Specific heat capacity of the Brenntag corrosion sample at 80°C, $C_{ps} = 2.30 \times 10^3$ J/ kg-K (From Section 4.1.3)

Mass of the test cell, $m_b = 38.71$ g = 3.87×10^{-2} kg

Specific heat capacity of the stainless steel test cell, $C_{pb} = 510$ J/ kg-K

Hence, the phi factor of the test cell is calculated as follows,

$$\phi = 1 + \frac{m_b C_{pb}}{m_s C_{ps}} = 1 + \frac{3.87 \times 10^{-2} \times 510}{7.16 \times 10^{-2} \times 2.30 \times 10^3} = 1.12$$

5.1.2.2 Temperature rate (\dot{T}) calculation:

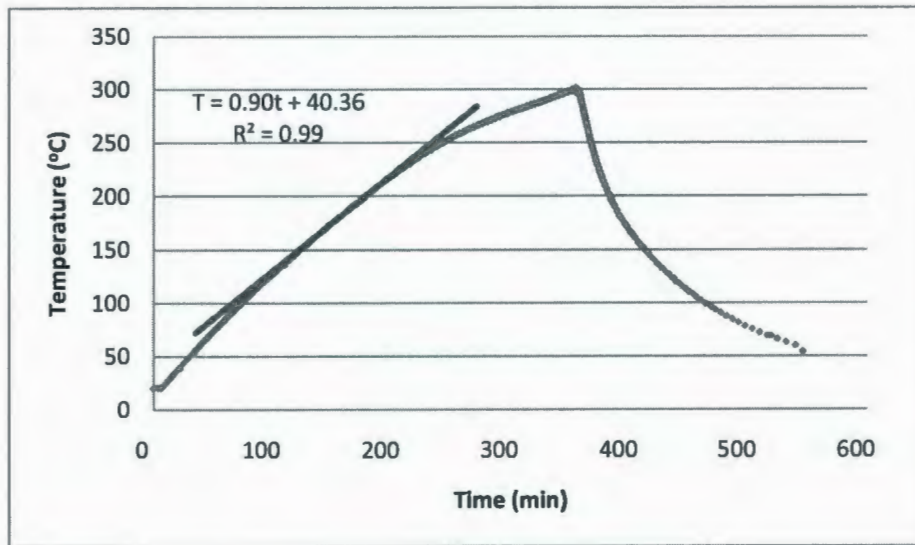


Figure 5.5: Temperature History for Brenntag Corrosion Inhibitor (VSP2 Test)

The slope of the temperature history plot shown in Figure 5.5 is used to calculate the temperature rate.

Hence, temperature rate, $\dot{T} = 0.90 \text{ }^\circ\text{C}/\text{min} = 1.5 \times 10^{-2} \text{ K/s}$

5.1.2.3 Calculation of heat release rate (q):

Leung (1986) developed a method to calculate heat release rate at set pressure and temperature for non-reactive systems, which is shown in Equation 5.1.

$$q = \phi C_p \dot{T}$$

Equation 5.1

Based on the data obtained for Brenntag, the heat release rate,

$$\begin{aligned} q &= 1.12 \times (2.30 \times 10^3 \text{ J/kg} \cdot \text{K}) \times (1.5 \times 10^{-2} \text{ K/s}) \\ &= 38.64 \text{ J/Kg} \cdot \text{s} \end{aligned}$$

5.1.2.4 Set pressure (P_s), set temperature (T_s) and $\frac{dP}{dT}$:

The set pressure or venting pressure at which the relief device is known to be opened is considered as 100 Psig. The pressure history (Figure 5.6) shows that the pressure rise increases rapidly after 100 Psig.

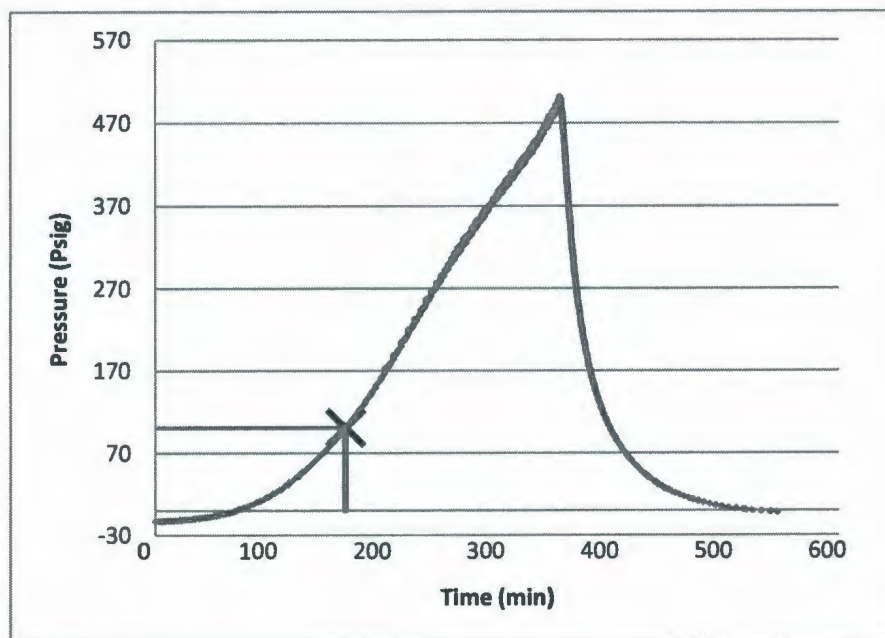


Figure 5.6: Pressure History for Brenntag Corrosion Inhibitor (VSP2 Test)

The pressure behavior as a function of temperature (Figure 5.7) is used to develop an equation to calculate the temperature at the set point that corresponds to the venting pressure. The steepest slope of the plot is used to calculate the set temperature, which will help to provide a more

conservative area to volume ratio. Equation 5.2 shows the relation between temperature and pressure.

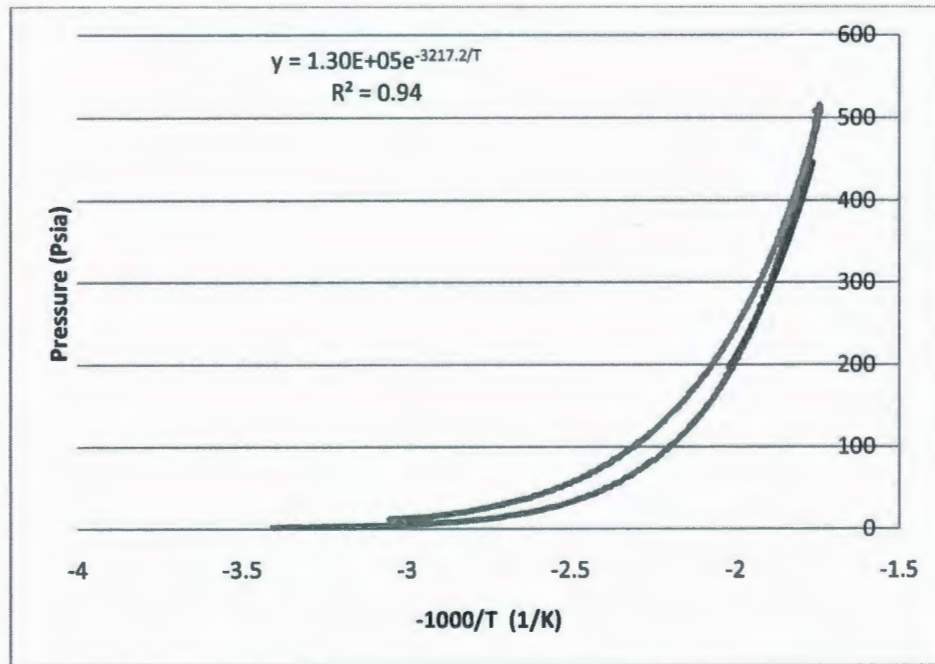


Figure 5.7: Pressure as a Function of Temperature for Brenntag Corrosion Inhibitor (VSP2 Test)

From Figure 5.7,

$$\ln P = \ln(1.30 \times 10^5) - \frac{3217.2}{T}$$

$$\text{So, } \ln P = 11.78 - \frac{3217.2}{T}$$

Equation 5.2

The pressure at set point is 100 Psig (7.91×10^5 Pa). Solving T from Equation 5.2, the temperature at set point is 457.14 K (183.99 °C).

Differentiating Equation 5.2, Equation 5.3 is achieved (Fauske, 1985) as follows:

$$\frac{1}{P} \frac{dP}{dT} = \frac{3217.2}{T^2}$$

$$\text{Hence, } \frac{dP}{dT} = \frac{3217.2 P}{T^2}$$

Equation 5.3

From Equation 5.3,

$$\frac{dP}{dT} (\text{at set pressure and temperature}) = \frac{3217.2 \times 7.91 \times 10^5}{457.14^2} \text{ Pa/K} = 1.22 \times 10^4 \text{ Pa/K}$$

5.1.2.5 Vapor density (ρ_v) and vapor specific volume (v_g) calculation:

Leung (1986) illustrates that the vapor density of an unknown sample can be calculated by considering that the system is following ideal gas behavior. Equation 5.4 expresses the ideal gas law.

$$\rho_v = \frac{M_w P}{RT}$$

Equation 5.4

The composition and the chemical properties of Brenntag corrosion inhibitor are proprietary protected, as mentioned in Chapter 4. Thus, the molecular weight of the corrosion inhibitor is assumed to be equal to the molecular weight of one of the major components, Naphtha.

Here,

Molecular weight, $M_w = 215.00 \text{ kg/Kmol}$ (Recochem Inc, 2007)

Molar gas constant, $R = 8.314 \times 10^3 \text{ J/Kmol} \cdot \text{K}$

From Equation 5.4, the vapor density and vapor specific volume is calculated as follows:

$$\rho_v = \frac{215.00 \times 7.91 \times 10^5}{8.314 \times 10^3 \times 457.14} \text{ Kg/m}^3 = 44.75 \text{ kg/m}^3$$

Therefore, vapor specific volume,

$$v_g = \frac{1}{\rho_v} = 2.23 \times 10^{-2} \text{ m}^3/\text{kg}$$

5.1.2.6 Latent heat of vaporization (h_g or λ) calculation:

Latent heat of vaporization (h_g) can be calculated from Clapeyron relation, as shown in Equation 5.5 (Leung, 1986),

$$\frac{h_g}{v_g} = T \frac{dP}{dT}$$

Equation 5.5

Solving for (h_g), the latent heat of vaporization is calculated as shown below,

$$h_g = \lambda = v_g T \frac{dP}{dT} = 2.23 \times 10^{-2} \times 457.14 \times 1.22 \times 10^4 \text{ J/kg} = 1.25 \times 10^5 \text{ J/kg}$$

5.1.2.7 Critical mass flux (G) calculation:

The critical mass flux for two phase flow is calculated using Equation 2.31, described in Chapter 2 (Leung, 1986),

$$G = 0.9 \frac{\lambda}{v_g} \left(\frac{1}{c_p T} \right)^{0.5} = 0.9 \times \frac{1.25 \times 10^5}{2.23 \times 10^{-2}} \times \left(\frac{1}{2.30 \times 10^3 \times 457.14} \right)^{0.5} \text{ kg/m}^2\text{-s} = 4.92 \times 10^3 \text{ kg/m}^2\text{-s}$$

5.1.3 Vent Sizing Calculation

The Brenntag corrosion inhibitor is a non-reactive system, so the vent sizing calculations are done only for external heating conditions. Leung's method for homogeneous vessel venting with external heating for no overpressure condition (described in Section 2.1.5.3 of Chapter 2), and

Fauske's method for a non-reactive system (described in Section 2.1.6.1 of Chapter 2), were used for such calculations.

5.1.3.1 Leung's method

The vent size design using Leung's method considers 1000 kg of initial mass for all the studied chemicals. This consideration facilitates the comparison between the vent sizes for the chemicals. The effective volume of the chemical in the vessel is calculated dividing the initial mass with the bulk density of that particular chemical.

Here,

Density of Brenntag, $\rho_l = 910 \text{ kg/m}^3$ (Brenntag Canada Inc, 2009)

Initial mass in vessel, $m_o = 1000 \text{ kg}$

Volume of the liquid, $V = \frac{m_o}{\rho_l} = 1.10 \text{ m}^3$

Leung's method for homogeneous vessel venting with external heating with no overpressure (Equation 2.27 in Chapter 2) is used to calculate the venting area (A_o) and the area to volume ratio, as shown below,

$$\begin{aligned} A_o &= \frac{m_o q \times m_o \times v_g}{G \times V \times h_g} \\ &= \frac{38.64 \times 1000 \times 1000 \times 2.23 \times 10^{-2}}{4.92 \times 10^3 \times 1.10 \times 1.25 \times 10^5} \text{ m}^2 \\ &= 1.27 \times 10^{-3} \text{ m}^2 \end{aligned}$$

So, the area to volume ratio for homogenous flow for no over pressure condition is,

$$\frac{A_o}{V} = 1.16 \times 10^{-3} \text{ m}^{-1}$$

5.1.3.2 Fauske's equation for non-reactive system with critical flow

The vent sizing calculation is also done considering ideal nozzle flow. The discharge co-efficient (C_D) of ideal nozzle flow is 1 (Fauske, 2000), where the discharge co-efficient is the ratio of the mass flow rate at the discharge end of the nozzle to that of an ideal nozzle.

Substituting the heat release rate, $\dot{Q} = \frac{V\rho_l C_p \dot{T}}{\lambda\rho_v}$ in Equation 2.32 (described in Chapter 2), the area to volume rate given is expressed as:

$$\begin{aligned} \frac{A}{V} &= \frac{C_p \rho_l \dot{T}}{0.61 C_D \rho_v \lambda \left(\frac{P}{\rho_v}\right)^{\frac{1}{2}}} \\ &= \frac{2.30 \times 10^3 \times 910 \times 1.5 \times 10^{-2}}{0.61 \times 1 \times 44.75 \times 1.25 \times 10^5 \times \left(\frac{7.91 \times 10^5}{44.75}\right)^{\frac{1}{2}}} m^{-1} \\ &= 6.92 \times 10^{-5} m^{-1} \end{aligned}$$

The area to volume ratio calculated using Fauske's method is only for a single phase flow or non-foamy behavior. For a homogeneous flow venting, multiplying this ratio by a factor of 2 gives a good approximation (Leung, 1986). Therefore, the area to volume ratio for homogenous flow is $1.38 \times 10^{-4} m^{-1}$.

5.2 Nox Rust 9800

5.2.1 ARSST Data

Two tests at 300 Psig pad pressure and two tests at 15 Psig pad pressure were carried out with 10 ml samples of Nox Rust 9800. Neither sudden pressure nor sudden temperature rises occurred due to external heat, as shown in Figure 5.8 and Figure 5.9. As a result, Nox Rust 9800 is classified as a non-reactive system, which is similar to the Brenntag corrosion inhibitor. However, the data sets for the ARSST screening tests do not show exact repeatability due to the reason described in Section 5.1.1.

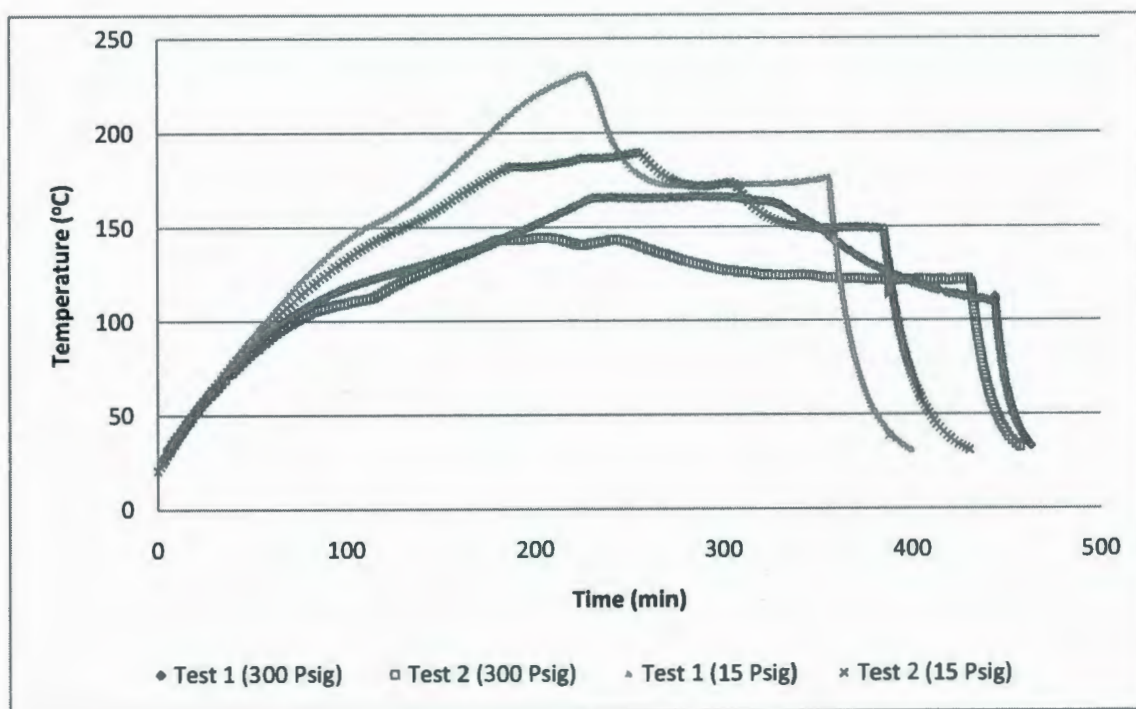


Figure 5.8: Temperature History for Nox Rust 9800 (ARSST Tests)

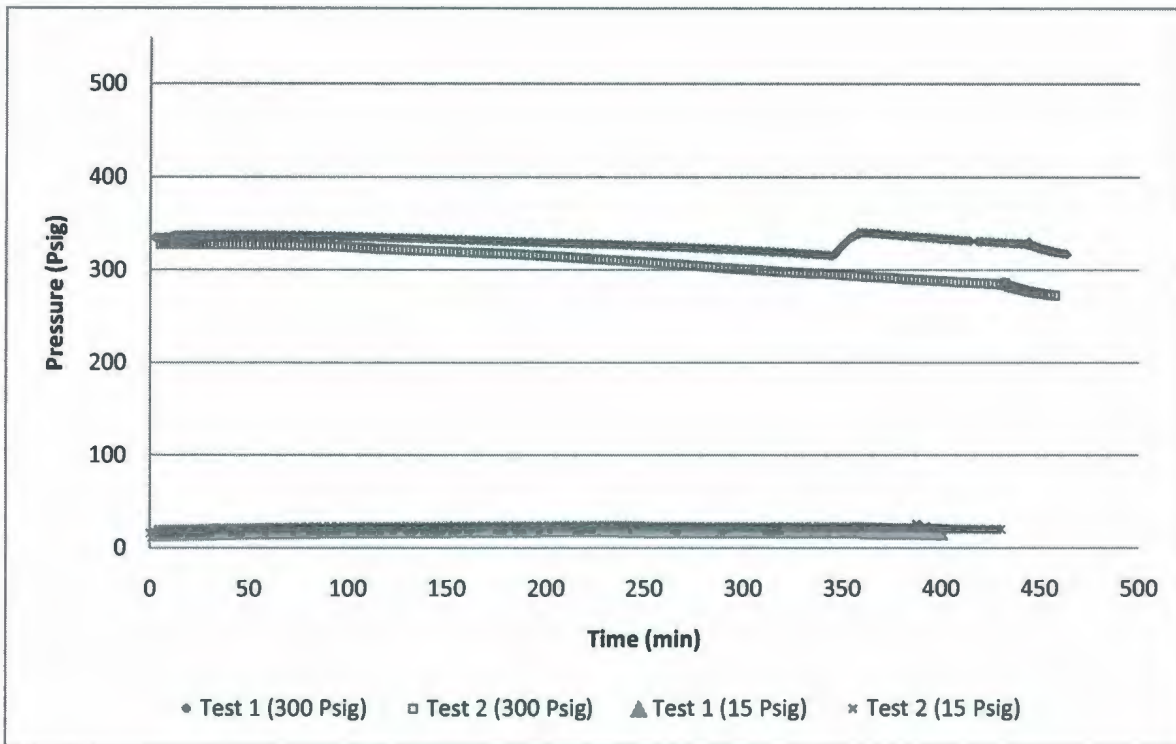


Figure 5.9: Pressure History for Nox Rust 9800 (ARSST Tests)

Table 5.2 lists the mass loss during the open cell tests in the ARSST. The mass loss for a 15 Psig pad pressure test is slightly higher than that for a 300 Psig pad gas pressure test, as lower pad pressure allows easier vaporization of the sample. But, mass loss of the samples is not affected by the experimental time, as shown in Figure 5.10, which presents the mass loss as a function of time plot.

Table 5-2: Mass Loss of Nox Rust 9800 for ARSST Tests

| | Initial Mass (g) | Final Mass (g) | Average Mass Loss (%) |
|-----------------------------------|------------------|----------------|-----------------------|
| 300 Psig Pad Pressure Test | 9.87±0.15 | 8.61±0.22 | 12.74±0.50 |
| 15 Psig Pad Pressure Test | 9.81±0.27 | 8.33±0.27 | 14.99±0.19 |

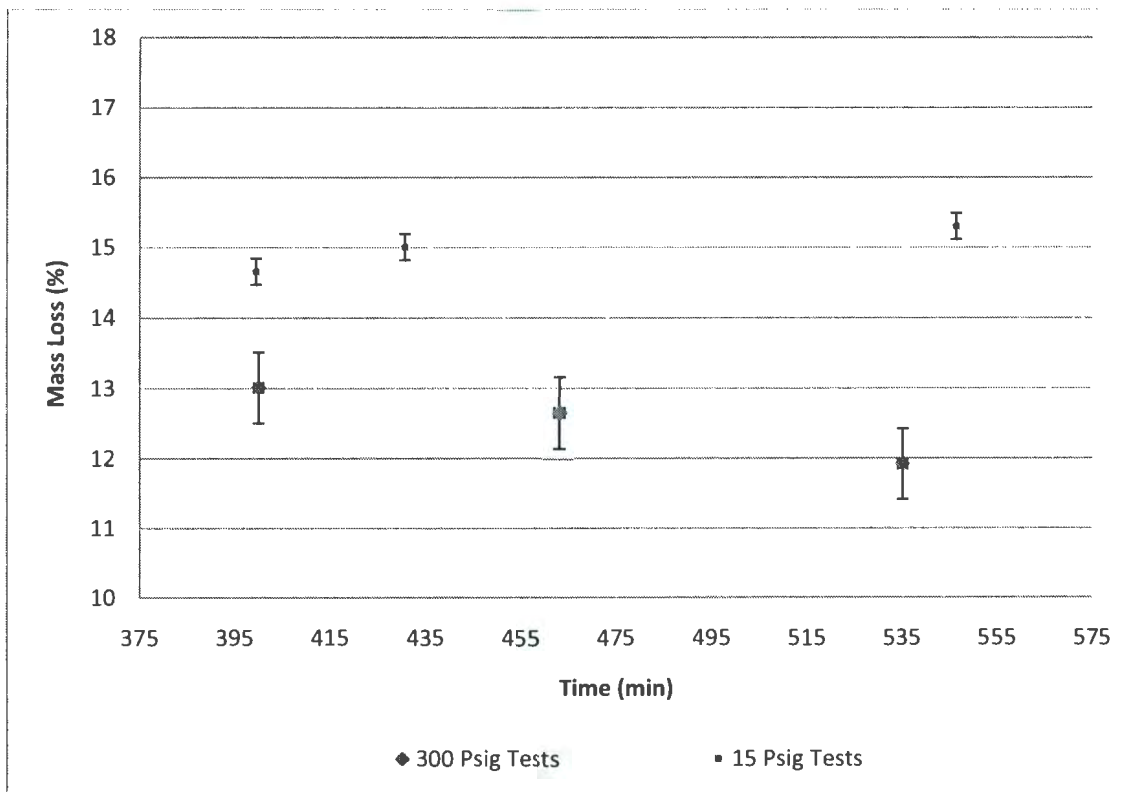


Figure 5.10: Mass Loss as a Function of Time for Nox Rust 9800 (ARSST Tests)

5.2.2 VSP2 Data

80 ml of Nox Rust 9800 was tested in a closed test cell in the VSP2. The sample was heated up to 275 °C and then the test was turned off as the pressure rise was as high as 510 Psig.

Figure 5.11 shows that there is no significant rise in the self heat rate. The temperature and pressure profile of the test are depicted in Figure 5.12 and Figure 5.13. For Nox Rust 9800, the set pressure is also considered as 100 Psig, as the pressure increased at a higher rate after this point. Figure 5.14 shows the pressure behaviour as a function of temperature (1/T) plot from

which the set temperature and $\frac{dP}{dT}$ are calculated. It is also observed (from Figure 5.14) that no gas was evolved during the test, as the initial pressure is equal to the end pressure.

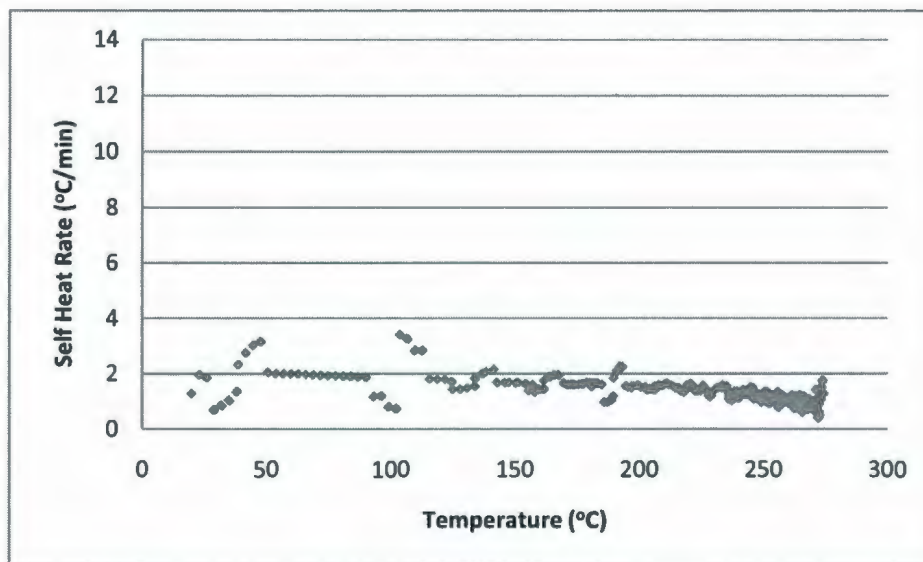


Figure 5.11: Self Heat Rate as a Function of Temperature for Nox Rust 9800 (VSP2 Test)

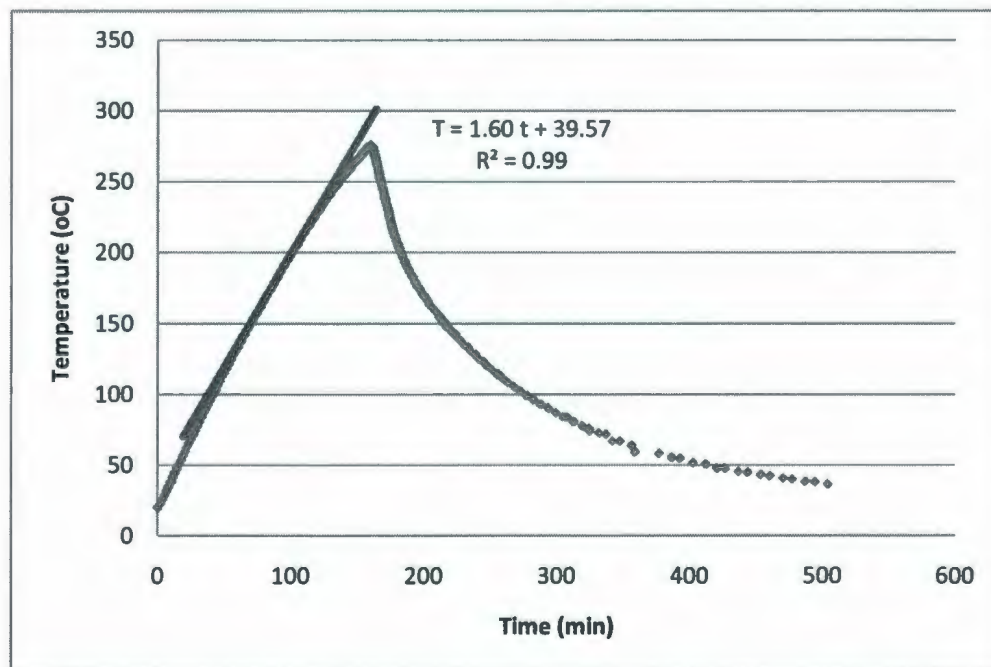


Figure 5.12: Temperature History for Nox Rust 9800 (VSP2 Test)

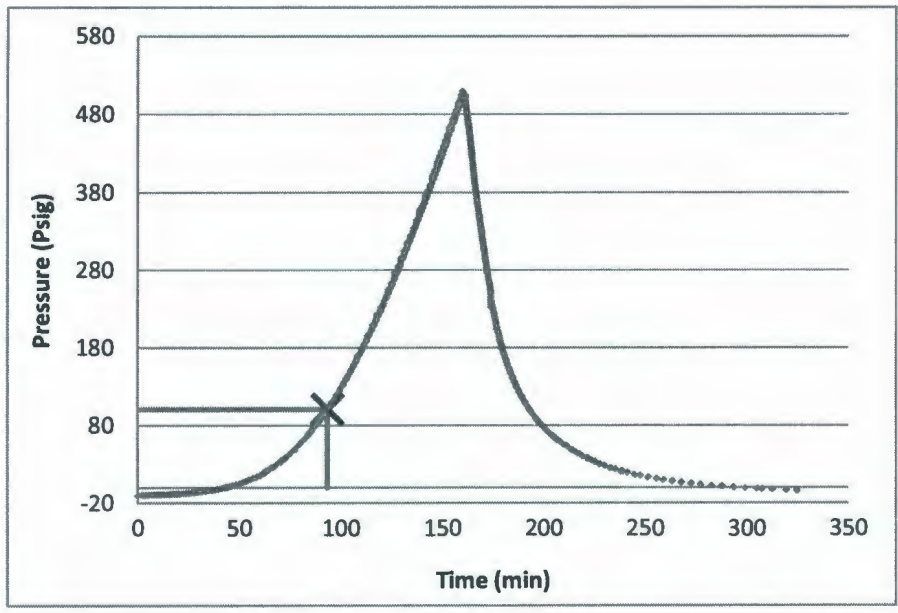


Figure 5.13: Pressure History for Nox Rust 9800 (VSP2 Test)

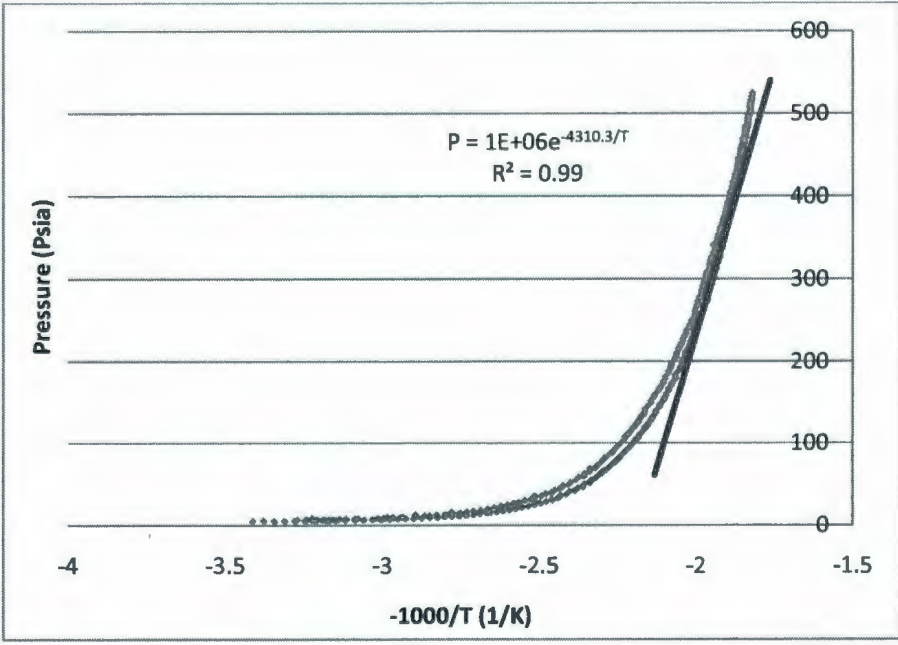


Figure 5.14: Pressure as a Function of Temperature for Nox Rust 9800 (VSP2 Test)

The necessary parameters for vent sizing are calculated using the given plots. The values are tabulated in Table 5-3. The procedure for calculating the parameters is the same as described in Section 5.1.3 for the Brenntag corrosion inhibitor. The detailed calculation is illustrated in Appendix 4.

Table 5-3: Independent and Dependent Variables for Vent Sizing for Nox Rust 9800

| | Parameters | Notation | Value | Unit |
|------------------------------|---|--------------------|-----------------------|----------------------|
| Independent Variables | Mass of the sample in test cell | m_s | 7.75×10^{-2} | kg |
| | Specific heat capacity of the Nox Rust 9800 at 90°C (Section 4.1.2) | C_{ps} | 2.92×10^3 | J/ kg-K |
| | Mass of the test cell | m_b | 4.30×10^{-2} | kg |
| | Specific heat capacity of the stainless steel test cell at 25°C | C_{pb} or C_p | 510 | J/ kg-K |
| | Pressure at set point | P | 7.91×10^5 | Pa |
| | Molecular weight (Sciencelab.com Inc, 2008) | M_w | 148.2 | kg/ Kmol |
| | Density of Nox Rust 9800 (Brenntag Canada Inc, 2009) | ρ_l | 970 | kg/m ³ |
| | Initial mass in vessel | m_o | 1000 | kg |
| Dependent Variables | Phi factor of the test cell | ϕ | 1.10 | No unit |
| | Temperature rate | \dot{T} | 2.7×10^{-2} | K/s |
| | Heat release rate | q | 86.72 | J/ kg-s |
| | Temperature at set point | T | 474.82 K | K |
| | $\frac{dP}{dT}$ @ set pressure | $\frac{dP}{dT}$ | 1.51×10^4 | Pa/ K |
| | Vapor density | ρ_v | 29.70 | kg/m ³ |
| | Vapor specific volume | v_g | 3.37×10^{-2} | m ³ / kg |
| | Latent heat of vaporization | h_g or λ | 2.41×10^5 | J/kg |
| | Critical mass flux | G | 5.47×10^3 | kg/m ² -s |
| | Volume of the chemical in the tank | V | 1.03 | m ³ |

5.2.3 Vent Sizing

Being a non-reactive corrosion inhibitor, the same vent sizing equations used for the Brenntag corrosion inhibitor are also used for Nox Rust 9800. A detail of the vent sizing calculation is given in Appendix 4.

5.2.3.1 *Leung's method for homogeneous vessel venting with external heating with no overpressure*

Area to volume ratio for homogenous flow for no over pressure condition,

$$\frac{A_o}{V} = 2.09 \times 10^{-3} m^{-1}$$

5.2.3.2 *Fauske's equation for non reactive system with critical flow and non foamy behavior*

Area to volume ratio for non-foamy flow,

$$\frac{A}{V} = 1.07 \times 10^{-4} m^{-1}$$

Area to volume ratio for homogenous flow,

$$\frac{A}{V} = 1.07 \times 10^{-4} \times 2 m^{-1} = 2.15 \times 10^{-4} m^{-1}$$

5.3 Nox Rust 1100

5.3.1 ARSST Data

For Nox Rust 1100, two tests at 300 Psig and two tests at 15 Psig pad pressure were also carried out similar to the other two liquid corrosion inhibitors. The temperature and pressure profile of the ARSST tests are depicted in Figure 5.15 and Figure 5.16. No pressure rise was found for the ARSST tests.

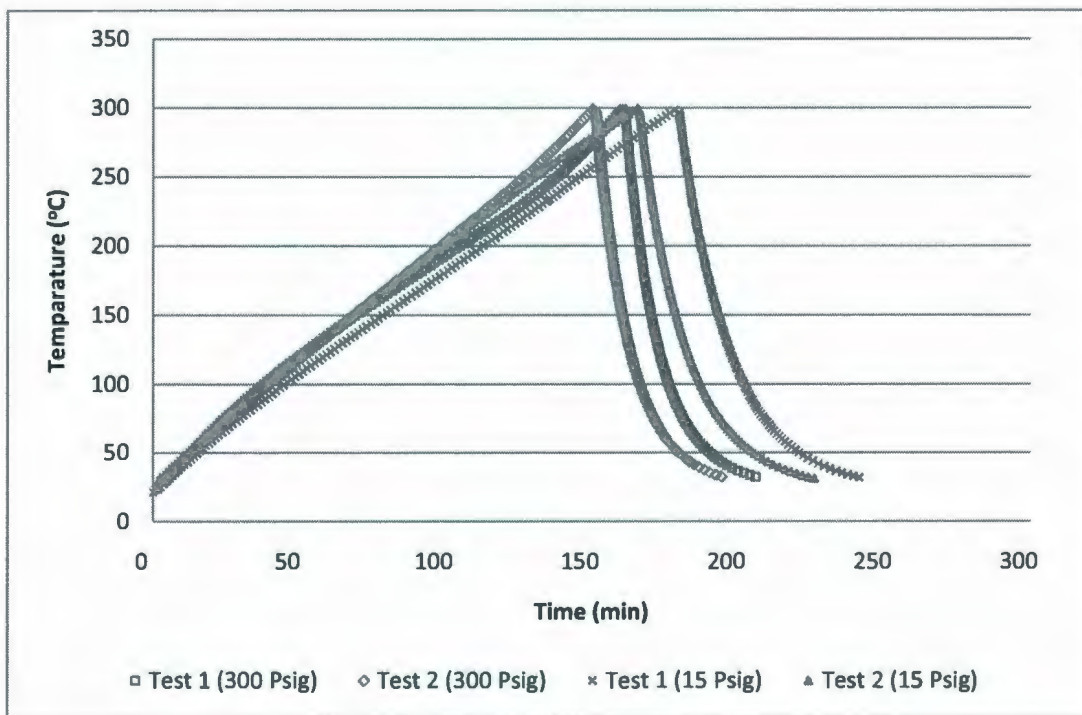


Figure 5.15: Temperature History for Nox Rust 1100 (ARSST Tests)

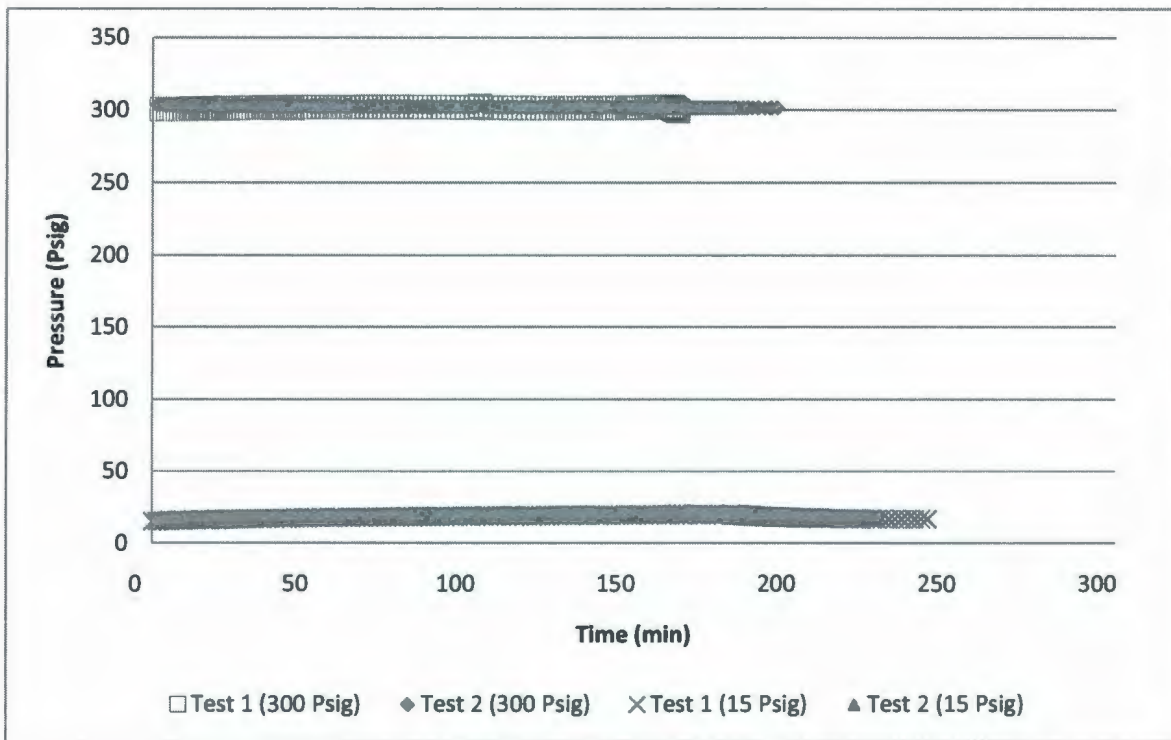


Figure 5.16: Pressure History for Nox Rust 1100 (ARSST Tests)

The mass losses during the open test cell tests are tabulated in Table 5-4. The mass losses observed for Nox Rust 1100 are lower than those for other liquid corrosion inhibitors. This is due to the percentage of volatile chemicals present in Nox Rust 1100 (32%) is lower than that present in Brenntag and Nox Rust 9800 corrosion inhibitors (KPR ADCOR Inc, 2009) .

Table 5-4: Mass Loss of Nox Rust 1100 for ARSST Tests

| | Initial Mass (g) | Final Mass (g) | Average Mass Loss (%) |
|-----------------------------------|------------------|----------------|-----------------------|
| 300 Psig Pad Pressure Test | 7.50±0.21 | 7.18±0.19 | 4.44±0.15 |
| 15 Psig Pad Pressure Test | 8.27±0.07 | 8.14±0.08 | 1.42±0.16 |

From Figure 5.17, which is mass loss as a function time plot for Nox Rust 110, it is apparent that the mass loss of Nox Rust 1100 also does not vary significantly with the experimental time.

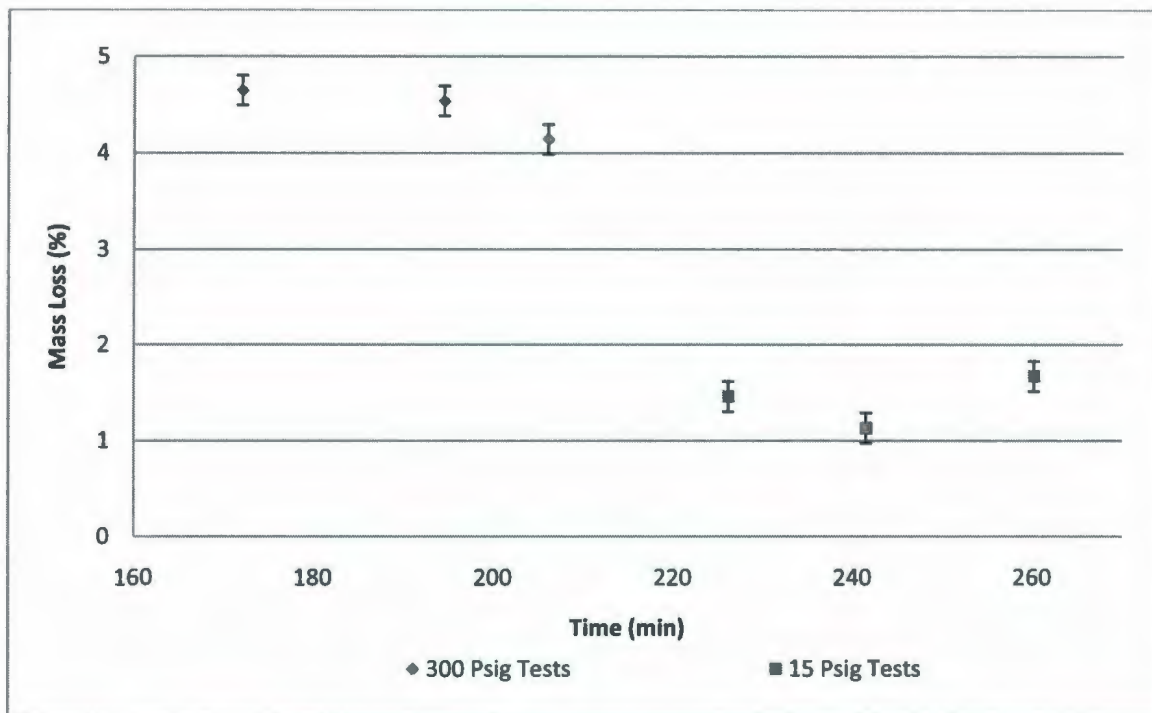


Figure 5.17: Mass Loss as a Function of Time for Nox Rust 1100 (ARSST Tests)

5.3.2 VSP2 Data

Two closed cell VSP2 tests were performed with 80 ml Nox Rust 1100 sample. In this section, one of the tests is characterized. Plots for another test are listed in Appendix 5. The plots for the second test follow the same trend as the first one. From the first test, it is found that the tempering point of the system was 387 °C. The tempering point of any system represents the point where the temperature and pressure of the system do not change while applying heat. From Figure 5.18, it is noticeable that there is no significant increase in the self heat rate. The noise observed during the tests can be explained by the following factors: (i) presence of the electrical wires close to the strong magnetic stirrer, (ii) the thermocouple of the test cell can be affected by the moisture in the air as the test cells were left unused for a long time, and (iii) improper

grounding. The noise due to above mentioned reasons can be minimized by taking the data log in interval 3 or 4. However, the data log in interval was set as 2 for these two tests for Nox Rust 1100 carried out in the VSP2, which could not minimize the noise. Figure 5.19 and Figure 5.20 depict the temperature and pressure histories. 40 Psig is considered as the venting pressure, because after this point the pressure increase is comparatively higher, as shown in Figure 5.20.

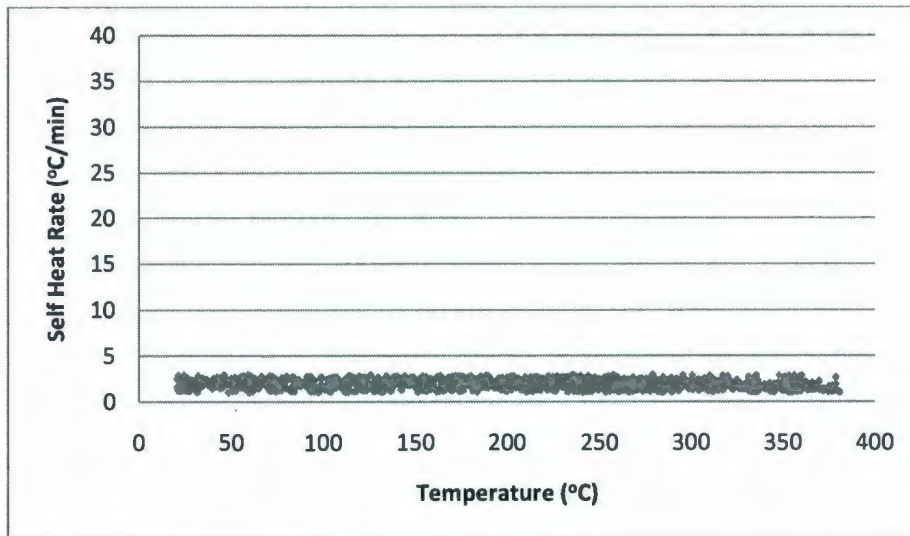


Figure 5.18: Self Heat Rate as a Function of Temperature for Nox Rust 1100 (VSP2 Test 1)

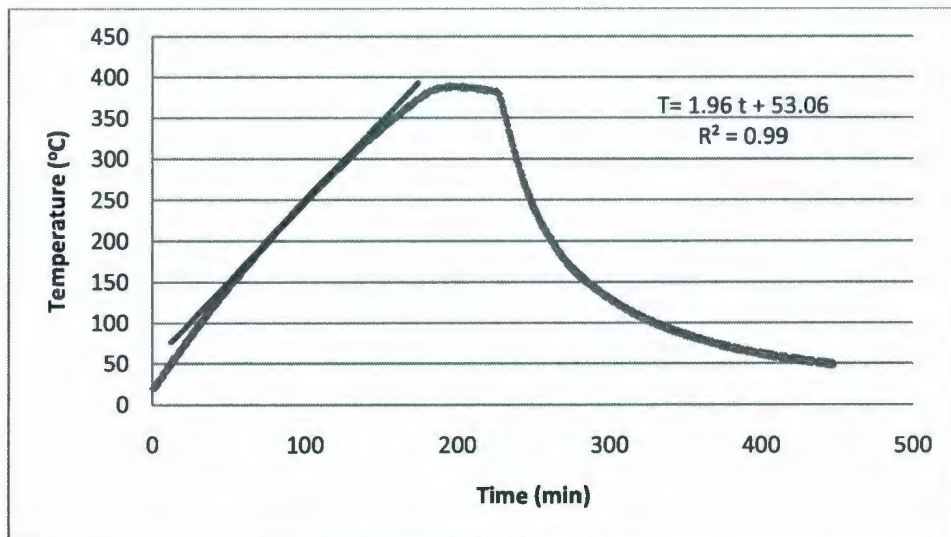


Figure 5.19: Temperature History for Nox Rust 1100 (VSP2 Test 1)

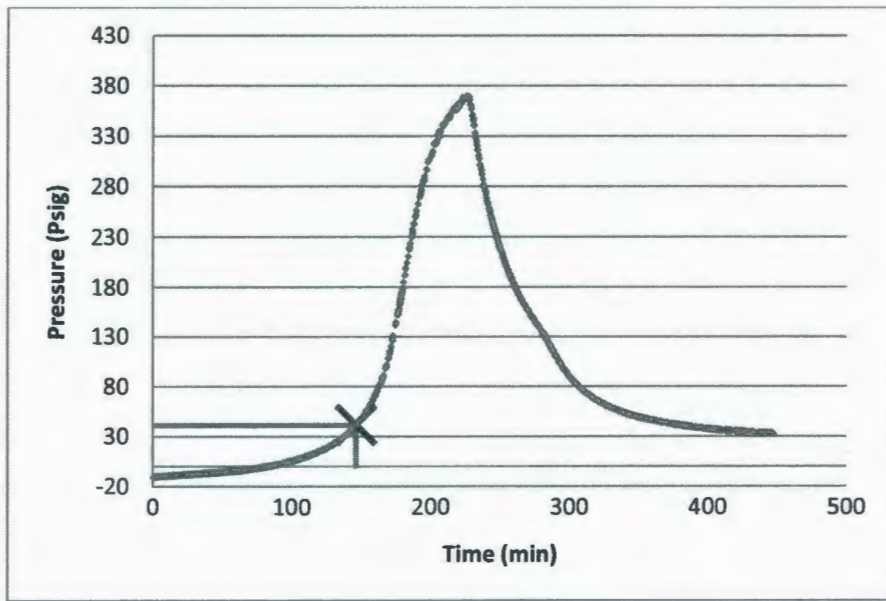


Figure 5.20: Pressure History for Nox Rust 1100 (VSP2 Test 1)

Figure 5.21 illustrates the pressure behavior as a function of temperature. It is observed that some non-condensable gas is generated during the heating. The end pressure is 50 Psia higher than the starting pressure. The same trend was also observed for the second test. Thus, Nox Rust 1100 can be classified as a gassy system.

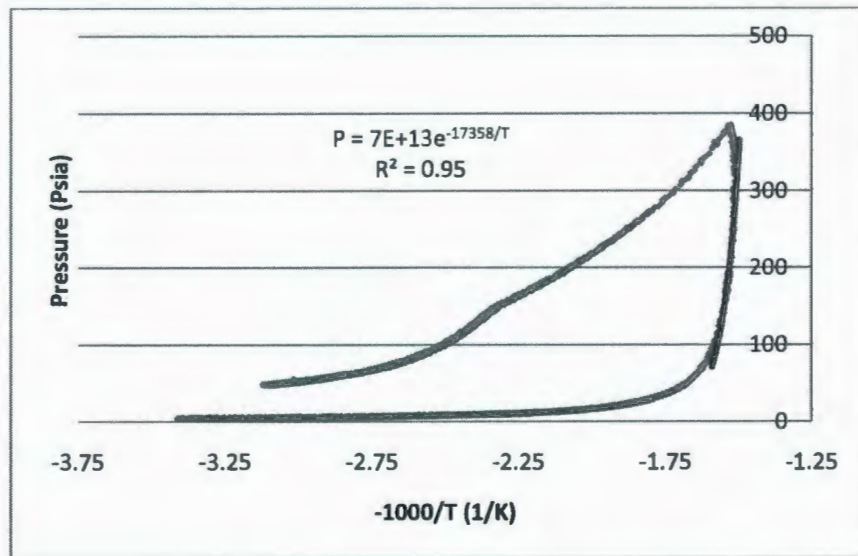


Figure 5.21: Pressure as a Function of Temperature for Nox Rust 1100 (VSP2 Test 1)

From Figure 5.21, the relation between pressure and temperature is drawn and given as:

$$\ln P = \ln(7 \times 10^{13}) - \frac{17358}{T}$$

$$\text{Or, } \ln P = 31.88 - \frac{17358}{T}$$

Equation 5.6

By substituting the venting pressure, which is 54.7 Psia, in Equation 5.6, the venting temperature is calculated as follows:

$$\text{Temperature at the set point, } T_s = 622.65 \text{ K} = 349.50 \text{ }^\circ\text{C}$$

5.3.3 Vent Sizing

Vent sizing for Nox Rust 1100 is done by using Fauske's screening equation as described in Section 2.1.9 and Fauske's detailed method for gassy systems as described in Section 2.1.6.5.

Figure 5.19, which is the pressure rate behavior as a function of temperature, shows a small increase in the pressure rate with the increase in temperature for the two VSP2 tests.

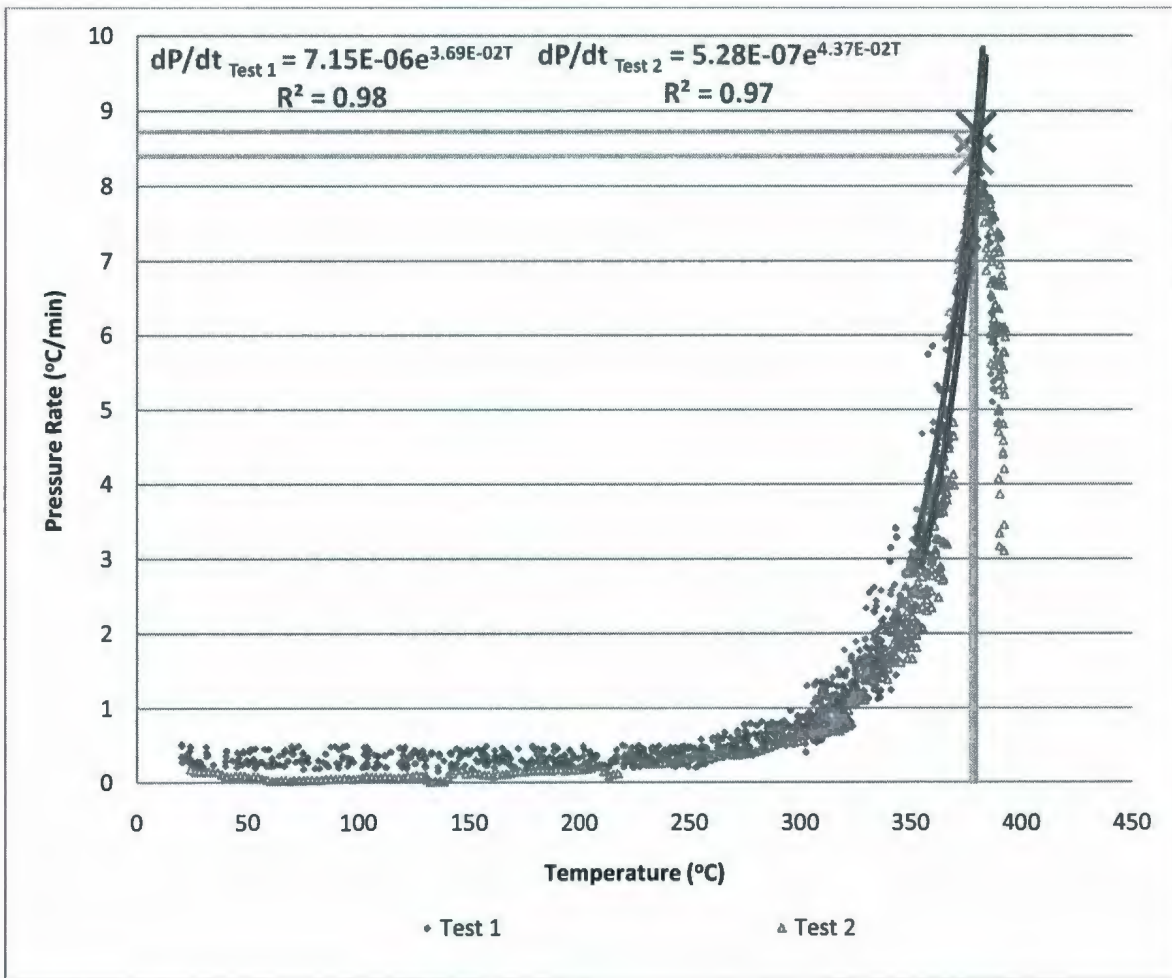


Figure 5.22: Pressure Rate as a Function of Temperature for Nox Rust 1100 (VSP2 Tests)

From Figure 5.22, the expression for pressure rate for the first test is given by Equation 5.7,

$$\dot{P} = 7.15 \times 10^{-6} e^{3.69 \times 10^{-2} T}$$

Equation 5.7

Maximum pressure rate is calculated from Equation 5.7. The temperature at the peak point of pressure rate is found to be 380 °C. Hence, the maximum pressure rate for the first test,

$$\dot{P} = 7.15 \times 10^{-6} e^{3.69 \times 10^{-2} \times 380} \text{ Psi/min} = 8.79 \text{ Psi/min}$$

For the second test the maximum pressure rate is also found to occur at 380 °C. And, the maximum pressure rate for the second test ($\dot{P} = 5.28 \times 10^{-7} e^{4.37 \times 10^{-2} \times 380}$ Psi/min) is 8.60 Psi/ min.

The discharge co-efficient (C_D), which is the ratio of the mass flow rate at the discharge end of the nozzle to that of an ideal nozzle, is considered as 1 for vent sizing calculation purposes. It means the area to volume ratio is determined considering ideal nozzle flow behavior.

5.3.3.1 Fauske's screening equation for gassy system

Section 2.1.9 (in Chapter 2) presents the details to determine the area to volume ratio from VSP2 closed cell tests using Fauske's screening equation for gaseous systems is expressed by Equation 5.8,

$$\frac{A}{V} = \frac{3.5 \times 10^{-3} \dot{P}}{C_D P \left[1 + \frac{1.98 \times 10^{-3}}{P^{1.75}} \right]^{0.286}} \times \frac{(120 - v)}{350} \times \frac{10}{m}$$

Equation 5.8

Here, for the first test,

Pressure at set point, $P = 40$ Psig = 54.7 Psi

Mass of the sample in test cell, $m = 69.42$ g

Volume of the sample, $v = 80$ ml

So, the area to volume ratio for Nox Rust 1100,

$$\frac{A}{V} = \frac{3.5 \times 10^{-3} \dot{P}}{C_D P \left[1 + \frac{1.98 \times 10^{-3}}{P^{1.75}} \right]^{0.286}} \times \frac{(120 - 80)}{350} \times \frac{10}{69.42}$$

$$\begin{aligned}
&= \frac{3.5 \times 10^{-3} \times 8.79}{1 \times 54.7 \left[1 + \frac{1.98 \times 10^{-3}}{54.7^{1.75}} \right]^{0.286}} \times \frac{(120 - 80)}{350} \times \frac{10}{69.42} m^{-1} \\
&= \frac{3.08 \times 10^{-4}}{54.7} \times 1.65 \times 10^{-2} m^{-1} \\
&= 9.29 \times 10^{-6} m^{-1}
\end{aligned}$$

The calculation for vent sizing by screening equation is given in Appendix 5. The average area to volume ratio for Nox Rust 1100 is $9.27 \times 10^{-6} m^{-1}$.

5.3.3.2 Fauske's detailed equation for gassy system

In Section 2.1.6.5, Fauske's detailed equation for gassy system is described. The molecular weight of gas in the system is required to use this equation. A compositional analysis is recommended to determine the molecular weight of the gas with accuracy. For this work, the compositional analysis of the evolved gas could not be done due to time constraints. As the main component of Nox Rust 1100 is Petroleum oil, it will produce carbon dioxide while introduced to fire (KPR ADCOR Inc, 2009), and, without fire involvement, methane along with different hydrocarbons can be produced (Ergon Refining Inc, 2003). The vent sizing calculations for Nox Rust 1100 by detailed Fauske's method is done by considering the gas molecular weight equal to carbon dioxide and methane separately. Therefore, a range of approximate vent area to volume ratio is estimated:

Here,

Test sample mass for the first test, $m_{t1} = 69.42 \text{ g} = 6.94 \times 10^{-2} \text{ kg}$

Test sample mass for the second test, $m_{t2} = 67.85 \text{ g} = 6.79 \times 10^{-2} \text{ kg}$

Test freeboard volume, which is the volume difference between test cell and the sample,

$$\vartheta = (120-80) \times 10^{-6} \text{ m}^3 = 4 \times 10^{-5} \text{ m}^3$$

Density of Nox Rust 1100, $\rho = 890 \text{ kg/m}^3$

Molecular weight of carbon di-oxide, $M_{\omega,g1} = 44.01 \text{ kg/Kmol}$

Molecular weight of methane, $M_{\omega,g2} = 16.04 \text{ kg/Kmol}$

Venting pressure, $P = 54.7 \text{ Psi} = 3.77 \times 10^5 \text{ Pa}$

Venting temperature, $T = 622.65 \text{ K}$

Maximum pressure rise rate for test 1, $\dot{P}_1 = 8.79 \text{ Psi/min} = 1.01 \times 10^3 \text{ Pa/s}$

Maximum pressure rise rate for test 2, $\dot{P}_2 = 8.60 \text{ Psi/min} = 9.88 \times 10^2 \text{ Pa/s}$

Gas constant, $R = 8.314 \times 10^3 \text{ J/Kmol} \cdot \text{K}$

Hence, considering that the molecular weights of gas and carbon dioxide are equal, the area to volume ratio for Nox Rust 1100 for test 1 can be calculated by using Equation 2.38, as follows:

$$\begin{aligned} \frac{A}{V} &= \frac{1}{0.61 C_D} \frac{\rho \vartheta \dot{P}_1}{m_{t1} P} \left(\frac{M_{\omega,g1}}{RT} \right)^{1/2} \\ &= \frac{1}{0.61 \times 1} \times \frac{890 \times 4 \times 10^{-5} \times 1.01 \times 10^3}{6.94 \times 10^{-2} \times 3.77 \times 10^5} \left(\frac{44.01}{8.314 \times 10^3 \times 622.65} \right)^{1/2} \text{ m}^{-1} \\ &= 6.57 \times 10^{-6} \text{ m}^{-1} \end{aligned}$$

The average areas to volume ratio for the two tests by considering the gas molecular weight equal to carbon di-oxide and methane separately are presented in Table 5-5.

Table 5-5: Area to Volume Ratio for Nox Rust 1100

| Gas Molecular Weight (kg/Kmol) | Area to Volume Ratio (m⁻¹) |
|--|---|
| Considering molecular weight of carbon dioxide (= 44.01) | $6.58 \times 10^{-6} \pm 1.58 \times 10^{-7}$ |
| Considering molecular weight of methane (= 16.04) | $3.98 \times 10^{-6} \pm 2.00 \times 10^{-7}$ |

From Table 5-5, it is evident that the area to volume ratio considering molecular weight of carbon dioxide provides higher value than that considering molecular weight of methane. In both cases, the orders of magnitude from the two tests are very similar. The area to volume ratio that considers the evolved gas consists of only carbon dioxide will be preferred, as it presents more conservative and safe estimation.

5.4 VCI 1 Powder

5.4.1 ARSST Data

Two tests at 300 Psig and two tests at 15 Psig were carried out with VCI 1 powder sample in the ARSST. The temperature and pressure profile for the ARSST tests are illustrated in Figure 5.23 and Figure 5.24, respectively. These profiles indicate that no sharp pressure increase or temperature increase (exotherm) occurred during the tests. As mentioned earlier, the VCI 1 sample is a white crystalline powder. It melted during the test and it is solidified as a lump after the cooling. The physical appearance of VCI 1 powder before and after the test is depicted in

Figure 5.25. The melting point of VCI 1 powder for 300 Psig tests is indicated in Figure 5.23. However, when the sample was heated at 15 Psig pad pressure, the temperature of the samples reached a plateau before 200 °C as shown in Figure 5.23. This means the samples started to melt at a lower temperature than the melting point for a lower pad gas pressure.

Mass loss was observed during the tests, which indicates that vent size is required. For obtaining detailed temperature and pressure behaviour to size vents, this chemical was also tested in a closed cell VSP2 test.

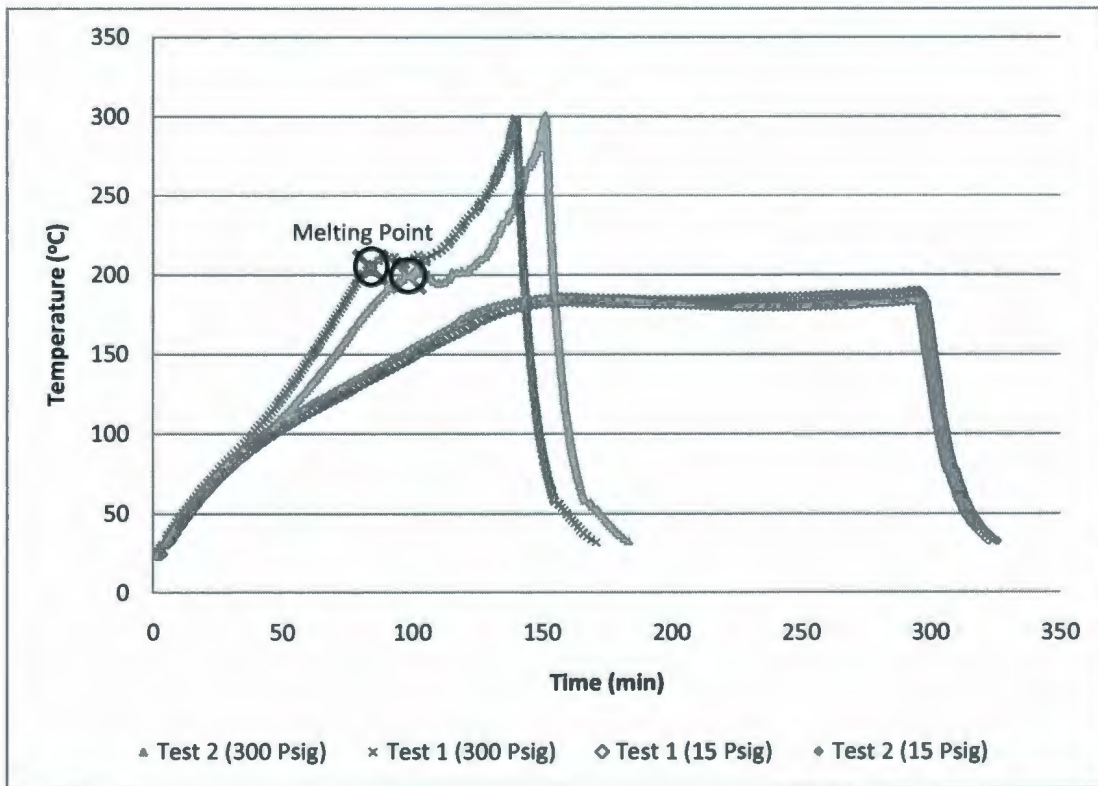


Figure 5.23: Temperature History for VCI 1 Powder (ARSST Tests)

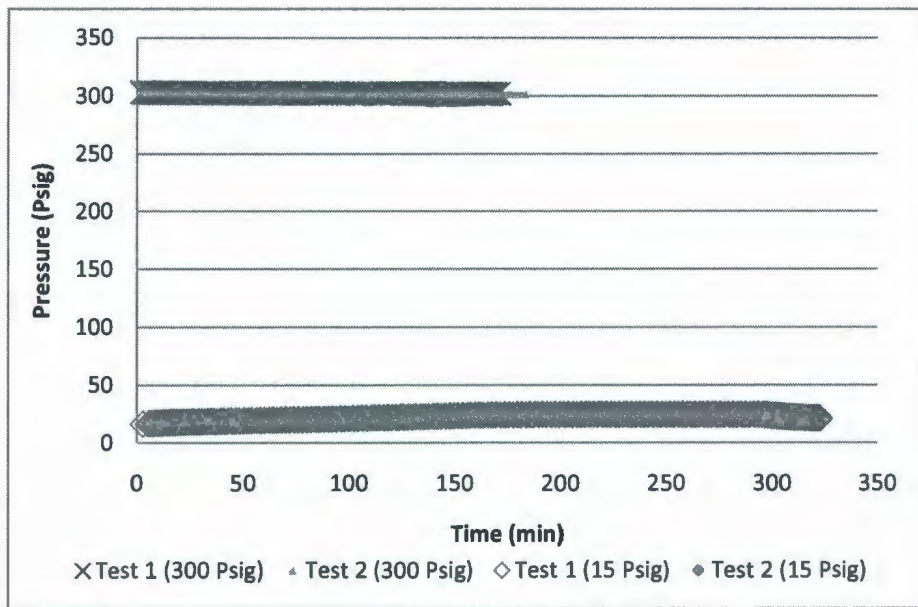


Figure 5.24: Pressure History for VCI 1 Powder (ARSST Tests)



Figure 5.25: VCI 1 Powder before Test (Left) and ARSST Test Cell Containing VCI 1 Powder after Test (Right)

Table 5-6 shows the mass loss for the ARSST tests and it is seen that the mass loss for the VCI powder is comparatively lower than the liquid corrosion inhibitor samples. This is due to the

negligible volatile organic compound presented in the VCI 1 powder sample (KPR ADCOR Inc, 2007).

Table 5-6: Mass Loss of VCI 1 Powder for ARSST Tests

| | Initial Mass (g) | Final Mass (g) | Average Mass Loss (%) |
|-----------------------------------|-------------------------|-----------------------|------------------------------|
| 300 Psig Pad Pressure Test | 3.23±0.19 | 3.02±0.32 | 1.76±0.65 |
| 15 Psig Pad Pressure Test | 3.82±0.02 | 3.61±0.01 | 5.43±0.46 |

5.4.2 VSP2 Data

A sample of 65 gm VCI 1 powder is tested in the VSP2 closed test. Figure 5.26 and Figure 5.27 show the temperature and pressure history, respectively. The melting point of the sample is close to 200 °C, which is also reflected from Figure 5.26. After reaching 200 °C, temperature was constant for certain period due to melting and then the temperature again started to increase. The test was stopped when the sample reaches 270 °C as the pressure rise was about 500 Psig at that peak temperature. The venting pressure is considered here as 135 Psig since the pressure increase is comparatively higher after this point.

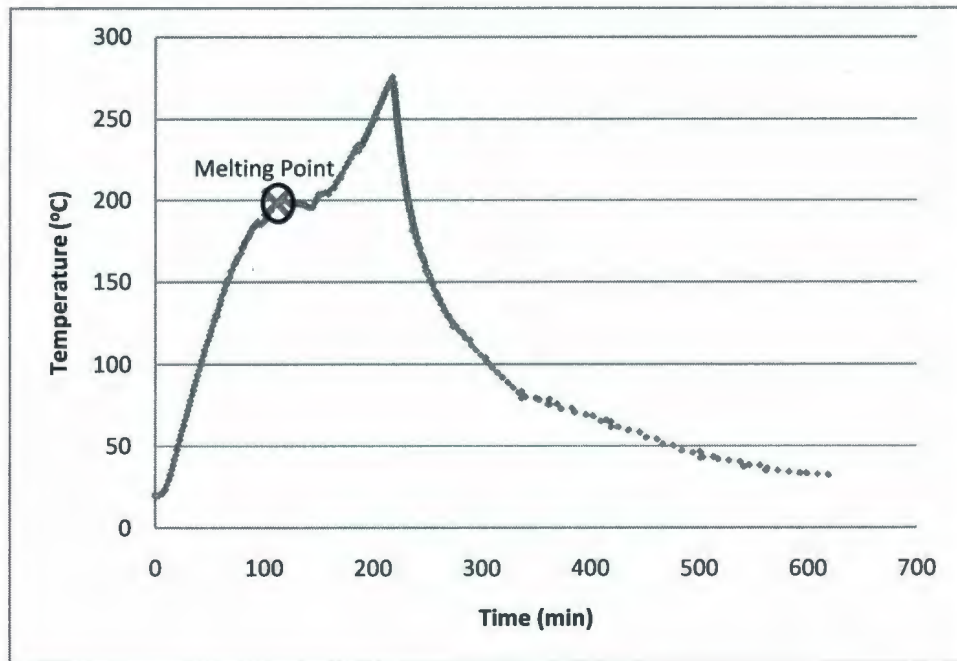


Figure 5.26: Temperature History for VCI 1 Powder (VSP2 Test)

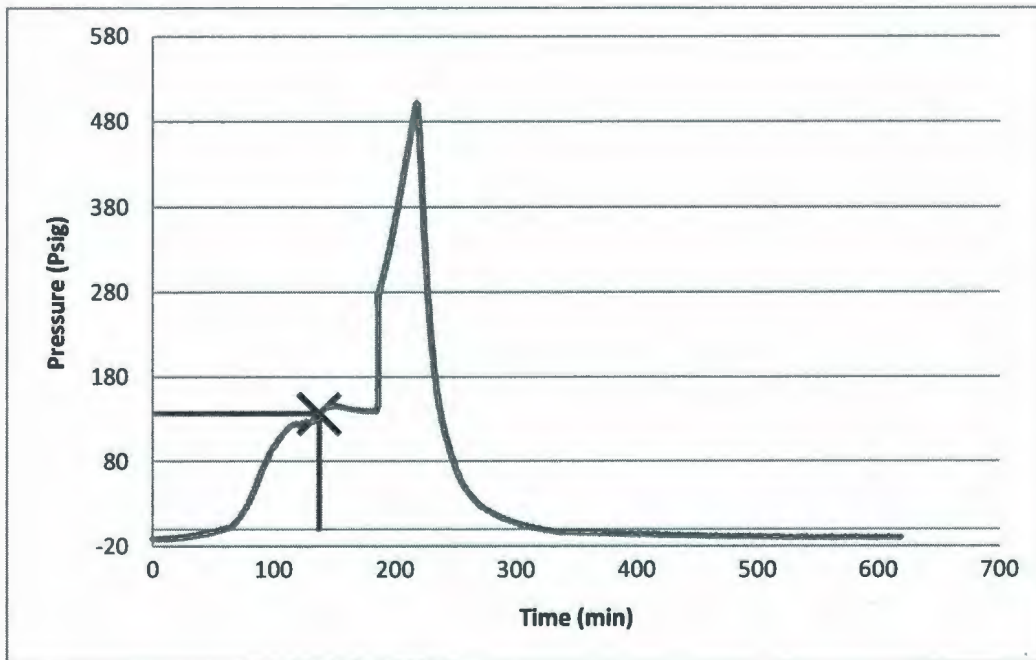


Figure 5.27: Pressure History for VCI 1 Powder (VSP2 Test)

There was no sharp increase in self heat rate found for the test as shown in Figure 5.28. The pressure behavior as function of temperature (Figure 5.29) indicates that the end pressure is close to the start pressure. But, there is a very sharp increase in pressure just after the melting point (200 °C) of the sample. While the sample is heated to high temperature, it is prone to produce various decomposition products such as carbon dioxide, carbon monoxide, and oxides of nitrogen (KPR ADCOR Inc, 2007). The closed test cell was deformed significantly after the VSP2 test as shown in Figure 5.30. Therefore, the system is considered as a gassy system and the vent sizing calculation is conducted in the following sections.

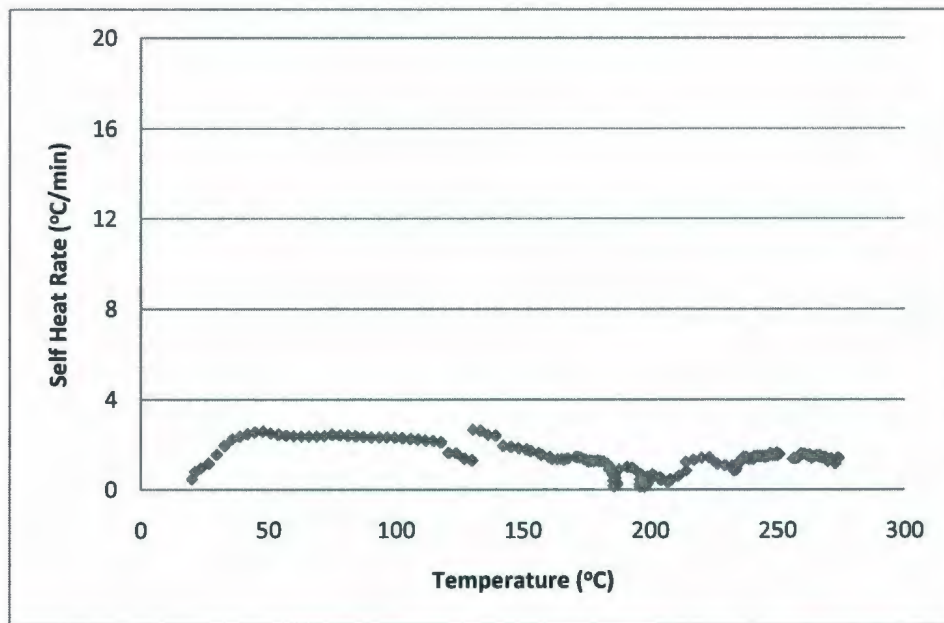


Figure 5.28: Self Heat Rate as a Function of Temperature for VCI 1 Powder (VSP2 Test)

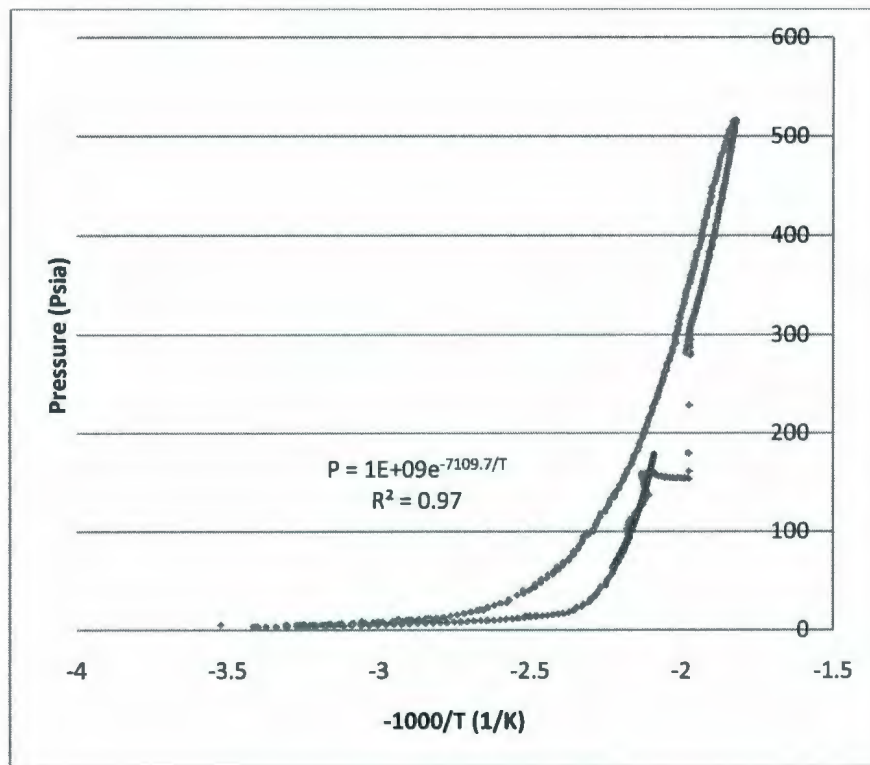


Figure 5.29: Pressure as a Function of Temperature for VCI 1 Powder (VSP2 Test)

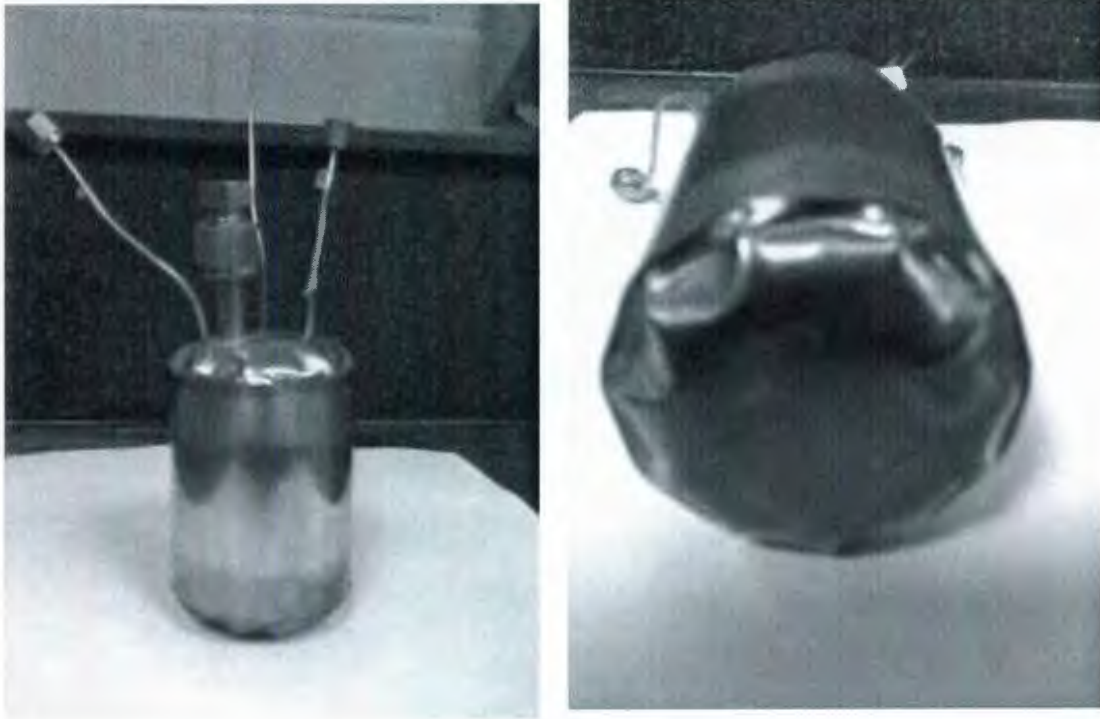


Figure 5.30: Deformed Closed Test Cell for VSP2 after Test with VCI 1 Powder

From Figure 5.29, the relation between pressure and temperature can be drawn which is given by Equation 5.9,

$$\ln P = \ln(1 \times 10^9) - \frac{7109.7}{T}$$

$$\text{Or, } \ln P = 20.72 - \frac{7109.7}{T}$$

Equation 5.9

By substituting the venting pressure, which is 149.7 Psia, in Equation 5.9, the venting temperature is calculated as follows:

$$\text{Temperature at the set point, } T_s = 452.43 \text{ K} = 179.28 \text{ }^\circ\text{C}$$

5.4.3 Vent Sizing

From the pressure rate as function of temperature (Figure 5.28), the pressure rate shows one peak prior to the melting point and another peak after the melting point. For vent sizing purposes the pressure rate corresponding to the second peak will be used because the second peak is higher than the first peak. And this will lead to a more conservative result. Fauske's short form of equation and Fauske's detailed method for gassy system will be used to calculate the vent size.

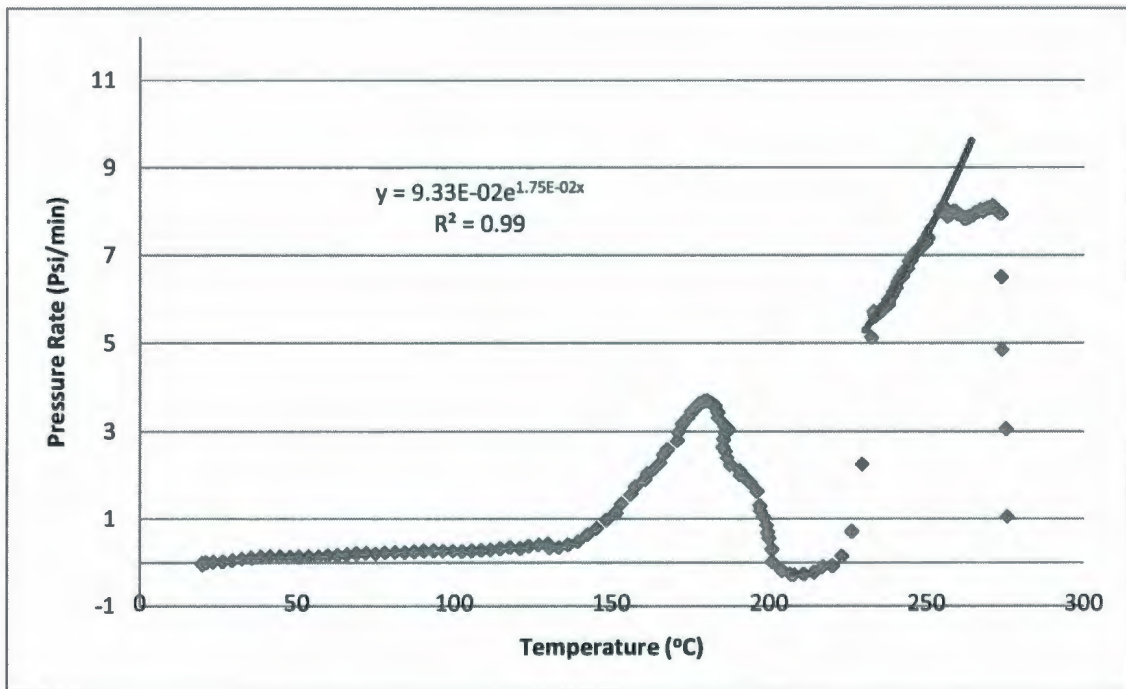


Figure 5.31: Pressure Rate as a Function of Temperature for VCI 1 Powder (VSP2 Test)

From Figure 5.31, the pressure rate is expressed as Equation 5.10. The temperature at which the pressure starts increasing sharply (255 °C) is used to calculate the maximum pressure rate as presented below,

$$\dot{P} = 9.33 \times 10^{-2} e^{1.75 \times 10^{-2} T}$$

Equation 5.10

So, maximum pressure rate, $\dot{P} = 9.33 \times 10^{-2} e^{1.75 \times 10^{-2} \times 255.00} \text{Psi/min} = 8.09 \text{Psi/min}$

5.4.3.1 Fauske's screening equation for gassy system

Here,

Pressure at set point, $P = 135 \text{ Psig} = 149.7 \text{ Psi}$

Mass of the sample in test cell, $m = 64.92 \text{ g}$

Density of the sample, $\rho = 1300 \text{ kg/m}^3$ (KPR ADCOR Inc, 2007)

Volume of the sample, $v = 50 \text{ m}^3$

The area to volume ratio for gassy system is calculated using Fauske's simplified equation for a VSP-2 closed cell test experiment (Equation 5.8) as shown below.

$$\begin{aligned} \frac{A}{V} &= \frac{3.5 \times 10^{-3} \dot{P}}{C_D P \left[1 + \frac{1.98 \times 10^{-3}}{P^{1.75}} \right]^{0.286}} \times \frac{(120 - 50)}{350} \times \frac{10}{64.92} \\ &= \frac{3.5 \times 10^{-3} \times 8.09}{1 \times 149.7 \left[1 + \frac{1.98 \times 10^{-3}}{149.7^{1.75}} \right]^{0.286}} \times \frac{(120 - 50)}{350} \times \frac{10}{64.92} \text{m}^{-1} \\ &= \frac{2.83 \times 10^{-2}}{149.7} \times 3.08 \times 10^{-2} \text{m}^{-1} \\ &= 5.83 \times 10^{-6} \text{m}^{-1} \end{aligned}$$

5.4.3.2 Fauske's detailed equation for gassy system

The composition and constituents of VCI 1 powder is completely proprietary protected. However, the manufacturer mentioned that the chemical can produce carbon dioxide, carbon monoxide, and oxides of nitrogen due to thermal decomposition or combustion (KPR ADCOR Inc, 2007). The percentage of each kind of gaseous components in the evolved gas mixture is

unknown. That's why the vent sizing calculation by Fauske's detailed method is done by considering the molecular weight of the gas equal to carbon dioxide, carbon monoxide, and nitrogen dioxide separately. This approach will give a range for area to volume ratio, which will help to choose a safe vent area.

Here,

Test sample mass, $m_t = 64.92 \text{ g} = 6.49 \times 10^{-2} \text{ kg}$

Test freeboard volume, which is the volume difference between test cell and the sample,

$$V = (120-50) \times 10^{-6} \text{ m}^3 = 7 \times 10^{-5} \text{ m}^3$$

Density of VCI 1 Powder, $\rho = 1300 \text{ kg/m}^3$ (KPR ADCOR Inc, 2007)

Venting pressure, $P = 149.7 \text{ Psi} = 1.03 \times 10^6 \text{ Pa}$

Venting temperature, $T = 452.43 \text{ K}$

Maximum pressure rise rate, $\dot{P} = 8.09 \text{ Psi/min} = 930 \text{ Pa/s}$

Gas constant, $R = 8.314 \times 10^3 \text{ J/Kmol} - \text{K}$

Discharge co-efficient, $C_L = 1$ (By considering ideal nozzle flow)

The vent area to volume ratios for VCI 1 powder by using Equation 2.38 for considering different gas molecular weight are tabulated in Table 5-7.

Table 5-7: Area to Volume Ratio for VCI 1 Powder

| Gas Molecular Weight, $M_{\omega,g}$ (kg/Kmol) | Area to Volume Ratio (m^{-1}) |
|--|-----------------------------------|
| Considering molecular weight of carbon dioxide (= 44.01) | 7.10×10^{-6} |
| Considering molecular weight of carbon monoxide (= 28.01) | 5.66×10^{-6} |
| Considering molecular weight of nitrogen dioxide (= 46.04) | 7.26×10^{-6} |

From Table 5-7, it is apparent that the area to volume ratio by considering molecular weight of gas is equal to that of nitrogen dioxide presents the highest value. Therefore, the recommended area to volume ratio for venting for VCI 1 powder is 7.26×10^{-6} , as it provides more conservative estimation.

An open test cell experiment was carried out with VSP2, as the closed test cell was distorted for evolvement of decomposition products. However, in the open cell test, no pressure or temperature rises were observed. The plots of this experiment are included in Appendix 4. When VCI 1 powder was tested with open test cell, the sample reacted badly with the glass fiber insulation,. The reaction product was found to be deposited on the deflector plate, inside the containment vessel and also on the wire connections and, as shown in Figure 5.32 and Figure 5.33. The auxiliary and guard heaters were found broken. So, more careful consideration should be taken if VCI 1 powder is tested with open test cell in the VSP2, or if it is used in open oxidizing environment under pressure.



Figure 5.32: Inside View of Containment Vessel after Performing Open Cell Test in VSP2



Figure 5.33: Deposited Product on the Deflector Plot after Open Cell Test in VSP2

5.5 Discussion

Figure 5.34 shows the area to volume (A/V) ratio for two liquid corrosion inhibitors calculated by Leung's method and Fauske's method for external heating. The vent sizing for both Brenntag corrosion inhibitor and Nox Rust 9800 are done for 1000 kg of initial mass in the vessel and 100 Psig of set pressure. It is seen that the vent area predicted by Leung's method is higher than that predicted by Fauske's method in both cases. Over estimation of the vent area by Leung's method is not unexpected as this method does not consider liquid-vapor disengagement (Leung, 1986). It is also seen that the required vent area for Nox Rust 9800 is higher than that for Brenntag corrosion inhibitor. The percentage of volatile product in Nox Rust 9800 is higher than that presented in Brenntag corrosion inhibitor (Brenntag Canada Inc, 2009; KPR ADCOR Inc, 2003). Hence, the larger vent area requirement for Nox Rust 9800 is apparent.

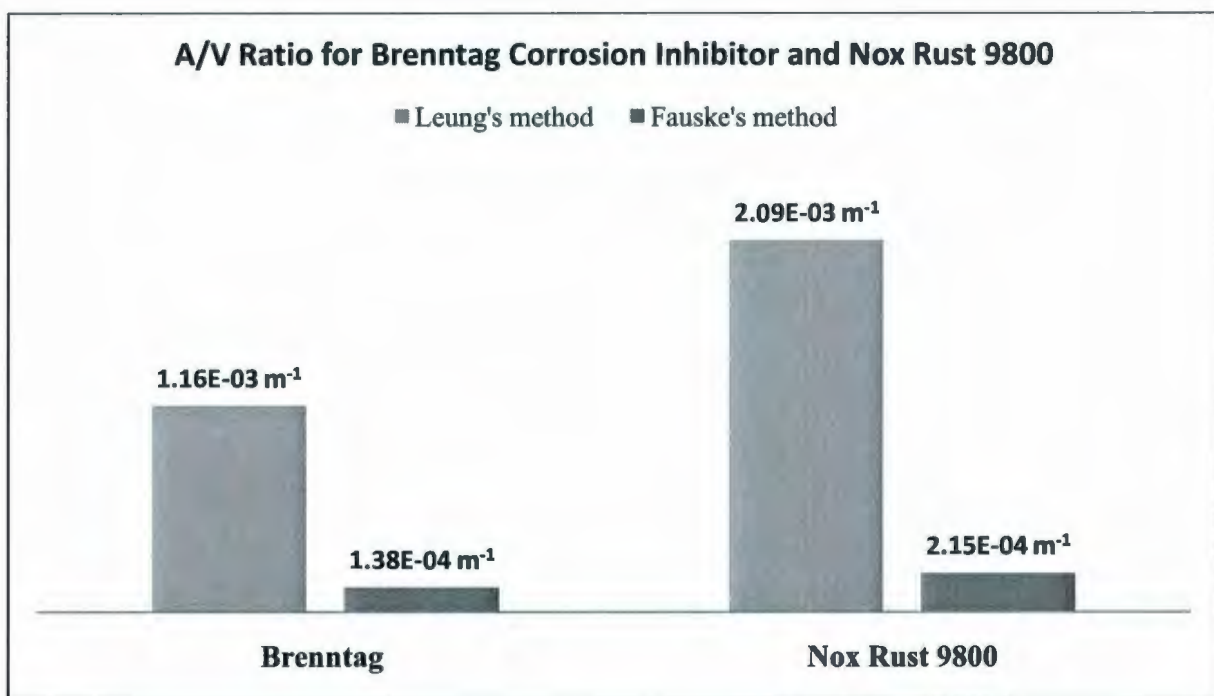


Figure 5.34: Comparison of A/V Ratio Calculated by Leung's Method and Fauske's method for External Heating

The calculations for vent sizing in both cases are done by considering various assumptions such as ideal gas behavior of the evolving vapor and abundance of Clapeyron relation. These assumptions were drawn to calculate the necessary parameters for vent sizing as the properties of the chemicals are proprietary protected. The precise value of these parameters will help to provide more realistic approximation of the vent sizing.

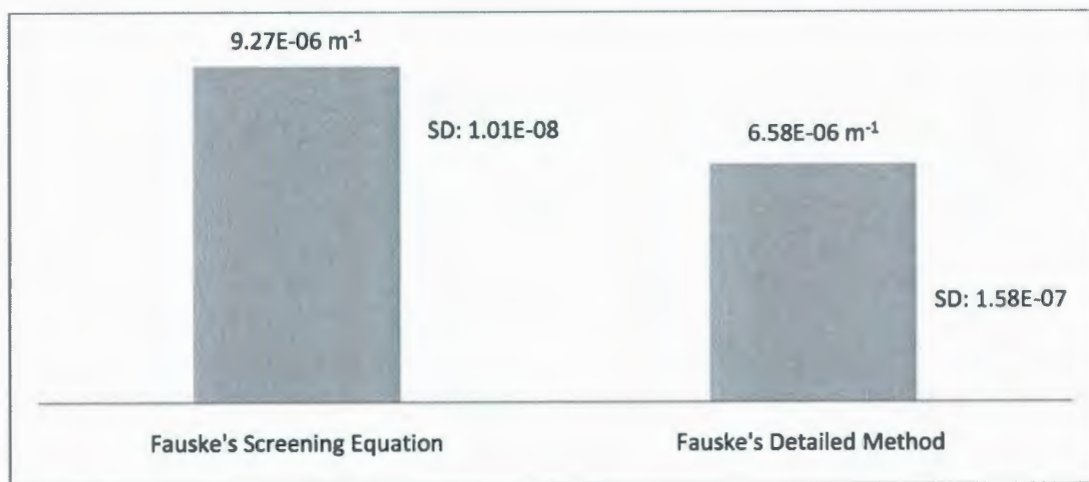


Figure 5.35: Comparison of A/V Ratio for Nox Rust 1100

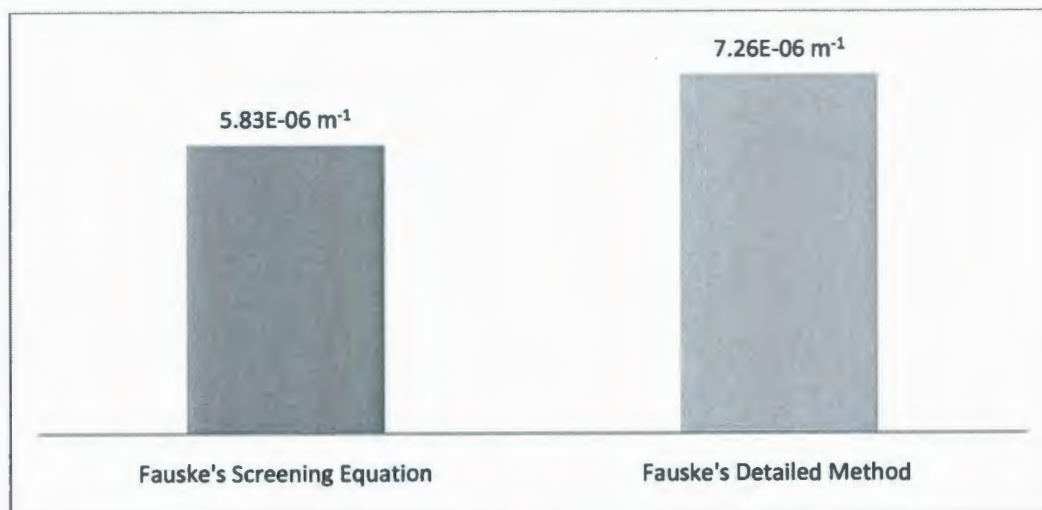


Figure 5.36: Comparison of A/V Ratio for VCI 1 Powder

The vent areas calculated for Nox Rust 1100 and VCI 1 powder have lower values than that for other two corrosion inhibitors. Both systems have small pressure increase rate, which gives smaller vent area requirement. The area to volume ratio calculated by screening equation provides higher value than that of detailed method for Nox Rust 1100. But, for VCI 1 powder, vent area calculated by detailed method provides higher value than that by screening method. So, area to volume ratio for Nox Rust 1100 calculated by screening equation and the area to volume ratio for VCI 1 powder calculated by detailed equation are recommended, as they provide conservative estimate. As VCI 1 powder shows unique reactive behavior in oxidizing environment in presence of metals, more detailed study about VCI 1 powder (e.g. identification of components) is recommended for having better vent size designs.

6 VENT SIZING: HYDROGEN SULFIDE SCAVENGER

This chapter represents the data analysis and vent sizing calculation conducted with VSP2 for formaldehyde solution, monoethanolamine and hydrogen sulfide scavenger samples. The thermal properties of the scavenger and its components have been studied by Vargas (2010). For this work, these samples were tested in the VSP2 with Hastelloy test cells. As the testing was performed in closed test cells, the mass loss for all the samples were less than 5%. As mentioned earlier, VSP2 tests are expensive. Hence, formaldehyde solution was tested in house once and the monoethanolamine was tested by Fauske. The mixture of these two, which is used as H₂S scavenger, was tested twice. The vent sizing calculations are done considering ideal nozzle flow (discharge co-efficient, C_D, is 1).

6.1 Formaldehyde

6.1.1 VSP2 Data

An ARSST test of the formaldehyde solution (37% Formaldehyde 14% Methanol) indicated high pressure (Vargas, 2010) with the increase in temperature. Therefore, 40 ml of the sample was tested in a closed cell VSP2 instead of typical 80 ml of sample volume. Figure 6.1 and Figure 6.2 depict the temperature and pressure profiles for the test respectively. For safety reasons, heating up the sample was stopped when the sample temperature reached 215 °C, as the pressure evolved at that point was 560 Psig. Figure 6.2 shows that a sharp increase in pressure occurs as it reaches

100 Psig. Thus, the venting pressure, which is the pressure at set point, is considered as 100 Psig or 114.7 Psia.

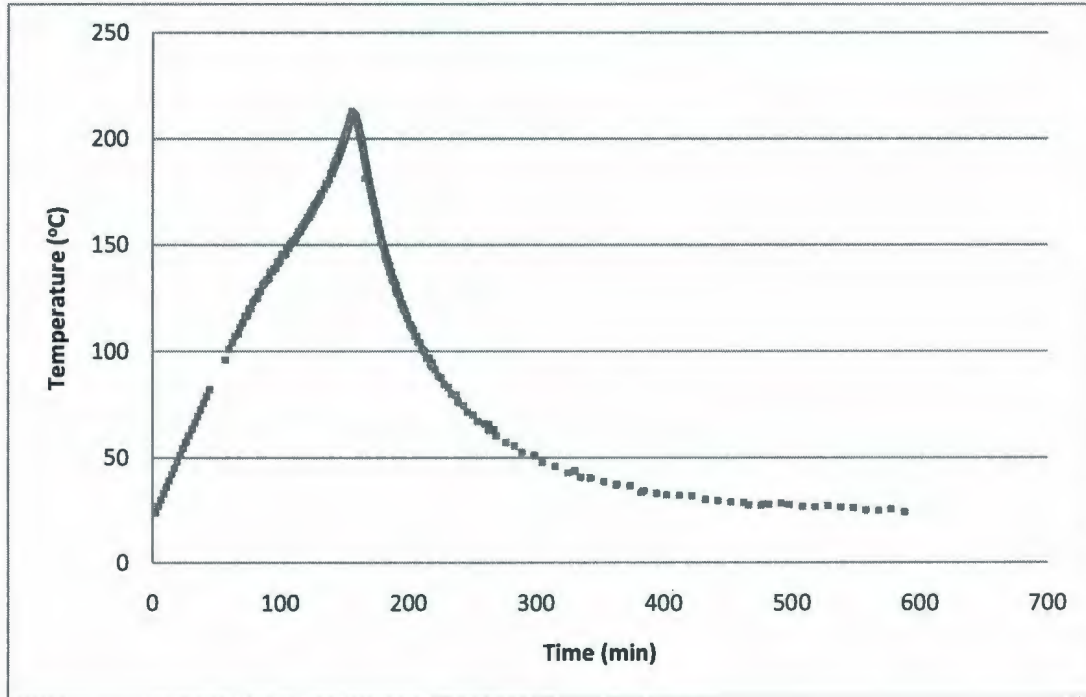


Figure 6.1: Temperature History for Formaldehyde (VSP2 Test)

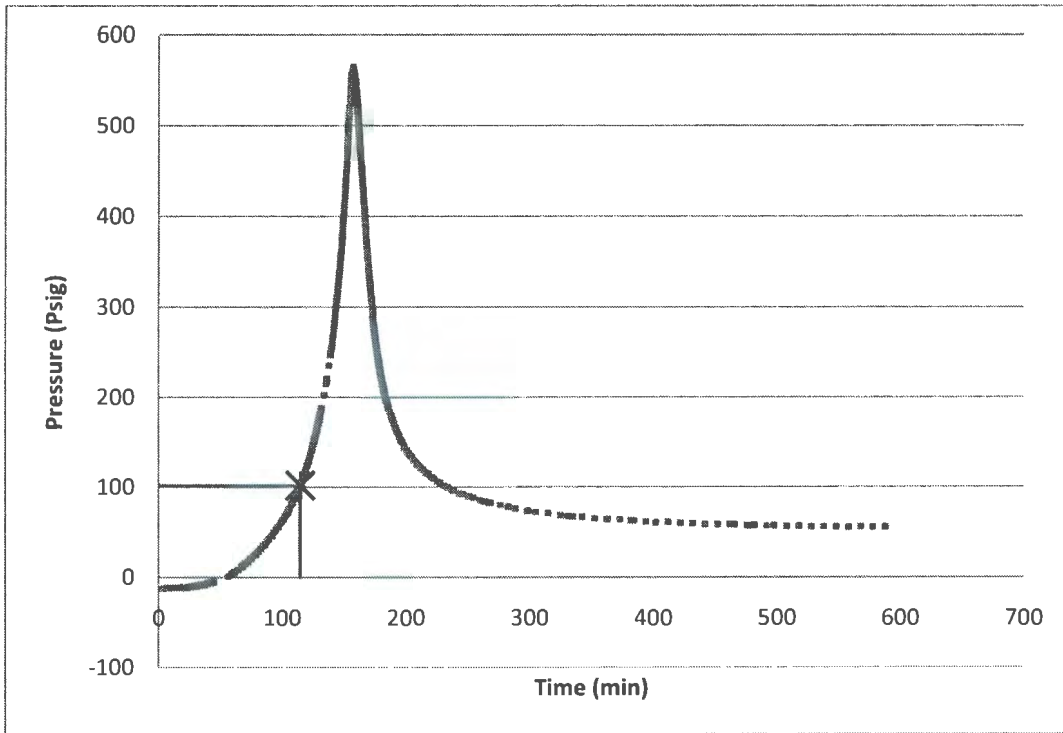


Figure 6.2: Pressure History for Formaldehyde (VSP2 Test)

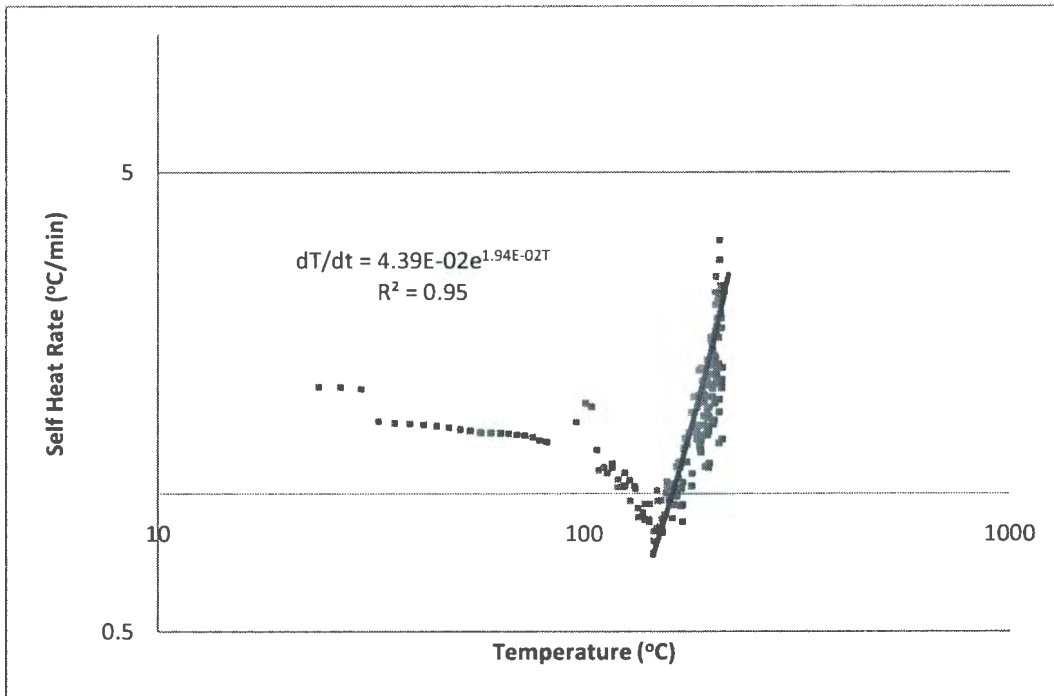


Figure 6.3: Self Heat Rate as a Function of Temperature for Formaldehyde (VSP2 Test)

From Figure 6.3, it is observed that the self heat rate increases with temperature. So, the sample has reactive behaviour. Figure 6.4, which is the plot of pressure as a function temperature ($1/T$) for formaldehyde solution, shows that the end pressure is 70 Psia higher than the starting pressure. Therefore, some non-condensable gas was generated during the heating of the sample and the system can be categorized as a gassy system.

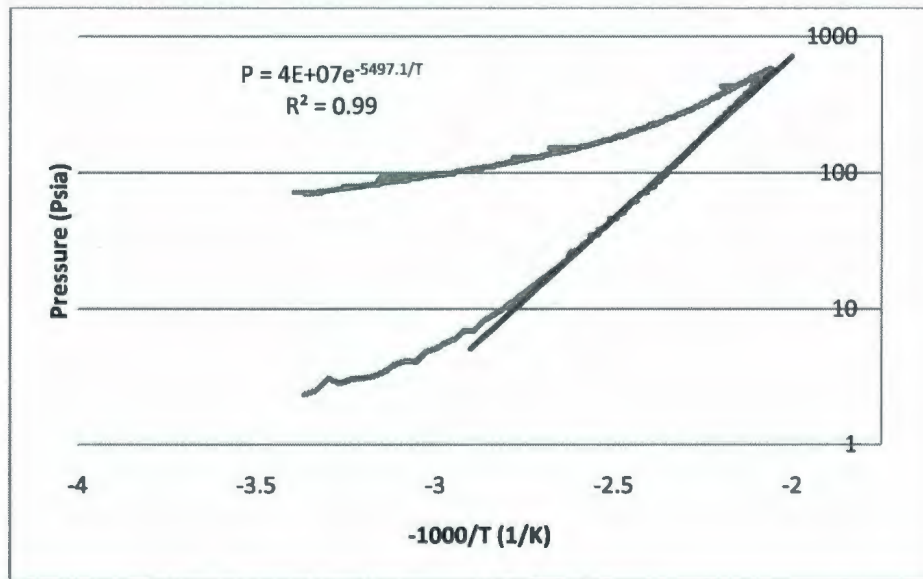


Figure 6.4: Pressure as a Function of Temperature for Formaldehyde (VSP2 Test)

From Figure 6.4, the relation between pressure and temperature is given by Equation 6.1:

$$\ln P = \ln(4 \times 10^7) - \frac{5497.1}{T}$$

$$\text{Or, } \ln P = 17.50 - \frac{5497.1}{T}$$

Equation 6.1

Substituting the venting pressure, which is 114.7 Psia, in Equation 6.1, the venting temperature is calculated as follows:

$$\text{Temperature at the set point, } T_s = 430.74 \text{ K} = 157.59 \text{ }^\circ\text{C}$$

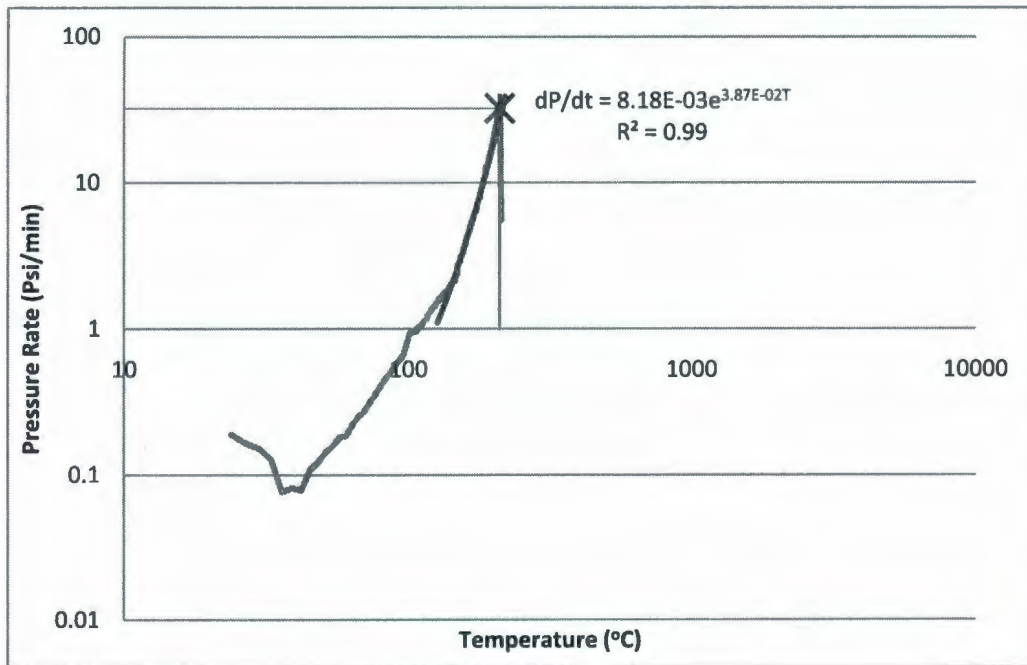


Figure 6.5: Pressure Rate as a Function of Temperature for Formaldehyde (VSP2 Test)

From the pressure as a function of temperature plot (Figure 6.5), an equation correlating the pressure rate with temperature is developed, which is given by Equation 6.2,

$$\dot{P} = 8.18 \times 10^{-3} e^{3.87 \times 10^{-2} T}$$

Equation 6.2

So, maximum pressure rate (\dot{P}), which is observed at 215 °C for this formaldehyde sample, is calculated from Equation 6.2 as follows:

$$\dot{P} = 8.18 \times 10^{-3} e^{3.87 \times 10^{-2} \times 215} \text{ Psi/min} = 33.60 \text{ Psi/min}$$

6.1.2 Vent Sizing

6.1.2.1 Fauske's screening equation for gassy system

Here,

Mass of the sample in test cell, $m = 42.49 \text{ g} = 4.25 \times 10^{-2} \text{ kg}$

Volume of the sample, $v = 40 \text{ ml}$

So, area to volume ratio for formaldehyde according to Equation 5.8,

$$\begin{aligned}\frac{A}{V} &= \frac{3.5 \times 10^{-3} \dot{P}}{C_D P \left[1 + \frac{1.98 \times 10^{-3}}{P^{1.75}} \right]^{0.286}} \times \frac{(120 - 40)}{350} \times \frac{10}{42.49} \\ &= \frac{3.5 \times 10^{-3} \times 33.60}{1 \times 114.7 \left[1 + \frac{1.98 \times 10^{-3}}{114.7^{1.75}} \right]^{0.286}} \times \frac{(120 - 40)}{350} \times \frac{10}{42.49} m^{-1} \\ &= \frac{0.12}{114.7} \times 5.38 \times 10^{-2} m^{-1} \\ &= 5.60 \times 10^{-5} m^{-1}\end{aligned}$$

6.1.2.2 Fauske's detailed equation for gassy system

To apply Fauske's detailed equation for gassy system as described in Section 2.1.6., molecular weight of the gassy system needs to be known. As mentioned earlier the studied sample contains 37% formaldehyde and 14% methanol. While both of the formaldehyde and methanol are heated in absence of oxygen, the main decomposition products at high temperature are carbon monoxide and hydrogen (Fletcher, 1934). The ratio of carbon monoxide and hydrogen present in the evolved gas during the experiment is unknown. However, the molecular weight of hydrogen is much lower than that of carbon monoxide thus could be neglected in this case. As a result, for

the calculation purpose, the gas molecular weight of the sample is considered to be equal to the molecular weight of carbon monoxide.

Here,

Test sample mass, $m_t = 42.49 \text{ g} = 4.25 \times 10^{-2} \text{ kg}$

Test freeboard volume, which is the available volume between test cell and sample,

$$\vartheta = (120-40) \times 10^{-6} \text{ m}^3 = 8 \times 10^{-5} \text{ m}^3$$

Density of formaldehyde solution, $\rho = 1090 \text{ kg/m}^3$

Gas molecular weight, $M_{\omega,g} = 28.01 \text{ kg/Kmol}$

Venting pressure, $P = 114.7 \text{ Psi} = 7.91 \times 10^5 \text{ Pa}$

Venting temperature, $T = 430.74 \text{ K}$

Maximum rate of pressure rise, $\dot{P} = 33.60 \text{ Psi/min} = 3.87 \times 10^3 \text{ Pa/s}$ (from Equation 6.2)

Gas constant, $R = 8.314 \times 10^3 \text{ J/Kmol} - \text{K}$

Hence, area to volume ratio for gassy system using Equation 2.38,

$$\begin{aligned} \frac{A}{V} &= \frac{1}{0.61 C_D} \frac{\rho \vartheta \dot{P}}{m_t P} \left(\frac{M_{\omega,g}}{RT} \right)^{1/2} \\ &= \frac{1}{0.61 \times 1} \times \frac{1090 \times 8 \times 10^{-5} \times 3.87 \times 10^3}{4.25 \times 10^{-2} \times 7.91 \times 10^5} \left(\frac{28.01}{8.314 \times 10^3 \times 430.74} \right)^{1/2} \text{ m}^{-1} \\ &= 4.60 \times 10^{-5} \text{ m}^{-1} \end{aligned}$$

6.2 Monoethanolamine

6.2.1 VSP2 Data

A sample of 40 ml of monoethanolamine was tested with a closed VSP-2 test cell at Fauske's Laboratory (Burr Ridge, Illinois, USA). The cut off temperature was 300 °C and the cut off pressure was 775 Psig. The temperature and pressure profile of the sample are depicted in Figure 6.6 and Figure 6.7, respectively. Figure 6.7 indicates that the pressure increases at a very high rate after reaching 25 Psig pressure. So, the venting pressure is considered as 25 Psig (39.7 Psia). The increase in self-heat rate with temperature is also high for monoethanolamine as shown in Figure 6.8.

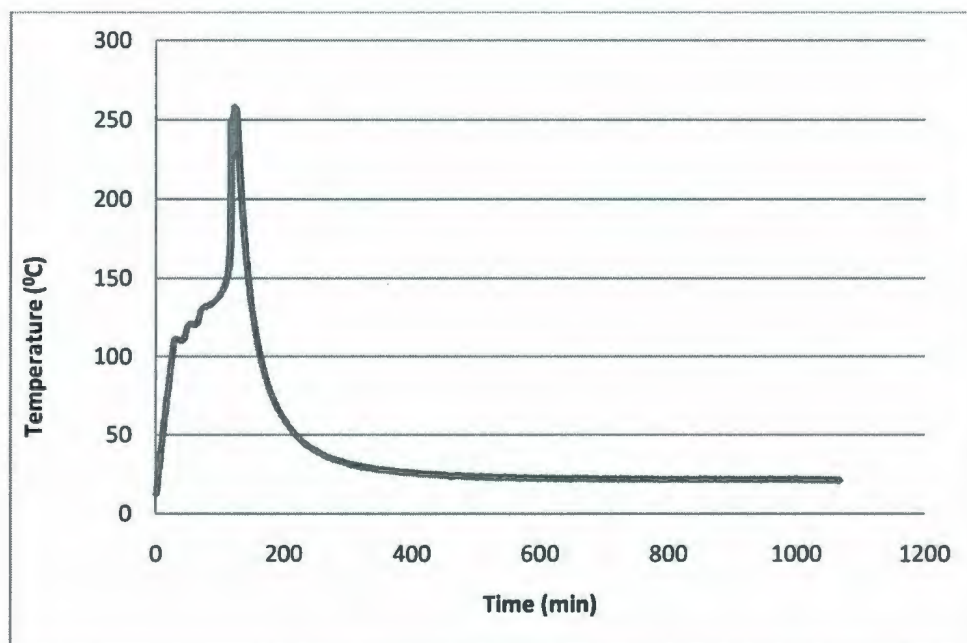


Figure 6.6: Temperature History for Monoethanolamine (VSP2 Test)

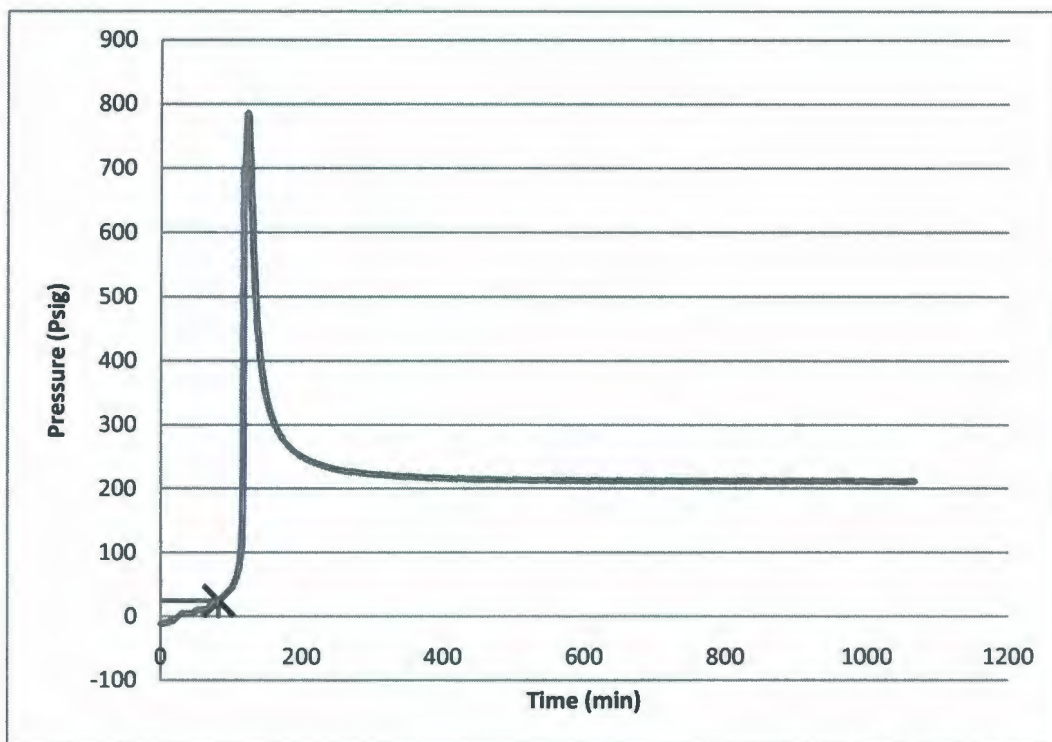


Figure 6.7: Pressure History for Monoethanolamine (VSP2 Test)

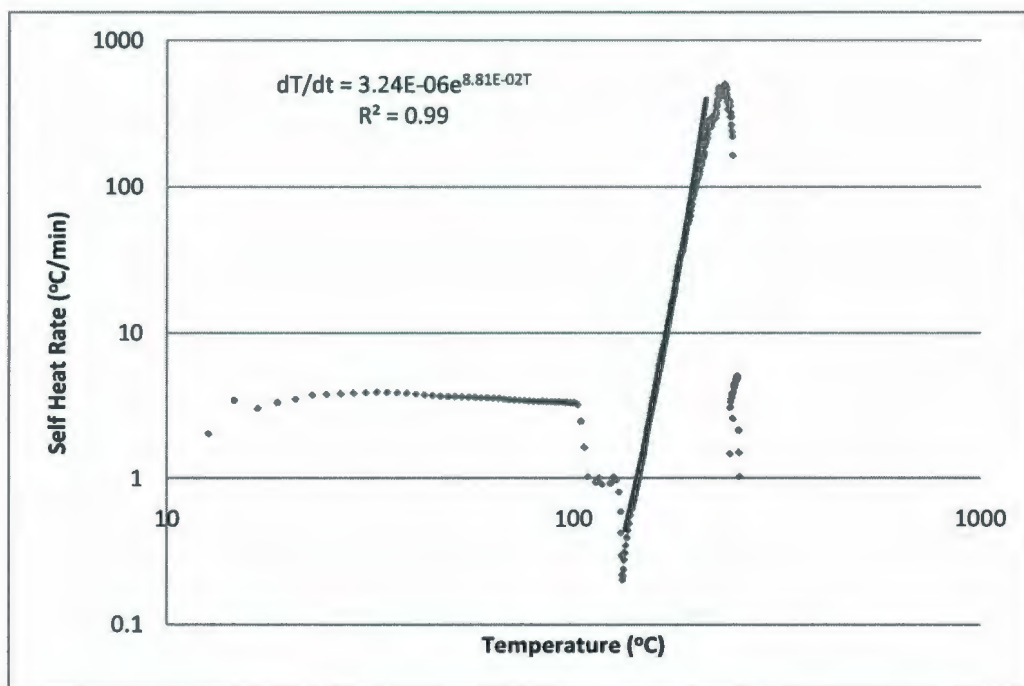


Figure 6.8: Self Heat Rate as a Function of Temperature for Monoethanolamine (VSP2 Test)

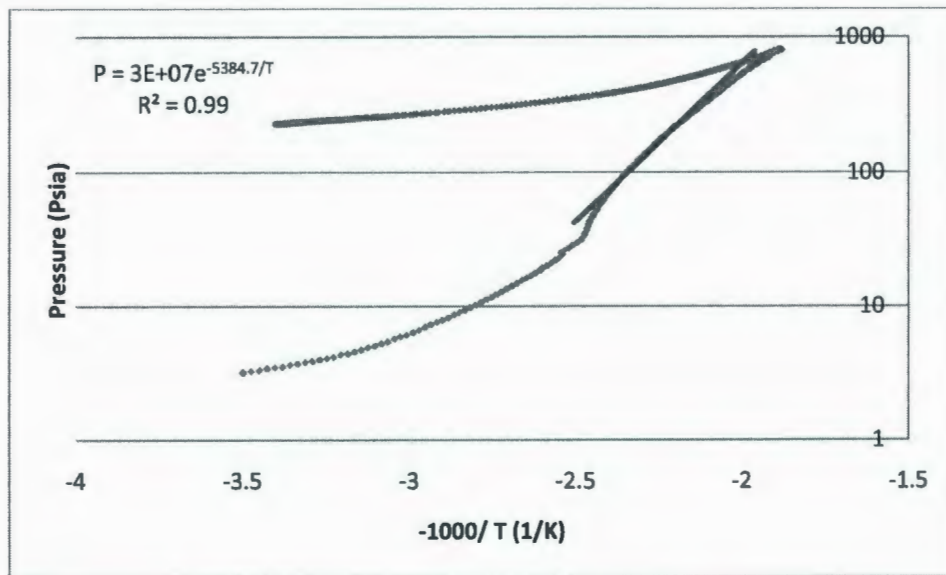


Figure 6.9: Pressure as a Function of Temperature for Monoethanolamine (VSP2 Test)

Figure 6.9, which depicts the pressure behavior as function of temperature ($1/T$), shows that the final pressure is about 230 Psia higher than the starting pressure. Therefore, this system is clearly a gassy system. From Figure 6.9, Equation 6.3 is derived, which shows the relation between temperature and pressure.

$$\ln P = \ln(3 \times 10^7) - \frac{5384.7}{T}$$

$$\text{Hence, } \ln P = 17.22 - \frac{5384.7}{T}$$

Equation 6.3

Substituting the set pressure (25 Psig as observed in Figure 6.7) into Equation 6.3, set temperature can be calculated.

Therefore, temperature at the set point, $T_s = 397.82 \text{ K} = 124.67 \text{ }^\circ\text{C}$

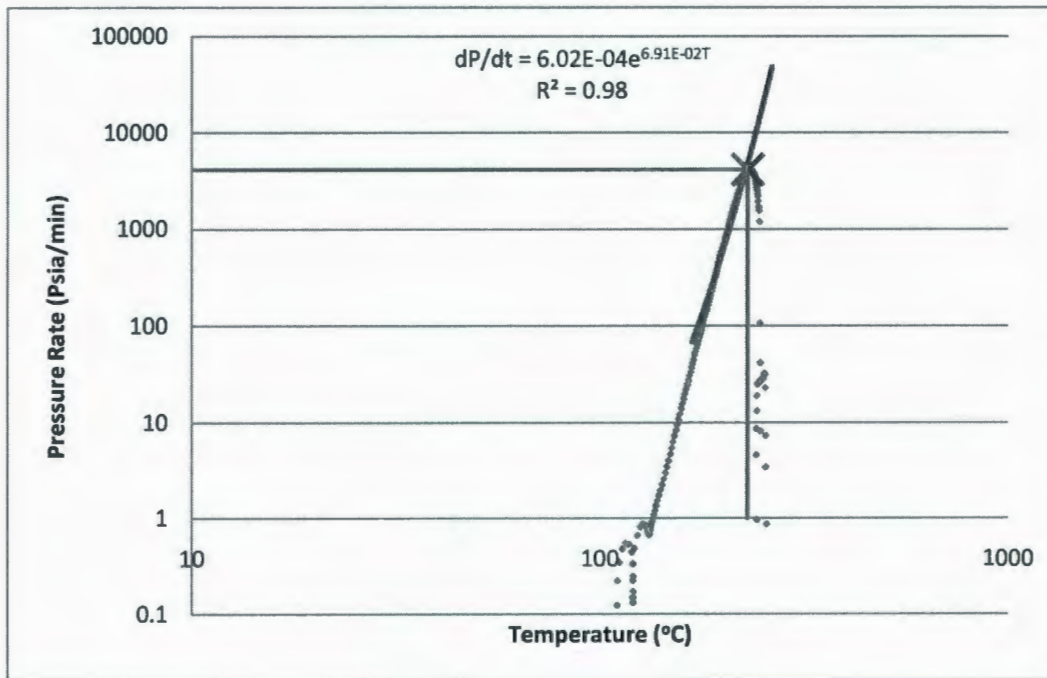


Figure 6.10: Pressure Rate as a Function of Temperature for Monoethanolamine (VSP2 Test)

From Figure 6.10, the pressure rate is expressed as follows:

$$\dot{P} = 6.02 \times 10^{-4} e^{6.91 \times 10^{-2} T}$$

Equation 6.4

Hence, the maximum pressure rate, which is the pressure rate at 230 °C, is calculated as shown below.

$$\dot{P} = 6.02 \times 10^{-4} e^{6.91 \times 10^{-2} \times 230} \text{Psi/min} = 4.81 \times 10^3 \text{Psi/min}$$

6.2.2 6.2.2 Vent Sizing

6.2.2.1 Fauske's screening equation for gassy system

Here,

Mass of the sample in test cell, $m = 45.46 \text{ g} = 4.55 \times 10^{-2} \text{ kg}$

Volume of the sample, $v = 45 \text{ ml}$

So, area to volume ratio for monoethanolamine according to Equation 5.8,

$$\begin{aligned}\frac{A}{V} &= \frac{3.5 \times 10^{-3} \dot{P}}{C_D P \left[1 + \frac{1.98 \times 10^{-3}}{\rho^{1.75}} \right]^{0.286}} \times \frac{(120 - 45)}{350} \times \frac{10}{45.46} m^{-1} \\ &= \frac{3.5 \times 10^{-3} \times 4.81 \times 10^3}{1 \times 39.7 \left[1 + \frac{1.98 \times 10^{-3}}{39.7^{1.75}} \right]^{0.286}} \times \frac{(120 - 45)}{350} \times \frac{10}{45.46} m^{-1} \\ &= \frac{16.84}{39.7} \times 4.71 \times 10^{-2} m^{-1} \\ &= 2.00 \times 10^{-2} m^{-1}\end{aligned}$$

6.2.2.2 Fauske's detailed equation for gassy system

Here,

Test sample mass, $m_t = 45.46 \text{ g} = 4.55 \times 10^{-2} \text{ kg}$

Test freeboard volume, $\vartheta = (120-45) \times 10^{-6} \text{ m}^3 = 7.5 \times 10^{-5} \text{ m}^3$

Density of monoethanolamine, $\rho = 1010 \text{ kg/m}^3$

Venting pressure, $P = 39.7 \text{ Psi} = 2.74 \times 10^5 \text{ Pa}$

Venting temperature, $T = 397.82 \text{ K}$

Maximum rate of pressure rise, $\dot{P} = 4.81 \times 10^3 \text{ Psi/min} = 5.53 \times 10^5 \text{ Pa/s}$

Gas constant, $R = 8.314 \times 10^3 \text{ J/Kmol} \cdot \text{K}$

A compositional analysis is recommended to determine the molecular weight of the evolved gas ($M_{\omega,g}$) with accuracy. However, it is beyond the scope of present study. For this work, the area to volume (A/V) ratio for monoethanolamine was calculated by considering molecular weight of different gases, which are the most possible products of monoethanolamine decomposition, separately. Several manufacturers of monoethanolamine listed in the MSDS of monoethanolamine that it decomposes into carbon dioxide, carbon monoxide, ammonia and oxides of nitrogen, when heated to high temperature (Equistar Chemicals, 2006; Brenntag Canada Inc, 2008; The Dow Chemical Company, 2001; Colonial Chemicals Solutions, Inc, 2008; Lindchem Ltd, 2005).

The values for area to volume ratio for monoethanolamine by using Equation 2.38 are tabulated in Table 6-1.

Table 6-1: Area to Volume Ratio for Monoethanolamine

| Gas Molecular Weight, $M_{\omega,g}$ (kg/Kmol) | Area to Volume Ratio (m^{-1}) |
|--|--|
| Considering molecular weight of carbon dioxide (= 44.01) | 2.01×10^{-2} |
| Considering molecular weight of carbon monoxide (= 28.01) | 1.60×10^{-2} |
| Considering molecular weight of ammonia (= 17.03) | 1.25×10^{-2} |
| Considering molecular weight of nitrogen dioxide (= 46.04) | 2.05×10^{-2} |

A/V ratio as a function of molecular weight is depicted in Figure 6.11 and it is apparent from the plot that the A/V ratio increases with the increase in molecular weight.

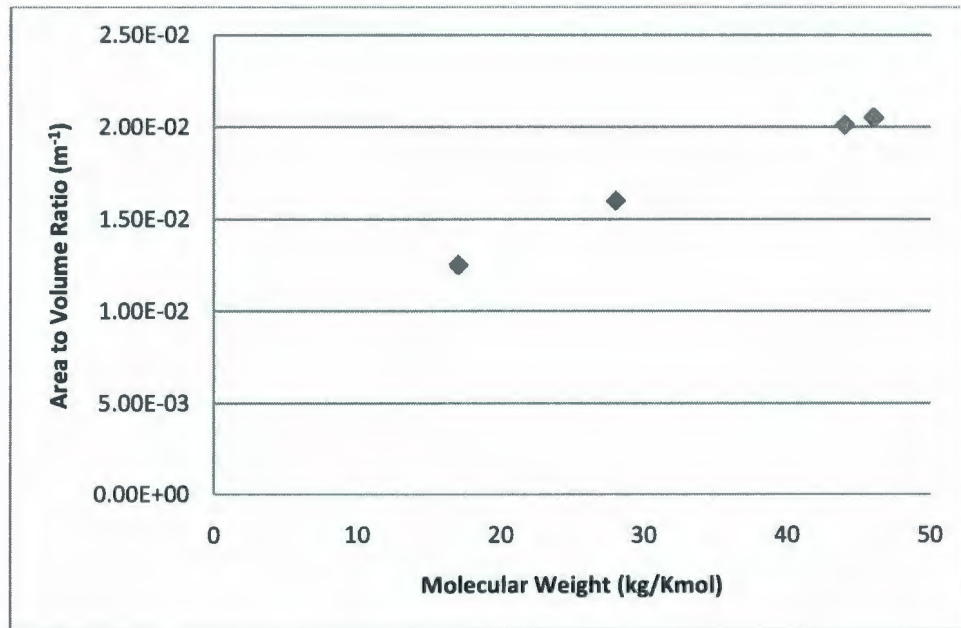


Figure 6.11: Area to Volume Ratio as a Function of gas Molecular Weight

The A/V ratio considering the gas molecular weight and carbon dioxide are equal, provides more conservative estimation. It is also mentioned by the manufacturers that the major decomposition product of monoethanolamine can be carbon dioxide (Equistar Chemicals, 2006; Brenntag Canada Inc, 2008; The Dow Chemical Company, 2001; Colonial Chemicals Solutions, Inc, 2008; Lindchem Ltd, 2005).

Hence, the recommended area to volume ratio for venting this monoethanolamine solution is $2.01 \times 10^{-2} \text{ m}^{-1}$ and this value is similar to the value obtained using Fauske's screening equation.

6.3 Hydrogen Sulphide Scavenger

Two tests were carried out for the hydrogen sulphide scavenger sample. The volume and mass of the sample used for the testing were 40 ml and 44 g, respectively. Hydrogen sulphide scavenger, which is a mixture of 5 units of 37% formaldehyde solution and 2 units of monoethanolamine, were tested in two steps:

1. Monoethanolamine was introduced to formaldehyde in a Hastelloy closed test cell confined in the VSP2 containment vessel through the auxiliary fill line. No heat was applied during this step and the insertion of the samples in the test cell was done at vacuum conditions. A sudden temperature and pressure rise was observed as soon as the two chemicals came into contact. Therefore, mixing these two chemicals results in an immediate exothermic reaction.

2. After the end of the first exotherm, the sample with the test cell was left in the adiabatic environment to cool down. While the temperature came down to around 30 °C, then heat was introduced. A second exotherm (sudden increase in pressure and temperature) was observed after heating up to 108 °C.

The heat of mixing evolved in the first step and the vent sizing characterization for the exotherm that occurred at the second step are discussed in the subsequent sections. The second exotherm is the most reactive exotherm and as a result the vent area is calculated for the second exotherm and this area will be adequate for the first and second pressurization condition.

6.3.1 Heat of Mixing Calculation

Heat of mixing can be calculated by using Equation 6.5 (Fauske and Associates Inc., 2007 a).

$$\Delta H_{mixing} = \frac{mC_p\Delta T}{n}$$

Equation 6.5

The mass and molar amounts of the components are tabulated in Table 6-2. For this mixture, monoethanolamine is the limiting reagent. The temperature rise due to the heat of mixing can be calculated from the temperature history for the first step of the test as depicted in Figure 6.12.

Table 6-2: Weight, Mass Fraction and Molar Quantity of the H₂S Scavenger Components

| Component | Units used in the test (by weight) | Mass fraction | Weight of the component used in the test (g) | Molecular weight of the component (g) | Component used (mol) |
|------------------|------------------------------------|---------------|--|---|----------------------|
| 37% Formaldehyde | 5 | 0.71 | 31.77 | 30.03 (Mallinckrodt Baker Inc, 2007) | 1.06 |
| Monoethanolamine | 2 | 0.29 | 12.91 | 61.08 (The Dow Chemical Company, 2001) | 0.21 |

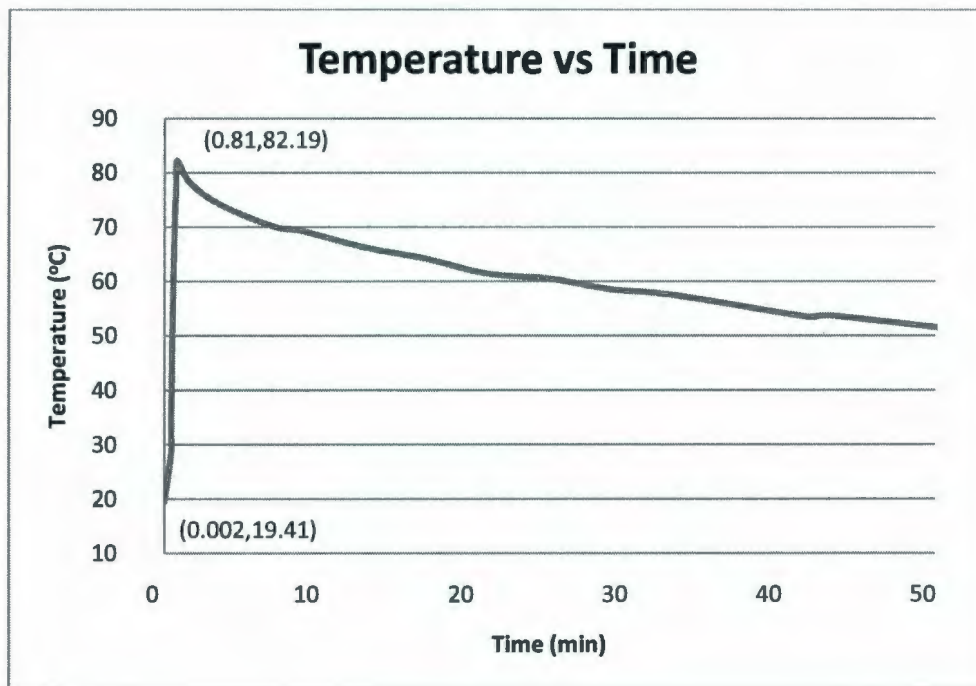


Figure 6.12: Temperature History due to the Heat of Mixing (VSP 2 Test)

Now,

Specific heat capacity of formaldehyde at 25 °C = 3121 J/ kg-K (Brenntag Canada Inc, 2007)

Specific heat capacity of monoethanolamine at 25 °C = 2784 J/kg-K (INEOS LLC)

Hence, the specific heat capacity of the H₂S scavenger at 25 °C,

$$C_p = (0.71 \times 3121 + 0.29 \times 2784) \text{ J/kg-K} = 3.02 \times 10^3 \text{ J/ kg-K}$$

Here,

Total mass of sample, $m = 44.68 \text{ g} = 4.47 \times 10^{-2} \text{ kg}$

Specific heat capacity of mixture, $C_p = 3.02 \times 10^3 \text{ J/ kg-K}$

Temperature rise after mixing, $\Delta T = (82.19 - 19.41) \text{ }^\circ\text{C}$

$$= \{(82.19 + 273) - (19.41 + 273)\} \text{ K}$$

$$= 62.78 \text{ K}$$

Moles of limiting reagent, $n = 0.21$

Therefore, heat of mixing of the H₂S scavenger mixture,

$$\Delta H_{mixing} = \frac{4.47 \times 10^{-2} \times 3.02 \times 10^3 \times 62.78}{0.21} \text{ J/mol} = 40.36 \text{ KJ/mol}$$

The heat of mixing calculation for the second sample test is given in Appendix 5. So, the average heat of mixing for this H₂S scavenger mixture in a closed environment is 38.83 KJ/mol with a standard deviation of 1.53 KJ/mol. Vargas (2010) measured the heat of mixing for the same mixture in an open test cell environment by using the ARSST. Heat of mixing for the scavenger sample in an open environment is 25.09 KJ/mol with a standard deviation of 0.8 KJ/mol (Vargas, 2010). Hence, the heat of mixing of this sample for a closed environment is higher than that for an open environment.

6.3.2 VSP-2 Data for Second Step

The temperature and pressure profiles for the two tests conducted for the scavenger sample in VSP-2 are depicted in Figure 6.13 and Figure 6.14, respectively. As mentioned earlier, a sharp increase in temperature was observed after reaching 108 °C. Figure 6.14 shows that there is a sharp increase in pressure after reaching 25 Psig. So, the venting pressure is considered 25 Psig for this sample. From the plots of these two tests, it is apparent that VSP2 data for reactive systems are more repeatable than ARSST data. It is because that VSP2 is capable of continuous and automatic tracking of pressure and adiabatic temperature.

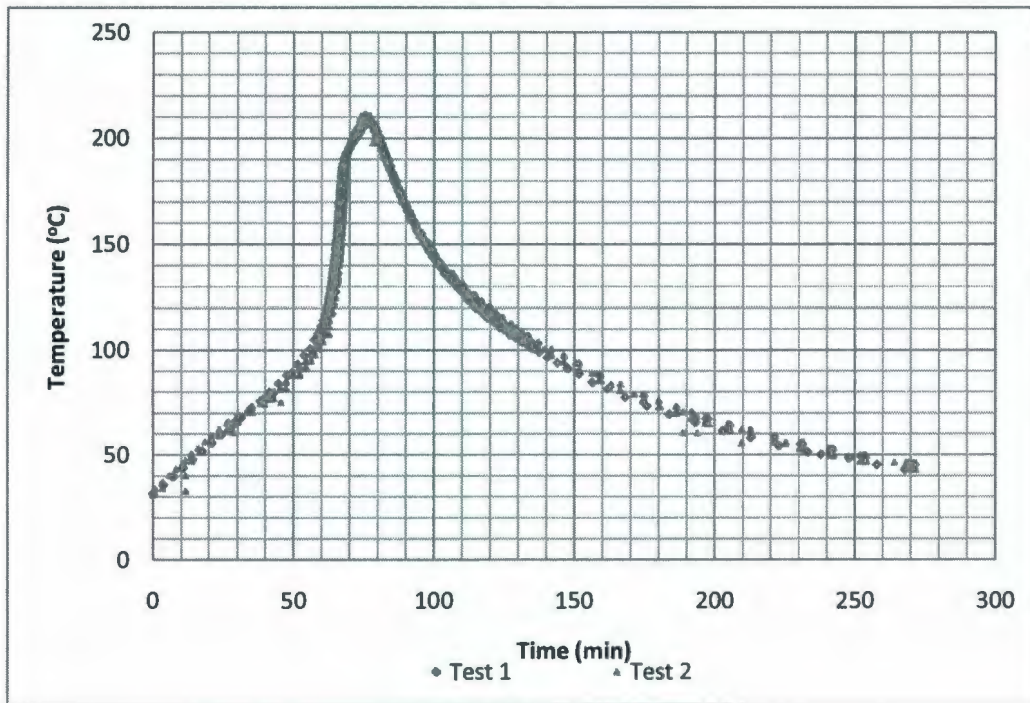


Figure 6.13: Temperature History for H₂S Scavenger (VSP2 Tests)

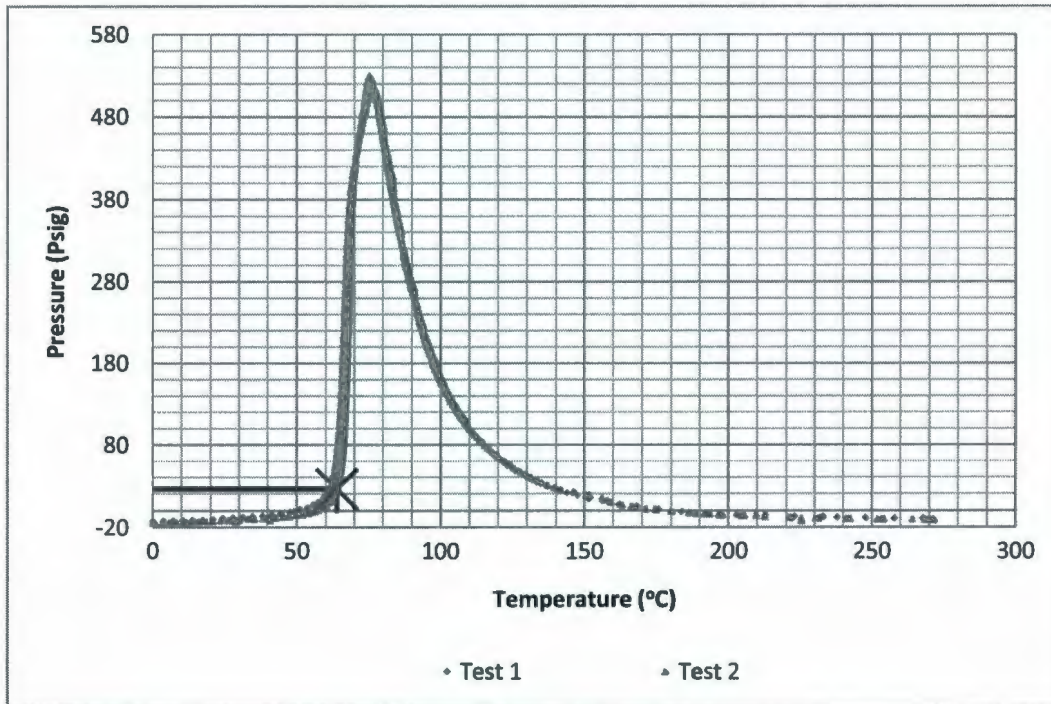


Figure 6.14: Pressure History for H₂S Scavenger (VSP2 Tests)

Figure 6.15 is the plot for pressure rate as a function of temperature and it is apparent from the plot that pressure rate increase significantly with temperature.

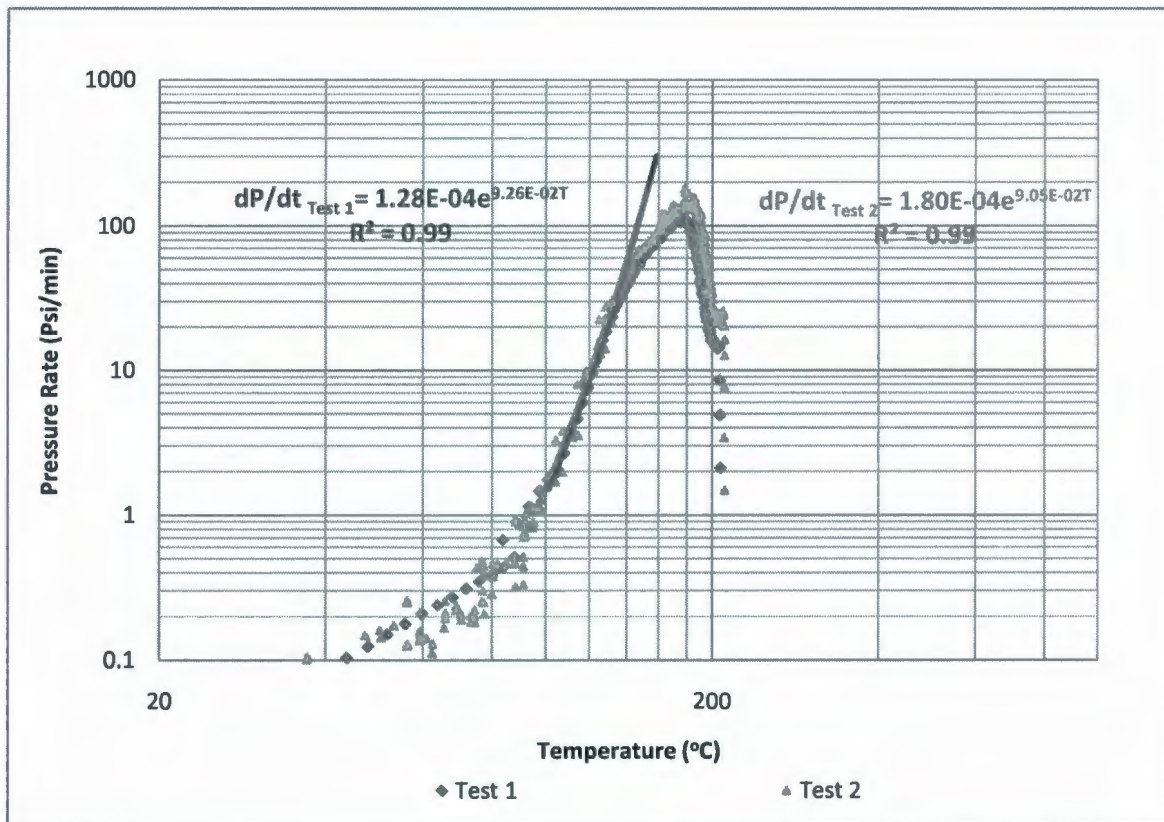


Figure 6.15: Pressure Rate as a Function of Temperature for H₂S Scavenger (VSP2 Tests)

Figure 6.16, which is the pressure as a function of temperature plot, shows that the end pressure is only 3 Psia higher than the initial pressure for both tests. The reason for this low pressure rise may be that the sample was not cooled down exactly to the room temperature after mixing and prior to the starting of the second step of the test. The temperature of the mixture at the starting of the second step was 32 °C. Moreover, the mixing was conducted in vacuum and formaldehyde was introduced in the test cell at the very start of the procedure. As formaldehyde has a very low boiling point, which is 19 °C, it might cause some decomposition at the condition that slightly

increase the system pressure. Any decomposition product due to the heating of the mixture did not produce and thus the sample can be categorized as a vapor system.

The necessary parameters for vent sizing will be described in the subsequent sections. The parameter calculation for only the first test will be described here and the parameter calculations for the other test are described in Appendix 5.

6.3.2.1 *Phi factor (ϕ) calculation (for Test 1):*

Given,

Specific heat capacity of the Hastelloy test cell, $C_{pb} = 425 \text{ J/kg-K}$ (Shanghai eshine Stainless steel Material Co., Ltd)

Specific heat capacity of 37% formaldehyde at $90^\circ\text{C} = 3.65 \times 10^3 \text{ J/kg-K}$ (Section 4.2.1)

Specific heat capacity of monoethanolamine at $90^\circ\text{C} = 3.17 \times 10^3 \text{ J/kg-K}$ (Section 4.2.2)

Hence, Specific heat capacity of H_2S Scavenger at 90°C ,

$$\begin{aligned} C_{ps} &= 0.71 \times 3.65 \times 10^3 + 0.29 \times 3.17 \times 10^3 \text{ J/kg-K} \\ &= 3.51 \times 10^3 \text{ J/kg-K} \end{aligned}$$

Mass of the sample, $m_s = 44.68 \text{ g} = 4.47 \times 10^{-2} \text{ kg}$

Mass of the test cell, $m_b = 50.27 \text{ g} = 5.03 \times 10^{-2} \text{ kg}$

So, Phi factor of the test cell by using Equation 2.1,

$$\phi = 1 + \frac{m_b C_{pb}}{m_s C_{ps}} = 1 + \frac{5.03 \times 10^{-2} \times 425}{4.47 \times 10^{-2} \times 3.51 \times 10^3} = 1.13$$

6.3.2.2 *Determining set pressure (P_s), set temperature (T_s) and $\frac{dP}{dT}$ (Test 1):*

As mentioned earlier, the set pressure for venting is considered 25 Psig as the pressure rise is comparatively higher after this point as shown in Figure 6.14. Set pressure is the pressure when

the relief device is known to be fully open. However, for a safety valve, a 10% overpressure is often needed to fully open the valve. Considering a 20% overpressure reduces the required vent area significantly for a reactive system vent sizing. Leung (1986) studied that calculated vent area considering 20% overpressure condition is able to give a safe but less conservative estimation.

Here,

$$\text{Pressure at set point, } P_s = 25 \text{ Psig} = 39.7 \text{ Psia} = 2.74 \times 10^5 \text{ Pa}$$

Let,

$$\text{Maximum allowable working pressure, MAWP} = 27.5 \text{ Psig} = 42.20 \text{ Psia} = 2.91 \times 10^5 \text{ Pa}$$

$$\text{Venting pressure by considering 20\% over pressure, } P_m = 30 \text{ Psig} = 44.7 \text{ Psia} = 3.08 \times 10^5 \text{ Pa}$$

$$\text{Pressure difference for considering 20\% over pressure, } \Delta P = P_m - P_s = (3.08 \times 10^5 - 2.74 \times 10^5) \text{ Pa}$$

$$= 3.40 \times 10^4 \text{ Pa}$$

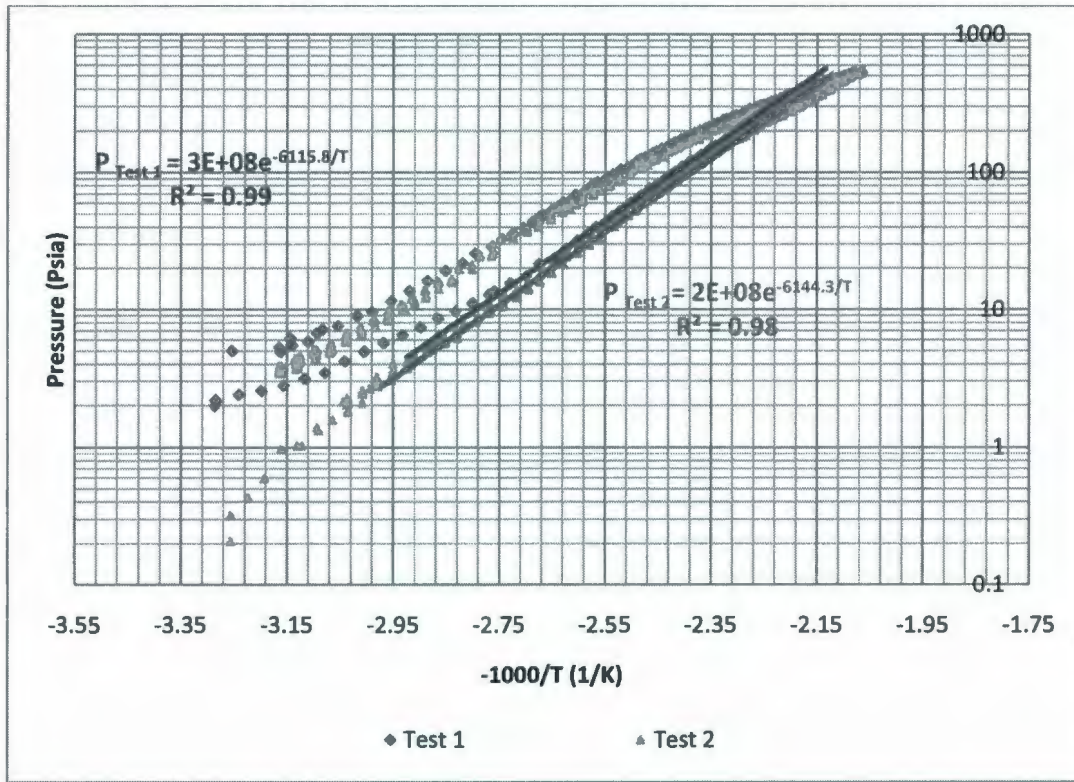


Figure 6.16: Pressure as a Function of Temperature for H₂S Scavenger (VSP 2 Tests)

From Figure 6.16, a relation between pressure and temperature is obtained, as given by Equation 6.5.

$$\ln P = \ln(3 \times 10^8) - \frac{6115.8}{T}$$

$$\text{So, } \ln P = 19.52 - \frac{6115.8}{T}$$

Equation 6.5

By substituting the value of set pressure (39.7 Psia), maximum allowable working pressure (42.20 Psia) and venting pressure (44.7 Psia) in Equation 6.5, the following values of temperature are calculated,

Temperature at the set point, $T_s = 386.15 \text{ K} = 113 \text{ }^\circ\text{C}$

Maximum allowable temperature, $T_{MAWP} = 387.64 \text{ K} = 114.50 \text{ }^\circ\text{C}$

Venting temperature, $T_m = 389.06 \text{ K} = 115.91 \text{ }^\circ\text{C}$

Temperature difference, $\Delta T = T_m - T_s = (389.06 - 386.15) \text{ K} = 2.91 \text{ K}$

By differentiating the Equation 6.5 (Fauske, 1985),

$$\frac{1}{P} \frac{dP}{dT} = \frac{6115.8}{T^2}$$

$$\text{Hence, } \frac{dP}{dT} = \frac{6115.8 P}{T^2}$$

Equation 6.6

$$\text{So, } \frac{dP}{dT} (\text{at set pressure and temperature}) = \frac{6115.8 \times 2.74 \times 10^5}{386.15^2} \text{ Pa/K} = 1.12 \times 10^4 \text{ Pa/K}$$

6.3.2.3 Temperature rate at set point $\left(\frac{dT}{dt}\right)_s$ and temperature rate at venting $\left(\frac{dT}{dt}\right)_m$ calculation (for Test 1):

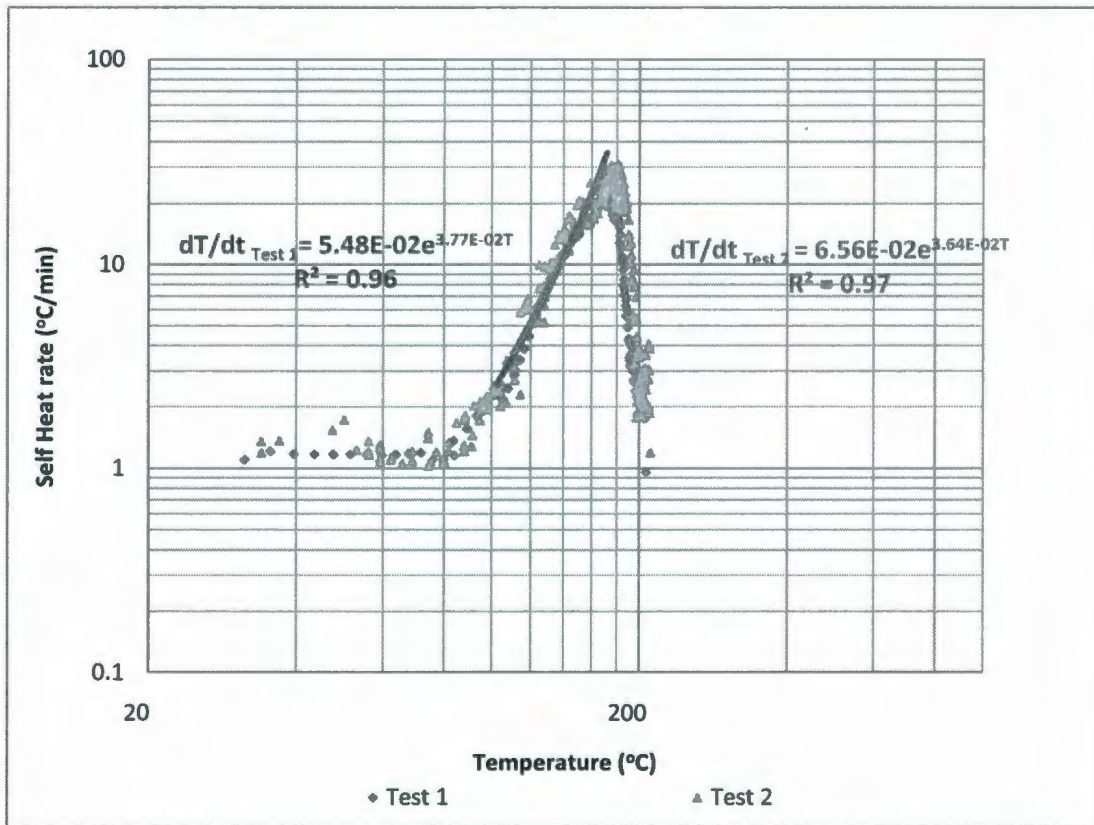


Figure 6.17: Self Heat Rate as a Function of Temperature for H₂S Scavenger (VSP 2 Tests)

From Figure 6.17,

$$\frac{dT}{dt} = 5.48 \times 10^{-2} e^{3.77 \times 10^{-2} T}$$

Equation 6.7

Hence, From Equation 6.7,

$$\begin{aligned} \text{Temperature rate at set point (113 } ^\circ\text{C)}, \left(\frac{dT}{dt}\right)_s &= 5.48 \times 10^{-2} e^{3.77 \times 10^{-2} \times 113} \text{ } ^\circ\text{C/min} \\ &= 3.88 \text{ } ^\circ\text{C/min} \\ &= 6.47 \times 10^{-2} \text{ K/s} \end{aligned}$$

$$\begin{aligned}
 \text{Temperature rate at venting (115.91 } ^\circ\text{C), } \left(\frac{dT}{dt}\right)_m &= 5.48 \times 10^{-2} e^{3.77 \times 10^{-2} \times 115.91} \text{ } ^\circ\text{C/min} \\
 &= 4.33 \text{ } ^\circ\text{C/min} \\
 &= 7.22 \times 10^{-2} \text{ K/s}
 \end{aligned}$$

6.3.2.4 Calculation of average heat release rate (q) and heat release rate at the set point (q_s) (for Test 1):

For H₂S scavenger, temperature rate is calculated from the self heat rate as a function of temperature plot as it is a reactive vapor system having a sharp increase in self heat rate. The equation for calculating heat release rate for the scavenger considers the average of the temperature rate at set point and the temperature rate at maximum point as suggested by Leung (1986).

Average heat release rate (Leung, 1986),

$$q = \frac{1}{2} \phi C_p \left[\left(\frac{dT}{dt}\right)_s + \left(\frac{dT}{dt}\right)_m \right]$$

Equation 6.8

Hence, Average heat release rate,

$$q = \frac{1}{2} \times 1.13 \times 3.51 \times 10^3 \times [6.47 \times 10^{-2} + 7.22 \times 10^{-2}] \text{ J/ kg-s} = 273.90 \text{ J/ kg-s}$$

Heat release rate at set temperature,

$$q_s = \phi C_p \left(\frac{dT}{dt}\right)_s$$

Equation 6.9

Hence, Heat release rate at set temperature,

$$q_s = 1.13 \times 3.51 \times 10^3 \times 6.47 \times 10^{-2} \text{ J/ kg-s} = 256.62 \text{ J/ kg-s}$$

6.3.2.5 Vapor density (ρ_v) and vapor specific volume (v_g) calculation (for Test 1):

Here,

Molecular weight of 37% formaldehyde solution = 30.03 kg/ Kmol (Mallinckrodt Baker Inc, 2007)

Molecular weight of monoethanolamine = 61.08 kg/ Kmol (The Dow Chemical Company, 2001)

Molecular weight of H₂S Scavenger, $M_w = (0.71 \times 30.03 + 0.29 \times 61.08)$ kg/ Kmol
= 39.03 kg/ Kmol

Molar gas constant, $R = 8.314 \times 10^3$ J/Kmol - K

From Equation 5.5, vapor density of H₂S scavenger at set temperature and pressure can be calculated as follows,

$$\rho_v = \frac{39.03 \times 2.74 \times 10^5}{8.314 \times 10^3 \times 386.15} \text{ Kg/m}^3 = 3.33 \text{ kg/m}^3$$

And, vapor specific volume,

$$v_g = \frac{1}{\rho_v} = 0.30 \text{ m}^3/\text{kg}$$

6.3.2.6 Latent heat of vaporization (h_g or λ) calculation (for Test 1):

Latent heat of vaporization (h_g) can be calculated from Clapeyron relation as shown in Equation 5.6 (Leung, 1986)

Hence, the latent heat of vaporization for H₂S scavenger for test 1,

$$\text{So, } h_g = \lambda = v_g T \frac{dP}{dT} = 0.30 \times 386.15 \times 1.12 \times 10^4 \text{ J/kg} = 1.30 \times 10^6 \text{ J/kg}$$

6.3.2.7 Critical mass flux (G) calculation:

The critical mass flux for two phase flow can be calculated by using Equation 2.31 described in Chapter 2 (Leung, 1986).

Hence, critical mass flux for test 1,

$$G = 0.9 \frac{\lambda}{v_g} \left(\frac{1}{c_p T} \right)^{0.5} = 0.9 \times \frac{1.30 \times 10^6}{0.30} \times \left(\frac{1}{3.51 \times 10^3 \times 386.15} \right)^{0.5} \text{ Kg/m}^2\text{-s} = 3.35 \times 10^3 \text{ kg/m}^2\text{-s}$$

The average value and standard deviation of the parameters from the two tests are depicted in Table 6-3 and details of the calculation are available in Appendix 5.

Table 6-3: Independent and Dependent Variables for Vent Sizing for H₂S Scavenger

| | Parameters | Notation | Value | Unit |
|-----------------------|--|---|---|----------------------|
| Independent Variables | Mass of the sample in test cell | m_s | $4.55 \times 10^{-2} \pm 1.50 \times 10^{-3}$ | kg |
| | Specific heat capacity of Nox Rust 9800 @ 90°C (Section 4.1.2) | C_{ps} | 3.51×10^3 | J/ kg-K |
| | Mass of the test cell | m_b | $5.11 \times 10^{-2} \pm 8.35 \times 10^{-4}$ | kg |
| | Specific heat capacity of the stainless steel test cell @ 25°C | C_{pb} or C_p | 425 | J/ kg-K |
| | Pressure at set point | P_s or P | 2.74×10^5 | Pa |
| | Molecular weight (Sciencelab.com Inc, 2008) | M_w | 39.03 | kg/ Kmol |
| | Density of Nox Rust 9800 (Brenntag Canada Inc, 2009) | ρ_l | 1066.80 | kg/m ³ |
| | Initial mass in vessel | m_o | 1000 | kg |
| Dependent Variables | Phi factor of the test cell | ϕ | 1.135 $\pm 5 \times 10^{-3}$ | Dimensionless |
| | Vent pressure for 20% over pressure | P_m | 3.08×10^5 | Pa |
| | Pressure difference | $\Delta P = P_m - P_s$ | 3.40×10^4 | Pa |
| | Temperature at set point | T_s or T | 392.15 ± 6.00 | K |
| | Venting Temperature | T_m | 395.14 ± 6.08 | K |
| | Temperature Difference | $\Delta T = T_m - T_s$ | 3.00 $\pm 8.5 \times 10^{-2}$ | K |
| | $\frac{dP}{dT}$ @ set pressure | $\frac{dP}{dT}$ | $1.09 \times 10^4 \pm 300$ | Pa/ K |
| | Temperature rate @ set point | $\left(\frac{dT}{dt}\right)_s$ or \dot{T} | $8.24 \times 10^{-2} \pm 1.77 \times 10^{-2}$ | K/s |
| | Temperature rate @ venting | $\left(\frac{dT}{dt}\right)_m$ | $9.11 \times 10^{-2} \pm 1.89 \times 10^{-2}$ | K/s |
| | Heat release rate | q | 347.03 ± 73.13 | J/ kg-s |
| | Heat release rate at set point | q_s | 328.38 ± 71.76 | J/ kg-s |
| | Vapor density | ρ_v | $3.28 \pm 5 \times 10^{-2}$ | kg/m ³ |
| | Vapor specific volume | v_g | $3.05 \times 10^{-1} \pm 5 \times 10^{-3}$ | m ³ / kg |
| | Latent heat of vaporization | h_g or λ | $1.305 \times 10^6 \pm 5 \times 10^3$ | J/kg |
| | Critical mass flux | G | $3.29 \times 10^3 \pm 65$ | kg/m ² -s |
| | Volume of the chemical in the tank | V | 0.94 | m ³ |
| | Specific volume of the liquid in vessel | v | 9.4×10^{-4} | m ³ /kg |

6.3.3 Vent Sizing Calculation

6.3.3.1 *Leung's method for homogenous venting with 20% overpressure*

The vent sizing by Leung's method are done by considering 1000 kg of initial mass and the effective volume of the chemical corresponding to this mass is calculated. At first, Vent rate (W) is calculated by using Equation 2.21. For calculating vent area by Equation 2.21, specific heat capacity at constant pressure is used instead of specific heat capacity at constant volume as suggested by Leung (1986). Subsequently, dividing this vent rate with heat mass flux, vent area is calculated. The average area to volume ratio for the performed two tests is $4.10 \times 10^{-3} \text{ m}^{-1}$. The detailed calculation is given in Appendix 5.

6.3.3.2 *Leung's method for homogenous venting with no overpressure*

For calculating vent area for homogeneous flow without overpressure, the limiting formula by considering $\Delta P = 0$ and $\Delta T = 0$ is used, as described in Section 2.1.5.1. In this case, the heat release at the set point is considered instead of the average heat release rate. The calculation details are given in Appendix 5. The established average area to volume ratio by Leung's method for no overpressure is $2.67 \times 10^{-2} \text{ m}^{-1}$ with a standard deviation of $6.60 \times 10^{-3} \text{ m}^{-1}$.

6.3.3.3 Fauske's short form equation for runaway chemical reaction under their own vapour pressure

This method was developed to have a screening value of vent area by considering homogenous flow. It is only applicable for a reactive system having a vapor phase behavior. A monogram was developed by Fauske (1984) by using the developed equation, Equation 2.39. This method is described in Section 2.1.7. Average area to volume ratio for H₂S scavenger sample by Fauske's short form of equation is found to be $8.76 \times 10^{-3} \text{ m}^{-1}$. The detail of the calculation is illustrated in Appendix 5.

6.3.3.4 Fauske's screening equation for vapour system

A screening equation was developed by Fauske to have an initial idea about the vent sizing for vapor system. It is a screening tool to characterize chemicals having unknown physical and chemical properties. The equation was developed by considering the physical and chemical properties of water at ambient condition. In Section 2.1.9, this method is already discussed. The estimated average area to volume ratio by this screening equation for H₂S scavenger sample is $8.87 \times 10^{-4} \text{ m}^{-1}$ with a standard deviation of $2.03 \times 10^{-4} \text{ m}^{-1}$ for the two performed tests. The calculation for vent area for the two conducted tests is given in Appendix 5.

6.4 Discussion

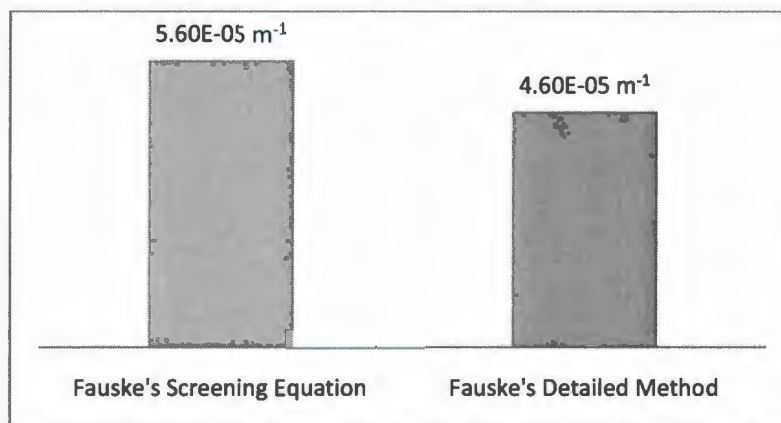


Figure 6.18: Comparison of A/V Ratio for 37% Formaldehyde

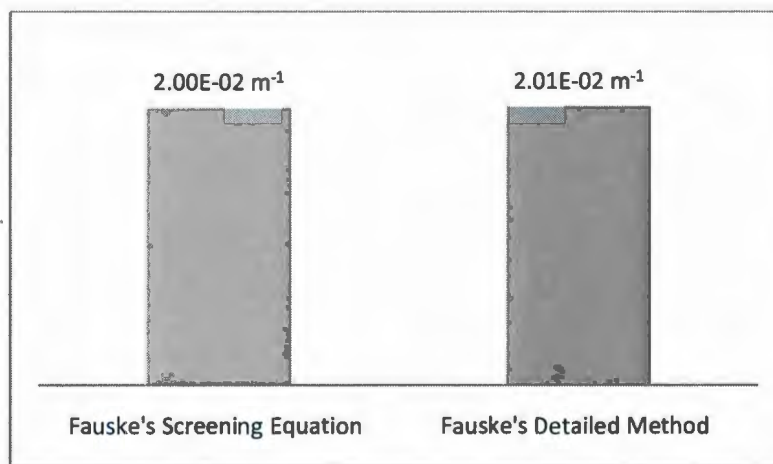


Figure 6.19: Comparison of A/V Ratio for Monoethanolamine

The calculated area to volume ratio for formaldehyde and monoethanolamine are depicted by Figure 6.18 and Figure 6.19 respectively. The area to volume ratios for both of the chemicals are calculated using Fauske's screening equation and Fauske's detailed method. This screening equation was developed from the detailed equation. For Formaldehyde, area to volume ratio calculated by Fauske's screening equation is higher than that calculated by Fauske's detailed

method considering gassy system. It is because the screening equation is based on the gas molecular weight of carbon dioxide, despite the real molecular weight of the sample. However, for the tested sample of formaldehyde solution, carbon monoxide is considered as the main decomposition product. As the molecular weight of carbon dioxide is higher than that of carbon monoxide, screening equation predicts a higher vent area. Figure 6.19 shows that the area to volume ratio calculated by Fauske's screening equation and Fauske's detailed method for monoethanolamine are equal. The reason behind this is that the calculation of vent diameter for monoethanolamine by Fauske's detailed method is done considering carbon dioxide as the main decomposition product.

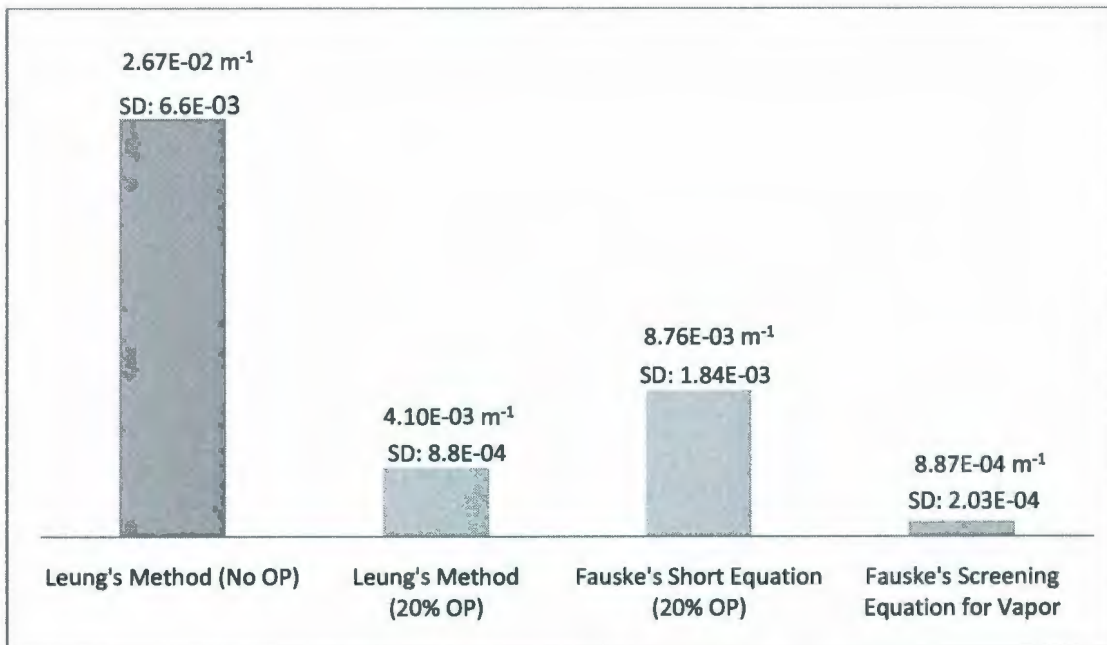


Figure 6.20: Comparison of A/V Ratio for H₂S Scavenger Sample

Figure 6.20 shows the area to volume ratio calculated by different methods for hydrogen sulphide scavenger sample. Though the two components of the hydrogen sulphide scavenger, formaldehyde solution and monoethanolamine, are categorized as gassy system, hydrogen sulphide scavenger is considered as a vapor system. The average and the standard deviation of the required vent diameters for each method for the two conducted tests are shown in Figure 6.20. The area to volume ratio calculated by Leung's method for no overpressure gives the largest value. When Leung's method is used for 20% overpressure, six fold reduced area to volume ratio is estimated for the vent. Hence, considering overpressure in vent sizing calculation for Leung's method can significantly decrease the required vent area. Fauske's short form of equation considering 20% overpressure predicts vent size area higher than the vent size area calculated by Leung's method considering 20% overpressure. So, Fauske's short form of equation is prone to over predict the required vent area. The lowest vent diameter is predicted by Fauske's screening equation for vapor system. As mentioned earlier, this method does not require any physical and chemical properties of the chemicals. It might cause such a low estimation of vent area for the studied chemical.

For the tested sample of scavenger, Leung's method considering 20% overpressure is most recommended for calculating the area to volume ratio because it neither over predicts nor underestimates the area to volume ratio.

7 CONCLUSION AND RECOMMENDATION

7.1 Conclusion

7.1.1 Specific Heat Capacity

All of the six chemicals were tested in the DSC and it is found that the specific heat capacity of the chemicals increases with the increase in temperature. Higher specific heat capacity values of chemicals provide higher area to volume ratio. The specific heat capacity values for formaldehyde and monoethanolamine determined experimentally are found to be similar to those provided by the manufacturer.

7.1.2 Oil Field Corrosion Inhibitor

ARSST and VSP-2 were successfully used to characterize three liquid corrosion inhibitors (Nox Rust 1100, Nox Rust 9800, and Brenntag) and one solid corrosion inhibitor (VCI 1 powder). The open cell ARSST tests indicated that the percentage of mass loss increases with the increase in volatile components. For the chemicals studied, higher mass loss is observed for lower pad gas pressure (15 Psig) test because it allows the samples to vaporize easily. However, mass loss of the corrosion inhibitors does not vary significantly with experimental time from 350 to 500 minutes.

the Brenntag corrosion inhibitors yields the highest mass loss (24% for 300 Psig tests and 37.25% for 15 Psig tests) as the percentage of volatile components ranges from 70-90%). The lowest mass loss is observed for the solid corrosion inhibitor (1.76% for 300 Psig tests and 5.43% for 15 Psig tests).

Both the Brenntag corrosion inhibitor and Nox Rust 9800 are categorized as non-reactive vapor systems. The vent area calculated by Leung's method is higher than that calculated by Fauske's method by an order of magnitude. Leung's method as used here did not allow for over pressure and thus, it provides higher and more conservative vent area requirements.

Nox Rust 1100 and VCI 1 powder are categorized as reactive gassy systems as both of them provide a higher end pressure than the starting pressure while tested in the VSP2. That means decomposition products are evolved due to the heating of the samples. Vent area calculations using Fauske's detailed method and Fauske's screening equations for gassy systems indicates that the required area to volume ratio for the corrosion inhibitors showing gassy system behavior is lower than that for those showing non-reactive vapor system behavior (e.g. Brenntag and Nox Rust 9800). This is because the corrosion inhibitors showing gassy system behavior have a low pressure increase rate (about 8-9 Psi/min).

7.1.3 Hydrogen Sulphide Scavenger

The hydrogen sulfide scavenger and its components (37% formaldehyde solution and monoethanolamine) were tested in VSP2 with Hastelloy closed test cells. As the samples were tested in closed test cells, the observed mass loss is lower than 5% for all of them.

Though the formaldehyde solution and monoethanolamine show gassy system behavior, the mixture of these two, which is categorized as a hydrogen sulfide scavenger, shows a reactive vapor system behavior. Both the formaldehyde solution and monoethanolamine evolve decomposition products due to heating up.

The area to volume ratio for these two chemical are calculated using Fauske's detailed method and Fauske's screening equations for gassy systems. The vent areas determined by these two methods for these two chemicals provide similar values.

The hydrogen sulfide scavenger sample, which is a mixture of 5 units of 37% formaldehyde and 2 units of monoethanolamine, is observed as the most reactive chemical among those tested. When the two components are mixed, an immediate exotherm is observed. . For the closed cell VSP2 tests for the scavenger, the observed heat of mixing is 38.83 KJ/mol. The second exotherm is observed at 108 °C, while the mixture is heated up after its first exotherm.

The vent sizing calculations for the scavenger sample is done by several different methods (Leung's method considering no over pressure and 20% overpressure, Fauske's short equation by considering 20% over pressure, and Fauske's screening equation for gassy system). The recommended vent area for H₂S scavenger is $4.10 \times 10^{-3} \text{ m}^{-1}$, which is achieved by Leung's method considering 20% overpressure, as it neither over predicts nor underestimates the area to volume ratio.

7.2 Recommendation

The oil field chemicals studied are protected and therefore assumptions were made during the calculations. For more representative results, the corrosion inhibitor provider should include the exact compositions (or a more representative one) to tune the results presented here.

To work on this area, a sound knowledge of adiabatic calorimetry, DIERS methodology, and emergency relief system design is required. The following can be the recommended future works to continue in this project:

- A mixture of corrosion inhibitors and hydrogen sulfide scavenger along with other oil field chemicals can be tested in the ARSST and VSP-2. It is worthwhile to characterize the thermal-pressure of this mixture of the chemicals with crude oil. This will provide vent area that better suit the operating conditions in oil fields, as complex mixtures of chemicals are subjected to high temperature and pressure conditions in oil and gas operations.
- The study of detailed physical and chemical properties of the tested chemicals (such as molecular weight, latent heat of vaporization, and vapor density) could be done to have a better data for relief system design.
- The sample of the decompositions products for Nox Rust 1100, VCI 1 powder, formaldehyde solution, and monoethanolamine could be collected during the test and detailed compositional analysis could be done. This will allow the knowledge of the constituents and molecular weight of the gas, as well as a better vent area approximation. Acquisition of the ARSST and VSP accessories for gas sampling is recommended.
- The vent area calculations are done by considering homogenous flow. It is worthwhile to characterize the real flow regime of the chemicals. A flow regime functionality can be

added to the ARSST. Also, blow down testing in the VSP 2 can be done to evaluate flow regime and vapor/ liquid disengagement.

- The area to volume ratios are calculated by considering ideal nozzle flow behavior for this current work. The real flow behavior of the chemicals and proper vent pipe design could also be an interesting sector for study for these oil field chemicals.
- This work indicates that the corrosion inhibitors and scavenger are susceptible to external fire exposure conditions. Thus, the choice of proper materials for the storage containers is recommended should consider the properties provided in this work. Actual process condition should be considered to better define credible upset conditions.
- Corrosion inhibitors are subjected to high temperature conditions in oil fields. A study of the corrosion resistance properties of these oil field chemicals with the increase in temperature is recommended to assess the efficiency of the inhibitors in oil and gas operations.
- The dust explosion hazards corresponding to the solid corrosion inhibitor sample, VCI 1 powder, can also be a worthwhile topic to study.
- For studying unknown chemicals in the ARSST, the single ramp polynomial control mode is used. It is recommended to develop a new polynomial on a non-reactive sample (such as pentadecane) for further testing with the instruments, as the existing polynomial is not capable of providing an external heating rate of 2 °C/min. This anomaly in the heating rate does not change the system characterization, but it prolongs the experiment

time. It is anticipated that the development of a polynomial requires numerous testing and calibrations. Another alternative is to modify and validate the existing polynomials.

- It is recommended to upgrade the ARSST in the Health and Safety lab as there is incompatibility between the available instrument and the installed software.

8 Bibliography

- American Petroleum Institute. (2008). *API RP 520 (Part I): Sizing and Selection of Pressure Relieving Devices in Refineries*. Washington, D.C.: American Petroleum Institute.
- American Petroleum Institute. (2003). *API RP 520 (Part II): Installation of Pressure Relieving Devices in Refineries*. Washington, D. C.: American Petroleum Institute.
- American Petroleum Institute. (2007). *API RP 521: Pressure Relieving and Depressurizing Systems*. Washington, D. C.: American Petroleum Institute.
- Andreev, N. N., & Kuznetsov, Y. I. (1998). Volatile Inhibitors for CO₂ Corrosion. *NACE Annual Conference and Exposition*, (pp. 22-28). San Diego.
- Askonas, C. F., Burelbach, J. P., & Leung, J. C. (2000). The Versatile VSP2: A Tool for Adiabatic Thermal Analysis and Vent Sizing Applications. *28th Annual Conference of North American Thermal Analysis Society*. Orlando.
- ASTM. (2005). *E 1269-05 Standard Test Method for Determining Specific Heat Capacity by Differential Scanning Calorimetry*. New York: ASTM International.
- Boyle, W. J. (1967). Sizing Relief Area for Polymerization Reactor. *Chemical Engineering Progress*, 63 (8), 61.
- Brenntag Canada Inc. (2009). *MSDS of Brenntag Corrosion Inhibitor*. Toronto: Brenntag Canada Inc.
- Brenntag Canada Inc. (2007). *MSDS of Formaldehyde*. Toronto: Brenntag Canada Inc.
- Brenntag Canada Inc. (2008). *MSDS of Monoethanolamine*. Toronto: Brenntag Canada Inc.
- Burelbach, J. P. (2001). Vent Sizing Application for Reactive Systems. *5th Bi-Annual Process Plant Safety Symposium*.
- Burelbach, J. P., & Theis, A. E. (2005). Thermal Hazards Evaluation Using the ARSST. *3rd International Symposium on Runaway Reactions, Pressure Relief Design and Effluent Handling*. Cincinnati.
- CCPS. (1993). Guidelines for Engineering Design for Process Safety. 409-420. New York, New York State, United States of America: American Institute for Chemical Engineers.
- Colonial Chemicals Solutions, Inc. (2008). *MSDS of Monoethanolamine*. Savannah: Colonial Chemicals Solutions, Inc.

- Coupe, P. J., & Cormon, E. B. (2004). Chemical Optimisation Case Histories and Cost Benefits. *1st International Symposium on Oilfield Corrosion*. Aberdeen: Society of Petroleum Engineers.
- Duffield, J. S., Nijssing, R., & Brinkhof, N. (1996). Emergency Pressure Relief Calculations Using the Computer Package: RELIEF. *Journal of Hazardous Materials* , 131-143.
- Duxbury, H. A. (1980). The Sizing of Relief Systems for Polymerization Reactors. *The Chemical Engineer* , 31-37.
- EMD Chemicals Inc. (2009 a). *MSDS of Acetone*. Gibbstown: EMD Chemicals Inc.
- EMD Chemicals Inc. (2009 b). *MSDS of Toluene*. Gibbstown: EMD Chemicals Inc.
- Environment Canada. (2008). *Guidance Document for responding to the Notice with respect to Certain High Priority Petroleum Substances*. Environment Canada.
- Environmental Protection Agency. (1991). *Locating and Estimating Air Emissions from Sources of Formaldehyde (Revised)*. Office of Air Quality Planning and Standards. Durham: U. S. Environmental Protection Agency.
- Equistar Chemicals. (2006). *MSDS of Monoethanolamine*. Houston: Equistar Chemicals.
- Ergon Refining Inc. (2003). *MSDS of Severly Hydrotreated Light Naphthenic Distillate*. Vicksburg: Ergon Refining Inc.
- Fauske and Associates Inc. (2007 b, June 20). Reduce Software User's Manual (Version 2.0.5). Burr Ridge, Illinois, United States of America.
- Fauske and Associates Inc. (2002, October). VSP2 User's Manual and Methodology. Burr Ridge, Illinois, United States of America.
- Fauske and Associates Inc. (2006, May 11). XY Plot 2 User's Manual (Version 5.15). Burr Ridge, Illinois, United States of America.
- Fauske and Associates Inc. (2007 a, October). Advanced Reactive Sytem Screening Tool System Manual Methodology and Operations. Burr Ridge, Illinois, United States of America.
- Fauske, H. K. (1984 a). A Quick Approach to Reactor Vent Sizing. *Plant/ Operation Progress* , 3 (3), 145.
- Fauske, H. K. (1985). Emergency Relief System Design. *Chemical Engineering Progress* , 81 (8), 53-56.
- Fauske, H. K. (1984 b). Generalized Vent Sizing Nomogram for Runaway Chemical Reactions. *Plant/ Operation Progress* , 3 (4), 213.

- Fauske, H. K. (1985). New Experimental Technique for Characterizing Runaway Chemical Reactions. *Chemical Engineering Progress*, 81 (8), 39-46.
- Fauske, H. K. (2000). Properly Size Vents for Non Reactive and Reactive Chemicals. *Chemical Engineering Progress*, 17-29.
- Fink, J. K. (2003). *Oil Field Chemicals*. USA: Gulf Professional Publications.
- Fisher, H. G. (1985). DIERS Research Program on Emergency Relief System. *Chemical Engineer Progress*, 81 (8), 33-36.
- Fisher, H. G., Forrest, H. S., Grossel, S. S., Huff, J. E., Muller, A. R., Noronha, J. A., et al. (1992). *Emergency Relief System Design Using DIERS Technology: The Design Institute for Emergency Relief Systems (DIERS) Project Manual*. New York: American Institute of Chemical Engineers.
- Fletcher, C. J. (1934). The Thermal Decomposition of Formaldehyde. *Proceedings of the Royal Society of London* (pp. 357-362). London: The Royal Society.
- Freedonia Group. (2008, November). *World Oilfield Chemicals to 2012*. Retrieved July 2, 2010, from Freedonia Group Web Site: <http://www.freedoniagroup.com/World-Oilfield-Chemicals.html>
- Hohne, G. W., Heminger, W. F., & Flammersheim, H. J. (2003). *Differential Scanning Calorimetry*. New York: Springer.
- Houston, C. W. (1996). *Hydrogen Sulfide Scavengers Market Assessment*. Gas Research Institute. Chicago: Gas Research Institute.
- INEOS LLC. (n.d.). *GAS/SPEC SS Specialty Amine*. Retrieved 05 10, 2010, from http://www.coastalchem.com/PDFs/GAS_SPEC/Ineos%20SS.pdf
- INEOS LLC. (2001). *GAS/SPEC SS Specialty Amine*. Retrieved 05 10, 2010, from http://www.coastalchem.com/PDFs/GAS_SPEC/Ineos%20SS.pdf
- ioMosaic Corporation. (2006). *Comprehensive Emergency Relief System Design Services*. Salem, New Hampshire, United States of America.
- Johnson, J. D., Hedges, W., & Dawson, J. (2004). *Working Party Report on the Use of Corrosion Inhibitors in Oil and Gas Production*. Maney: EFC 39 (European Federation of Corrosion).
- Kelland, M. A. (2009). *Production Chemicals for the Oil and Gas Industry*. CRC Press.
- Kemp, H. S. (1983). Formation and Management of AIChE Design Institutes. *Chemical Engineering Progress*, 79 (6), 9-14.

- KPR ADCOR Inc. (2009). *MSDS of Nox Rust 1100*. Hamilton: KPR ADCOR Inc.
- KPR ADCOR Inc. (2003). *MSDS of Nox Rust 9800*. Hamilton: KPR ADCOR Inc.
- KPR ADCOR Inc. (2007). *MSDS of VCI-1 Powder*. Hamilton: KPR ADCOR Inc.
- Leung, J. C. (1986). Simplified Vent Sizing Equations for Emergency Relief Requirements in Reactors and Storage vessels. *AIChE*, 32 (10), 1623-1635.
- Lindchem Ltd. (2005). *MSDS of Monoethanolamine*. Great Yarmouth: Lindchem Ltd.
- Mallinckrodt Baker Inc. (2007). *MSDS of Formaldehyde*. Philipsburg: Mallinckrodt Baker Inc.
- Mannan, M. S., Aldeeb, A. A., & Rogers, W. J. (2002). Understanding the Role of Process Chemistry in Fires and Explosions. *Process Safety Progress*, 21 (4), 323-328.
- Mannan, S., & Frank, P. L. (2005). *Lees' Loss Prevention in the Process Industries: Hazard Identification, Assessment and Control* (Vol. 2). Burlington: Butterworth-Heinemann Publications.
- Marshall, V., & Ruhemann, S. (2001). *Fundamentals of Process Safety*. Glasgow, UK: Institution of Chemical Engineers (IChemE).
- McKetta, J. J., & Cunningham, W. A. (1985). *Encyclopedia of Chemical Processing and Design: Fluid Flow, Two - Phase Design to Froth Flotation* (Vol. 23). New York: Marcel Dekker.
- METTLER TOLEDO. (2007). *DSC 1 STARe System Operating Instructions*. METTLER TOLEDO.
- Muller, S., Rizvi, S. Q., Yokose, K., & Jackel, M. (2009, October). *Specialty Chemicals Update Program (SCUP): Available SCUP Reports*. Retrieved June 22, 2010, from SRI Consulting Website: <http://www.sriconsulting.com/SCUP/Public/Reports/CORRO000/>
- Noronha, J. (1999). Why DIERS Technology Should be Used in Risk Assessment: Call for a 1999 Worldwide Benchmarking Survey on Various Risk Reduction Methods Used. *Process Safety Progress*, 18 (2), 115-120.
- OECD/SIDS. (2001). *SIDS Initial Assessment Report for 12th SIAM*. Paris: UNEP Publications.
- Palmer, W. J., Hedges, W., & Dawson, J. L. (2004). *The use of Corrosion Inhibitors in Oil and Gas Production*. Institute of Materials, Minerals and Mining. London: Maney Publishing.
- Rasmussen, B. (1988). Occurrence and Impact of Unwanted Chemical Reactions. *Journal of Loss Prevention in the Process Industries*, 1 (2), 92-95.
- Recochem Inc. (2007). *MSDS of Shellite*. Lytton: Recochem Inc.

- Rosenfeld, I. L. (1977). *Corrosion Inhibitors*. Moscow: M. Khimia Publisher.
- Ruschau, G. R., & Al-Anezi, M. A. (2006). *Print Report / PDF Files: Oil & Gas Exploration Production*. Retrieved 06 22, 2010, from Cost of Corrosion: <http://www.corrosioncost.com/pdf/oilgas.pdf>
- Ruschau, G. R., & Al-Anezi, M. A. (2006). *Production & Manufacturing: Oil & Gas Exploration - Production*. Retrieved June 22, 2010, from Cost of Corrosion: <http://www.corrosioncost.com/prodmanu/oilgas/index.htm>
- Sastri, V. S. (1998). *Corrosion Inhibitors: Principles and Applications*. Chickester, UK: Wiley.
- Sciencelab.com Inc. (2008). *MSDS of Dipropylene Glycol Methyl Ether*. Houston: Sciencelab.com Inc.
- Sestak, E. J. (1965). *Venting of Chemical Plant Equipment*. Hartford: Factory Insurance Association.
- Shanghai eshine Stainless steel Material Co., Ltd. (n.d.). *Home: News: Hastelloy Introduction*. Retrieved 05 10, 2010, from Shanghai Eshine Stainless Steel Material Co. Ltd Web site: <http://www.sh-yixiang.com/01900013/php/newsshow.php?menuid=5&getnewslistid=5212&lang=3>
- Sigma-Aldrich Canada. (2009). *MSDS of Tert-Butyl Peroxide*. Oakville: Sigma-Aldrich Canada.
- Swift, I. (1984). Development in Emergency Relief System Design. *The Chemical Engineer* , 30-33.
- TA Instruments. (2002). *Guide for Choosing DSC Pans*. TA Instruments.
- The Dow Chemical Company. (2001). *Ethanolamines*. Midland: The Dow Chemical Company.
- Townsend, D. I., & Tou, J. C. (1980). Thermal hazard evaluation by an accelerating calorimeter. *Thermochemica Acta* , 37 (1).
- Tulstar Products Inc. (1996). *MSDS of Petroleum Hydrocarbon Oil*. Tulsa: Tulstar Products Inc.
- Tung, N. P., Hung, P. V., Tien, H. D., & Loi, C. M. (2001). Study of Corrosion Control Effect of H₂S Scavengers in Multiphase Systems. *SPE International Symposium on Oilfield Chemistry*. Houston.
- Vargas, S. (2009 a). *Basic Theory Behind Differential Scanning Calorimetry*. St. John's.
- Vargas, S. (2009 b). *Hazard Evaluation of Corrosion Inhibitors Use in Oil and Gas Operation*. Post Doctorial Research Proposal, Memorial University of Newfoundland, Process Engineering, St. John's.

Vargas, S. (2010). Thermal characterization of oil field chemicals. *Fauske & Associates, LLC Free Users Group Training Seminar*. Chicago.

Vargas, S. (2010). Thermal Characterization of Oil Field Chemicals. *Fauske & Associates, LLC Free Users Group Training Seminar*. Chicago.

APPENDIX 1

A1.1 EXPERIMENTAL SETUP

A1.1.1 Pre Test Steps

The first step is to weigh and record the test cell with magnetic stir bar which will be around 1.2-1.6 gm. The stir bar size, whether it is large or small should also be recorded.



Figure 1: Measuring the weight of the test cell.

It is necessary to check the resistance between the connector of the heater and the foil. It should be O.L., which denotes that no short exists within the heater.



Figure 2: Assuring no short exists within the heater.

The resistance of the heater should range between 23.5 to 24.5 Ω as shown in Figure 3.



Figure 3: Measuring resistance of the heater.

A1.1.2 Making Test Cell Assembly

The heater is wrapped around the test cell in a comfortable way as shown in Figure 4.



Figure 4: Wrapping the heater around the test cell.

The heater test cell assembly is again wrapped by a heater belt (Figure 5), and the copper wires of the heater are manually twisted as much as possible (Figure 6). After that, needle nose pliers are used to twist the copper wire (Figure 7) till the test cell heater assembly becomes unmovable inside the heater belt and stays stable .



Figure 5: Wrapping the test cell-heater assembly with heater belt.



Figure 6: After manually twisting the copper wires of the heater belt



Figure 7: Twisting the copper wire of the heater belt more with needle nose pliers.

After the twisting is done, the assembly will look like as shown in the figure 8.

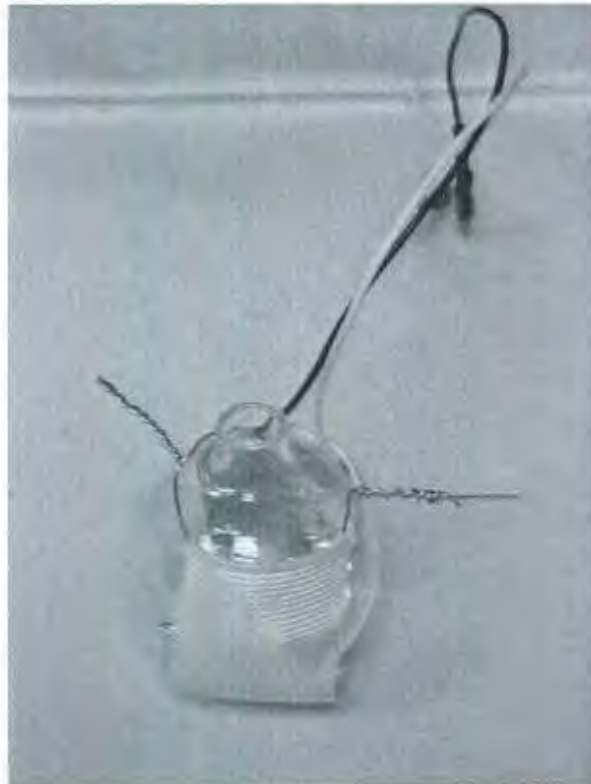


Figure 8: After twisting the copper wires of the heater belt with needle nose pliers.

Then the extra portion of the twisted wire should be clipped to an extent (Figure 9) so that there will remain approximately 3 twists next to the test cell.



Figure 9: Cutting the extra portion of the twisted wires.

The final test cell- heater assembly with heater belt will look like as shown in the Figure 10.



Figure 10: Final test cell- heater assembly with heater belt.

The next step is to wrap the assembly with foil paper (Figure 11). The shiny side of the foil should be towards the cell to assure better reflection of heat inside the cell (Figure 12). After placing the assembly on the foil, the foil is at first folded diagonally (Figure 13). Then, it should be tightly pressed against the test cell to minimize air pockets and reduce bulkiness (Figure 14).



Figure 11: Foil paper- Shiny side (Left), Dull side (Right)



Figure 12: Putting the assembly on the shiny side of the foil.



Figure 13: Folding the foil diagonally.

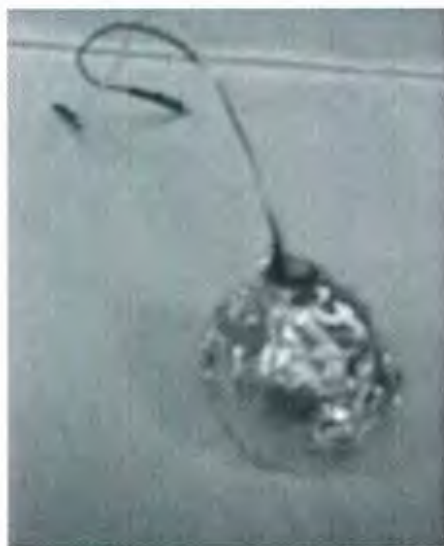


Figure 14: After tightly pressing the foil against test cell.

Each test cell comes with six pieces of precut insulation which is capable of holding the test cell. Thus, the test cell is insulated.



Figure 15: Insulation for test cell.

(The left most part will be at the bottom while the right most will be at the top)



Figure 16: Insulation for test cell.



Figure 17: Putting the test cell in insulation.

A notch should be cut half way through the top most part of the insulation, and the heater wire should be pulled through the notch in the insulation as shown in Figure 18.

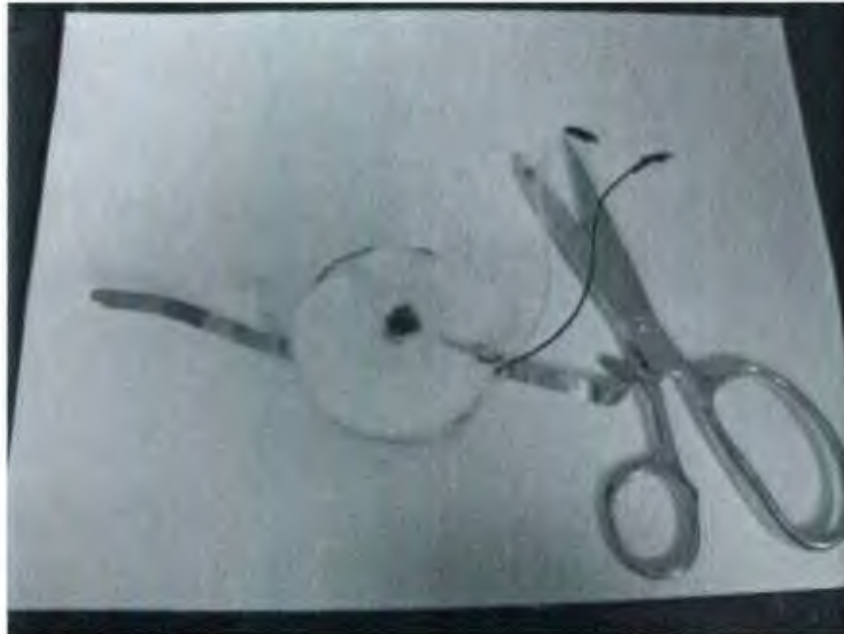


Figure 18: Test cell with insulation.

The next step is to insert the magnetic stir bar inside the test cell (Figures 19 and 20).



Figure 19: Magnetic stir bar.



Figure 20: Inserting magneting stir bar into test cell.

The insulated test cell assembly is hold together and placed inside the bottom piece of the insulation sheath (Figure 21). The sheath is placed on a flat place and the insulation is pressed

inside it. The heater wire is pulled through the hole in the top piece of the sheath. Then the top piece of the sheath is placed over the bottom piece.



Figure 21: Insulation sheath.

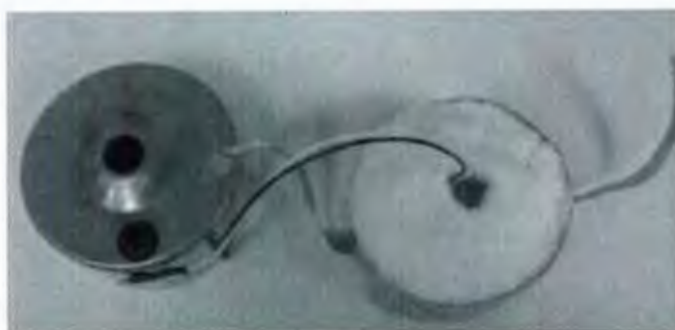


Figure 22: After placing the test cell-insulation assembly inside the bottom piece of the insulation sheath.



Figure 23: After placing the top piece of the sheath on the bottom piece of the sheath.

The top and bottom sheath pieces should be maintained together by applying tape across the bottom part of the assembly.



Figure 24: After applying tape to the assembly – Side view (Left), Top view (Right)

The neck of the test cell should be in the center of the hole in the top of the sheath. During the assembly, the test cell and the sheath undergo a lot of movement. Therefore, a recheck is required to ensure that the magnetic bar is still in the cell.



Figure 25: Ensuring the proper alignment of the test cell and inserting magnetic stirrer.

The thermocouple and its holder are inserted into the hole in the top sheath. Before inserting the thermocouple, it is necessary to assure that the thermocouple connection is not shorted to sheath.

Thus, the resistance of the male connector to the sheath should be O.L. on the 4 M Ω scale. It is also advisable to check the resistance of the thermocouple.



Figure 26: Checking resistance of the thermocouple.



Figure 27: Checking resistance of the the male connector of the thermocouple to the sheath.



Figure 28: After inserting thermocouple in the thermocouple holder.



Figure 29: After inserting the thermocouple in the test cell-sheath assembly.

ARSST tests are open tests, so it is easier to place the sample in the test cell by injecting it through the hole of the top sheath before inserting the assembly in the vessel. The required amount of materials for one test in ARSST is generally 10 ml.



Figure 30: Measuring the weight of the test cell assembly.



Figure 31: The weighing machine showing the weight of the sample.

A1.1.3 Making Final Vessel Assembly

The whole assembly is carefully inserted in the vessel (Figure 32).



Figure 32: After inserting the whole assembly to the vessel.

The male connection of the heater and the thermocouple are dipped in vacuum grease and appropriate connection are made inside the vessel. Before applying grease to the heater wires, the female connections on the heater gland should be slightly pinched for a better connection. The connections for the heater as well as for the thermocouple should be taped to have a better protection.



Figure 33: After crimping heater connectors inside the vessel for better contact.



Figure 34: Applying vacuum grease to the heater wire.



Figure 35: The inside view of the containment vessel after all connections.

The heater gland and the wires of the thermocouple glands must not be shorted to the vessel or not. For an appropriate condition, the resistance should be O. L. on the 4 M Ω scale for both cases as shown in Figure 36.



Figure 36: Checking the resistance of the heater gland to the vessel.



Figure 37: Checking the resistance of the heater gland to the wires of the thermocouple glands.

The sealing surface of the vessel and the lid should be cleaned to ensure a proper seal. A small amount of grease is applied to lid around o-ring. Then the lid is placed on the vessel with gentle movement so that the fill line does not interfere with the connection wires inside the vessel.

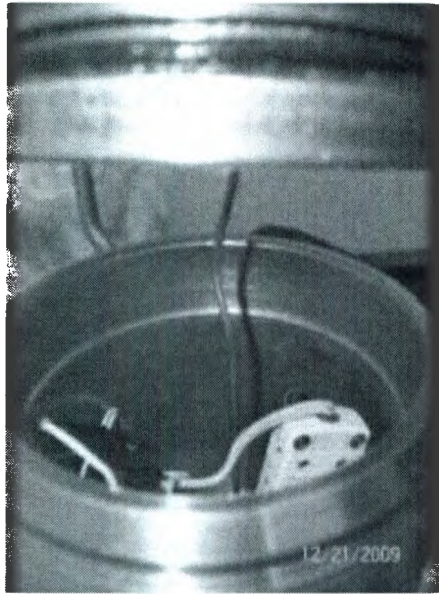


Figure 38: Carefully placing the lid.

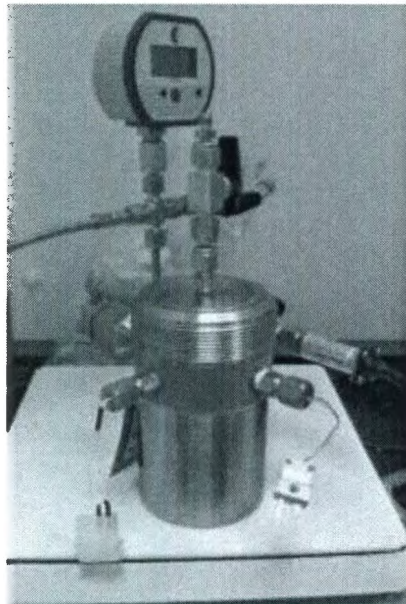


Figure 39: After placing the lid in the containment vessel.

Then top part is screwed around the lid until it becomes hand tight.



Figure 40: Screwing the lid around the top part of the containment vessel.

The next step is to check the resistance of the heater (Figure 41) and the resistance of the thermocouple (Figure 42).



Figure 41: Double checking resistance of the thermocouple.



Figure 42: Double checking the resistance of the heater.



Figure 43: Double checking the resistance of the thermocouple

The last step for set up is to make the thermocouple and heater connections to the control box. The connections of the pressure transducer should also be checked.



Figure 44: After making all connections.

A1.1.4 Pressure Calibration

For conducting ARSST experiment, an initial pad gas pressure is applied to the containment vessel. Generally an initial pressure of 300 psig is applied for the first experiment. Lower applied pressure can be used to investigate tempering at relief conditions.

For calibrating pressure, at first make sure that the pressure gauge reading is 0 psig. Then the zero pressure is inserted in the “A (psig)” box and the “Enter” button is pressed twice (Figures 45 and 46).

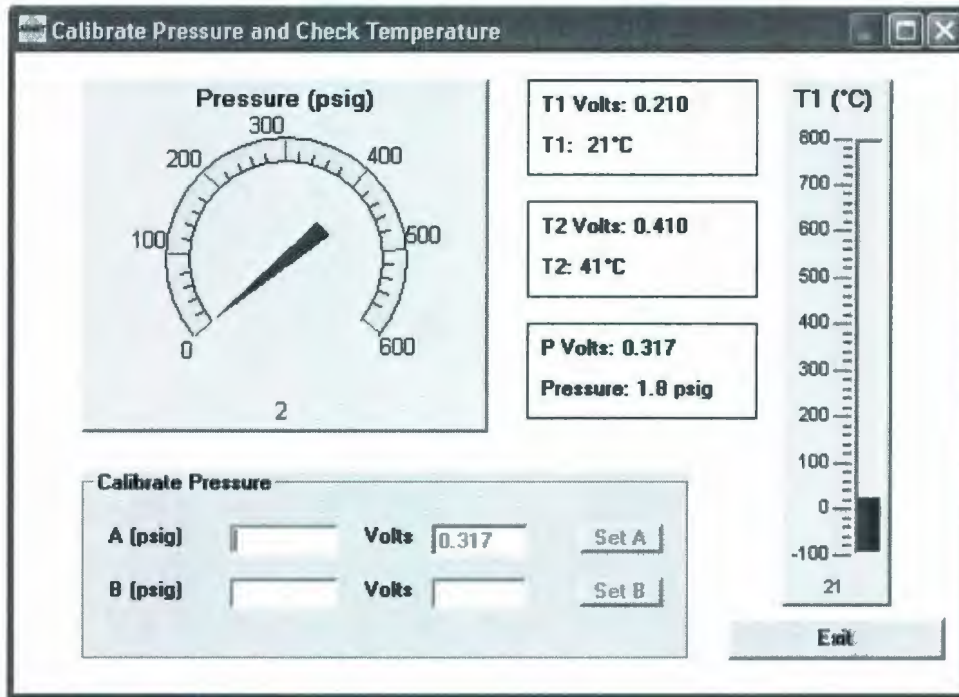


Figure 45: Pressure calibration wizard before entering the lower limit of the pressure range.

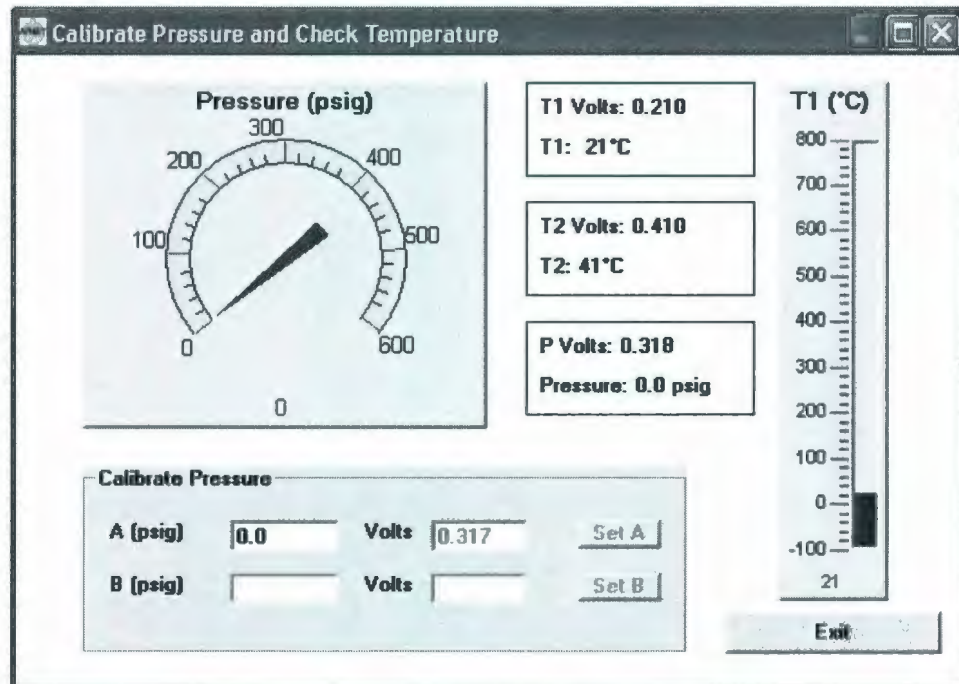


Figure 46: Pressure calibration wizard after entering the lower limit of the pressure range.

Then the vessel is pressurized by opening the valve of the nitrogen tank and the value of the upper limit of the pressure is inserted “B (psig)” box and the “Enter” button is pressed twice similarly.

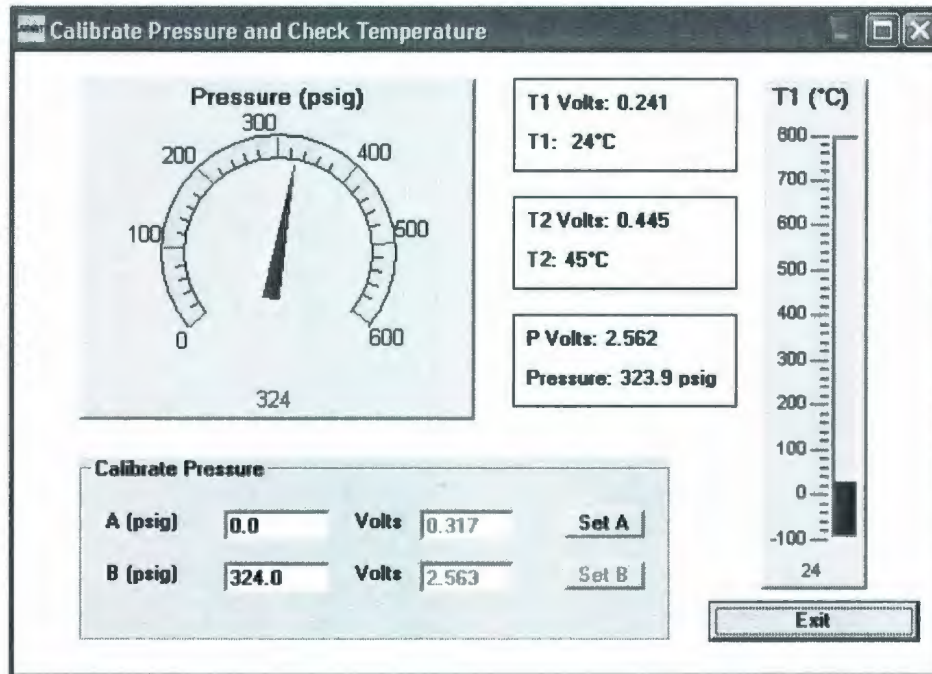


Figure 47: Pressure calibration wizard after entering the upper limit of the pressure range.

A1.1.5 Experimental Run

After calibrating the pressure, the experiment is then started. The cut-off criteria and the data log in interval are selected in the “Test Setup Wizard”. For a single ramp - polynomial control mode of operation, a pre developed polynomial is chosen from the “Select Ramp Polynomial” option for running the experiment (Figures 48 and 49). There are two established polynomial- one for an experiment starting with an initial pressure of 300 psig (2CPM300PSI066) and another for an experiment starting with an initial pressure of 15 psig (2CPM15PSI066). For choosing perfect experimental mode for a particular system it is recommended to go through the ARSST manual (FAI/07-136, 2007).

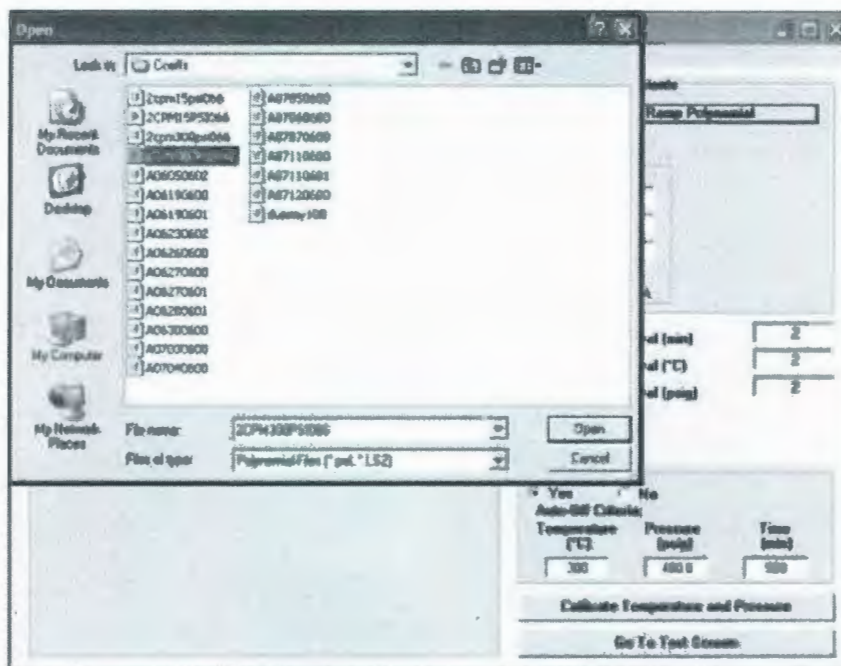


Figure 48: Choosing a pre developed polynomial in the “Test Setup Wizard”.

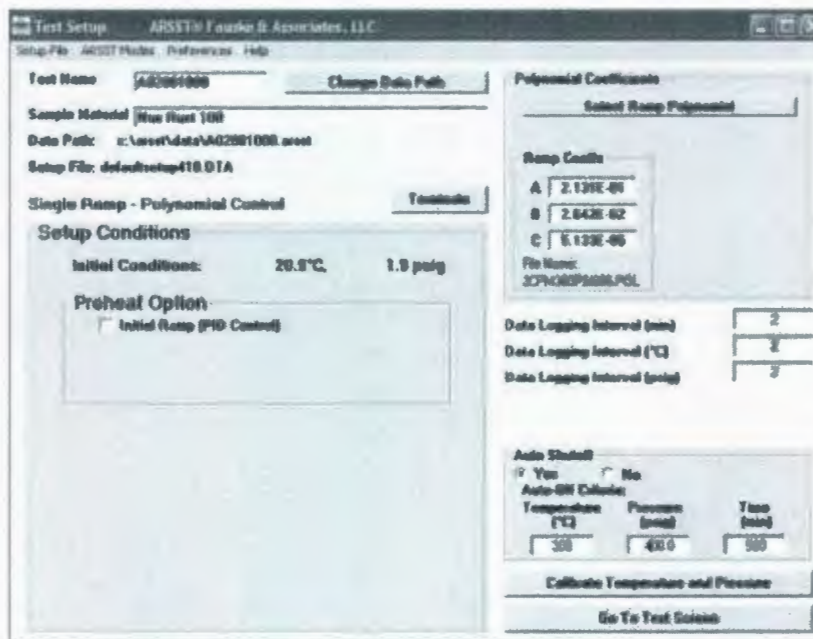


Figure 49: Test setup wizard after selecting all the criteria.

Then the experiment is started by hitting the “Run” button in the “Test Screen”. It is necessary to make sure that magnetic stirrer is turned on and the main control box is also turned on.

A1.2 TROUBLESHOOTING

A1.2.1 Changing Heater Gland

Lack of continuity along the wires of the heater gland is a common problem as the wires are susceptible to breaking while twisting. In that case, the heater gland needs to be changed. At first heater gland is removed from the containment vessel. The threads of the new heater gland need to be cleaned properly with the help of needle and acetone (Figures 50 and 51). Any contaminant particles in the threads will hinder the connection to be properly sealed. The threads for connecting heater gland of the connecting vessel also need to be cleaned properly in a similar fashion. Then the threads of the heater gland are covered with a Teflon tape (Figure 52). The Teflon tape should be applied in the same direction of the threads. It is necessary to apply the tape as less as possible to cover the whole thread to avoid difficulties while installing the heater gland in the containment vessel. The anti seize cream is applied around the thread and then the heater gland is installed to the containment vessel with wrench as tight as possible (Figure 53 and 54).



Figure 50: Cleaning the threads of the heater gland.

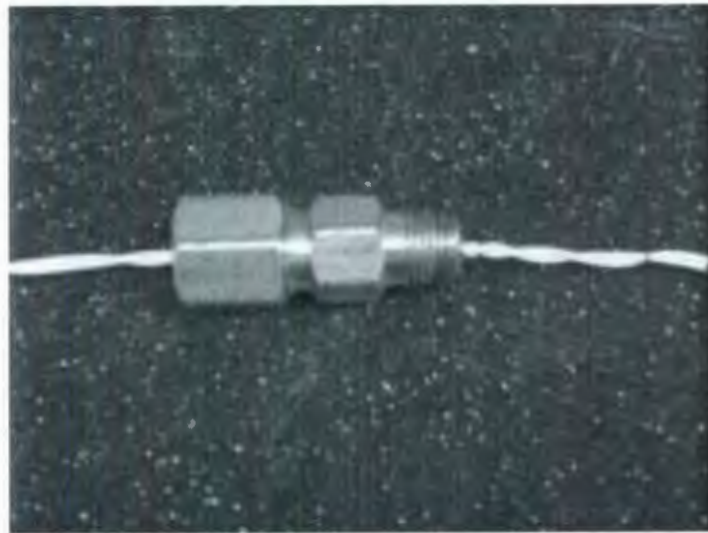


Figure 51: Properly Cleaned threads of heater gland.

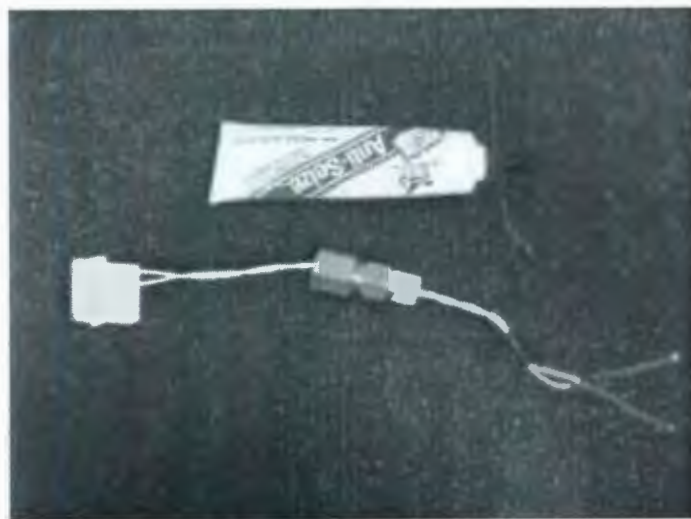


Figure 52: After application of Teflon tape to the threads of heater gland.



Figure 53: Heater gland thread with Teflon tape after application of Anti seize.



Figure 54: Installing heater gland in the containment vessel.

Thermocouple gland can also be changed in the same way while broken.

A1.2.2 Checking Pressure leak

To check pressure leak, the vessel is sealed with the lead without any test cell assembly inside. The valve at the fill line of the containment vessel is also closed. Then the containment vessel is dipped into water. The occurrence of any bubble indicates that there is a pressure leak.

A1.2.3 Fixing Nonzero Gauge Pressure Reading in Atmospheric Condition

The calibration potentiometer cover on the front of the unit to access the zero control is removed. Then the gauge reference units should be re-zeroed with a small screw driver without affecting the span calibration. The gauge port must be open to the ambient with no pressure or vacuum applied. Adjust The Zero control should be adjusted until the gauge reads zero with the minus (-) sign occasionally flashing.

APPENDIX 2

A2.1 EXPERIMENTAL SETUP

A major part in the experimental set up is to continuously monitor the operating conditions to make sure that everything is working properly. The experimental setup can be sub divided into several parts. The accuracy of a VSP2 test depends on the proper execution of each part as described in the subsequent sections.

A2.1.1 Test Cell Setup

A2.1.1.1 Choice of test cell and the primary information

Appropriate test cell should be chosen according to the characteristics of the sample and the expected experimental conditions. There are three general kinds of test cells available for VSP2: (1) Type I or closed test cell, which is only open through 1/16 inch fill line, (2) Type II or open test cell, which is provided with a top mounted vent tube of varying diameter, (3) Type III, bottom vented, or dip tube test cell. Type III is vented with vent tube extended to almost bottom floor of the test cell. Some specially designed test cells with a larger diameter of filling port are also available for solid samples. However, the Health and Safety Lab at MUN only have the first two kind test cells made with stainless steel as well as Hastelloy.



Figure 1: Closed test cell (Left one) and Open test cell (Right one) made of stainless steel.

The next step is to record the test cell tare mass. The test cell mass should be around 35 gm.



Figure 2: Recording test cell tare mass.

The test cell configurations such as type and material of stir bar (standard/ large/ glass/ none), material of test cell (stainless/ Hastelloy/ other), venting type (yes/ no/ other), number of fill lines (single/ dual) should be recorded.

A2.1.1.2 Checking continuity and resistance of different parts

There are two heaters: auxiliary heater and guard heater which have the coils made of stainless steel Nichrome heater wire. The guard heater is constructed of two parts: guard heater can and lid.

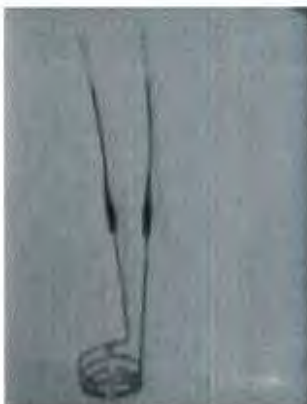


Figure 3: Auxiliary heater.



Figure 4: Guard heater can (Left) and Lid of guard heater (Right).

It is necessary to check the continuity of auxiliary heater and guard heater. The resistance of auxiliary heater should be around 18Ω . The resistances of the lid of the guard heater and guard heater should be around 12Ω and 44Ω consecutively.



Figure 5: Checking continuity of auxiliary heater.



Figure 6: Checking continuity of lid of the guard heater (Left) and guard heater can (Right)

The next step is to check resistance of heater leads to sheath for each component which should be greater than 1 M Ω .



Figure 7: Checking resistance of TC1 lead to test cell



Figure 8: Checking resistance of TC2 leads to guard can



Figure 9: Checking resistance of guard heater lead to sheath.



Figure 10: Checking resistance of guard heater lid's lead to sheath.

A2.1.1.3 Insulating and installing test cell into heaters

The first step is to install the auxiliary or main heater on the test cell. The fill lines of the test cell and the leads of the test cells need to be parallel to each other.



Figure 11: Test cell with auxiliary heater.

The test cell needs to be insulated with 7 cm wide flat paper insulation. Four full rounds of the insulation should be done around the test cell and masking tape can be used to hold it in place.



Figure12: Placing strip flat paper insulation around test cell.

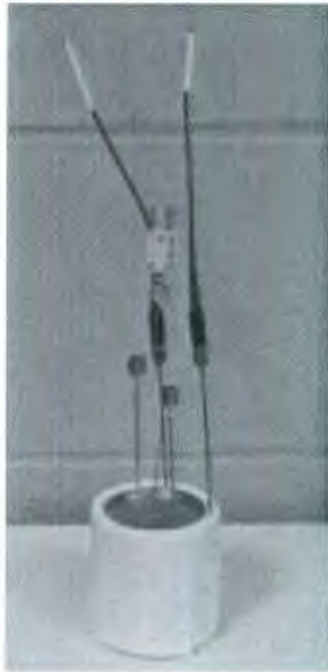


Figure 13: After completing four full rounds of flat paper insulation around test cell-
Side view (Left), Top view (Right)

Masking tape should be applied across the bottom so that it can easily fit into guard heater can.



Figure 14: Covering bottom of the test cell- auxiliary heater assembly with masking tape.

The test cell should be insulated from the guard heater on all sides along the wall, top and bottom with the same thickness of the insulation layer. As a result, a glass fiber insulation disk should be inserted inside the guard heater.



Figure 15: Half thickness glass fiber insulation disk.



Figure 16: Putting insulation disk inside guard heater.

The next step is to insert the insulated test cell into guard heater. While inserting, the guard heat leads are parallel to test cell fill lines, but placed at the opposite side of the auxiliary heater leads (as shown in Figure 17). Thus, the auxiliary heater leads and the guard heater leads should be opposite to each other in respect of the test cell fill lines, and both of them need to be parallel with the test cell fill lines as well as with each other (Figure 17).



Figure 17: Inserting test cell – auxiliary heater assembly into guard heater can.

A glass fiber insulation disk needs to be cut into half and place at the top of the test cell to insulate it (Figure 18).



Figure 18: Insulating the top of the test cell.

The top of the guard heater that is the lid of the guard heater should be installed and connected as shown in Figure 19.



Figure 19: Installing lid of the guard heater.

A completed test cell set up is shown in the Figure 20.

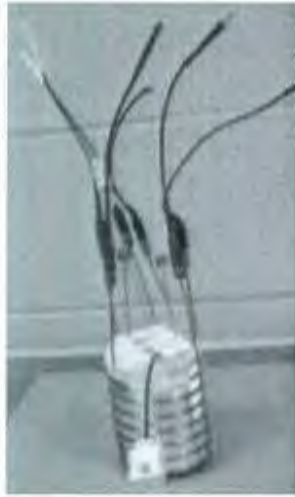


Figure 20: Completed test cell set up.

A2.1.1.4 Double checking continuity of heaters

The last part of the test cell set up is to double check continuity of auxiliary and guard heaters as shown in Figures 21 to 23.



Figure 21: Double checking continuity of auxiliary heater



Figure 22: Double checking continuity of guard heater can.



Figure 23: Double checking continuity of the lid of guard heater.

A2.1.2 Containment Vessel Setup

A2.1.2.1 Test cell and vessel connectoins

Pressurized air is blown through the fill lines ports to make it clean. Then, the fill lines are temporarily covered with masking tape. A single layer of fiber insulation disk is placed on the bottom of the containment vessel, and some pre-cut fiber insulation rings are placed up to the fill line ports as show in Figure 24.



Figure 24: Placing insulation in the containment vessel up to the fill line ports.

The completed test cell set up is inserted in the containment vessel. The test cell fill lines are in proper orientation with the containment vessel fill line ports to be connected as shown in Figure 25. The masking tapes should be removed then.



Figure 25: Inserting the test cell assembly inside the containment vessel.

The fill lines of the test cell should be connected with the fill line ports. For this purpose, the fill line tube should be bended without making a sharp corner. The test cell fill line tubes should be inserted in the containment vessel fill line ports in a proper orientation. This allows for easy connection and tightening (refer to Figure 26). While the test cell fill line is aligned with the bulkhead fitting, the nut should be rotated clockwise until a click is heard. Any over pressure should not be applied to make the connection, which should not be over tightened. Otherwise, the grooves in the fill line port will be damaged which will lead to replacement of that part.



Figure 26: Connecting the fill lines.

To prevent unnecessary electrical noise (which leads to erroneous reading) the guard heater can and the lead of the guard heater should be grounded with the containment vessel through jumper wires (Figures 27 and 28).

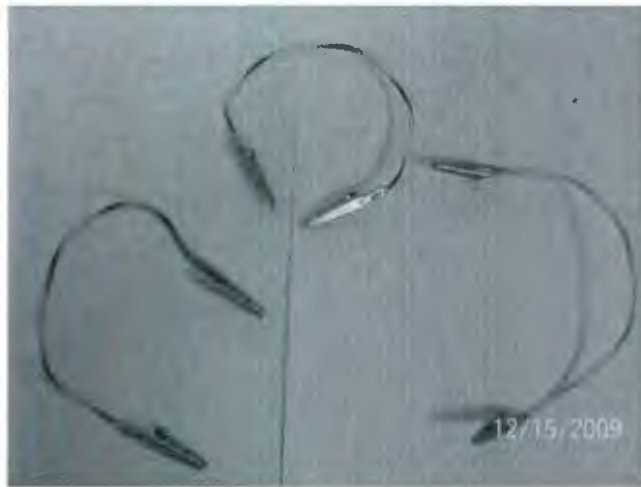


Figure 27: Jumper wires.

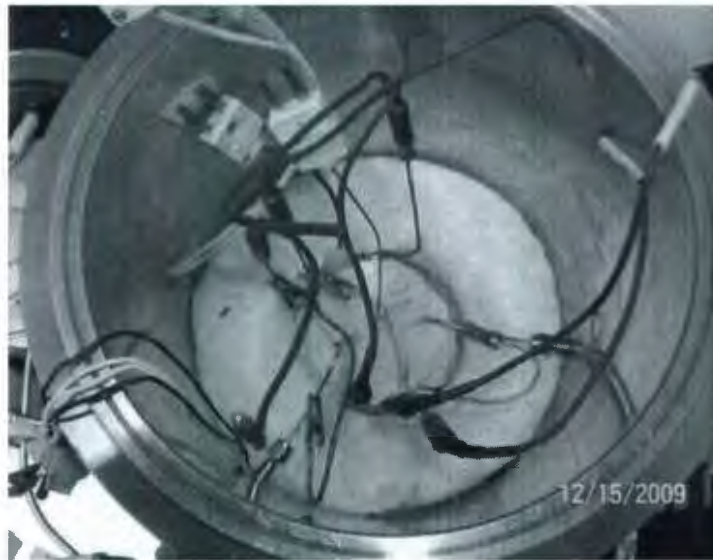


Figure 28: Grounding guard heater can and lid of the guard heaters to fill lines.

At this stage, the connections between test cell and vessel should be complete. Before making any connection (no matter whether it is a wire connection or a thermocouple connection) inside the containment vessel, it is necessary to apply vacuum grease. The connected place should also be taped.



Figure 29: Applying vacuum grease before each connection.

The first wire connection, for an easy management, is between the smallest male port with the smallest female port. This means the connection between the guard heater can and the lid of the guard heater. Next, connect the yellow male ports to the white female ports. That is the connection for the auxiliary heater (Figure 30). The rest of female and male parts are for the guard heater connection.



Figure 30: Connecting auxiliary heater connections (yellow to white).

A2.1.2.2 Thermocouple connections inside the vessel

The TC1 leads should be connected with the female thermocouple port noted as “1” and the TC2 leads should be connected with the female thermocouple port noted as “2”. While doing the

connections, the negative male part should be inserted to the negative female part and the positive male part should be inserted to the positive female part (Figure 31).



Figure 31: Correct thermocouple connections ('-' to '-' and '+' to '+')

For the thermocouples, vacuum grease should be applied to the outer side of the thermocouple connections and then it should be covered by tape.

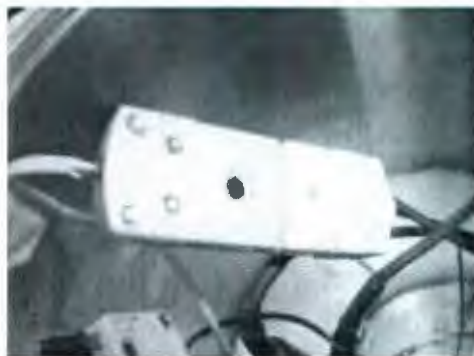


Figure 32: Applying vacuum grease and taping outside of the thermocouple connections.

Figure 33 shows the inside of the containment vessel after all the connections are made.



Figure 33: Inside view of the containment vessel after all connections.

The resistance of the auxiliary heater and the guard heater should be rechecked (Figure 34). The resistance of the auxiliary heater should be around $18\ \Omega$ and the resistance of the guard heater should be around $58\ \Omega$.



Figure 34: Re checking auxiliary heater resistance



Figure 35: Rechecking guard heater resistance.

It is also necessary to check the continuity of guard heater sheath to the containment vessel (Figure 35).



Figure 36: Confirming guard heater sheath to vessel continuity.

A2.1.2.3 Insulation

Pre-cut insulation fiber rings are placed around the wires, and small fiber disks are placed on the top of test cell assembly (Figure 37). However, excessive amount of insulation should not be pressed inside the vessel. In case of open tests, a hole should be maintained along the vent line for proper ventilation.

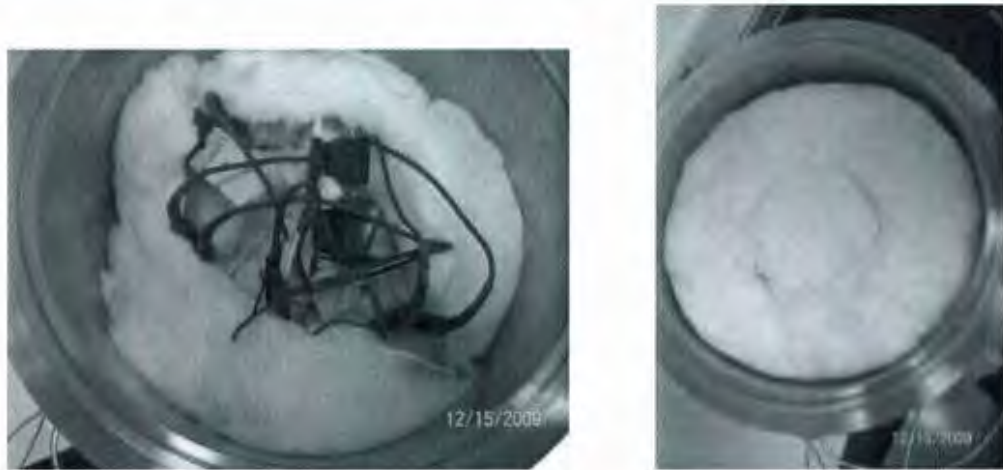


Figure 37: Installing upper fiber insulation to cover pressure and vent ports.

A2.1.3 Vessel Assembly

A deflector plate should be placed on the top of the insulation which will make the nitrogen stream to enter the containment vessel in a well distributed way (Figure 38).



Figure 38: Inserting deflector plate on the top of the insulation.

Then the top of the containment vessel should be placed as shown in Figure 39.



Figure 39: Placing the top of the containment vessel.

The next step is to place the ring on the top of the containment vessel. One should be very careful to put the ring in a way so that the side having deeper marks of bolts will be upwards as shown in Figure 40. Otherwise, the containment vessel will not be able to hold the pressure. As a result, the increased pressure in the test cell will deform the test cell, which might be burst.



Figure 40: Ring on the right direction (Top and side view)



Figure 41: Ring on the wrong direction (Top and side view)

The ring and the top of the vessel are held together with two pieces of half round jaws. It is necessary to make sure that the jaws are adjacently placed around the top portions of the containment vessel (Figure 42). Otherwise, the two parts will not be contacted with each other properly.



Figure 42: Proper placement of the jaws around the top parts, the right image is showing a closer view.

The mating portions of the two half round jaws should be as close as possible as shown in the Figure 43.



Figure 43: A closer view of the mating portion of the two half round jaws.

While putting the jaws together, one should be careful that the two adjacent lid bolts of the jaws around the rupture disk are in an equal and sufficient distance from the rupture disk (Figure 44). Otherwise, it will be difficult to tighten the lid bolts.



Figure 44: Maintaining equal and sufficient distances between the rupture disk part and two adjacent screws.

Figure 45 shows the proper sequence to tighten the lid bolts of the jaws. This sequence will help to maintain least distance between the mating parts. The lid bolts need to be tightened as much as possible by hand at first. Then the balanced tightening pattern should be used to make it properly tightened for preventing pressure leakage.

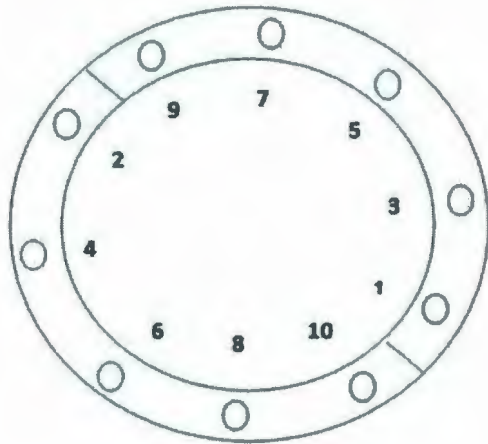


Figure 45: Schematic diagram (top view) showing the sequence of tightening the lid bolts.



Figure 46: Tightening the lid bolts in a proper sequence.

A2.1.4 Checking Resistance of Thermocouples and Heater Glands

It is a significant important part for the containment vessel set up.

The resistances of thermocouple leads (both TC1 and TC2) to vessel should be greater than 20 M Ω , and the resistance of TC1 to TC2 should be greater than 1 M Ω .



Figure 47: Checking resistance of TC1 leads to vessel.



Figure 48: Checking resistance of TC2 leads to vessel.



Figure 49: Checking resistance of TC1 leads to TC2 leads.

The resistance of the heaters (both auxiliary and guard) leads to the vessel and as well as the resistance of the auxiliary heater leads to guard heater leads should be more than 1 M Ω (Figure 50).

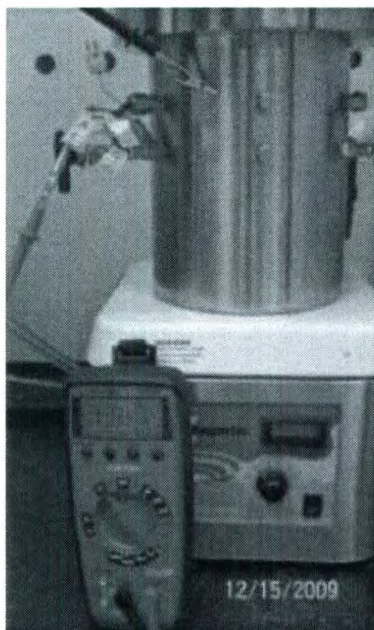


Figure 50: Checking resistance of auxiliary heater leads to vessel.

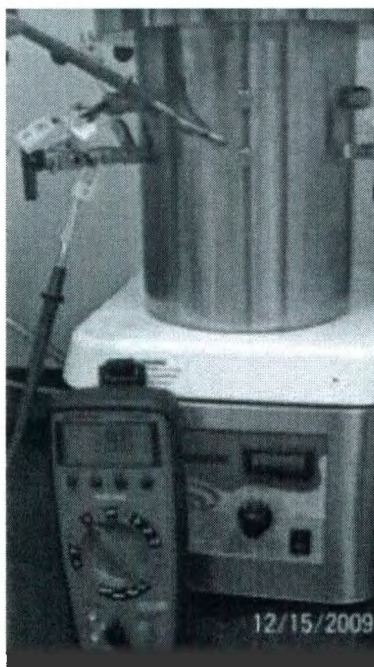


Figure 51: Checking resistance of guard heater leads to vessel.



Figure 52: Checking resistance of auxiliary heater leads to vessel.

The resistance between each of the heaters and each of the thermocouple should also be out of limit.

A2.1.5 Thermocouple Connections outside the Vessel

The next step is to make the thermocouple connections ('1' to '1' and '2' to '2') outside the vessel (Figure 53). Both of the thermocouples need to be grounded with the containment vessel by using jumper wire (Figure 54).



Figure 53: After making thermocouple connections.



Figure 54: Grounding both thermocouples to the containment vessel.

The connections for both auxiliary heater and the guard heater should be made as shown in Figure 55.



Figure 55: After making heater and thermocouple connections and grounding thermocouples to vessel.

To minimize noise, it is very important to ground the containment vessel to the main electronic console by a long jumper wire. This grounding connection is illustrated in Figures 56 and 57.



Figure 56: The view of the jumper wire (orange one) near vessel grounding vessel to main electronic console.



Figure 57: Grounding the containment vessel to main electronic console.

All the connections wires should be kept as far as possible from the magnetic stirrer. Otherwise, unwanted electronic signals will cause erroneous and huge amount of data points while running the experiment.



**Figure 58: Complete connection – right way.
(as the wires are managed to place away from the magnetic stirrer)**

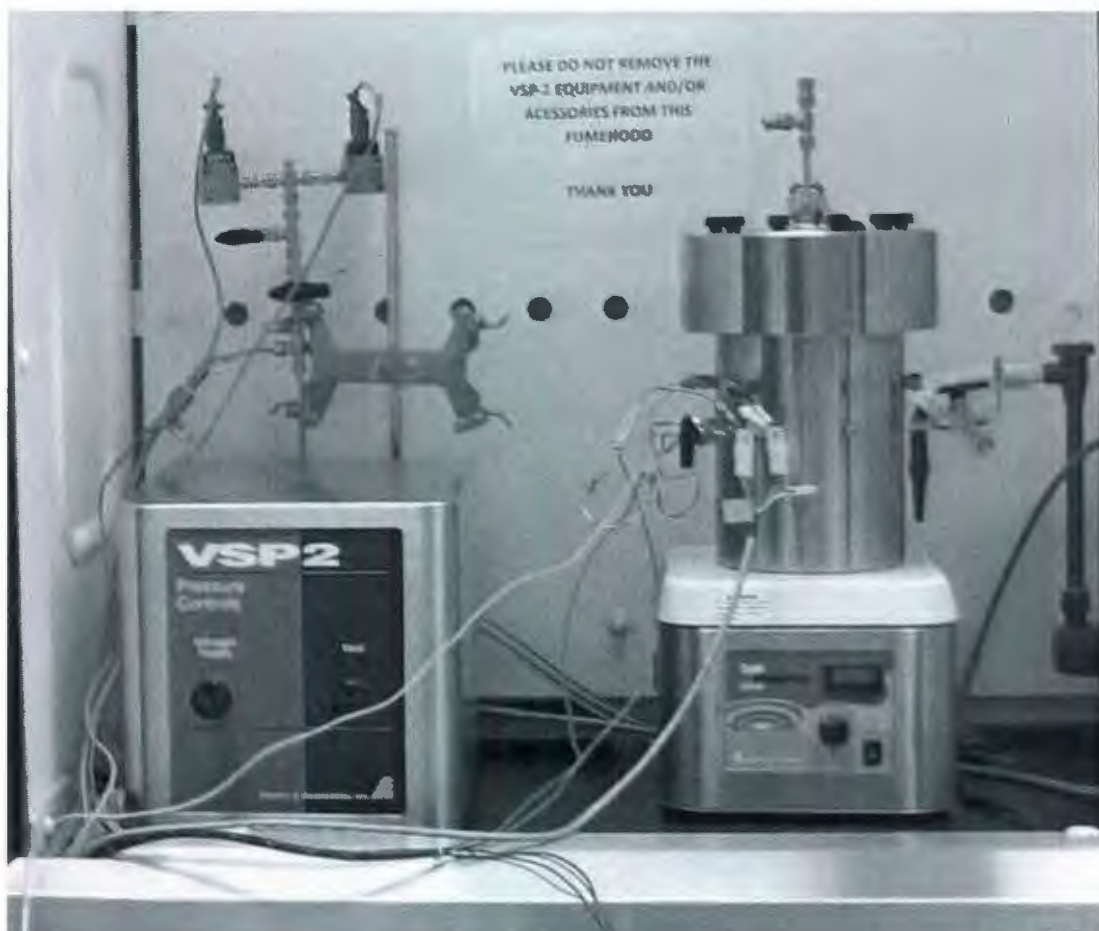


Figure 59: Complete connection - wrong way.
(as the wires are a bit closer to the magnetic stirrer)

A2.1.6 Calibration of Thermocouples

With the new software, it is not necessary to calibrate the temperature. However, a simple correction can be made for more accurate results. At first, an arbitrary temperature is set in the temperature calibrator device, which is then connected to the thermocouple connection wire coming from the main electronic console (Figure 60). The VSP2 setup screen menu should show the same arbitrary temperature that is set in the temperature calibrator device. If the computer screen temperature does not match the calibration device temperature, it is necessary to input the required offset temperature value in the “Reference Temperature Offset” box in the screen menu to make the two values almost equal (Figure 61). The temperatures shown in the screen should be accurate within 1°C with the set arbitrary temperature. Both of the thermocouples (TC1 and TC2) can be calibrated in this way.



Figure 60: Setting an arbitrary temperature in the temperature calibrator device.

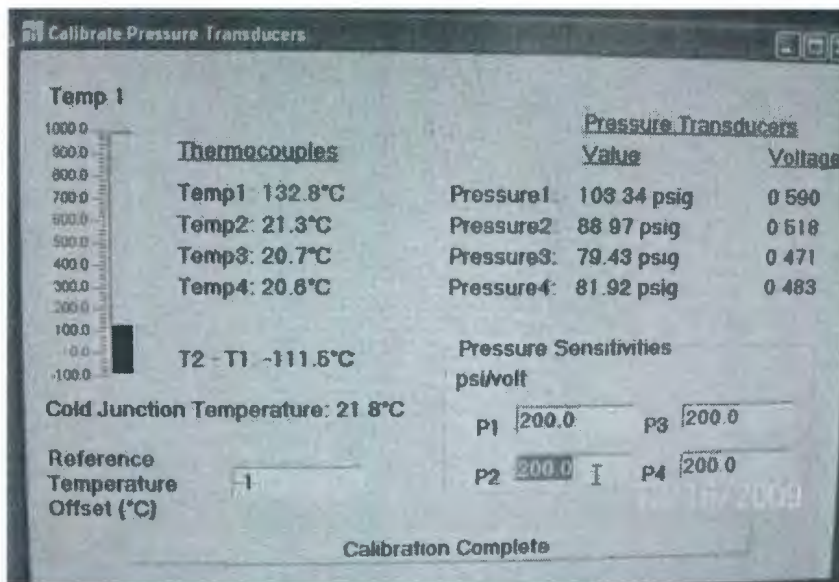


Figure 61: Offsetting the value of TC1 in the screen by “-1” for making it almost equal to the arbitrary temperature value.

After doing the adjustment, the thermocouples can be subjected to the room environment to see that whether it is perfectly sensing the room temperature or not. In that case, TC1 and TC2 should agree within 1°C (Figure 62).

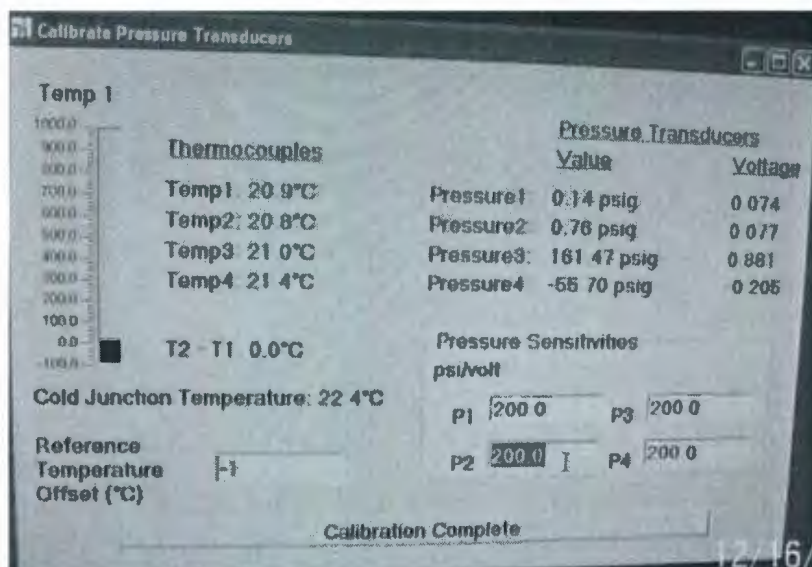


Figure 62: Checking whether the VSP2 console is perfectly sensing room temperature or not.

A2.1.7 Calibration of Pressure Transducers

Two pressure transducers (one for measuring the pressure in the test cell and another one for measuring the pressure in the containment vessel) need to be mounted on the calibration tree (Figure 63).

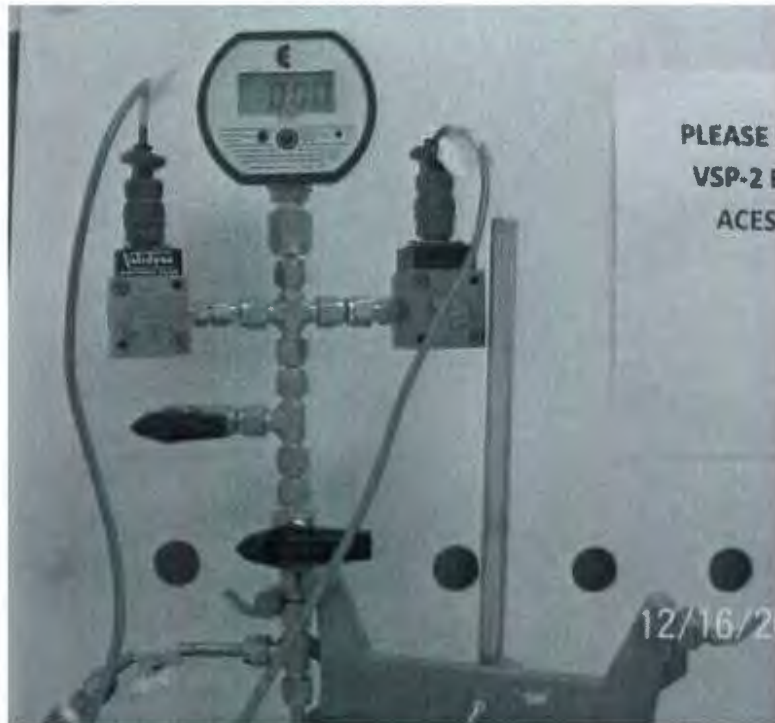


Figure 63: Calibration tree showing 0 psig while the valve is opened.

Depressurization is done to make the pressure zero psig by opening the valve near to the pressure gauge. The P1 and P2 of the zero pot in the main electronic console is adjusted with a screw driver so that the P1 and P2 readings in the software interface are as close as possible to zero (Figures 64 and 65). Once the zero pot is adjusted, a pressure up to the maximum test range is applied (in most cases, 800 psig), and the P1 and P2 of the gain pot in the main electronic console is adjusted in the same fashion (Figures 66 and 67).



Figure 64: P1 and P2 of of the zero pot and gain pot of the main electronic console.



Figure 65: Screw driver to adjust the zero pot & gain pot.

Then the pressure is decreased by couple of hundreds psig while checking whether the pressure sensed by the pressure gauge and the pressure sensed by the VSP2 console are similar or not. If they are not similar, re-adjusting of the pots in the main electronic console is necessary. The re-

checking of the pressures and re-adjusting of the pots will be repeated til the pressure sensed be the VSP2 console is within 1 psig of the pressure sensed by the pressure calibrator.



Figure 66: Calibration tree showing 807 psig after applying some pressure.

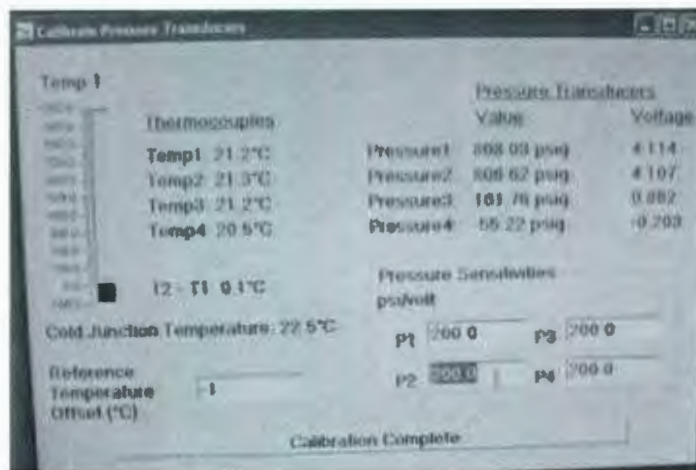


Figure 67: Set up screen menu after adjusting the gain pots in the main electronic console.

After calibrating the pressure, the transducers are separated from the calibration tree and mounted to the containment vessel (Figure 68). It is important to note that the pressure transducers with diaphragms should be mounted to the containment vessel in a proper vertical direction. Otherwise they might be deflected by the magnetic field of the stirrer.

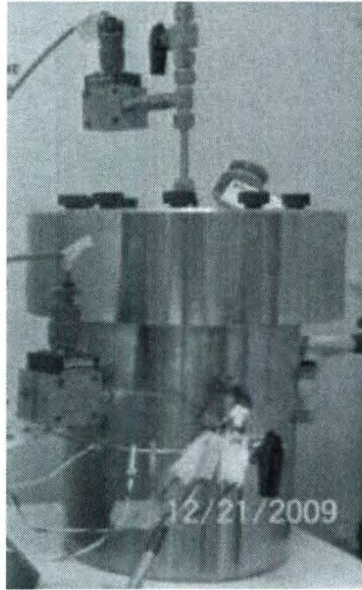


Figure 68: Pressure transducers mounted vertically to the containment vessel.

A2.1.8 Checking Leak in the Test Cell

One of the most important things is to check whether the test cell is holding the pressure or not. The necessary steps for this checking will be described as follows:

1. Make sure that there is no leak in the assembly due to opened valves. That is the valve from the control box to the pressure gauge and the valve from the test cell to the atmosphere (the line which is used is to charge sample for closed cell test) are closed (Figures 69 and 70).



Figure 69: Valve near to pressure gauge.



Figure 70: Valve for sample charging.

2. The nitrogen tank must provide the pressure to the assembly. The applied pressure is generally 800 psig.
3. Apply 30 psig in both the test cell and containment cell. Make sure that valve from the nitrogen tank to the top of the containment vessel and the valve from the containment vessel to the test cell are opened. (Figure 71 and 72)



Figure 71: Valve for nitrogen inlet in the containment vessel.



Figure 72: Valve linking vessel and test cell.
(Note: it is in closed direction in the figure)

Then the “nitrogen” box in the software interface is set to open the solenoid valve, and the “nitrogen supply” valve of the control box is also turned slowly to the left till the pressure of the test cell and the containment vessel is around 30 psig. The manual valve in the control box should be closed as soon as the pressure reaches 30 psig, and then the “all closed” box in the software interface is set (Figure 73 and 74).



Figure73: Manual Nitrogen supply and Vent valve in the Pressure control box.

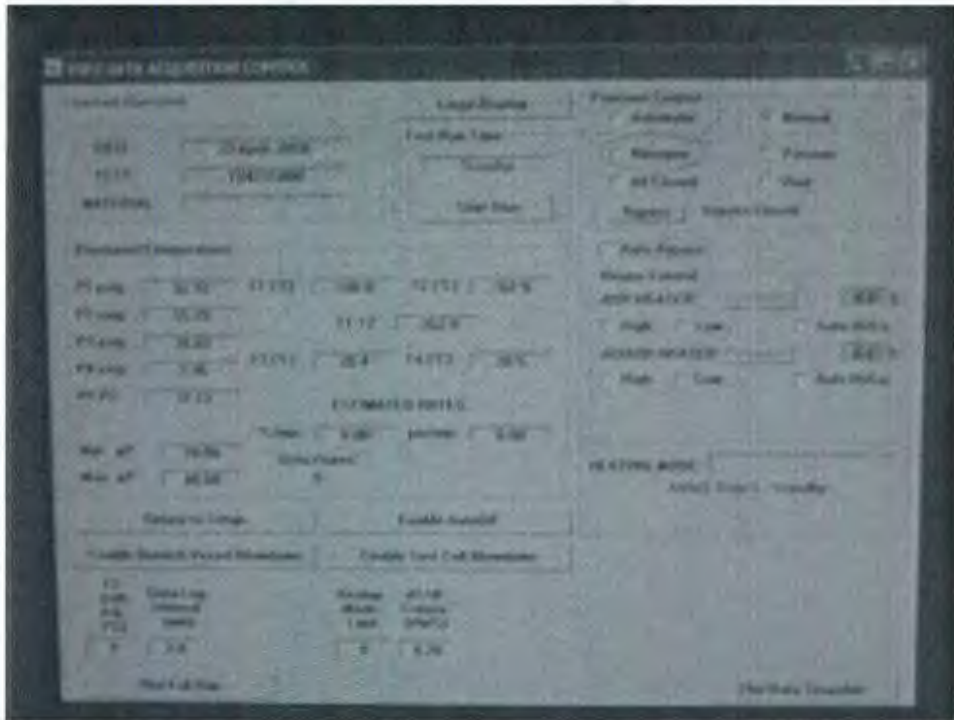


Figure74: Software interface showing “Nitrogen” box as well as “Vacuum”, “All Closed” and “Vent” boxes.

4. Make the pressure difference between test cell and the containment vessel by closing the valve, which linked the test cell to the containment vessel. Then, vent the pressure from the containment vessel by pressing “vent” in the software and manually opening the “vent” valve in the control box. (Figure 73 and 74)
5. When the pressure of the containment vessel (P2) is around ambient pressure (0 psig), the vent valve in the control box is manually closed and the “all closed” box in the software interface is pressed. The pressure of test cell (P1) is observed to check whether it is constant or not for about 10 minutes. This indicates whether the test cell is capable of holding the pressure or not.
6. After checking the leak in the test cell, the valve from the test cell is opened to the containment vessel to release the pressure in the test cell to the containment vessel.

A2.1.9 Applying Vacuum in the Test Cell and Containment Vessel

The reason for applying vacuum is to avoid pad gas correction while analyzing the data.

1. Make sure that the linking valve between the test cell and the containment vessel is opened.
2. The vacuum pump needs to be switched on. It is also necessary to make sure that the valve from the vacuum pump to the control box is open (Figure 75).

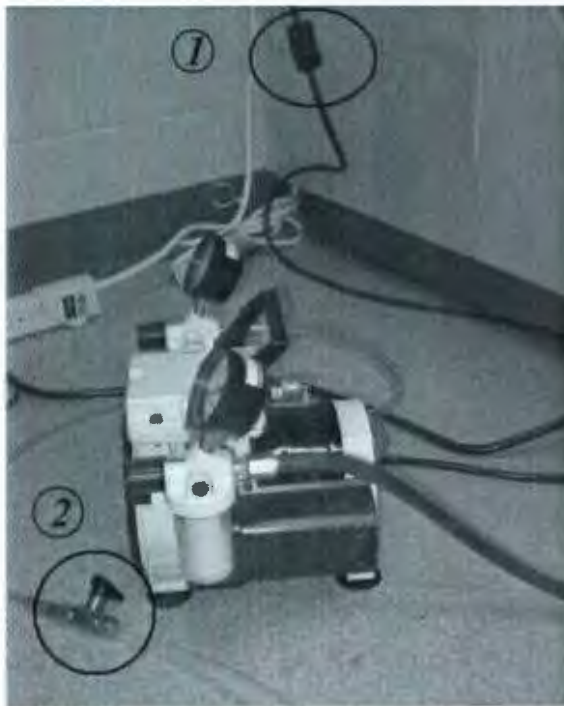


Figure75: Vacuum pump showing turn on switch (1) and valve from the vacuum pump to the control box (2).

Then “vacuum” box in the software interface (Figure 74) is pressed, and the pressure decreases to about “-14.7psig”.

3. The valve from the containment vessel to the test cell is closed. Then, the vacuum pump is switched off, the valve from the vacuum pump to the control box is closed, and the “all closed” box in the software interface is pressed

A2.1.10 Loading Sample in the Test Cell

A2.1.10.1 Liquid sample

A syringe is loaded with the required amount of sample and placed on the fill line (Figure 76). The valve of the fill line is opened slowly so that the sample can enter into the test cell. As there is a vacuum condition in the test cell, it is not necessary to push the piston. The sample will automatically enter through the fill line due to the vacuum and its own weight. After injecting all the samples the valve is closed and the syringe is disassembled from the fill line.



Figure 76: Installed syringe with sample in the fill line.

A2.1.10.2 Solid sample

For solid samples, it is necessary to load the sample in the test cell before installing it in the containment vessel. In that case, the general procedure of applying vacuum will not be applicable. The containment vessel is evacuated at first and then the test cell is vented very slowly to the evacuated containment vessel by tapping to vacuum using the bypass line. Otherwise the test can be done without applying vacuum and pad gas correction is performed while analyzing the data.

A2.1.11 Running Test

The mode of the operation should be selected and the appropriate test name, test material and other parameters should be entered.

The sample is then entered to the test cell through the fill line. The magnetic stirrer should be set approximately from 400 to 500 rpm for good stirrer option. Then the heater switches should be turned on (both in main control box and software interface). For auxiliary heater, low power mode and for guard heater, auto power mode is used typically (Figure 77 and 78).



Figure 77: Knobs for controlling the heaters in the main control box.

(Note that the main control box as well as both of the heaters is switched off in this figure)



Figure 78: The heater control portion in the software interface during experimental run.

The following checks should be conducted while doing the experiment:

- The nitrogen supply valve is opened.
- The nitrogen supply needle valve needs to be opened by about $\frac{1}{4}$ turn at the beginning of the experiment.
- The vessel inlet valve on top of the containment vessel should be opened.
- The vent throttle valve needs to be fully opened.
- The pressure control needs to be in the automatic mode.

The power supply in the control box should not be switched off during test experiment. Otherwise, the pressure inside the test cell will be less than the pressure in containment vessel and this will destroy the test cell.

After completion of the experiment, the heater switches should be turned off and the nitrogen supply should be isolated. The valve in the nitrogen must be closed before leaving the lab.

A2.2 BASIC CONCERNS

Direction of tightening and loosening?

When the nut is turning around in the clockwise direction, it is tightening up and it is loosening while turning in the anti clockwise direction. The easy way to remember this is to memorize “Righty tighty, Lefty loosy”.

Open and closing direction of valves?

When the knob of the valve is in parallel direction with the flow line, it is opened. The valve is closed, while the knob is at a perpendicular direction to the flow line.

How to open and depressurize the nitrogen tank?

Valve 1 is turned in left direction, valve 2 is opened, and valve 3 is screwed till the pressure reaches up to the required pressure (Figure 77).



Figure 77: Opening the nitrogen tank.

For depressurizing, close valve 1 first, then open the valve near the pressure tree slowly till it is totally depressurized. Lastly turn valve 3 to the right to make it as loose as possible. Otherwise while pressurizing next time; there will be a sudden rise in pressure in the system.

How to clean a pressure transducer?

It is recommended to clean the pressure transducer adjacent to the test cell after each experiment. The little set screw in the bleed port which is situated on the opposite side of the connecting thread of the pressure transducer is loosened by using a ball ended hexagonal screw driver (Figure 78 and 79). Then, acetone is flowed through the bleed port which will come out through the connecting thread of the pressure transducer. After washing with acetone, air is also passed through the acetone. While passing acetone and air through the bleed line, one should be very careful so that the o-ring adjacent to the bleed port is not lost with the flow.



Figure 78: Bleed port (1) and connecting thread (2) of the pressure transducer.



Figure 79: Ball ended hexagonal screw driver.

A2.3 TROUBLESHOOTING

What to do when ΔP is very high?

In the emergency condition when the ΔP is very high (>40 psig), the valve from the containment vessel to the test cell needs to be opened, but only with the valve from the nitrogen tank to the top of the containment vessel being closed. If the valve at the top of the containment vessel is opened, all the chemicals would be sucked up by the solenoid valve in the control box.

What to do while having frequent pressure drop during pressure calibration?

The first reason behind it is that there is some pressure leak in the system. Make sure that all the connections are leak proofed by applying soapy water in the connections. If the soapy water is bubbling, make that connection leak proof by applying anti seize and Teflon tape.

As long as there is no leak in the two connections in the containment vessel for pressure transducers, the system is alright to run. However, to have a better collection adjust the zero pot and gain pot for at least three times by pressurizing and depressurizing the vessel for three times. Then increase the pressure with a 100 psig increment up to the required pressure and observe the reading of the pressure gauge and the software. If the difference between these two readings for each increment ranges from 1 psig to 3 psig, the pressure calibration is alright.

Having a loose swage lock?

Tight the screw in the knob of the lock with a ball ended hexagonal screw driver.

Getting too much data points while the experiment is running?

The test data points should be monitored very closely at the beginning of the experiments. If the test is at the very beginning stage, it is better to stop the test and restart it. Accumulation of large number of data points can be due to the following reasons:

- (i) The electrical wires might be close to the strong magnetic stirrer which is providing error signals. Make sure that the wires were placed as far as possible from the magnetic stirrer.

- (ii) The ground connections inside and the outside of the containment vessel might not be connected properly. Make sure that they are OK.
- (iii) The thermo couple of the test cell might be affected by the moisture in the air, as they are not used for a long time. While making the test cell assembly, the resistance between TC1 and test cell wall should be carefully checked. If the resistance is lower, the test cell can be heated up in an oven at around 50°C for a 12hr to 24hr period to get back the proper resistance.
- (iv) If neither of the above reasons is valid make the data log in interval to 3 or 4. That will for surely have less noisy data. But remember that for a fast runaway reaction, making the data log in interval so wide will cause to lose important data points.

Nonstop clicking sound at the cooling stage of the experiment?

The possible reason behind that “Automatic” box is pressed in the pressure control section of the software interface. During the cooling stage, the pressure in the test cell is dropping other than increasing. As a result, the pressure difference between the test cell and the containment vessel becomes negative. While in an automatic mode, the solenoid valve is opened to try to minimize the pressure difference between them. As the solenoid valve is only capable of supplying nitrogen to the containment vessel, it can’t help to counterbalance the negative pressure difference. And as a result, nonstop clicking sounds are heard. Press the “Manual” box in the pressure control section of the software interface. But remember that it is necessary to vent the pressure time to time while the pressure control of the experiment is in manual stage, otherwise the test cell will be collapsed.

APPENDIX 3

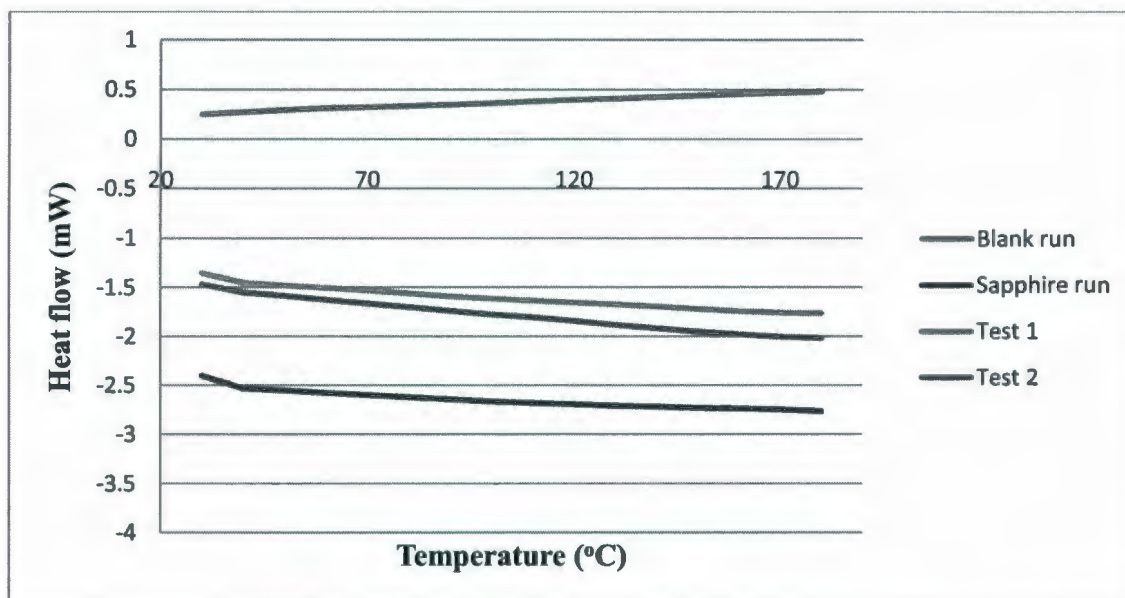


Figure 1: Heat Flow as a Function of Temperature for Nox Rust 1100

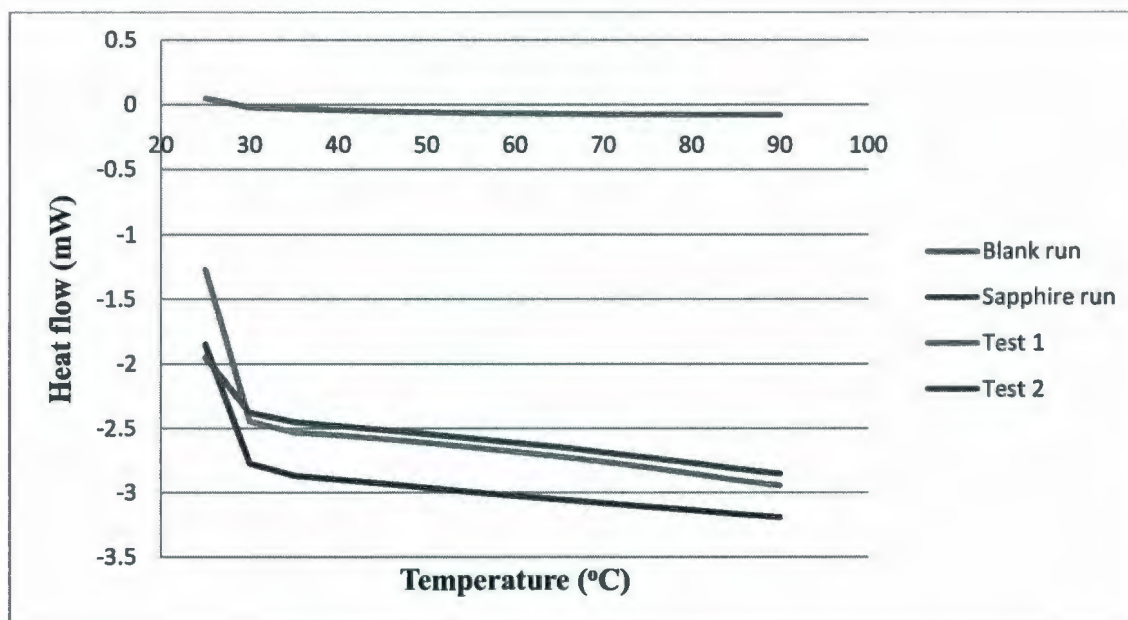


Figure 2: Heat Flow as a Function of Temperature for Nox Rust 9800

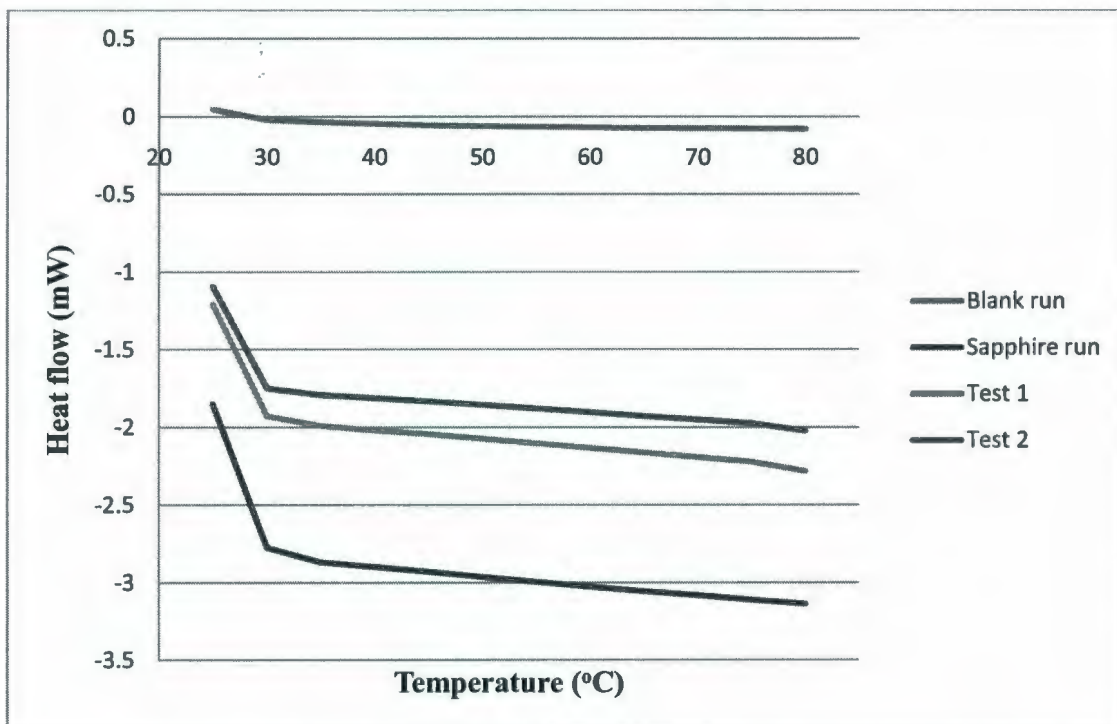


Figure 3: Heat Flow as a Function of Temperature for Brenntag Corrosion Inhibitor

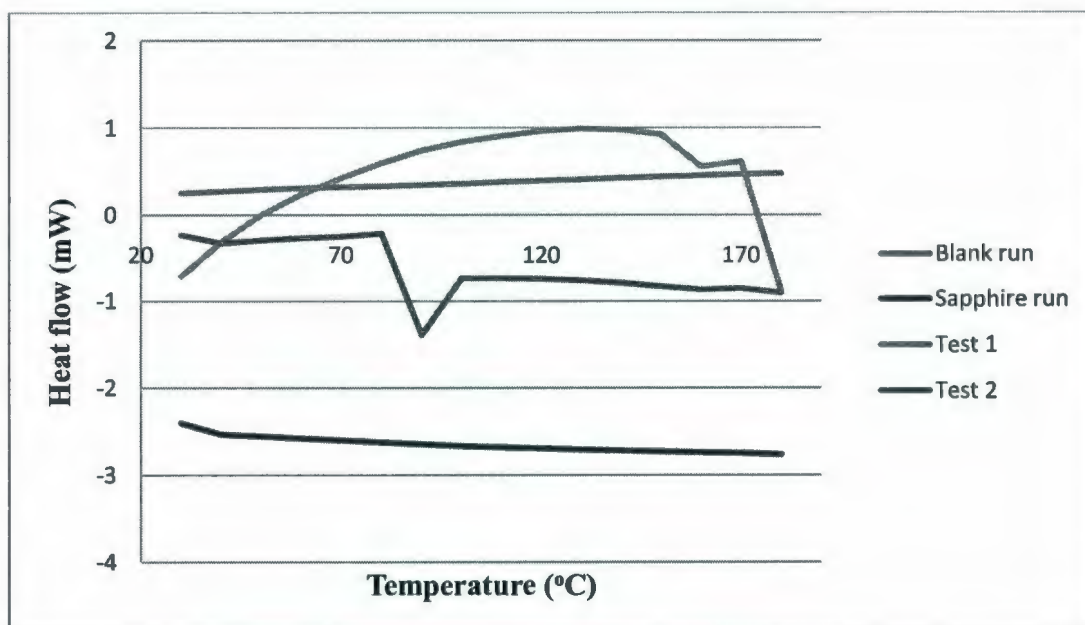


Figure 4: Heat Flow as a Function of Temperature for VCI 1 Powder

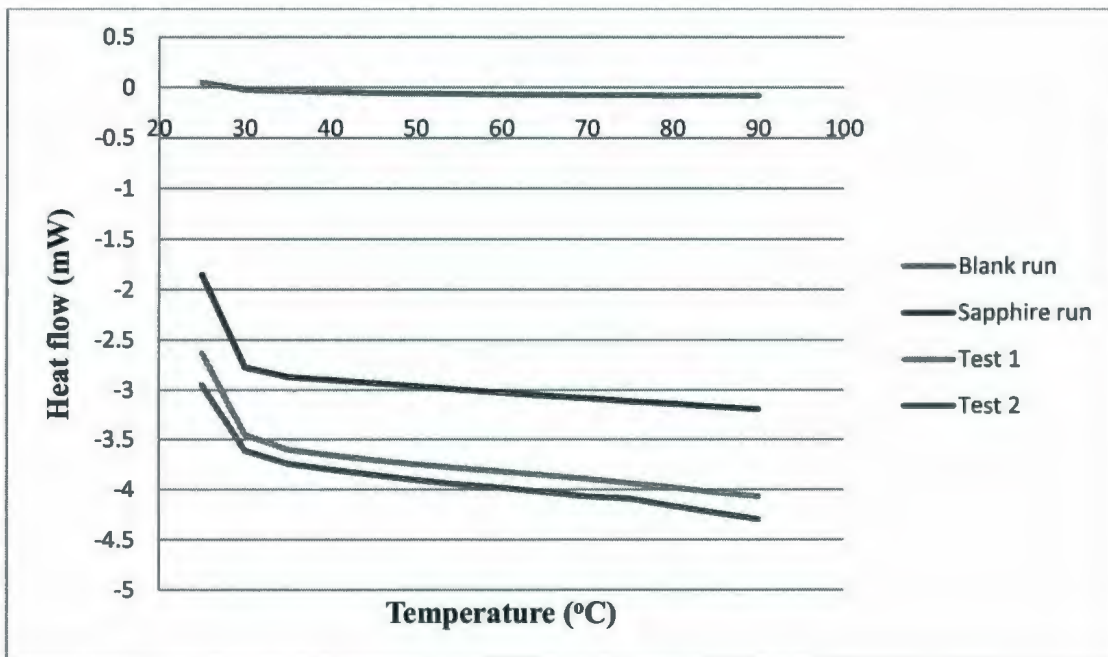


Figure 5: Heat Flow as a Function of Temperature for Formaldehyde

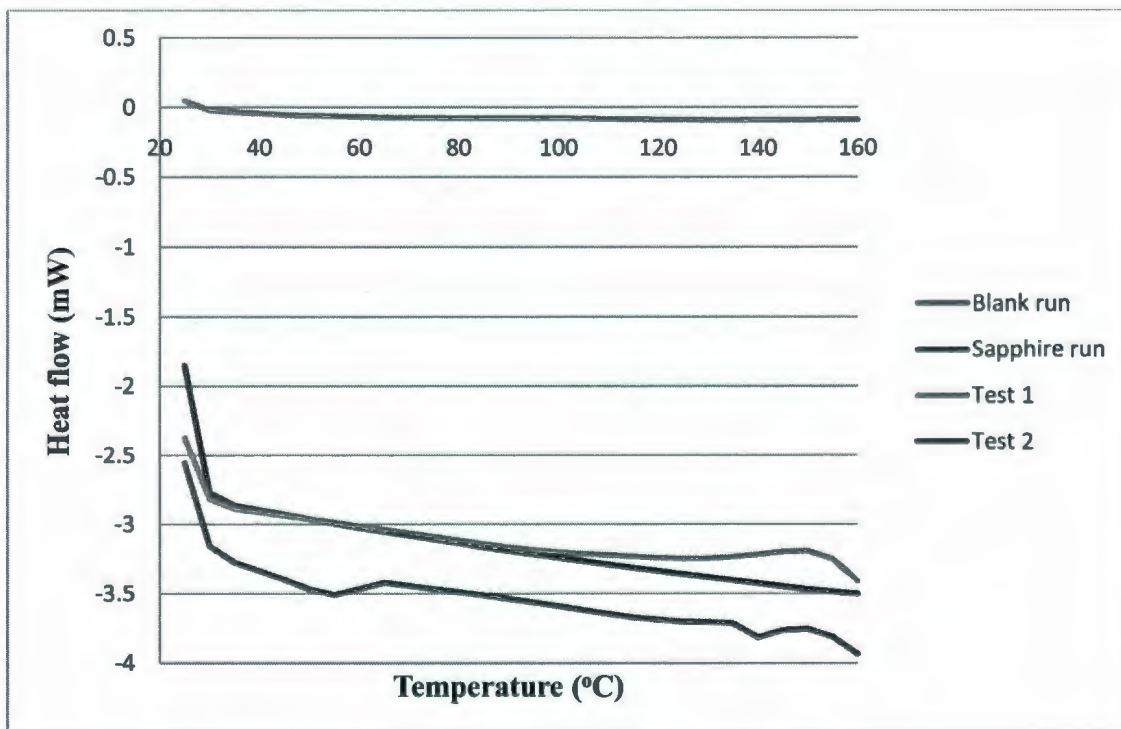


Figure 6: Heat Flow as a Function of Temperature for Monoethanolamine

Table 1: Specific Heat Capacity Values for Nox Rust 1100

| Temperature (°C) | Specific Heat Capacity (J/ kg-K) | | Average Specific Heat Capacity (J/ kg-K) | Standard Deviation | Standard Error |
|---------------------|----------------------------------|---------|--|-----------------------|-------------------|
| | Test 1 | Test 2 | | | |
| 30 | 1940.54 | 2206.36 | 2073.45 | 132.91 | 93.98 |
| 40 | 2022.88 | 2274.33 | 2148.60 | 125.72 | 88.90 |
| 50 | 2098.35 | 2366.80 | 2232.58 | 134.23 | 94.91 |
| 60 | 2164.94 | 2455.32 | 2310.13 | 145.19 | 102.67 |
| 70 | 2225.73 | 2539.62 | 2382.68 | 156.95 | 110.98 |
| 80 | 2292.61 | 2623.51 | 2458.06 | 165.45 | 116.99 |
| 90 | 2359.39 | 2704.57 | 2531.98 | 172.59 | 122.04 |
| 100 | 2416.70 | 2781.37 | 2599.03 | 182.33 | 128.93 |
| 110 | 2475.89 | 2859.35 | 2667.62 | 191.73 | 135.57 |
| 120 | 2528.86 | 2939.46 | 2734.16 | 205.29 | 145.17 |
| 130 | 2578.51 | 3022.79 | 2800.65 | 222.14 | 157.08 |
| 140 | 2636.67 | 3101.66 | 2869.16 | 232.49 | 164.40 |
| 150 | 2698.41 | 3180.03 | 2939.22 | 240.81 | 170.28 |
| 160 | 2754.05 | 3251.77 | 3002.91 | 248.86 | 175.97 |
| 170 | 2799.36 | 3313.68 | 3056.52 | 257.16 | 181.84 |
| 180 | 2823.07 | 3349.25 | 3086.16 | 263.09 | 186.03 |

Table 2: Specific Heat Capacity Values for Nox Rust 9800

| Temperature (°C) | Specific Heat Capacity (J/ kg-K) | | Average Specific Heat Capacity (J/ kg-K) | Standard Deviation | Standard Error |
|---------------------|----------------------------------|---------|--|-----------------------|-------------------|
| | Test 1 | Test 2 | | | |
| 30 | 2492.05 | 2420.09 | 2456.07 | 35.98 | 25.44 |
| 35 | 2528.55 | 2443.28 | 2485.91 | 42.63 | 30.14 |
| 40 | 2552.19 | 2477.19 | 2514.69 | 37.49 | 26.51 |
| 45 | 2583.25 | 2509.73 | 2546.49 | 36.76 | 25.99 |
| 50 | 2614.65 | 2542.13 | 2578.39 | 36.26 | 25.64 |
| 55 | 2650.05 | 2577.53 | 2613.79 | 36.26 | 25.64 |
| 60 | 2687.03 | 2612.89 | 2649.96 | 37.06 | 26.21 |
| 65 | 2725.62 | 2647.57 | 2686.59 | 39.03 | 27.59 |
| 70 | 2770.25 | 2692.25 | 2731.25 | 39.02 | 27.58 |
| 75 | 2816.94 | 2734.59 | 2775.77 | 41.18 | 29.11 |
| 80 | 2868.41 | 2780.88 | 2824.64 | 43.76 | 30.95 |
| 85 | 2918.84 | 2824.31 | 2871.57 | 47.27 | 33.42 |
| 90 | 2963.61 | 2868.23 | 2915.92 | 47.69 | 33.72 |

Table 3: Specific Heat Capacity Values for Brenntag Corrosion Inhibitor

| Temperature (°C) | Specific Heat Capacity (J/ kg-K) | | Average Specific Heat Capacity (J/ kg-K) | Standard Deviation | Standard Error |
|---------------------|----------------------------------|---------|--|-----------------------|-------------------|
| | Test 1 | Test 2 | | | |
| 30 | 1988.81 | 2008.58 | 1998.69 | 9.89 | 6.99 |
| 35 | 2007.38 | 2008.17 | 2007.77 | 0.39 | 0.28 |
| 40 | 2037.87 | 2031.51 | 2034.69 | 3.18 | 2.25 |
| 45 | 2062.54 | 2053.94 | 2058.24 | 4.29 | 3.04 |
| 50 | 2091.83 | 2078.81 | 2085.32 | 6.51 | 4.60 |
| 55 | 2124.03 | 2105.59 | 2114.81 | 9.22 | 6.52 |
| 60 | 2154.34 | 2131.36 | 2142.85 | 11.49 | 8.12 |
| 65 | 2186.05 | 2159.72 | 2172.89 | 13.17 | 9.31 |
| 70 | 2218.36 | 2188.61 | 2203.49 | 14.88 | 10.52 |
| 75 | 2250.27 | 2216.32 | 2233.29 | 16.98 | 12.00 |
| 80 | 2316.62 | 2276.79 | 2296.71 | 19.91 | 14.08 |

Table 4: Specific Heat Capacity Values for VCI 1 Powder

| Temperature (°C) | Specific Heat Capacity (J/ kg-K) | | Average Specific Heat Capacity (J/ kg-K) | Standard Deviation | Standard Error |
|---------------------|----------------------------------|---------|--|-----------------------|-------------------|
| | Test 1 | Test 2 | | | |
| 30 | 1228.31 | 673.39 | 950.85 | 277.46 | 196.19 |
| 40 | 713.26 | 800.94 | 757.09 | 43.84 | 30.99 |
| 50 | 346.83 | 793.53 | 570.18 | 223.35 | 157.93 |
| 60 | 71.30 | 789.75 | 430.53 | 359.22 | 254.01 |
| 70 | -157.61 | 784.41 | 313.40 | 471.01 | 333.06 |
| 80 | -365.86 | 764.28 | 199.21 | 565.07 | 399.57 |
| 90 | -535.92 | 2338.45 | 901.26 | 1437.19 | 1016.24 |
| 100 | -648.47 | 1500.25 | 425.89 | 1074.36 | 759.69 |
| 110 | -713.25 | 1530.90 | 408.83 | 1122.08 | 793.43 |
| 120 | -773.59 | 1568.26 | 397.34 | 1170.93 | 827.97 |
| 130 | -791.89 | 1614.85 | 411.48 | 1203.37 | 850.91 |
| 140 | -758.17 | 1683.44 | 462.64 | 1220.80 | 863.24 |
| 150 | -668.64 | 1763.68 | 547.52 | 1216.16 | 859.95 |
| 160 | -157.02 | 1842.08 | 842.53 | 999.55 | 706.79 |
| 170 | -221.38 | 1847.95 | 813.29 | 1034.66 | 731.62 |
| 180 | 1815.34 | 1935.67 | 1875.50 | 60.16 | 42.54 |

Table 5: Specific Heat Capacity Values for Formaldehyde

| Temperature (°C) | Specific Heat Capacity (J/ kg-K) | | Average Specific Heat Capacity (J/ kg-K) | Standard Deviation | Standard Error |
|---------------------|----------------------------------|---------|--|-----------------------|-------------------|
| | Test 1 | Test 2 | | | |
| 30 | 2967.13 | 3244.47 | 3105.80 | 138.67 | 98.05 |
| 35 | 3035.51 | 3297.48 | 3166.49 | 130.98 | 92.62 |
| 40 | 3089.41 | 3358.52 | 3223.96 | 134.55 | 95.14 |
| 45 | 3137.93 | 3412.56 | 3275.25 | 137.31 | 97.09 |
| 50 | 3176.65 | 3460.09 | 3318.37 | 141.72 | 100.21 |
| 55 | 3209.90 | 3500.29 | 3355.10 | 145.19 | 102.67 |
| 60 | 3239.23 | 3533.26 | 3386.25 | 147.01 | 103.95 |
| 65 | 3274.44 | 3572.80 | 3423.62 | 149.18 | 105.49 |
| 70 | 3310.76 | 3616.69 | 3463.73 | 152.97 | 108.16 |
| 75 | 3348.29 | 3635.94 | 3492.12 | 143.82 | 101.70 |
| 80 | 3387.70 | 3706.33 | 3547.01 | 159.31 | 112.65 |
| 85 | 3427.09 | 3765.54 | 3596.31 | 169.22 | 119.66 |
| 90 | 3463.02 | 3828.44 | 3645.73 | 182.71 | 129.19 |

Table 6: Specific Heat Capacity Values for Monoethanolamine

| Temperature (°C) | Specific Heat Capacity (J/ kg-K) | | Average Specific Heat Capacity (J/ kg-K) | Standard Deviation | Standard Error |
|---------------------|----------------------------------|---------|--|-----------------------|-------------------|
| | Test 1 | Test 2 | | | |
| 30 | 2830.90 | 2904.50 | 2867.70 | 36.80 | 26.02 |
| 35 | 2842.79 | 2954.04 | 2898.41 | 55.63 | 39.33 |
| 40 | 2873.33 | 3016.19 | 2944.77 | 71.43 | 50.51 |
| 45 | 2899.02 | 3080.18 | 2989.60 | 90.58 | 64.05 |
| 50 | 2923.81 | 3146.77 | 3035.29 | 111.48 | 78.83 |
| 55 | 2949.43 | 3184.76 | 3067.09 | 117.66 | 83.20 |
| 60 | 2975.53 | 3143.01 | 3059.27 | 83.74 | 59.21 |
| 65 | 3002.99 | 3101.78 | 3052.39 | 49.40 | 34.93 |
| 70 | 3031.67 | 3124.95 | 3078.31 | 46.64 | 32.98 |
| 75 | 3058.92 | 3146.97 | 3102.95 | 44.03 | 31.13 |
| 80 | 3086.93 | 3167.19 | 3127.06 | 40.13 | 28.37 |
| 85 | 3112.15 | 3187.89 | 3150.02 | 37.87 | 26.78 |
| 90 | 3137.45 | 3210.01 | 3173.73 | 36.28 | 25.65 |
| 95 | 3155.77 | 3234.23 | 3195.00 | 39.23 | 27.74 |
| 100 | 3172.15 | 3259.01 | 3215.58 | 43.43 | 30.71 |
| 105 | 3184.64 | 3287.65 | 3236.15 | 51.51 | 36.42 |
| 110 | 3190.87 | 3310.29 | 3250.58 | 59.71 | 42.22 |
| 115 | 3201.58 | 3333.46 | 3267.52 | 65.94 | 46.63 |
| 120 | 3213.06 | 3349.88 | 3281.47 | 68.41 | 48.37 |
| 125 | 3216.11 | 3361.60 | 3288.86 | 72.75 | 51.44 |
| 130 | 3211.84 | 3362.08 | 3286.96 | 75.12 | 53.12 |
| 135 | 3166.55 | 3333.50 | 3250.02 | 83.48 | 59.03 |
| 140 | 3181.53 | 3465.41 | 3323.47 | 141.94 | 100.37 |
| 145 | 3156.94 | 3410.80 | 3283.87 | 126.93 | 89.75 |
| 150 | 3149.94 | 3399.62 | 3274.78 | 124.84 | 88.28 |
| 155 | 3213.07 | 3457.52 | 3335.29 | 122.22 | 86.43 |
| 160 | 3379.37 | 3578.39 | 3478.88 | 99.51 | 70.36 |

A4.1 Brenntag Corrosion Inhibitor

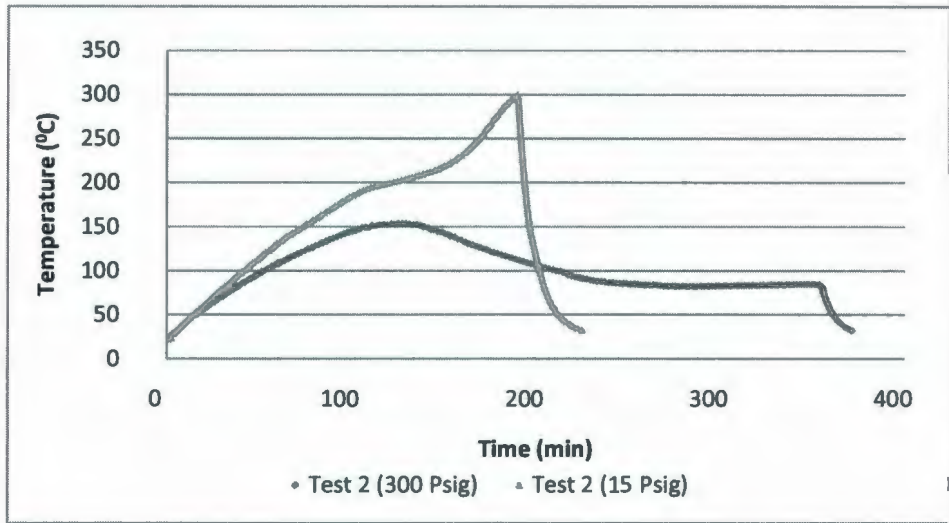


Figure 1: Temperature History for Brenntag Corrosion Inhibitor (ARSST Tests)

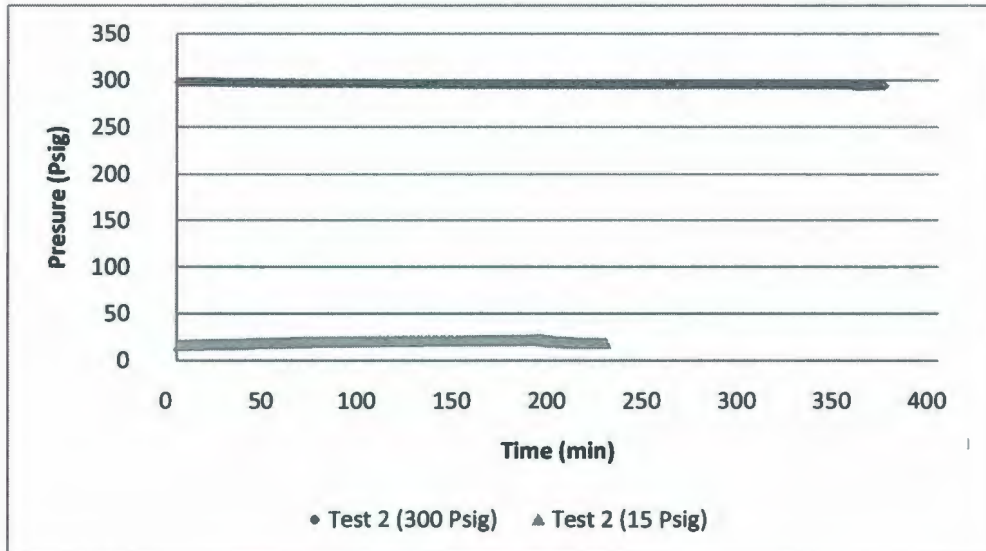


Figure 2: Pressure History for Brenntag Corrosion Inhibitor (ARSST Tests)

A4.2 Nox Rust 9800

A4.2.1 Different Parameters to design Vent size

A4.2.1.1 Phi factor (ϕ) calculation:

Given,

Mass of the sample, $m_s = 7.75 \times 10^{-2}$ kg

Specific heat capacity of the sample at 90°C, $C_{ps} = 2.92 \times 10^3$ J/ kg-K (From Section 4.1.2)

Mass of the test cell, $m_b = 43.04\text{g} = 4.30 \times 10^{-2}$ kg

Specific heat capacity of the stainless steel test cell, $C_{pb} = 510$ J/ kg-K = 510 J/ kg-K

So, Phi factor of the test cell by using Equation 2.1,

$$\phi = 1 + \frac{m_b C_{pb}}{m_s C_{ps}} = 1 + \frac{4.30 \times 10^{-2} \times 510}{7.75 \times 10^{-2} \times 2.92 \times 10^3} = 1.10$$

A4.2.1.2 Temperature rate (\dot{T}) calculation:

From Figure 5.10, the following equation represents the temperature rate (\dot{T}):

$$T = 1.59t + 39.57$$

Temperature rate, $\dot{T} = 1.59$ °C/min = 2.7×10^{-2} K/s

A4.2.1.3 Calculation of heat release rate (q):

Heat release rate (Leung, 1986),

$$q = \phi C_p \dot{T}$$

So, $q = 1.10 \times 2.92 \times 10^3 \times 2.7 \times 10^{-2} \text{ J/kg-s} = 86.72 \text{ J/kg-s}$

A4.2.1.4 Determining set pressure (P_s), set temperature (T_s) and $\frac{dP}{dT}$:

The set pressure for venting is considered as 100 Psig as the pressure rise is comparatively higher after this point as shown in Figure 5.13.

From the Pressure behavior as a function of Temperature (Figure 5.14),

$$\ln P = \ln(1 \times 10^6) - \frac{4310.3}{T}$$

$$\text{So, } \ln P = 13.82 - \frac{4310.3}{T}$$

Here, pressure at set point, $P = 7.91 \times 10^5 \text{ Pa}$

Temperature at the set point, $T = 474.82 \text{ K} = 201.67 \text{ }^\circ\text{C}$

By differentiating the equation (Fauske, 1985),

$$\frac{1}{P} \frac{dP}{dT} = \frac{4310.3}{T^2}$$

$$\text{So, } \frac{dP}{dT} = \frac{4310.3 P}{T^2}$$

$$\text{So, } \frac{dP}{dT} (\text{at set pressure and temperature}) = \frac{4310.3 \times 7.91 \times 10^5}{474.82^2} \text{ Pa/K} = 1.51 \times 10^4 \text{ Pa/K}$$

A4.2.1.5 Vapor density (ρ_v) and vapor specific volume (v_g) calculation:

Vapor density (ρ_v) can be calculated by considering the system is following ideal gas behavior (Leung, 1986) as follows:

$$\rho_v = \frac{M_w P}{RT}$$

The composition and the chemical properties of Brenntag corrosion inhibitor is proprietary protected. So, the molecular weight of the corrosion inhibitor is assumed to be equal to the molecular weight of one of the major component which is DPGME.

Here,

Molecular weight, $M_w = 148.2 \text{ kg/Kmol}$ (Sciencelab.com Inc, 2008)

Molar gas constant, $R = 8.314 \times 10^3 \text{ J/Kmol} \cdot \text{K}$

Vapor density,

$$\rho_v = \frac{148.2 \times 7.91 \times 10^5}{8.314 \times 10^3 \times 474.82} \text{ Kg/m}^3 = 29.70 \text{ kg/m}^3$$

And, vapor specific volume,

$$v_g = \frac{1}{\rho_v} = 3.37 \times 10^{-2} \text{ m}^3/\text{kg}$$

A4.2.1.6 Latent heat of vaporization (h_g or λ) calculation:

Latent heat of vaporization can be calculated from Clapeyron relation (Leung, 1986).

$$\frac{h_g}{v_g} = T \frac{dP}{dT}$$

$$\text{So, } h_g = \lambda = v_g T \frac{dP}{dT} = 3.37 \times 10^{-2} \times 474.82 \times 1.51 \times 10^4 \text{ J/kg} = 2.41 \times 10^5 \text{ J/kg}$$

A4.2.1.7 Critical mass flux (G) calculation:

This parameter is calculated by using Equation 2.31.

$$G = 0.9 \frac{\lambda}{v_g} \left(\frac{1}{C_p T} \right)^{0.5} = 0.9 \times \frac{2.41 \times 10^5}{3.37 \times 10^{-2}} \times \left(\frac{1}{2.92 \times 10^3 \times 474.82} \right)^{0.5} \text{ kg/m}^2\text{-s} = 5.47 \times 10^3 \text{ kg/m}^2\text{-s}$$

A4.2.2 Vent Sizing Calculation

The vent sizing by Leung's method considers 1000 kg of initial mass and the effective volume of the chemical corresponding to this mass is calculated.

Here,

Density of Brenntag, $\rho_l = 970 \text{ kg/m}^3$ (KPR ADCOR Inc, 2003)

Initial mass in vessel, $m_o = 1000 \text{ kg}$

Volume of the liquid, $V = \frac{m_o}{\rho_l} = 1.03 \text{ m}^3$

A4.2.2.1 Leung's method for homogeneous vessel venting with external heating with no overpressure:

From Equation 2.27,

$$\begin{aligned} A_o &= \frac{Q_T m_o v_g}{G V h_g} \\ &= \frac{86.72 \times 1000 \times 1000 \times 3.37 \times 10^{-2}}{5.47 \times 10^3 \times 1.03 \times 2.41 \times 10^5} \text{ m}^2 \\ &= 2.15 \times 10^{-3} \text{ m}^2 \end{aligned}$$

Area to volume ratio for homogenous flow for no over pressure condition,

$$\frac{A_o}{V} = 2.09 \times 10^{-3} \text{ m}^{-1}$$

A4.2.2.2 Fauske's equation for non-reactive system with critical flow:

The vent sizing calculation is done in this case by considering ideal nozzle flow. And for ideal nozzle flow, the discharge co-efficient (C_D) is considered to be 1 (Fauske, 2000).

Area to volume ratio,

$$\begin{aligned} \frac{A}{V} &= \frac{C_p \rho_l \dot{T}}{0.61 C_D \rho_v \lambda \left(\frac{P}{\rho_v}\right)^{\frac{1}{2}}} \\ &= \frac{2.92 \times 10^3 \times 970 \times 2.7 \times 10^{-2}}{0.61 \times 1 \times 29.70 \times 2.41 \times 10^5 \times \left(\frac{7.91 \times 10^5}{29.70}\right)^{\frac{1}{2}}} m^{-1} \\ &= 1.07 \times 10^{-4} m^{-1} \end{aligned}$$

The area to volume ratio calculated here is only for a single phase flow. This ratio is multiplied with a factor of 2 for a homogeneous flow (Fauske, 2000).

Hence, area to volume ratio for homogenous flow,

$$\frac{A}{V} = 1.07 \times 10^{-4} m^{-1} \times 2 m^{-1} = 2.15 \times 10^{-4} m^{-1}$$

A4.3 Nox Rust 1100

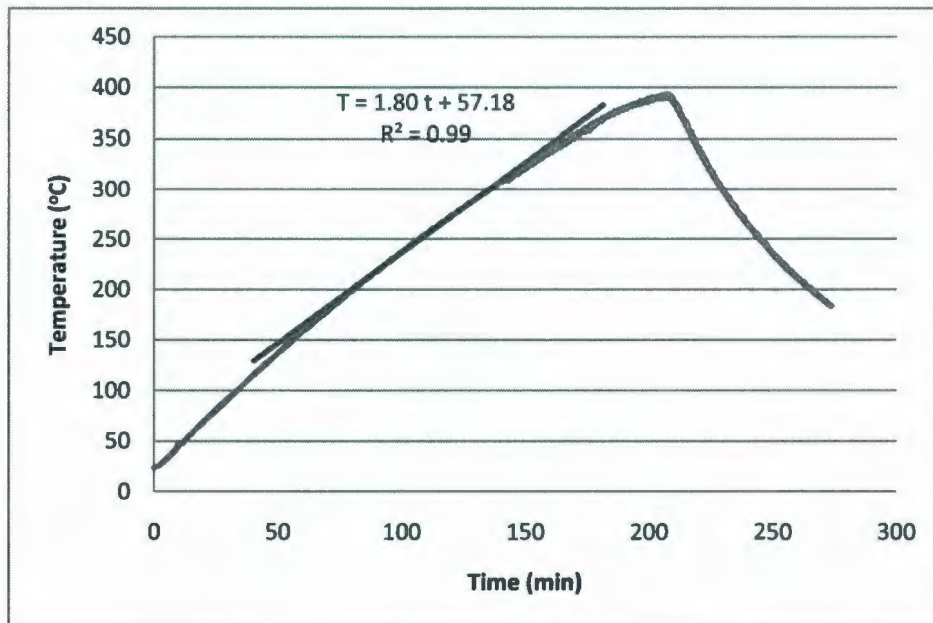


Figure 3: Temperature History for Nox Rust 1100 (VSP2 Test 2)

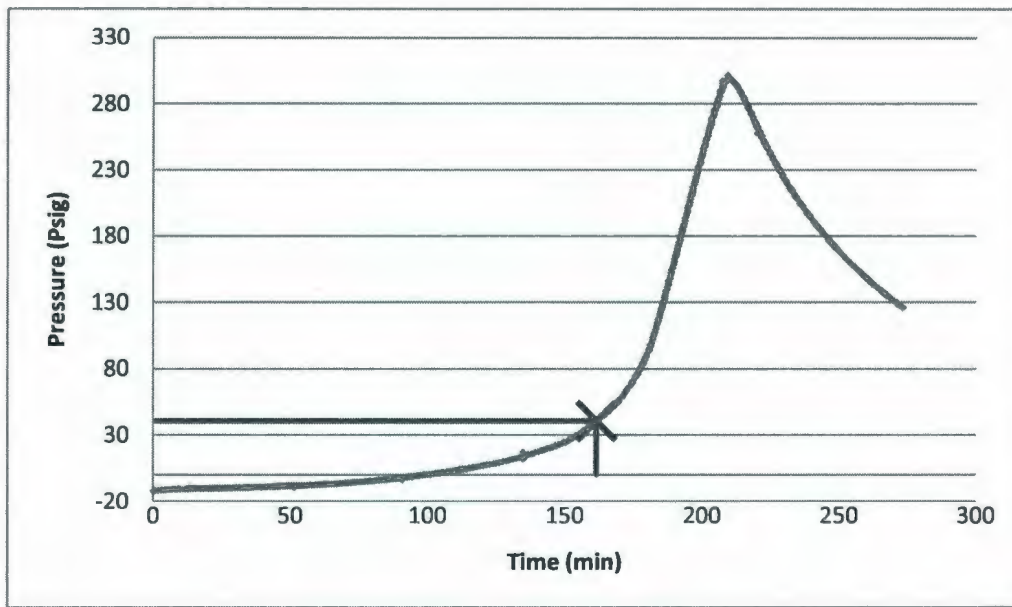


Figure 4: Pressure History for Nox Rust 1100 (VSP2 Test 2)

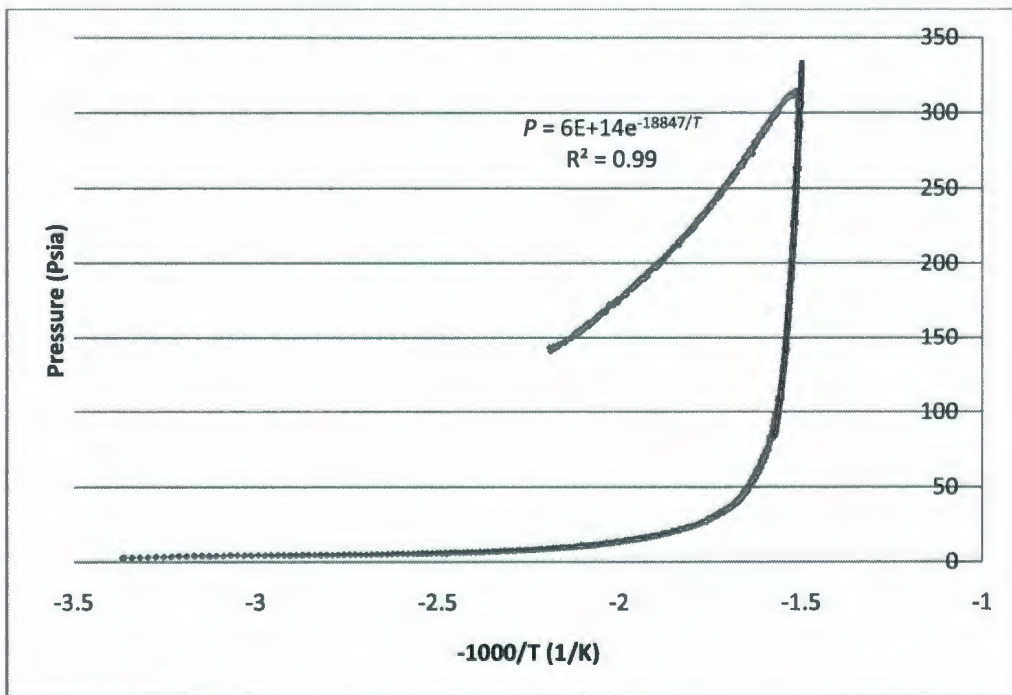


Figure 5: Pressure as a Function of Temperature for Nox Rust 1100 (VSP2 Test 2)

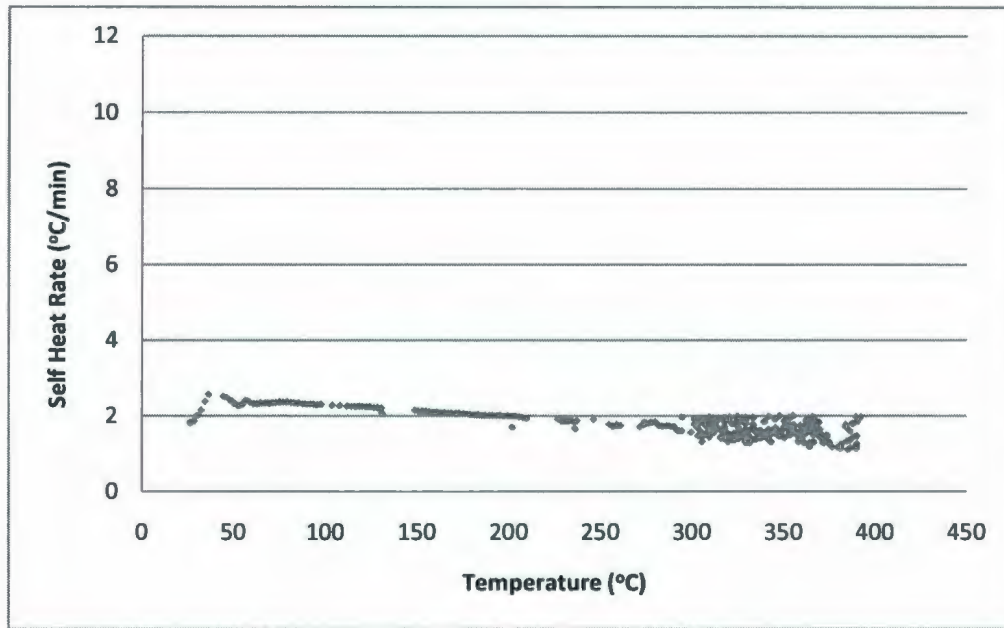


Figure 6: Self Heat Rate as a Function of Temperature for Nox Rust 1100 (VSP2 Test 2)

A4.4 VCI 1 Powder

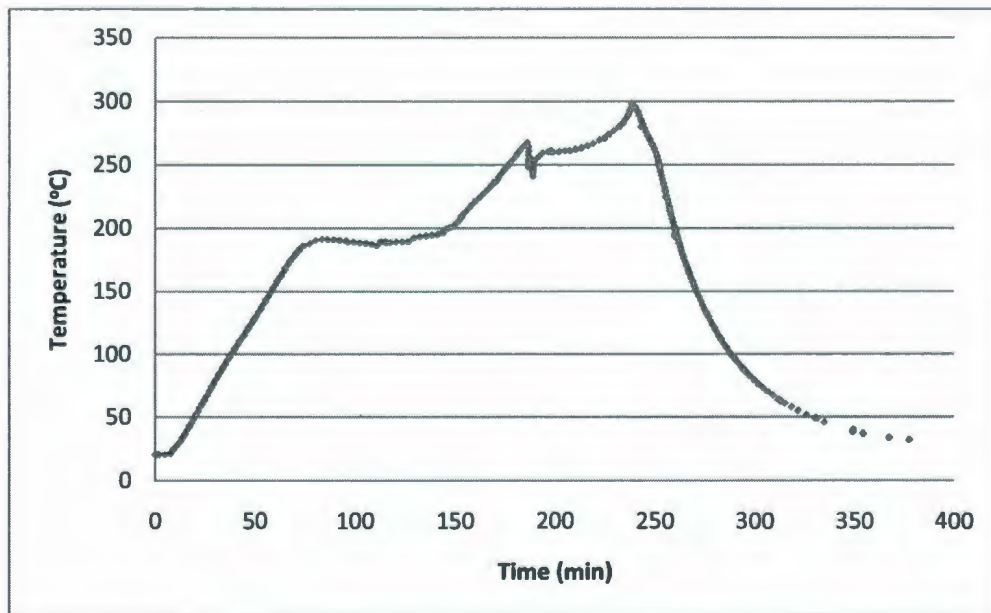


Figure 7: Temperature History for VCI 1 Powder (VSP2 Open Cell Test)

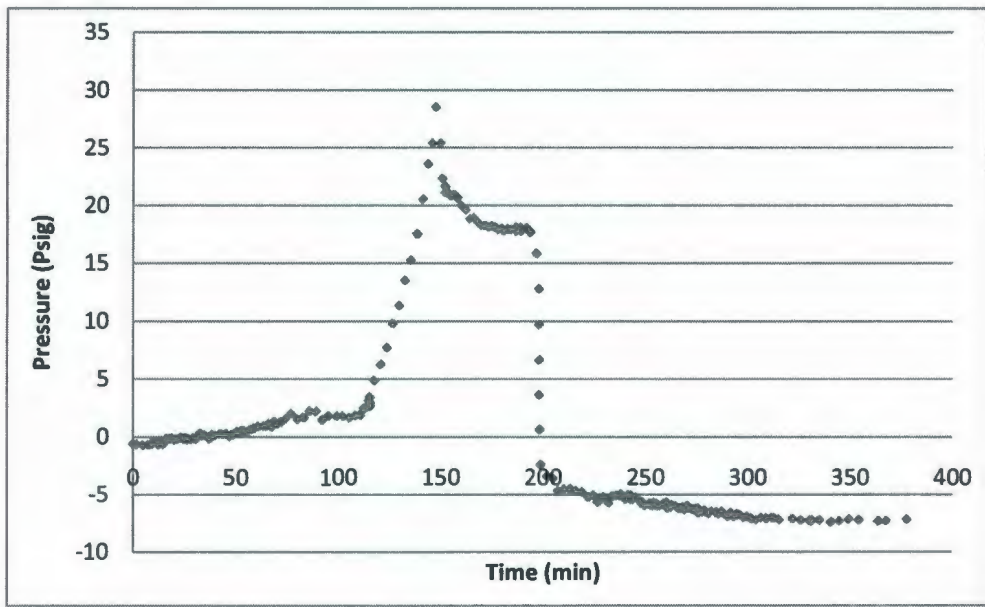


Figure 8: Pressure History for VCI 1 Powder (VSP2 Open Cell Test)

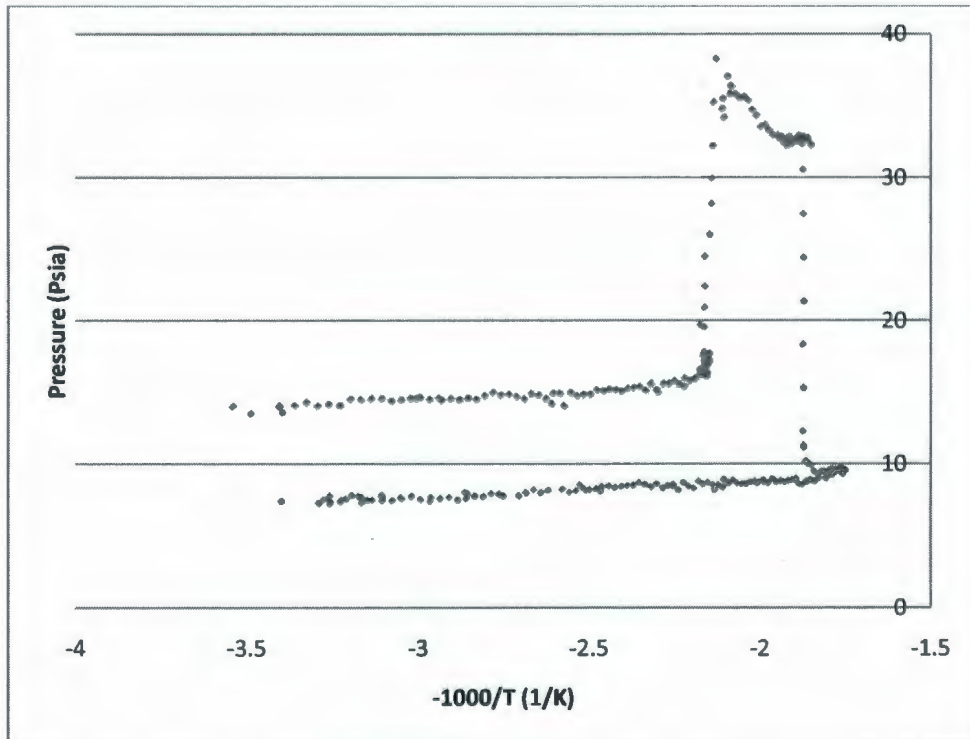


Figure 9: Pressure as a Function of Temperature for VCI 1 Powder (VSP2 Open Cell Test)

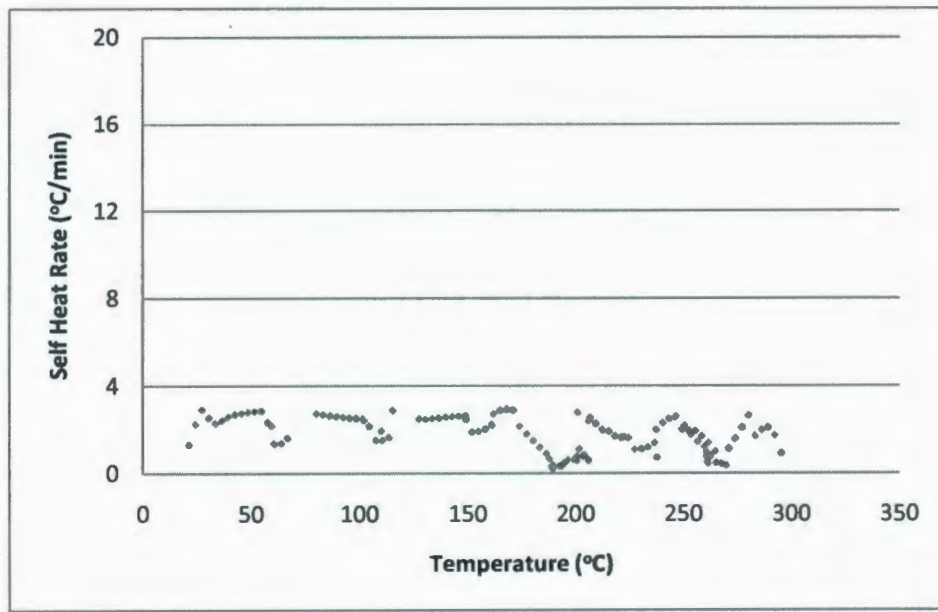


Figure 10: Self Heat Rate as a Function of Temperature for VCI 1 Powder (VSP2 Open Cell Test)

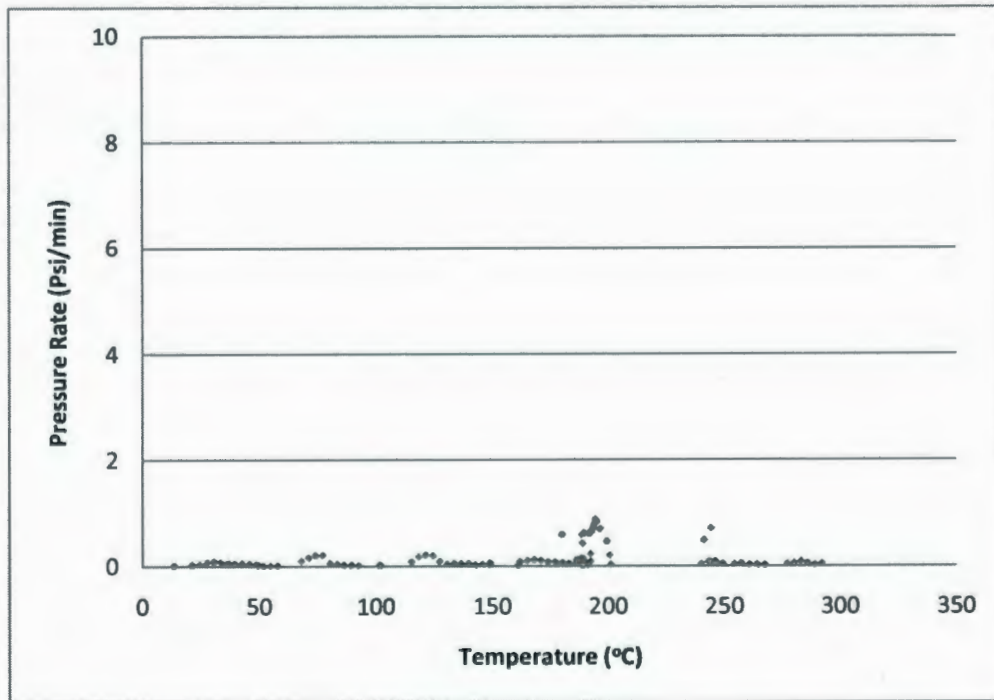


Figure 11: Pressure Rate as a Function of Temperature for VCI 1 Powder (VSP2 Open Cell Test)

APPENDIX 5

As mentioned in Chapter 6, the hydrogen sulphide scavenger was tested twice with the VSP 2. The heat of mixing calculation for the second test and the vent sizing calculations for both of the tests are described in this appendix.

A5.1 Heat of Mixing Calculation for Test 2

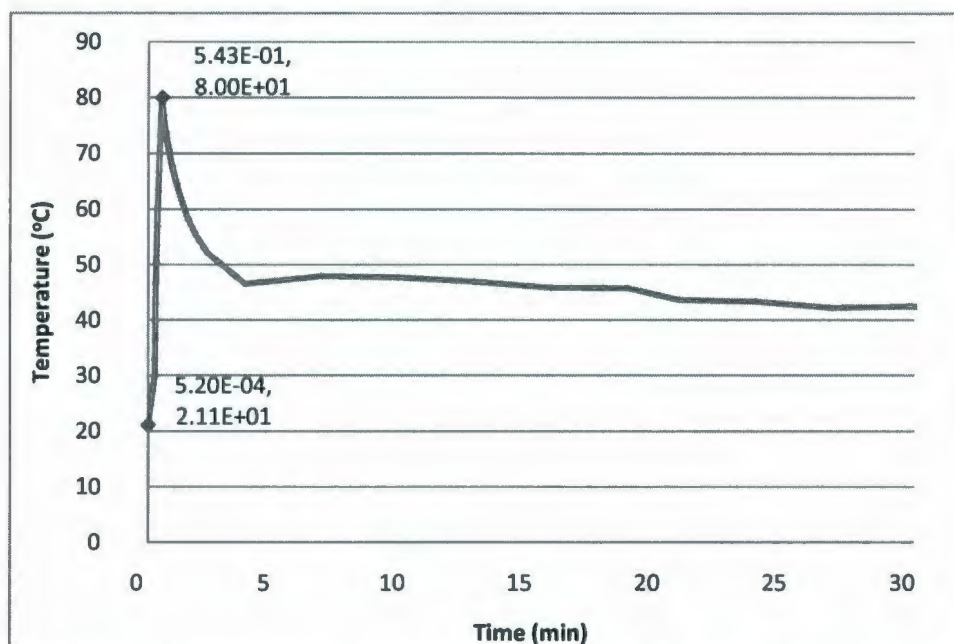


Figure 1: Temperature History due to the Heat of Mixing (VSP2 Test 2)

Table 1: Weight, Mass Fraction and Molar Quantity of the H₂S Scavenger Components

| Component | Units used in the test (by weight) | Mass fraction | Wt of the component used in the test (g) | Molecular weight of the component (g) | Component used (mol) |
|------------------|------------------------------------|---------------|--|--|----------------------|
| 37% Formaldehyde | 5 | 0.71 | 31.69 | 30.03 (Mallinckrodt Baker Inc, 2007) | 1.06 |
| Monoethanolamine | 2 | 0.29 | 12.82 | 61.08 (The Dow Chemical Company, 2001) | 0.21 |

Here,

Specific heat capacity of the H₂S scavenger at 25 °C, $C_p = 3.02 \times 10^3$ J/ kg-K

Total mass of sample, $m = 44.00$ g = 4.40×10^{-2} kg

Temperature rise after mixing, $\Delta T = (80.00 - 21.1) ^\circ\text{C} = \{(80.00+273) - (21.1+273)\}$ K = 58.9 K

Moles of limiting reagent, $n = 0.21$

Therefore, heat of mixing of the H₂S scavenger mixture,

$$\Delta H_{\text{mixing}} = \frac{mC_p\Delta T}{n} = \frac{4.40 \times 10^{-2} \times 3.02 \times 10^3 \times 58.9}{0.21} \text{ J/mol} = 37.28 \text{ kJ/mol}$$

A5.2 Different Parameters

A5.2.1 Phi factor (ϕ) calculation (for Test 2):

Given,

Specific heat capacity of the Hastelloy test cell, $C_{pb} = 425$ J/ kg -K (Shanghai eshine Stainless steel Material Co., Ltd)

Hence, Specific heat capacity of H₂S scavenger at 90°C, $C_{ps} = 3.51 \times 10^3$ J/ kg -K

Mass of the sample, $m_s = 44$ g = 4.40×10^{-2} kg

Mass of the test cell, $m_b = 51.94$ g = 5.19×10^{-2} kg

So, Phi factor of the test cell by using Equation 2.1,

$$\phi = 1 + \frac{m_b C_{pb}}{m_s C_{ps}} = 1 + \frac{5.19 \times 10^{-2} \times 425}{4.40 \times 10^{-2} \times 3.51 \times 10^3} = 1.14$$

A5.2.2 Determining set pressure (P_s), set temperature (T_s) and $\frac{dP}{dT}$ (for Test 2):

The set pressure for venting is considered as 25 Psig as the pressure rise is comparatively higher after this point as shown in Figure 6.14.

Here,

$$\text{Pressure at set point, } P_s = 25 \text{ Psig} = 39.7 \text{ Psia} = 2.74 \times 10^5 \text{ Pa}$$

Let,

$$\text{Maximum allowable working pressure, MAWP} = 27.5 \text{ Psig} = 42.20 \text{ Psia} = 2.91 \times 10^5 \text{ Pa}$$

$$\text{Venting pressure by considering 20\% over pressure, } P_m = 30 \text{ Psig} = 44.7 \text{ Psia} = 3.08 \times 10^5 \text{ Pa}$$

$$\text{Pressure difference for considering 20\% over pressure, } \Delta P = P_m - P_s = (3.08 \times 10^5 - 2.74 \times 10^5) \text{ Pa}$$

$$= 3.40 \times 10^4 \text{ Pa}$$

From Figure 6.16,

$$\ln P = \ln(2 \times 10^8) - \frac{6144.3}{T}$$

$$\text{So, } \ln P = 19.11 - \frac{6144.3}{T}$$

Equation 1

By substituting the value of set pressure (42.20 Psia), maximum allowable working pressure (42.20 Psia) and venting pressure (44.7 Psia) in Equation 1, the following values if temperature can be calculated,

$$\text{Temperature at the set point, } T_s = 398.14 \text{ K} = 125 \text{ }^\circ\text{C}$$

$$\text{Maximum allowable temperature, } T_{MAWP} = 399.72 \text{ K} = 126.57 \text{ }^\circ\text{C}$$

Venting Temperature, $T_m = 401.22 \text{ K} = 128.07 \text{ }^\circ\text{C}$

Temperature difference, $\Delta T = T_m - T_s = (401.22 - 398.14) \text{ K} = 3.08 \text{ K}$

By differentiating the Equation 1 (Fauske, 1985),

$$\frac{1}{P} \frac{dP}{dT} = \frac{6144.3}{T^2}$$

$$\text{Hence, } \frac{dP}{dT} = \frac{6144.3 P}{T^2}$$

Equation 2

$$\text{So, } \frac{dP}{dT} (\text{at set pressure and temperature}) = \frac{6144.3 \times 2.74 \times 10^5}{398.14^2} \text{ Pa/K} = 1.06 \times 10^4 \text{ Pa/K}$$

A5.2.3 Temperature rate at set point $\left(\frac{dT}{dt}\right)_s$ and temperature rate at venting $\left(\frac{dT}{dt}\right)_m$ calculation (for Test 2):

From Figure 6.17,

$$\frac{dT}{dt} = 6.56 \times 10^{-2} e^{3.64 \times 10^{-2} T}$$

Equation 3

Hence, From Equation 3,

$$\text{Temperature rate at set point (125 }^\circ\text{C), } \left(\frac{dT}{dt}\right)_s = 6.56 \times 10^{-2} e^{3.64 \times 10^{-2} \times 125} \text{ }^\circ\text{C/min}$$

$$= 6.20 \text{ }^\circ\text{C/min}$$

$$= 0.10 \text{ K/s}$$

$$\text{Temperature rate at venting (126.57 }^\circ\text{C), } \left(\frac{dT}{dt}\right)_m = 6.56 \times 10^{-2} e^{3.64 \times 10^{-2} \times 128.07} \text{ }^\circ\text{C/min}$$

$$= 6.94 \text{ }^\circ\text{C/min}$$

$$= 0.11 \text{ K/s}$$

A5.2.4 Calculation of average heat release rate (q) and heat release rate at the set point (q_s) (for Test 2):

Heat release rate by using Equation 6.8,

$$q = \frac{1}{2} \times 1.14 \times 3.51 \times 10^3 \times [0.10 + 0.11] \text{ J/ kg -s} = 420.15 \text{ J/ kg -s}$$

Heat release rate at set temperature by using Equation 6.9,

$$q_s = 1.14 \times 3.51 \times 10^3 \times 0.10 \text{ J/ kg -s} = 400.14 \text{ J/ kg -s}$$

A5.2.5 Vapor density (ρ_v) and vapor specific volume (v_g) calculation (for Test 2):

Here,

Molecular weight of H₂S Scavenger, M_w = 39.03 kg / Kmol

Molar gas constant, R = 8.314 × 10³ J/Kmol - K

From Equation 5.5, vapor density of H₂S Scavenger at set temperature and pressure for test 2,

$$\rho_v = \frac{39.03 \times 2.74 \times 10^5}{8.314 \times 10^3 \times 398.14} \text{ kg /m}^3 = 3.23 \text{ kg /m}^3$$

And, vapor specific volume,

$$v_g = \frac{1}{\rho_v} = 0.31 \text{ m}^3 / \text{kg}$$

A5.2.6 Latent heat of vaporization (h_g or λ) calculation (for Test 2):

Latent heat of vaporization for H₂S scavenger for test 2, by using Clapeyron relation described by Equation 5.6,

$$\text{So, } h_g = \lambda = v_g T \frac{dP}{dT} = 0.31 \times 398.14 \times 1.06 \times 10^4 \text{ J/ kg} = 1.31 \times 10^6 \text{ J/ kg}$$

A5.2.7 Critical mass flux (G) calculation:

Critical mass flux for test 2 can be calculated by using Equation 2.31 described in Chapter 2 (Leung, 1986), as follows,

$$G = 0.9 \frac{\lambda}{v_g} \left(\frac{1}{c_p T} \right)^{0.5} = 0.9 \times \frac{1.31 \times 10^6}{0.31} \times \left(\frac{1}{3.51 \times 10^3 \times 398.14} \right)^{0.5} \text{ kg/m}^2\text{-s} = 3.22 \times 10^3 \text{ kg/m}^2\text{-s}$$

A5.3 Vent Sizing Calculation

A5.3.1 Leung's method for homogenous venting with 20% overpressure

The vent sizing by Leung's method are done by considering 1000 kg of initial mass and the effective volume of the chemical corresponding to this mass is calculated

Here,

Density of formaldehyde = 1090 kg/m³

Density of monoethanolamine = 1010 kg/m³

Density of H₂S scavenger, $\rho_l = 1066.80 \text{ kg/m}^3$

Initial mass in vessel, $m_o = 1000 \text{ kg}$ (710 Kg formaldehyde + 290 Kg monoethanolamine)

Volume of the liquid, $V = \frac{m_o}{\rho_l} = 0.94 \text{ m}^3$

Specific volume of the liquid in vessel, $v = \frac{V}{m_o} = \frac{0.94}{1000} \text{ kg} = 9.4 \times 10^{-4} \text{ m}^3/\text{kg}$

Test 1:

At first, vent rate (W) is calculated by using Equation 2.21. The specific heat capacity at constant pressure is considered instead of specific heat capacity at constant volume for the calculation purpose as suggested by Leung (1986). The calculation is shown as follows:

$$\begin{aligned} W = GA &= \frac{m_o q}{\left[\left(\frac{V}{m_o} \frac{h_g}{\vartheta_g} \right)^{1/2} + (C_p \Delta T)^{1/2} \right]^2} \\ &= \frac{1000 \times 273.90}{\left[\left(\frac{0.94}{1000} \times \frac{1.30 \times 10^6}{0.30} \right)^{1/2} + (3.51 \times 10^3 \times 2.91)^{1/2} \right]^2} \text{ kg/s} \\ &= 10.07 \text{ kg/s} \end{aligned}$$

$$\text{Hence, vent area, } A = \frac{W}{G} = \frac{10.07}{3.35 \times 10^3} \text{ m}^2 = 3.01 \times 10^{-3} \text{ m}^2$$

$$\text{Therefore, area to volume ratio, } \frac{A}{V} = \frac{3.03 \times 10^{-3}}{0.94} \text{ m}^{-1} = 3.22 \times 10^{-3} \text{ m}^{-1}$$

Test 2:

Vent rate for test 2 by using Equation 2.21,

$$\begin{aligned} W = GA &= \frac{m_o q}{\left[\left(\frac{V}{m_o} \frac{h_g}{\vartheta_g} \right)^{1/2} + (C_p \Delta T)^{1/2} \right]^2} \\ &= \frac{1000 \times 420.15}{\left[\left(\frac{0.94}{1000} \times \frac{1.31 \times 10^6}{0.31} \right)^{1/2} + (3.51 \times 10^3 \times 3.08)^{1/2} \right]^2} \text{ Kg/s} \\ &= 15.06 \text{ kg/s} \end{aligned}$$

$$\text{Hence, vent area, } A = \frac{W}{G} = \frac{15.06}{3.22 \times 10^3} \text{ m}^2 = 4.68 \times 10^{-3} \text{ m}^2$$

$$\text{Therefore, area to volume ratio, } \frac{A}{V} = \frac{4.68 \times 10^{-3}}{0.94} \text{ m}^{-1} = 4.98 \times 10^{-3} \text{ m}^{-1}$$

A5.3.2 Leung's method for homogenous venting with no overpressure

Vent area for no over pressure for Leung's method as given by Equation 2.22,

$$A_o = \frac{m_o q_s v_g}{G v h_g}$$

Test 1:

Vent area for no over pressure,

$$A_o = \frac{1000 \times 256.62 \times 0.30}{3.35 \times 10^3 \times 9.4 \times 10^{-4} \times 1.30 \times 10^6} \text{ m}^{-1} = 1.89 \times 10^{-2} \text{ m}^{-1}$$

Hence, area to volume ratio is $2.01 \times 10^{-2} \text{ m}^{-1}$.

Test 2:

Vent area for no over pressure,

$$A_o = \frac{1000 \times 400.14 \times 0.31}{3.22 \times 10^3 \times 9.4 \times 10^{-4} \times 1.31 \times 10^6} \text{ m}^{-1} = 3.13 \times 10^{-2} \text{ m}^{-1}$$

Hence, area to volume ratio is $3.33 \times 10^{-2} \text{ m}^{-1}$.

A5.3.3 Fauske's short form equation for runaway chemical reaction under their own vapour pressure

Area to volume ratio by Fauske's short form equation as given by Equation 2.39,

$$\frac{A}{V} = \rho (TC_p)^{-1/2} \frac{q_s}{\Delta P}$$

Test 1:

Area to volume ratio for homogeneous flow,

$$\begin{aligned} \frac{A}{V} &= 1066.80 \times (386.15 \times 3.51 \times 10^3)^{-1/2} \times \frac{256.62}{3.40 \times 10^4} \text{ m}^{-1} \\ &= 6.92 \times 10^{-3} \text{ m}^{-1} \end{aligned}$$

Test 2:

Area to volume ratio for homogeneous flow,

$$\begin{aligned}\frac{A}{V} &= 1066.80 \times (398.14 \times 3.51 \times 10^3)^{-1/2} \times \frac{400.14}{3.40 \times 10^4} \text{ m}^{-1} \\ &= 1.06 \times 10^{-2} \text{ m}^{-1}\end{aligned}$$

A5.3.4 Fauske's screening equation for vapour system

The vent sizing calculation is done in this case by considering ideal nozzle flow. And for ideal nozzle flow, the discharge co-efficient (C_D) is considered to be 1 (Fauske, 2000).

$$\frac{A}{V} = \frac{3.5 \times 10^{-3} \dot{T}}{C_D P \left[1 + \frac{1.98 \times 10^{-3}}{P^{1.75}} \right]^{0.286}}$$

Test 1:

Area to volume ratio for non- foamy flow,

$$\begin{aligned}\frac{A}{V} &= \frac{3.5 \times 10^{-3} \times 3.88}{1 \times 39.7 \left[1 + \frac{1.98 \times 10^{-3}}{39.7^{1.75}} \right]^{0.286}} \text{ m}^{-1} \\ &= \frac{1.36 \times 10^{-2}}{39.7} \text{ m}^{-1} \\ &= 3.42 \times 10^{-4} \text{ m}^{-1}\end{aligned}$$

For foamy flow, $\frac{A}{V} = 3.42 \times 10^{-4} \times 2 \text{ m}^{-1} = 6.84 \times 10^{-4} \text{ m}^{-1}$

Test 2:

Area to volume ratio for non- foamy flow,

$$\begin{aligned}\frac{A}{V} &= \frac{3.5 \times 10^{-3} \times 6.20}{1 \times 39.7 \left[1 + \frac{1.98 \times 10^{-3}}{39.7^{1.75}} \right]^{0.286}} m^{-1} \\ &= \frac{2.17 \times 10^{-2}}{39.7} m^{-1} \\ &= 5.47 \times 10^{-4} m^{-1}\end{aligned}$$

For foamy flow, $\frac{A}{V} = 5.47 \times 10^{-4} \times 2 m^{-1} = 1.09 \times 10^{-3} m^{-1}$



